ROLE OF OSTEO-PROGENITORS IN THE PATHOGENESIS OF VASCULAR CALCIFICATION

Thesis submitted by

SHRIPAD NAGESH PAL

MSc. (INDIA)

AUGUST 2009

for the degree of Doctor of Philosophy (Vascular Biology)

in the School of Medicine and Dentistry

James Cook University, QLD

AUSTRALIA

Table of contents

DECLARATION

I, the undersigned declare that this research investigation is carried out on my own and it has not been previously submitted anywhere for another degree or diploma at any university or institution of tertiary education in or out of Australia. Information derived from the published or unpublished works of others has been acknowledged in the text and a list of references is given.

Shripad Nagesh PAL,

August 2009

STATEMENT OF ACCESS TO THESIS

I, the undersigned, author of this thesis, understand that James Cook University will make this work available for use within the university library and, by microfilm or other photographic means, allow access to users in other approved libraries. All users consulting this thesis will have to sign the following statement.

'In consulting this thesis, I agree not to copy or paraphrase it completely in whole or in part without written consent of the author, and to make proper written acknowledgement for any assistance which I have obtained from it.'

Apart from this, I do not wish to place any restriction on access to this research thesis.

Shripad Nagesh PAL,

August 2009

DECLARATION ON ETHICS

The research presented and reported in this thesis was conducted within the guidelines for research ethics outlined in the *National Statement on Ethics Conduct in Research Involving Human* (1999), the *joint NHMRC/AVCC Statement and Guidelines on Research Practice* (1997), the *James Cook University Policy on Experimental Ethics. Standard Practices and Guidelines* (2001), and the *James Cook University Statement and Guidelines on Research Practice* (2001). The proposed research methodology received clearance from the James Cook University Experimental Ethics Review Committee (approval number H-2196)

Shripad N. Pal **August 2009**

ACKNOWLEDGEMENTS

The completion of this research thesis would have remained an unfulfilled dream without the untiring and selfless support from a number of people throughout my research student tenure. It is to all of them that I wish to extend my heartfelt gratitude without which this task would not have been possible.

First and foremost, I thank the Almighty Lord for providing me the opportunity, determination and perseverance which I could invest bit by bit, day by day to reach this stage. Secondly, I owe a lot to my parents (Nagesh K Pal and Mangala N Pal), my younger brother Pratik, my dearest wife Rucha and her family who loved, cared, supported, and believed in me in the toughest of times. This journey would not have been possible without their love, prayers and blessings.

In Australia, I am sincerely thankful to my supervisor Professor Jonathan Golledge, co-supervisors Dr Lynn Woodward and Dr Mirko Karan. I am grateful for their able supervision, professional guidance, and many words of thought during my research. I really appreciate them for their continuing belief in me which kept on reigniting the lamp of hope throughout the PhD candidature, especially during the darkest of research moments. Professor Golledge also provided me with all the necessary financial support required for my research candidature and survival in Townsville for which I am deeply indebted.

Sincere thanks and thoughts go towards Dr Catherine Rush and Dr Ann Van Campenhout for their willingness to pass on their research experience. It's their patience and selfless guidance that helped me to efficiently focus on the candidature. I extend my appreciation to Dr Monsur Kazi, Dr Paula Clancy, Mrs Frances Wood and Ms. Simone Mangan for their friendship, words of support, guidance and technical assistance throughout my tenure. The time and efforts of Dr Bradford Cullen and Dr Julie Mudd in their work with the mouse model which provided me with tissue samples is gratefully acknowledged.

A warm and a heartfelt thanks goes towards my fellow PhD colleague, office buddy and partner in crime, Venkat Vangaveti, for his company, tolerance, and support. Very special thanks go to Dr. Adam Parr, Ms Barbara Bradshaw from the Townsville General Hospital and Sullivan and Nicolaides Pathology, Townsville for assisting me in arranging the patient samples without which the research investigation would not have been complete. I also

extend my gratitude towards the Biomedical and Tropical veterinary sciences faculty for providing all the required facility for undertaking mouse work.

I am also obliged to thank my faculty, The School of Medicine and Dentistry and Graduate research school, James Cook University for all financial and administrative support that assisted me in completing my research candidature.

Last but not the least; I would convey a heartfelt thankyou to all the friends in Townsville, both compatriots and local fellows who supported me socially throughout my candidature. Without their first-hand social and emotional support it would have been tough to survive and thrive in Townsville.

LIST OF ABBREVIATIONS

µg/kg: Microgram/ kilogram

µl: Microliter

A.A: Aortic arch

AAA: Abdominal aortic aneurysm

ACI: Aortic calcification index

ACK: Ammonium chloride and potassium chloride

ALP: Alkaline phosphatase

ApoE: Apolipoprotein E

BL/6: Black 6

BM: Bone marrow

BMP-2: Bone matrix protein-2

BMT: Bone marrow transplantation

COV: Coefficient of variation

CT: Computed tomography

CTA: Computed tomography angiogram

CVC: Calcifying vascular cells

D/W: Distilled water

DAPI: 4', 6-diamidino-2-phenylindole

dL: Deciliter

EDTA: Ethylene diamine tetra-acetic acid

ELISA: Enzyme linked Immunosorbent assay

EPC: Endothelial progenitor cells

ESRD: End stage renal disease

FC: Flow cytometry

FCS: Fetal calf serum

FSC: Forward scatter

G-CSF: Granulocyte colony-stimulating factor

GFP: Green fluorescent protein

GM-CSF: Granulocyte-macrophage colony-stimulating factor

HDL: High density lipoprotein

HEPES: 4-(2-hydroxyethyl)-1-piperazineethanesulfonic acid

hMSC: Human mesenchymal stem cells

HSC: Hematopoietic stem cells

hVSMC: Human vascular smooth muscle cells

I. R: Infra renal

I-CAM-1: Intercellular adhesion molecule-1

IL- 6: Interleukin 6

IL-1β: Interleukin 1- beta

IL-8: Interleukin 8

IQR: Inter quartile range

LDLR: Low-density lipoprotein receptor

MACS: Magnetic assorting cell separator

mg: Milligrams

MGP: Matrix gamma-carboxyglutamic acid protein

Min: Minutes

ml: Mililiter

mM- Milimolar

mm^3: Cubic milimeter

Mmol/L: Milimolar/liter

MNC: Mononuclear cells

MS: Magnetic separation

MSC: Mesenchymal stem cells

ng/ml: Nanogram/milliliter

nm: Nanometer

O.D: Optical density

^oC: Degrees centigrade

OCN^+: Osteocalcin positive

$OPG^{-/-}$: Osteoprotegerin deficient

$OPG^{+/+}$: Osteoprotegerin present

OPN: Osteopontin

PBS: Phosphate buffered saline

PDGF: Platelet derived growth factor

PE: Phycoerythrin

pg/ml: picogram/milliliter

PPi: Pyrophosphate

R.T: Room temperature

RANK: Receptor activator of nuclear kappa

RANK-L: Receptor activator of nuclear kappa ligand

RBC: Red blood cells

rpm: Revolutions per minute

S.D: Standard deviation

S.R: Supra renal

SCF: Stem cell factor

SDF-1α: Stromal cell derived factor 1 alpha

SMC: Smooth muscle cells

SNP: Sullivan Nicolaides pathology

SSC: Side scatter

T.A: Thoracic arch

TGF-β: Tumor growth factor-beta

TNF α: Tumor necrosis factor- alpha

V-CAM-1: Vascular cell adhesion molecule-1

VEGF: Vascular endothelial growth factor

VSMC: Vascular smooth muscle cells

ABSTRACT

Vascular calcification, until recently, was considered to be a passive process which occurred as a nonspecific response to tissue injury or necrosis. Since the severity of vascular calcification has been correlated with that of atherosclerosis and its risk factors, it was postulated that the process is linked to these events. However recent findings from a number of mouse model studies suggest that the mechanisms involved in vascular calcification may be distinct from those underlying atherosclerosis.

Current theories regarding the pathogenesis of vascular calcification suggest a number of possible mechanisms. These include passive models in which vascular calcification is observed as a result of loss of molecular inhibitors and those where active cell mediated process is involved. Calcification has also been reported as result of apoptosis or death of vascular smooth muscle cells (VSMC). Current evidence favours a cell mediated mechanism of vascular calcification.

The origin of the cells responsible for vascular calcification is not clearly defined. One novel source of cells controlling vascular calcification is from the bone marrow (BM). A circulating immature BM-derived population has been identified. A small subset of this BM population has been reported to possess bone forming properties *invitr*o and hence called osteo-progenitors. In the present investigation, it was hypothesized that these circulating osteo-progenitors contribute to vascular calcification. It was postulated that the osteo-progenitors are recruited from the BM environment under the influence of stem cell mobilising cytokines such as stromal cell derived factor-1 α (SDF-1α), granulocyte-colony stimulating factor (G-CSF) and stem cell factor (SCF). Further, it was suggested that these stem cell mobilising cytokines facilitate the homing of immature circulating osteo-progenitors to vascular lesions and contribute to calcification.

These hypotheses were tested in two mouse models and one human patient cohort. The aims of the investigation included:

a) To establish a suitable mouse model for vascular calcification studies.
b) To assess the association of the circulating osteo-progenitor population with the severity of aortic calcification in mouse models.
c) To identify if the osteo-progenitor population was deposited within the vasculature at sites of vascular calcification.

d) To assess the relationship between the circulating osteo-progenitor population and aortic calcification in a human patient group suffering from peripheral artery disease.
e) To assess the relationship between the stem cell mobilising cytokines and the severity of vascular calcification in a mouse model and a human patient cohort.

The findings of this work suggest, for the first time, an association between circulating osteocalcin positive mononuclear cells (OCN^+ MNC) and aortic calcification in two mouse models and a human patient cohort diagnosed with peripheral artery disease. It was found that the severity of vascular calcification was increased in 52 week old osteoprotegerin knockout ($OPG^{-/-}$) mice and even more elevated in younger (14 week old) $OPG^{-/-}$ mice receiving controlled doses of calcitriol. It was further observed that in both mouse models the percentage of circulating OCN^+ MNC was correlated to the aortic calcium content. These results suggest a possible role for BM-derived osteo-progenitors in vascular calcification. It was also observed that OCN^+ population deposited within the vasculature was directly associated with the severity of extractable aortic calcium in the $OPG^{-/-}$ mouse model. These results suggest a three-way association between osteo-progenitor population in circulation, its cellular deposition within vasculature and the severity of aortic calcification.

The investigation undertaken in the human patient cohort also supported the initial hypothesis and confirmed the research findings obtained from the two mouse models. In the patient study the percentage of circulating OCN^+ MNC was observed to be associated with the severity of infra-renal aortic calcification.

The present study also supported the hypothesis that the stem cell mobilizing cytokines could be involved with the release of osteo-progenitors and may facilitate their homing to the vasculature. The concentrations of SDF-1α, G-CSF and SCF were associated with the percentage of circulating OCN^+ MNC and the severity of aortic calcification in the mouse models and patient cohort investigated. These results suggest that the BM- derived osteo-progenitors are mobilised into the peripheral circulation from the marrow environment under the influence of these cytokines. Further, the circulating osteo-progenitors may home to vascular lesions and differentiate into bone-forming cells. This process may contribute to the pathogenesis of vascular calcification.

Further work, however, is necessary to confirm the role of these BM-derived immature cells in vascular calcification as there are a number of limitations of the present investigation. Firstly, both mouse models employed were based on OPG deficiency. Thus it is possible that the increased OCN^+ MNC was related to this rather than the aortic calcification in these animals. Secondly, the role of OPG within the vasculature is also not entirely clear. While depletion of OPG in mouse models is reported to induce vascular calcification, in patients serum OPG levels are positively associated with peripheral artery disease. This difference in results between mouse models and human patient illustrates the current uncertainty regarding the role of OPG in cardiovascular disease. The patient group investigated in this study was small. A larger group would be ideal to confirm the association between circulating osteo-progenitors and aortic calcification. The absence of a healthy control group is a further limitation of the human investigation.

Overall, the current research suggests an important new mechanism underlying vascular calcification with implications for treatment. Results obtained from this study may also be useful in the investigation of other pathology types, and may assist in establishing collaboration with external groups. Since vascular calcification is also linked to other clinical conditions such as atherosclerosis, diabetes, obesity and bone related disorders, this investigation can build on those areas within research groups with broader clinical perspectives.

LIST OF TABLES

LIST OF FIGURES

CHAPTER 1. INTRODUCTION AND LITERATURE REVIEW

INTRODUCTION

Vascular calcification, or hardening of the arteries, has long been considered a complication of ageing and hence little significance has been given to its clinical consequences[1]. However, in the past two decades vascular calcification has been shown to be a age progressive complication of patients which significantly contributes to high cardiovascular mortality[2] resulting in greater research focus on its aetiology, mechanisms and consequences[1-3]. Vascular calcification affects a significant proportion of elderly people[2]. Recent studies revealed that in the western world it is evident in 55 percent of men and women under 40 years, and a considerable extent of calcification was present in all men by age 50 and by the age of 60 in all women[2,4]. In Australia, despite increased research in areas such as atherosclerosis and calcification, cardiovascular diseases remain one of the biggest causes of death and continues to generate a considerable burden on the population in terms of illness and disability[5]. Despite extensive laboratory and clinical research the precise mechanisms leading to the process of calcification remains unclear.

Literature suggests that one of the known key hallmarks of vascular calcification is the deposition of calcium phosphate in the form of bioapatite[4,6]. This can occur in blood vessels, myocardium and cardiac valves[6]. In blood vessels, calcified deposits are found in distinct layers of the blood vessels and are related to underlying pathology[7]. Intimal calcification is observed in atherosclerotic lesions whereas medial calcification is found to be associated with vascular stiffening and arteriosclerosis observed with age, diabetes and end stage renal disease (ESRD)[3,8-10]. The introduction of new techniques to measure vascular calcification noninvasively, such as electron beam computed tomography, has changed the current perspective about the risks of vascular ailment[11-13]. Calcification is now positively correlated with atherosclerotic plaque burden, increased risk of myocardial infarction and plaque instability[13-15]. Although some of these findings may relate to the correlation of calcification with the extent of underlying atherosclerotic disease[14], it is also been thought that vascular calcification itself can contribute to initiation of cardiovascular disease[2,16,17]. Vascular calcification has been reported to be prevalent in the medial layers of the larger arteries such as the aorta which leads to increased stiffening and therefore decreased elasticity of the arteries[18-20]. The consequent loss of the important cushioning function of these arteries is associated with increased arterial pulse wave velocity and pulse

pressure[21] leading to impaired arterial flexibility[2], ventricular hypertrophy[12] and compromised coronary perfusion[22].

Previously, vascular calcification was considered to be a passive process in which elevated calcium and phosphorous levels promoted apatite nucleation and crystal growth[23-25]. However, scientific evidence over the past two decades suggests that calcification could be an actively regulated process that may arise via several different mechanisms[1,11,18]. Human and mouse findings have determined that blood vessels normally express certain inhibitors of mineralization and a lack of these molecules leads to spontaneous vascular calcification[3,26]. The presence of bone proteins such as osteopontin (OPN)[27-29], OCN[8,30], bone matrix protein-2(BMP-2)[6,31,32], and matrix vesicles, in calcified vascular lesions has suggested that osteogenic mechanisms may also play a role in vascular calcification[6,33]. Release of circulating nucleation complexes, due to bone turnover, has also been reported to link vascular calcification and osteoporosis[34,35]. Similarly cell apoptosis has also been reported to provide phospholipid-rich membranous debris and apoptotic bodies that may serve to nucleate apatite[36,37], particularly in diseases such as atherosclerosis[14,38].

More recently, a new mechanism of vascular calcification has been postulated. Ongoing studies suggest an active role for circulating cells stemming from sources such as BM and spleen. These cells are thought to contribute to the process of calcification in vasculature[39-41].

The focus of this current research is to investigate the role of such circulating cells originating from the BM and their contribution to disease formation. Two hypotheses are proposed:

The immature progenitor cells released from the BM environment home in on diseased arteries and develop into an osteogenic lineage

This osteogenic cell population in circulatory blood is directly associated with the severity of vascular calcification.

Specifically, the aims of the study are to:

i) Assess the extent of calcification formation in vasculature using an osteoprotegerin knock out animal model
ii) Study the role of circulating BM- derived osteo-progenitor cells and their association with severity of aortic calcification.

iii) Study a human patient cohort to determine the association between the circulating BM- derived osteo-progenitor cells and the severity of vascular calcification

iv) Investigate protein expression studies relating to the association of BM mobilising cytokines with severity of aortic calcification using animal and human patient system.

The circulating cell theory and its contribution towards vascular diseases is novel. Bone marrow derived progenitor cells have been reported to contribute towards atherosclerosis in mouse models such as $MGP^{-/-}$, $ApoE^{-/-}$ and $OCN^{-/-}$. However the results obtained from these studies remain controversial. Our studies would be based in an $OPG^{-/-}$ mouse model which is reported to undergo vessel wall calcification devoid of atherosclerosis. Choosing this mouse model would enable us to highlight the role of bone marrow progenitors specific to vascular calcification. Also, the assessment of circulating progenitors with respect to the severity of calcification has not been previously reported in an $OPG^{-/-}$ mouse model. We also used calcitriol to accelerate vascular calcification. To further support our animal findings, a human patient cohort diagnosed with peripheral artery diseases was also assessed.

Overall, these investigations have enabled a better understanding of the disease mechanism and may have significant therapeutic application.

LITERATURE REVIEW

1. Atherosclerosis and vascular calcification

Atherosclerosis is a major cause of cardiovascular morbidity globally[42,43]. The disease is characterized by inflammatory lesions of the vasculature resulting in the narrowing of vessel walls[43]. It involves a defective lipid metabolism which leads to the formation of a fatty streak lesion characterised by the presence of macrophages in the endothelium followed by accumulation of lipids, fibrosis and finally thrombosis[42-44].

There is considerable scientific evidence suggesting that these atherosclerotic lesions frequently become calcified[11,14]. This calcification process can begin early and can accelerate as the disease progresses which results in complicated lesion progresssion[17,38]. Since calcification is a surrogate measure of coronary atherosclerosis, clinical interest has now focused on the usefulness of non-invasive detection of calcium as a measure of coronary risk[38,45] with reports of high histological correlation between total atherosclerotic plaque burden and the extent of coronary calcium deposition[38,46].

Atherosclerotic calcification has been suggested to be an active process[38,46]. To date, several groups have isolated subpopulations of VSMC that undergo osteoblastic differentiation *in vitro*[47-51]. Calcification is also thought to be the result of accumulation of necrotic foam cells which could serve as a source for vessel mineralization[29,52-54]. The necrotic cells release high concentrations of mitochondrial phosphate and display crystal-nucleating molecules[54,55] thus, creating a perfect microenvironment within an atherosclerotic lesion for calcification to take place[14,15,17].

In spite of vascular calcification being positively associated with atherosclerosis it has been reported that the two diseases could be studied separately[1,3,56]. Mouse genomic studies have suggested that atherosclerosis and vascular calcification are separate genetic entities[6,7,38]. Firstly, the analysis of a genetic cross between several inbred and genetically engineered mouse strains showed that there is no co-segregation of aortic calcification and atherosclerotic lesion development[57-59]. Secondly, in mouse models of atherosclerosis, mice lacking apolipoprotein E (ApoE) or low-density lipoprotein receptor (LDLR), calcification of atherosclerotic lesions is a rare and secondary event[57,60]. Finally, engineered mouse strains such as $OPG^{-/-}$ mice[58] and matrix gla protein ($MGP^{-/-}$)[59] have been reported to develop vascular calcification in the absence of atherosclerosis[61,62]. This evidence supports an independent study of vascular calcification and the various mechanisms involved.

1.1. Clinical Background

1.1.1 Prevalence

Cardiovascular diseases contribute to a major morbidity and mortality rate in the world[63]. In 2004-05, the prevalence of cardiovascular disease was reported highest in North-West Europe (29%) followed by the United Kingdom and Southern Eastern Europe (both at 28%), North Africa and the Middle East (19%), Australia (17%) and South East Asia (15%)[63]. In Australia also, the incidences of these conditions are increasing at alarming rates[5]. Despite steady improvement in medical research over the last three decades, cardiovascular disease remains one of the biggest causes of death in Australia[5]. In 2004-05, 18% (approximately 3.5 million) of Australians reported having a long-term cardiovascular condition out of which a significant proportion was diagnosed for atherosclerosis and vascular calcification. Out of all the patients who report vascular conditions, 28% of them suffer from angina, 27 % are reported with artery diseases and 20% for other ischaemic heart disease[5].

The prevalence of cardiovascular disease increases with age[2,63,64]. In 2003-04, of those aged 35 to 44 years, 13% reported a long term cardiovascular condition[63]. This increased to 23% for those aged 45 to 54 years and 63% for 75 years and over[5]. The proportion of males reporting cardiovascular disease was higher than for females in all age group (Figure 1.1).[5,64-66]

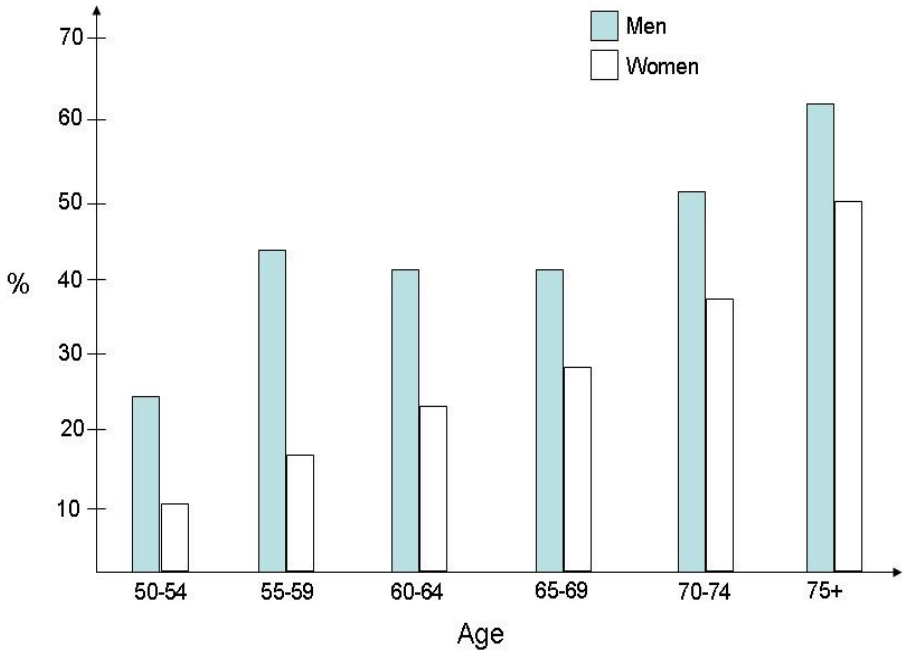

Figure 1.1. Prevalence of vascular calcification in males and females with age progression. (Figure adapted from Cannata *et al*, 2006)

The reports suggested that males were more susceptible than females to ischaemic heart diseases (30% compared to 18%) and diseases of the arteries, arterioles and capillaries (17% compared to 10% respectively)[5]. 65% of the males who were aged 75 and above were reported to develop vascular calcification compared with 50 % women[5,63,66,67].

1.1.2. Risk factors

Some of the major risk factors which contribute towards vascular calcification are smoking, hypertension, high blood cholesterol, inadequate physical activity, overweight and obesity, poor nutrition and diabetes[63,66-68] (Table 1.1).

Table1.1. Risk factors for vascular calcification

Non modifiable risk factors Older age, male gender, race, diabetes Modified risk factors Hypertension, smoking, high LDL cholesterol, low HDL cholesterol, serum phosphorous and serum calcium, calcium-phosphorous product, high dosage vitamin D metabolites

1.1.2.1. Smoking

Tobacco smoking increases the risk of coronary heart disease and peripheral artery disease[69,70,71,72]. Cigarette smoking leads to a reported seven-fold increase in the risk of peripheral artery disease[73,74,75]. Dyslipidemia is another important risk factor for peripheral artery disease[73,76].

1.1.2.2. Diabetes Mellitus

People suffering from type I diabetes are prone to develop disease that affects small arteries whereas those with type II diabetes are prone to atherosclerosis in larger arteries such as the aorta[64,65]. The affected people also tend to develop atherosclerosis at an earlier age than do people who do not have diabetes[65,77]. The risk of developing atherosclerosis is reported to be 2 to 6 times higher for people with diabetes[65,78].

1.1.2.3. Obesity

Obesity levels also increases the risk of coronary artery disease including atherosclerosis[74,79]. It also multiplies the onset of other risk factors for atherosclerosis such as high blood pressure, type II diabetes, and high cholesterol levels[73,79].

1.1.2.4. Physical inactivity

Physical dormancy over a longer span of time contributes passively to increase the risk of developing coronary artery disease. Reports suggest that regular exercise even to a moderate degree reduces this risk and decreases mortality[66,73].

1.1.2.5. Alcohol

Excessive consumption is a major risk factor[66,67,80] and if coupled with smoking, poor diet and physical inactivity it can lead to cardiovascular complications[80].

1.1.2.6. Hyperhomocysteinemia

People having very high blood levels of homocysteine, an amino acid, usually because of a hereditary disorder, have an increased risk of coronary artery disease, which may occur at a young age[63,81]. High levels of homocysteine may directly injure the lining of arteries, instigating the formation of calcified plaques[11].

1.2. Vascular calcification

1.2.1. Association with atherosclerosis

There is considerable scientific evidence suggesting that atherosclerotic lesions frequently become calcified[11,14]. The calcification process can begin early and can accelerate as the disease progresses resulting in complicated lesion progresssion[17,38].

1.2.2. Pathogenesis

The pathogenesis of vascular calcification is similar to that of atherosclerosis in many ways.[1,43]. As most of the calcified areas are found around the plaque regions it is considered that the onset of both diseases is similar[3,17,38,82]. As reported with atherosclerosis, endothelial cells and VSMC have been reported to contribute towards calcification[14,15].

Under the influence of the major risk factors, lesion formation occurs under an intact but dysfunctional endothelium[42]. Consequently the endothelial cells reduce in numbers and de-endothelialized areas appear over advanced lesions[42,83]. Depending on the size and area of the lesions, plasma molecules and lipoprotein particles pass through this dysfunctional endothelium into the sub endothelial space, where atherogenic lipoproteins are retained and later become cytotoxic and proatherogenic[42,43]. The dysfunctional endothelium is activated by proinflammatory stimuli, and the expression of adhesion molecules, such as vascular cell adhesion molecule-1 (VCAM-1) are elevated resulting in monocyte and T cell recruitment[83,84]. In addition to VCAM-1, other adhesion molecules such as intercellular adhesion molecule-1 (ICAM-1), E selectin, and P selectin, may contribute to the recruitment of blood-borne cells to the atherosclerotic lesion[83-85].

Circulating monocytes, lymphocytes and activated mast cells contribute to the formation of calcified plaques[15,86,87]. However, the mere adhesion of these blood cells to the endothelium is not enough for lesion formation[88]. An endothelial migration is required to initiate the process and for this migration to happen, one or more chemokines are necessary[88,89]. In calcified plaques, chemokines, also termed chemo attractants are found to facilitate this migration[90,91]. The levels of these chemokines are found to be elevated in and around the calcified lesions suggesting a possible role for them in atherosclerosis and calcification[39].

Apart from the endothelial cells and leukocytes, VSMC also contribute to the calcified lesions within the vasculature[42]. These VSMC are the principal connective tissue producing cell in the normal and diseased atherosclerotic intima (Figure 1.2)[45,92]. The impaired functions of these cells may result in plaque rupture[42,45].

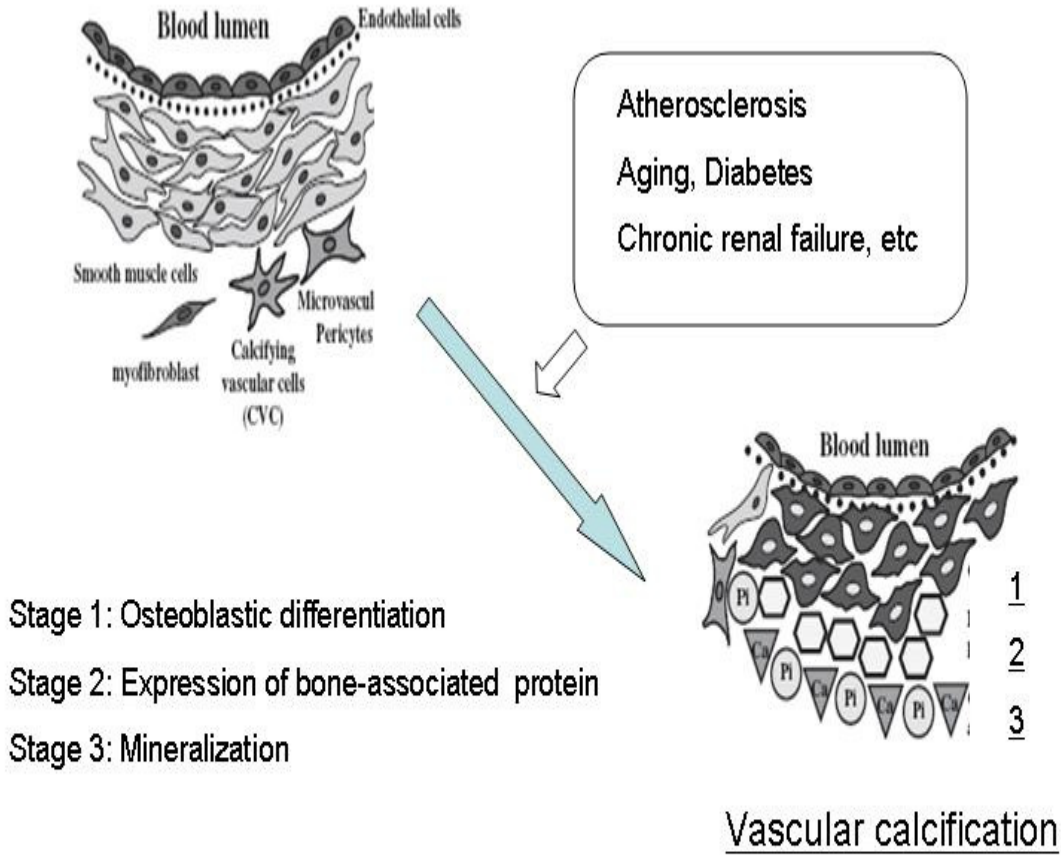

Figure 1.2. Risk factors leading to the disease progression. (Figure adapted from Jono *et al*, 2006)

Calcification in the vessel wall reportedly occurs in two sites; the intima and the media[2]. Medial calcification is a result of the inflammation of the atherosclerotic plaque and its presence is associated with atherosclerotic burden[10,87,93]. It is localized in two functionally major arteries, such as the aorta and the coronaries[94]. Medial calcification occurs in the elastic lamina of large and medium size arteries[10,15]. The complications of intimal and medial vascular calcifications are different[1,38] (Table 1.2). Intimal calcification is mainly associated with occlusion of the vessels, while the latter is associated with vascular stiffness[95,96].

Table 1.2. Characteristics of intimal vs. medial calcification

	Intimal calcification	Medial calcification
Morphology	Patchy scattered deposits	Continuous linear deposits
Histological association	Inflammatory cells lipids Vascular smooth muscle cells	Vascular smooth muscle cells Elastin
Disease association	Atherosclerosis	Diabetes Chronic renal failure Monckeberg's sclerosis

The mechanism of vascular calcification is complex[1,52]. It does not consist of a simple precipitation of calcium and phosphate as earlier thought[52]. It is instead an active and modifiable process involving VSMC apoptosis and vesicle formation. These apoptotic changes of VSMC leads to osteoblast-like cells within the vessel wall thus, inducing matrix formation and attraction of local factors involved in the mineralization process[1,52,93,97].

Vascular calcification consists primarily of noncrystalline calcium phosphate and apatite, with apatite being the predominant crystalline form in vessels[9]. Although commonly referred to as hydroxyapatite, the apatite is actually an carbonate apatite, $(Ca_{10}(PO_4)_6(OH)_2$[9,54,98]. This apatite forms a good indicator for understanding the process of calcification[98]. Calcium hypophosphate ($CaHPO_4 \cdot 2H_2O$) is formed in a reversible reaction with a solubility product above the product of free Ca_2 and H_2PO_4 as illustrated in Figure 1.3[9,98,99]. The $CaHPO_4 \cdot 2H_2O$ gradually transforms into apatite, which is insoluble under physiologic conditions (Figure 1.4)[98]. *In vivo*, this latter reaction is prevented by two reported inhibitors of calcification, pyrophosphate (PPi) and MGP[100,101].

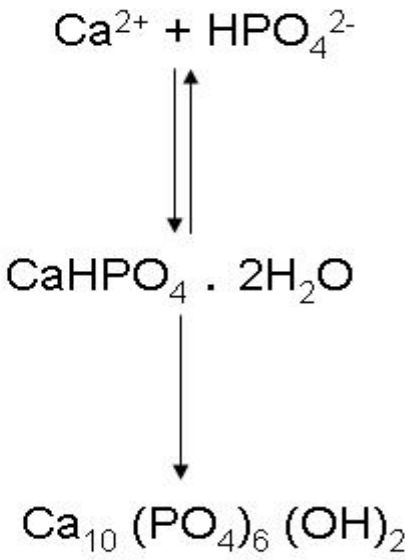

Figure 1.3. Formation of apatite in vasculature: A two-step process beginning with formation of amorphous calcium phosphate followed by spontaneous conversion to apatite. (Figure adapted from O'Neil *et al*, 2007)

1.2.3. Molecular determinants

There are several molecules which have been associated with the process of vascular calcification, many of which have been extensively investigated in animal and patients studies[1-3,102]. Table 1.3 below describes a list of molecular proteins that may play a role in determining vascular calcification.

Table 1.3. Molecular determinants for vascular calcification and modes of action

Protein	Function
Collagen type I	May act as nucleator
Elastin	May act as nucleator
Bone sialoprotein	May act as nucleator
Osteopontin	Adhesion molecules binding cells to apatite and inhibiting crystal growth by binding to crystal surfaces
Osteoprotegerin	Osteoclastogenesis inhibitory factor Inhibitor of vascular calcification, knock out mouse has medial calcification
Matrix Gla protein	Found in association with areas of calcification Gla residues inhibitor of vascular calcification, knock out mouse has medial calcification capable of binding to apatite
Osteonectin	High affinity for apatite and collagen
Osteocalcin	Gla residues capable of binding the hydroxyapatite
Klotho	Inhibitor of vascular calcification, knock out mouse has medial calcification

1.2.3.1. Matrix Gla Protein

MGP was originally isolated from bones but has since been reported to be expressed in several tissues including kidney, lung, heart, cartilage and VSMC from the vessel walls[103,104]. The only reported function of Gla residues is to bind calcium ions or calcium crystals[105,106,107]. MGP protects against calcification by complexing of calcium within tissues to inhibitors of calcification such as MGP[3,8,107].

The function of MGP as an inhibitor of calcification was demonstrated in a MGP knockout rats[108]. These rats were normal at birth but developed calcification of elastic arteries, which ruptured causing premature death within a few weeks[108]. It was reported that the calcification of arteries resulted from the replacement of the medial VSMC by chondrocyte-

like cells which was accompanied by deposition of a calcified matrix[59,108]. More recently, it was also demonstrated that restoration of MGP expression in MGP null mice, specifically in the vasculature, prevented arterial calcification[59,61].

Studies in MGP null mice demonstrated that the production of MGP, specifically induced in VSMC, is essential in preventing vascular calcification[59]. Expression of MGP in the liver of these mice and its subsequent release into the circulation failed to have effects on rescuing the vascular calcification phenotype[59]. These observations demonstrate that either circulating MGP was not taken up by artery wall cells or that the process of MGP entering through the circulation makes the protein inactive, possibly via binding other serum components[59,103,108]. Alternatively, MGP activity may possibly depend on the interaction with a matrix component upon release from VSMC[109]. Further MGP has been detected intracellularly in chondrocytes *in vivo* and also in VSMC induced to over express MGP in human VSMC[103,109].

1.2.3.2. Osteoprotegerin

The recent discovery of OPG, a member of the tumor necrosis factor (TNF) receptor super family, introduced a new link between bone and vascular metabolism[110,111]. OPG is an indirect inhibitor of osteoclastogenesis[111,112]. It functions as a soluble decoy receptor which binds and inhibits receptor activator of nuclear kappa ligand (RANKL). The activation of its receptor, RANK by RANKL is essential for maturation of osteoclast precursors[112,113].

Recently, evidences have demonstrated a positive correlation between endogenous serum OPG levels and the severity of coronary artery disease, stroke and the progression of atherosclerosis[110,114-117]. Reports also suggest that circulating OPG levels are associated with the extent of vascular calcification[99,118]. Since OPG is a known inhibitor of bone resorption, it is possible that altered mineral metabolism can result in reducing the extent of atherosclerotic calcification[57,112]. An increase in the circulating calcium-phosphate product has been associated with ectopic mineralization and OPG treatment has been shown to block this process[110,118]. An $OPG^{-/-}$ mouse model have also been demonstrated to develop vascular calcification[58]. These will be discussed in greater detail later in this Chapter (section 1.3.2).

1.2.3.3. Osteopontin

OPN is an phosphorylated glycoprotein which was first reported in bone and is thought to be involved in the regulation of biomineralization by promoting osteoclast function[119,100,120].

Although OPN is not found in most normal soft tissues, it is reported to be abundant at sites of ectopic calcification in human atherosclerotic lesions[121]. In calcified arteries OPN is highly localized to the surfaces of calcified deposits[27,29,47]. Along with histological studies, it has also been reported that OPN inhibits calcium deposition in calcifying VSMC *in vitro* which suggests a regulatory role for OPN in vascular calcification[28,47].

1.2.3.4. Alkaline phosphatase

ALP is an essential component of matrix vesicles where it increases the phosphates levels resulting in the growth of hydroxyapatite crystal[100,122]. The essential role of ALP in bone formation is demonstrated by the disease hypophosphatasia, characterized by lack of functional ALP and defective bone mineralization[9,34]. ALP is also reported to be present in systemic arteries, arterioles, and some capillaries and is considered to play a role in arterial calcification by the same mechanism as reported in bone[8,34,123].

1.2.4. Clinical factors

Many clinical factors influence vessel mineralization[1,12]. Since vascular calcification can include osteogenesis, effects on bone and vessel mineralization has to be taken into account while considering treatment that affects mineralization[1,2].

1.2.4.1. Osteoporosis

Osteoporosis is a condition involving excessive demineralization of bone, which begins after a certain age[113,124,125]. Causes of osteoporosis include a decrease in osteoblast function, a change in parathyroid activity as a compensatory factor for decreased calcium absorption, decreased ability to synthesize vitamin D, or insufficient dietary intake of vitamin D[113,126,127]. Patients with osteoporosis have been observed to frequently display vascular

diseases including atherosclerosis and calcification[34,128]. Osteoporosis, like atherosclerosis, is positively associated with aging, diabetes, smoking, inactivity, and elevated cholesterol levels[125,129]. Osteoporosis and atherosclerosis tend to occur in the same patients and correlate in severity[125].

Vascular calcification also has been reported to co-exist with bone loss in numerous epidemiological studies, suggesting a relationship with osteoporosis[34,37,124]. A transfer in bone growth, from the skeleton to the vasculature has been proposed to explain the association of bone loss and vascular calcification[37,130]. There have been previous studies in which $OPG^{-/-}$ mouse groups have been shown to develop severe osteoporosis and medial vascular calcification suggesting a clinical link between bone modelling and calcification[58,61].

Recently, sophisticated imaging techniques that combine non-invasive evaluation with high resolution electron-beam computed tomography, multi-detector computed tomography (CT) and ultrafast spiral CT have been developed which allows detailed assessment of coronary artery disease and arterial calcification *in vivo*[63,129,131].

1.2.4.2 Diabetes

Diabetes mellitus is reported to be one of the more common diseases in the world, found in as many as 6.2% of the population of the world[77]. Its prevalence is on the rise owing to an increasingly obese and aging population[77]. Interestingly, 80 % of patients with diabetes mellitus are reported to die from complications related to coronary and peripheral artery diseases[64,77,78]. Diabetes mellitus also has been positively correlated with renal disease, and is the leading cause of disease ESRD[20,132].

Diabetes is also clinically associated with vascular calcification[16,64]. The presence of detectable arterial calcification is a strong marker of future cardiovascular events in diabetic patients[65,117]. At the cellular level, advanced glycation end products associated with diabetes are known to promote mineralization in cultures of micro vascular pericytes[78,132]. Previous studies have demonstrated that in genetically modified mice, inducing type II diabetes activates expression of developmental osteogenic transcription factors and proteins within vasculature[67,117].

1.3. Mouse models of aortic calcification

Mouse knockout models have demonstrated roles for number of proteins in regulating vascular calcification[61,97]. Studies have focused attention on proteins involved in the regulation of both calcification and bone mineralization suggesting that the process of calcification and bone mineralisation may, in some way, be pathologically linked[1,34,97,124]. These genetic approaches were applied in distinct combinations in order to explore the hierarchy of factors such as calcium, phosphate and calcification inhibitors in their involvement in the regulation of the disease[3,26]. There are several such models which have been investigated in the past including $MGP^{-/-}$ mice, $OPG^{-/-}$, $OPN^{-/-}$, $Ldr^{-/-}$ and $ApoE^{-/-}$ models[61]. Out of these models, $MGP^{-/-}$ and $OPG^{-/-}$ were widely studied for investigating the mechanism involved in the pathogenesis of the calcification[58,59,61].

1.3.1. Matrix Gla protein knockout model

MGP is found in the matrix of cartilage as well as VSMC of the artery wall[61]. It is a key physiological inhibitor of soft-tissue calcification that acts as a direct inhibitor of calcium crystal formation[99,103,133].

This mouse model suggests that MGP has an important role in preventing vascular calcification. Since MGP has Gla residues, it has been thought that MGP binds to hydroxyapatite, producing a protein layer that inhibits mineralization[103,134]. Mice lacking matrix Gla protein have extensive calcification of the aorta, its branches, and all elastic and muscular arteries including the coronary arteries[50,59]. These mice die at about 2 months from rupture of a brittle and calcified aorta[59]. Histological examination of these calcified aorta demonstrated that calcification occurred exclusively in the media and therefore it shares similarities with Monckeberg's sclerosis, suggesting an evident role of MGP in medial calcification[59,108]. Since these knockout mice do not develop atherosclerosis, it is not known if the absence of MGP will affect atherosclerotic intimal calcification[59]. However, it is been thought that MGP acts to liberated calcium from the vessel wall and that the high levels of MGP demonstrated in human atherosclerotic lesions are due to MGP binding to calcified within the lesion[59,103,134].

1.3.2. Osteoprotegerin knockout model- old model

It has been demonstrated that OPG is a physiological regulator of normal bone mass and its targeted deletion in mice results in severe, early-onset osteoporosis[112,135,136]. Depletion of OPG also results in calcification of the aorta and renal arteries which are sites of endogenous OPG expression in normal animals[56,112]. These findings suggest that OPG does play an important role in regulating physiological bone formation in the postnatal mice and suggest an additional role for OPG in regulating pathological calcification of arteries[61,135].

OPG is a molecule secreted from osteoblasts which functions as a decoy receptor for RANK-L[126,137]. As discussed in section 1.2.3.2, the RANK-L/RANK/OPG system is critically involved in the regulation of bone metabolism and structure[137]. $OPG^{-/-}$ mice display medial calcification of their large arteries and are reported to die prematurely[58,115]. The decrease in $OPG^{-/-}$ mouse movement is positively associated with an increase in the incidence of vertebral bone fractures[58,61]. A decrease in bone mineral density was evident by radiography at one month of age in $OPG^{-/-}$ mice[58]. Changes in the mineral density were more pronounced by four months of age as it becomes more severe with age[1,58].

Histological analysis reported that calcification occurred primarily in the aorta and renal arteries[61]. Like $MGP^{-/-}$ mice, dystrophic calcification was not observed in smaller arteries, capillaries or veins, suggesting that these vessels express additional unknown inhibitors of calcification[56,99]. The calcified arteries, determined by histology, in $OPG^{-/-}$ vasculature are also sites of endogenous OPG expression, thus suggesting a specific role for OPG in protecting these arteries from calcification[58,113]. Calcification is mainly evident in the media and is associated with mild to moderate intimal and medial proliferation in 3 to 6 month-old $OPG^{-/-}$ mice[58]. Endogenous OPG expression is localized within the medial smooth muscle layer of the aortic and renal arteries, suggesting a role for OPG in maintaining normal structure in vasculature[58,137].

1.3.3. Limitations of the current mouse models

Although $MGP^{-/-}$, $OPG^{-/-}$, $OPN^{-/-}$, $ApoE^{-/-}$ and $LDLR^{-/-}$ models have been extensively investigated to understand vascular calcification *in vivo*, there remains a few limitations in these existing models[1,61]. The distribution of calcification in vasculature varies considerably in all the models[1,58]. The extent of vascular calcification is also observed to be from mild to moderate degrees in all the reported knockout models[28,59,103]. Calcification in the $OPG^{-/-}$ knockout mouse is more limited and is extremely localized[61,138]. The $MGP^{-/-}$ model has reported calcification of smaller coronary arteries, while the remaining models involve primarily the aorta[50,103]. Along with this, in $ApoE^{-/-}$ and $LDLR^{-/-}$ models dyslipidemia is an integral feature making it difficult to separate effects due to calcification and those due to abnormalities of circulation lipoproteins.

Also, in vasculature, the function of OPG is unknown because it is unclear whether vascular calcification takes place in $OPG^{-/-}$ mice or not[138]. Mouse groups in this model system along with $MGP^{-/-}$ mice have a life span of 8-12 months which makes the vascular calcification study too long[58]. Hence a suitable and feasible method had to be designed to quickly induce calcification in the vasculature to understand the process and mechanisms better and quicker[138].

1.3.4. Modified calcitriol induced osteoprotegerin knockout model

1.3.4.1. Need for a modified model system

As the limitations of the existing mouse models became more evident, the development of suitable modifications was required[138]. Also, the extent of calcification had to be more consistently distributed throughout the vasculature unlike the previous models where calcification was localised[61]. The degree of calcification also needed to be considered while designing and adopting any modified model as the previous murine models demonstrated only low to moderate degrees of calcification[61,138]. A severe degree of calcification within the vasculature was essential in understanding the mechanism convincingly[138]. The modified mouse model eliminates some, if not all, of the limitations which were evident in previous models [58,138].

1.3.4.2 Calcitriol induced calcification & mode of action

Calcitriol or 1-, 25-dihydroxyvitamin D3 was recently introduced into the study of vascular calcification. Also referred to as bioactive Vitamin D, calcitriol is a steroid hormone known for its important role in regulating body levels of calcium and phosphorus, and in mineralization of bone[54,139].

Calcitriol is reported to generate in animal skin when light energy is absorbed by a precursor molecule 7-dehydrocholesterol[138]. Vitamin D is metabolized within the body to the hormonally-active form known as 1, 25-dihydroxycholecalciferol[138,140]. This is known to occur in two ways: in the liver where cholecalciferol is hydroxylated to 25-hydroxycholecalciferol by the enzyme 25-hydroxylase[139,141] and within the kidneys where 25-hydroxycholecalciferol serves as a substrate for 1-alpha-hydroxylase, yielding 1, 25-dihydroxycholecalciferol[54,139]. The active form of calcitriol bind to intracellular receptors which functions as transcription factors to modulate gene expression[54]. In most cases studied, the effect is to activate transcription, but situations are also known in which calcitriol suppresses transcription[142].

Calcitriol is known to be involved in mineral metabolism and bone growth[138]. It facilitates intestinal absorption of calcium and also stimulates the expression of a number of proteins involved in transporting calcium from the lumen of the intestine into blood[28,141]. In other words, calcitriol is designed to increase the amount of circulating calcium in the

bloodstream. Also, as a transcriptional regulator of bone matrix proteins, it induces the expression of OCN and suppresses synthesis of type I collagen.[30,143]. More recently, a modified mouse model receiving doses of calcitriol was also designed to address the shortcomings of the existing knock out models of vascular calcification[138].

A sub-cutaneous injection of calcitriol at a controlled dosage induced rapid calcification in vasculature of $OPG^{-/-}$ mice. The administration of calcitriol (5 μg/kg for 3 days) also resulted in significant calcification in the arterial wall of $OPG^{-/-}$[138]. The bone morphology in these $OPG^{-/-}$ mice showed an osteoporotic phenotype including increased porous area and decreased bone volume[138]. Histological examinations confirmed that in $OPG^{-/-}$ mice receiving calcitriol, calcification was detected at a considerably high level [138]. In addition, the serum ALP and serum calcium levels were significantly elevated in $OPG^{-/-}$ injected with calcitriol when compared to those without calcitriol[138].

Increased calcium deposition was reported in the medial aortic layer in $OPG^{-/-}$ mice receiving calcitriol treatment. However the calcified area was confined to the media of arterial wall. Electron microscopic analysis also suggested a needle-like calcium matrix in the cytoplasm of VSMC and calcium deposits around VSMC was seen in $OPG^{-/-}$ mice given a high phosphate diet and calcitriol treatment[138].

1.4. Human investigation for vascular calcification

Human research investigations have also been undertaken to understand vascular calcification mechanism[1,2]. Research studies have demonstrated the role of various proteins and cytokines which are involved in the pathogenesis of the disease[4,8,144]. Cellular approaches in human studies have also been implemented to determine the role of various cell types associated with disease[145]. One of the most robust and reproducible ways of studying calcifying vasculature is protein expression research analysis, performed at serum and plasma levels in patients diagnosed with peripheral artery diseases[99,107,146,147]. *In vitro* studies have also been undertaken to monitor the effect of various cytokines and inflammatory factors in differentiation of vascular cells into osteogenic lineage[49,55,148].

Serum expression studies involving OPG, OPN, ALP bone markers and other inflammatory makers have been widely investigated in humans[57,100,144].

1.4.1. Serum osteoprotegerin association with calcification

Vascular calcification is reported to be influenced by several inhibitory molecular proteins. Among these, OPG is considered to be a primary inhibitor directly associated with the advent of disease[116,144,149,150]. OPG inhibits the differentiation of macrophages into osteoclast and also regulates the resorption of bone *in vitro* and *in vivo* as previously discussed[33,49,151,152]. Recently OPG has also been shown to be associated in human atherosclerosis and vascular calcification[57,144,150]. A high serum OPG level is reportedly associated with severe coronary atherosclerosis and overall vascular mortality[150]. Additionally, increased OPG levels were recently reported to be associated with cardiovascular mortality in patients suffering from diabetes[114,153,154].

Patients diagnosed with chronic kidney diseases were also found to have elevated serum OPG levels which were statistically significant to the aortic calcification levels[155] (Figure 1.4).

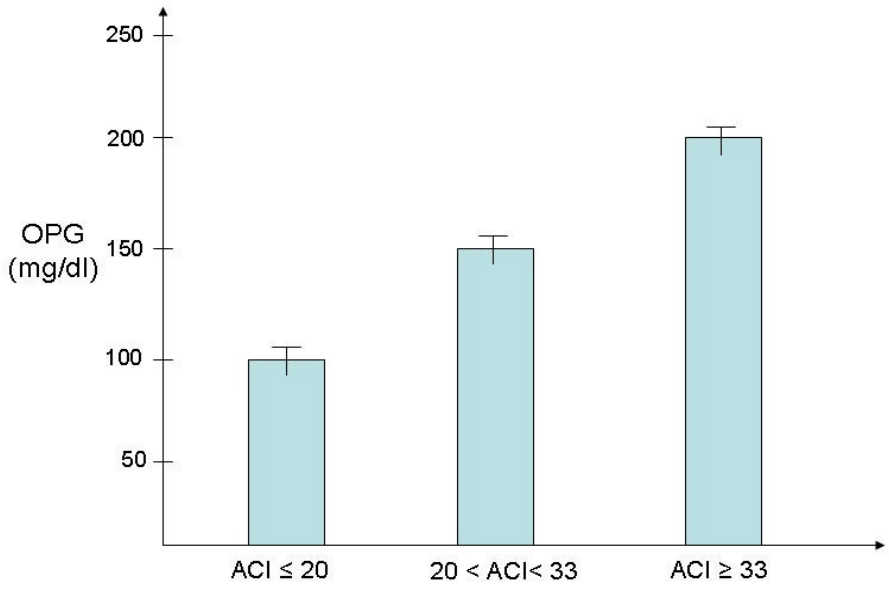

Figure 1.4. Elevated serum OPG levels in cardiovascular patients undergoing haemodialysis. (ACI: aortic calcification index, Figure adapted from Nishiura *et al*, 2007)

An inverse correlation was also observed between the serum levels of OPG and OCN, which is a crucial osteoblastic lineage marker for mineralisation[144]. These results suggest that the OPG may be an independent and important predictor of vascular calcification which can be robustly studied in human patient cohorts[155].

1.4.2. *In vitro* calcification studies of human vascular cells

Along with the serum protein studies, *in vitro* cell culture work with human vascular smooth muscle cells (hVSMC) have yielded significant results which are equally robust and reproducible[146]. The *in vitro* culture work involves studying the contribution of vascular cells towards the mineralisation process of the vasculature[156]. *In vitro* culture work provides a flexible platform to analyse and clarify the effect of different proteins and other inflammatory cytokines on vascular cells [18,49]. Vascular cells derived from other clinical complications such as diabetes and kidney disease have also been studied in association with mineralisation in vasculature[99,148].

These hVSMC have been consistently seen to undergo calcification *in vitro* under the action of calcification inducing factors such as β-glycerophosphate[145,157] and dexamethasone[158,159]. Similar experiments have suggested a role of calcifying vascular cells

(CVC) of human origin to undergo *in vitro* calcification at a quicker rate, suggesting an osteogenic lineage for smooth muscles cells and CVC in atherosclerotic plaques[31,160].

OPG levels were observed to decrease in cell culture studies of calcifying SMC[49]. When calcium levels were raised in the culture medium, there was a significantly decreased level of secreted OPG, suggesting its association with calcification[49,149]. Similar experiments have been performed to analyse any effect of insulin on VSMC[49]. Along with insulin and β-glycerophosphate, the roles of inflammatory cytokines such as TNF- α, interleukin (IL)-1β, and IL-6 in *invitro* calcification has been widely investigated [11,41,161]. Human osteoblastic cells have been cultured with these cytokines and ALP activity and deposited calcium was measured in these cells[110,162]. When tested at different concentrations, these cytokines resulted in significant decreases in ALP levels while the deposition of calcium within the cell layer decreased in cells treated with TNF-α and IL-1β[41,163] suggesting that these cytokines are capable of influencing osteoclast activity within vasculature.

1.5. Mechanism of vascular calcification: existing concepts

For the past century, vascular calcification was considered to be a passive process which leads to uncontrolled precipitation of calcium phosphate associated with tissue necrosis and metabolic calcium and phosphate imbalance[1,3].

1.5.1. Existing concepts

To understand the mechanism, four different and non-mutually exclusive theories of vascular calcification had been previously reported[1,4,33]. These theories are illustrated in Figure 1.5.

a) Loss of inhibition; b) Induction of bone formation; c) Circulation nucleational complex; d) Cell death

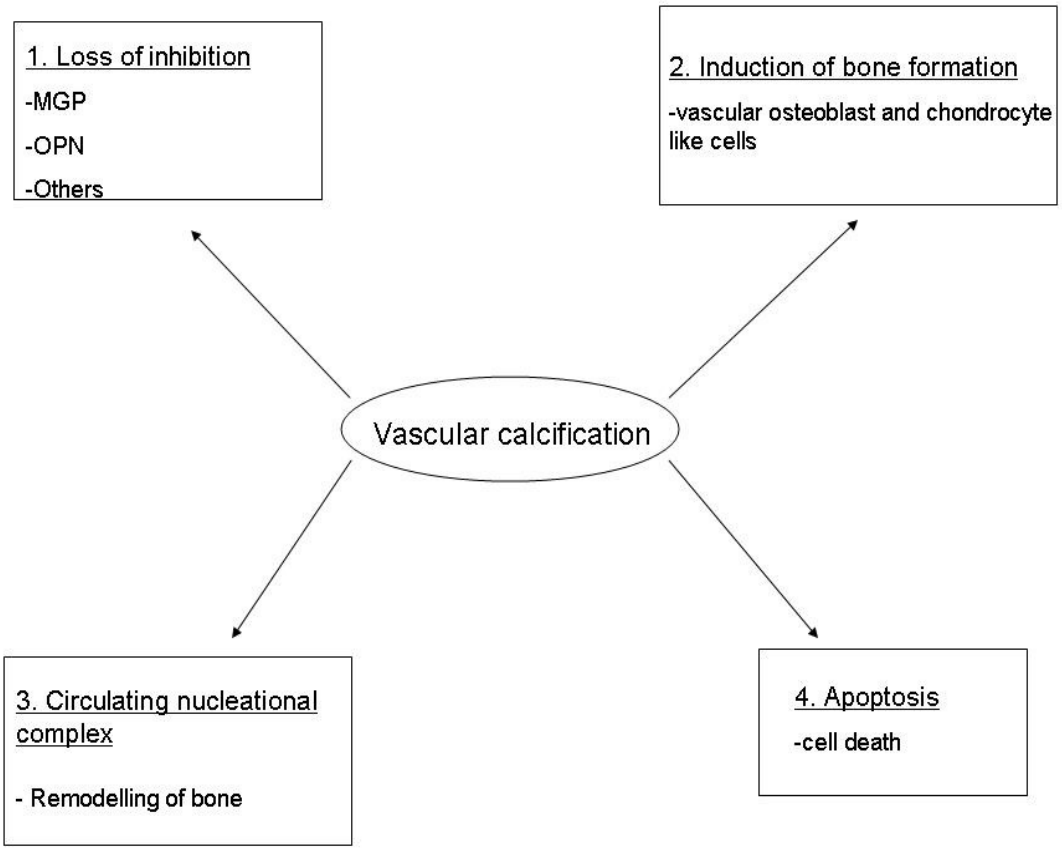

Figure 1.5. Schematic illustration summarizing four current theories illustrating molecular mechanisms of vascular calcification. (Figure adapted from Giachelli *et al*, 2004)

1.5.1.1. Loss of Inhibition

It is increasingly becoming clear that most body fluids and organs contain inhibitors of calcium and phosphate deposition. These theories explain why spontaneous mineralization does not occur even though body fluids contain calcium and phosphate[50,56,100]. A growing number of such molecules have been identified using mouse mutational analyses and are listed in Table 1.4.

Table 1.4. Vascular calcification phenotypes in mouse strains

Gene	Mouse mutant	Phenotype
MGP	$MGP^{-/-}$	Vascular, valve and cartilage calcification
OPN	$OPN^{-/-}$	Enhanced calcification of subcutaneously implanted valve; increased medial calcification in $MGP^{-/-}$ background.
OPG	$OPG^{-/-}$	Osteoporosis, vascular calcification
β Glucosidase	$Kloth^{-/-}$	Vascular calcification, aging

Genes such as MGP, OPG and OPN have been widely studied in mouse models[3,7,56,61] (Table 1.4). As mentioned earlier in section 1.2.3, mouse knockout models of these proteins result in osteoporosis and varied degree of mineralisation at different areas in the vasculature confirming the inhibitory roles of these genes in calcification[61]. It was observed that MGP was found to inhibit BMP-2 activity which inhibits osteogenic differentiation[31]. Similarly OPN and OPG have also been reported as primary osteogenic inhibitor, the absence of which leads to osteoporosis and mineralisation of aorta[48,100,120]. These studies showed that OPN and OPG act as an inducible inhibitor in an adaptive response of vascular injury by inhibiting crystal growth[135,136].

1.5.1.2. Induction of bone formation

As mentioned previously, ectopic bone, in addition to matrix mineralization, is often found in calcified arteries[3,52]. This theory suggests that vascular calcification represents a similar process as bone formation[125,130,164]. Literature suggests that CVC has a role in vasculature and that this subpopulation of vascular medial cells spontaneously formed nodules that mineralized *in vitro*[31]. In contrast to CVC, heterogeneous uncloned populations of SMC do not spontaneously mineralize in culture but can be induced to mineralize by elevating phosphate levels in the medium[31,98]. Furthermore, elevated phosphate levels induced

VSMC to undergo a phenotypic transition characterized by loss of VSMC lineage and gain osteogenic markers such as OPN, ALP and OCN[24,26,100].

Using an *in vivo* gene delivery model groups have also provided evidence in support of the transdifferentiation of VSMC[156,165]. The existing data support the presence of a pluripotent population within the artery wall which is capable of osteogenic differentiation that might be involved in vascular calcification under pathological conditions[41,52,125].

1.5.1.3. Circulating nucleational complexes

A growing number of studies have associated bone remodelling, specifically osteoclastic resorptive activity, with vascular calcification[3,126,136]. These findings suggest that vascular calcification is linked to osteoclastic resorption[113]. It is reported that soft tissue calcification is promoted by crystal nuclei generated at sites of bone resorption that facilitate through circulating blood and lodge in soft tissue, thereby inducing tissue mineralization[113,126]. These studies have observed that calcium and phosphate mineral complexes are released from bone which can be detected in blood. The release of these complex can be inhibited by osteoclastic inhibition[26,98,103]. This theory seems logical given the link between osteoporosis and cardiovascular calcification[17,34,124,125].

1.5.1.4. Apoptosis

Apoptosis or programmed cell death has long been regarded as a major mechanism for vascular calcification, especially in the case of dystrophic calcification as seen in atherosclerotic lesions where large areas of necrosis are typically observed[2,85,97]. Matrix vesicles, the known nucleation sites for calcium phosphate crystal formation in cartilage and bone, were observed in calcifying vascular lesions which were thought to be derived from dying VSMC[6,87,166]. Associative *in vitro* VSMC studies between cell death and calcification suggest that apoptosis occurs before the onset of calcification of VSMC and stimulation of apoptosis results in SMC calcification[148,156]. Apoptotic bodies derived from VSMC cultures were also observed to accumulate calcium[24]. Similar to matrix vesicles, the calcium concentrated inside the apoptotic bodies were found to be in a crystallized state[38,61,85] (Figure 1.6). These observations provide evidence that apoptotic bodies derived

from cultured VSMC can act as initiating and nucleating sites for calcium phosphate deposition[24].

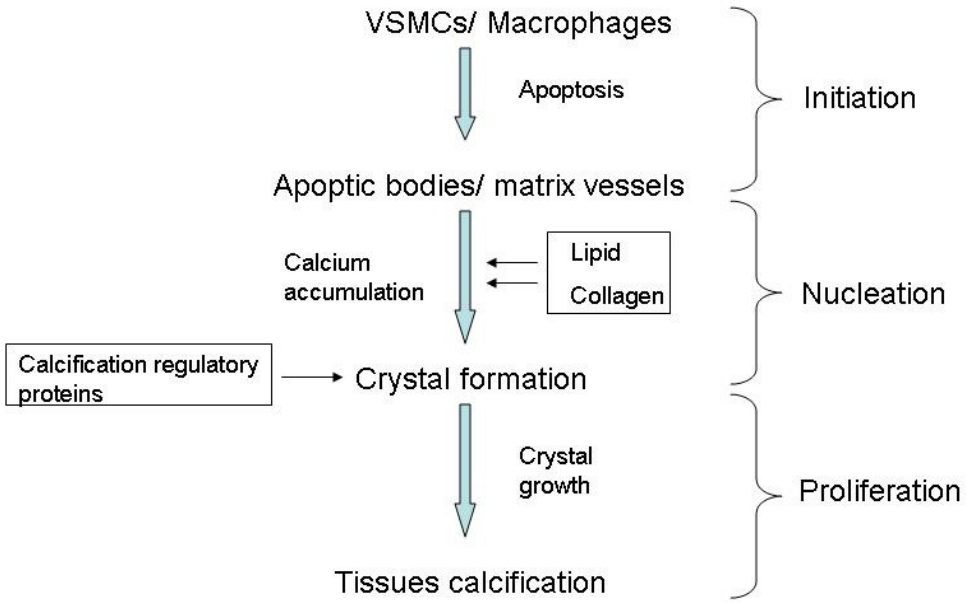

Figure 1.6. Tissue calcification initiated by apoptosis and cell nucleation complex. (Figure adapted from Abedin *et al,* 2004)

1.5.2. Circulating cells and calcification: A novel concept

Amidst the above mentioned theories, stem cell and circulating progenitor biology is evolving as one of the most promising fields under current investigation, with huge potential in the field of regeneration medicine[167,168]. Reports in the past decade have hypothesised a role for circulating immature cells derived from sources like the BM and the spleen in the contribution of vascular diseases including atherosclerosis and vascular calcification[168-171].

1.5.2.1. Background theory

According to previous active cell theories, VSMC migrate from the media to the sub endothelial space, where they proliferate and contribute towards atherogenesis[42,168]. However, there are several observations that challenge this model of VSMC migration from the media to the intimal lesion[168]. Researchers have documented VSMC migration across the internal elastic lamina from the tunica media into the sub endothelial layer[167,168]. On the other hand studies have demonstrated that blood cells attach to the lumina of the injured artery prior to the development of neointimal hyperplasia[172]. The neointima has been observed to form rapidly in the absence of medial cells, which can be killed by severe injury[172,173]. Neointimal VSMC has also been reported to express a number of hematopoietic lineage markers and proinflammatory proteins[174,175]. Collectively, these findings suggest that some of the neointimal VSMC, if not all, may be derived from circulatory blood cells rather than medial cells[44,175]. These investigations suggested that there is more to atherosclerosis and vascular calcification disease progression than migration of VSMC from media to intima[42,175-177]. These findings lead to a new theory in which immature cells from various sources were thought to be released into the blood circulation, which then home to the vascular lesions[40,168,169,177,178]. Under ideal proliferation conditions these cells differentiate into various cell lineages, one of which could potentially be an osteogenic lineage[179].

1.5.2.2. Association with vascular diseases

Immature progenitors such as endothelial progenitor cells (EPC) are reported to instigate new vessel formation *via* angiogenesis and neovascularisation[180,181]. However these cells also have the potential to provide ongoing endothelial repair by homing to sites of endothelial damage[181]. These cells in peripheral circulation may play a crucial contribution towards vascular diseases[90,177].

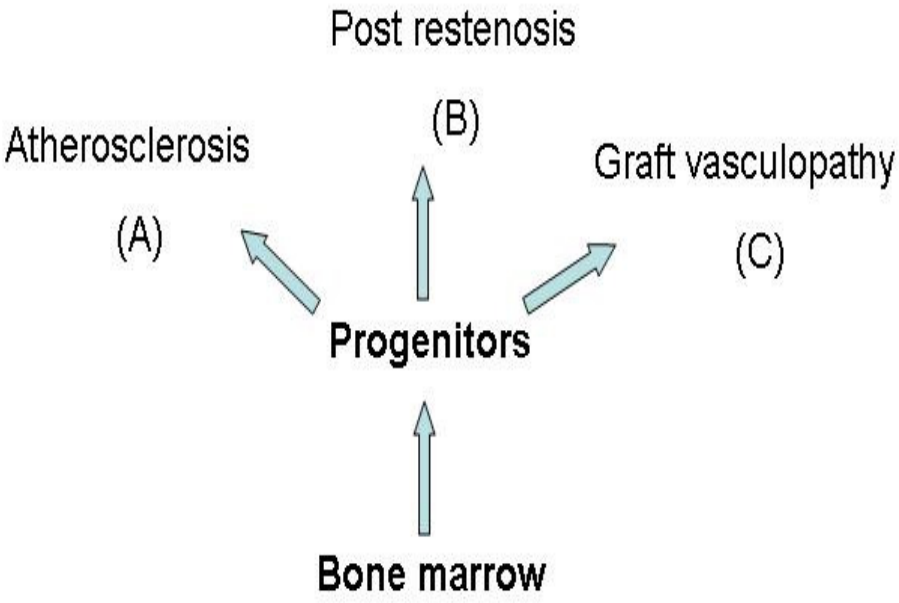

Figure 1.7. Contribution of BM- derived vascular progenitors towards vascular diseases. A) BM-derived cells detected in atherosclerotic plaques which lead to mineralisation. B) Contribution of BM cells to lesion formation after mechanical injury. C) BM-derived neointimal cells in transplant-associated arteriosclerosis. (Figure adapted from Sata *et al*, 2005)

As illustrated in Figure 1.7, the immature cells are thought to be released from the BM into the peripheral circulation[39,182,183]and home to atherosclerotic plaque region under the influence of chemo attractants[91,184,185]. This is further followed by proliferation and differentiation of these cells within vessel walls[186-188]. Histological examination of aortic sections in animal studies has confirmed the role of immature progenitors in contributing towards complications in vasculature[167,189]. *In vitro* studies also complement the animal studies providing further support for the circulating cell concept[30,190].

1.5.2.3. Evidence supporting circulating theory

1.5.2.3. a. Bone marrow transplant studies

The contribution of BM cells towards vascular lesions was first investigated in graft vasculopathy, a form of atherosclerosis which progressively develops in transplanted organs[171,191]. To identify the potential source of recipient cells that contribute to allograft vasculopathy, BM transplantation (BMT) was performed from LacZ mice to wild-type

mice (BMT LacZ-wild mice)[179,192]. After eight weeks, wild-type hearts were transplanted into the BMT LacZ-wild mice. Four weeks after cardiac transplantation, most of the neointimal cells were LacZ positive[193,194]. Similarly, when wild-type hearts were transplanted into wild-type mice whose BM had been reconstituted with that of transgenic mice that express green fluorescent protein (GFP); the GFP-positive cells then accumulated on the luminal side of the graft coronary arteries[191,192] hence indicating that recipient BM cells can substantially contribute to neointimal formation in transplanted grafts[191].

1.5.2.3. b. Histological studies

Animal studies which involve direct transplantation of unselected marrow cells into the acutely infarcted myocardium have been reported to cause significant intramyocardial calcification[194]. In this experiment, rats received standard intramyocardial injections of either DiI-labeled total BM cells or the same number of DiI-labeled, clonally expanded BM-derived multipotent stem cells[194]. The rats were euthanized for histological examinations after 2 weeks. Spotty calcified lesions in these infracted areas were reported[194].

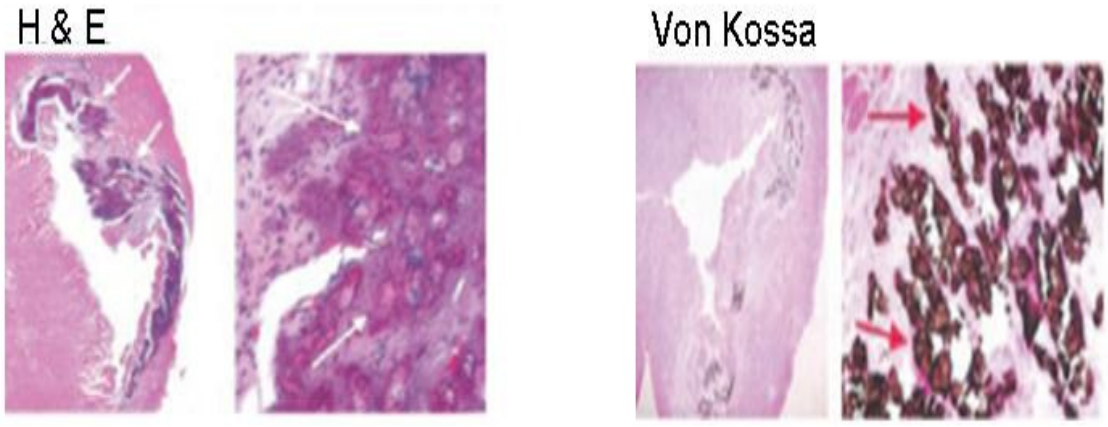

Figure 1.8. Examination with haematoxylin and eosin (H & E) staining to identify calcified lesions. (Figure downloaded from Yoon *et al*, 2004)

Haematoxylin and eosin staining demonstrated deep blue to purple regions of stained area suggesting the presence of calcium particles spread within regions of fibrosis (Figure 1.8). Further analysis was performed by von kossa staining by which black metallic deposits of calcification were noted[194].

ALP staining also demonstrated strong staining surrounding the calcified area suggesting the possibility of osteogenic activity. 4', 6-diamidino-2-phenylindole (DAPI) staining on the frozen sections, which preserved the red fluorescence of the transplanted DiI-labeled BM cells, revealed that DAPI-negative calcified areas were surrounded by DiI-labeled BM cells. These observations suggest the involvement of transplanted BM cells in calcification[194]. These results demonstrate that transplantation of BM cells into the acutely infracted myocardium may cause significant intramyocardial calcification[179].

1.5.3. Sources of circulating cells

The circulating immature cells are known to originate primarily from human BM and hence they are also termed marrow cells or stromal cells[39,40]. BM is considered to be a huge reservoir for such immature potential cells[39,188]. Apart from the BM pool, the spleen is thought to be another less significant potential source of these cells [167].

1.5.3.1. Bone marrow: reservoir for immature cells

BM is a special, spongy tissue that acts as a reservoir for immature stem cells, and is located inside a few large bones (Figure 1.9)[182]. In adults, marrow in large bones produces new blood cells and constitutes to 4% of overall body weight[183,188,189].

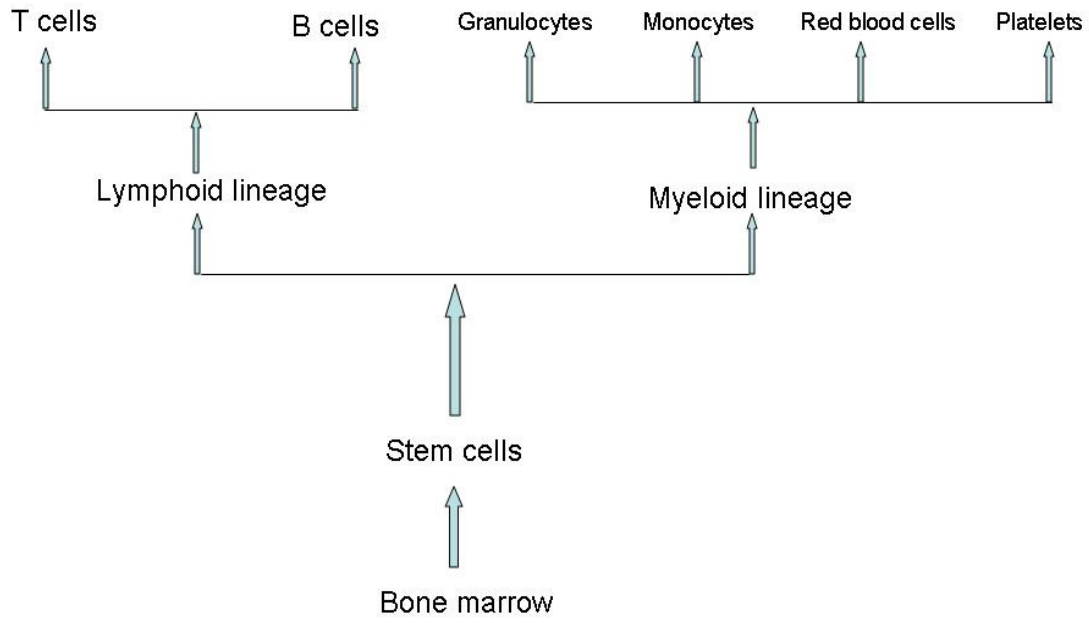

Figure 1.9. Bone marrow cells differentiating into various cell types. (Adapted from Stem cells and the future of regenerative medicine, 2004)

The BM stroma constitutes of fibroblasts, macrophages, adipocytes, osteoblasts and blood vessels[195,196,197,198]. It also contains mesenchymal stem cells (MSC) which are multipotent cells are able to differentiate into a variety of cell types[195]. These MSC have been shown to differentiate into osteoblasts, chondrocytes, myocytes, adipocytes and β-pancreatic islets cells[195,199,200]. They can also trans-differentiate into neuronal cells[195]. The blood vessels constitute a barrier, inhibiting immature blood cells from leaving the BM[199]. Only mature blood cells contain the membrane proteins required to attach to and pass the blood vessel endothelium[199].These immature cells are released from the BM stroma and enter peripheral circulation in response to any endothelial damage caused by the various risk factors[39]. These cells are known to contribute towards the repair process within the vasculature. However their impact on the contribution towards vascular diseases including calcification is not specifically known and demands in-depth research[167].

1.5.3.2. Spleen

Research shows that splenic cells also contribute to the pool of immature cells in a small, yet significant way[201]. Recent research on splenic cells suggests that the spleen may be a potential source of adult stem cells that could contribute to the regeneration of many cell

types including insulin producing islets of pancreas[187]. The finding supports the existence of these splenic stem cells and also suggests they may be able to produce an even greater variety of tissues and contribute towards different types of damage healing in tissues[187]. Researchers also noted that the spleen develops from embryonic tissue that is known not only to generate precursors to many types of blood cells, a function shared by the BM, but potentially to form such diverse organs as the small intestine, uterus, vascular system and lung[202,203]. These cells are also thought to also produce bone cells which can be linked with osteoblastic lineage and vasculature[202].

1.6. Bone marrow and calcification: A cellular approach

16.1. Bone marrow

BM is a major resource for immature progenitor cells. These cells are categorized into different lineages based on the characteristics and the potential of the immature cells[39].

1.6.1.1. Stem cells and progenitors

Stem cells are known to have two important characteristics that separate them from other types of cells[90,177,204] (Table 1.5). Firstly, they are unspecialized cells which renew themselves for long periods through cell division[177,205]. Secondly, under experimental conditions, these cells can be induced to become cells with specific functions[177,183]. To date, scientists have identified two kinds of stem cells from human and animal origins; adult stem cells and embryonic stem cells each of which have different functions and characteristics[195,206]. Progenitor cells, like stem cells, have only been researched in the last decade and understanding of their role is evolving. Progenitor cells have a capacity to differentiate into a specific type of cell (Figure 1.10)[167]. They are far more specific than stem cells. Most progenitors are reported to be of unipotent or multipotent lineages[205] (Table 1.5). From this point of view, they may be compared to adult stem cells. But progenitors are said to be in a further stage of cell differentiation. They are in the intermediate stage between stem cells and fully differentiated cell[182].

Table 1.5. Characteristics of stem cells and progenitor cells

	Stem cell	Progenitor cell
Self renewal *in vivo*	Unlimited	Limited
Self Renewal *in vitro*	Unlimited	Limited
Potentiality	Multipotent	Unipotent
Maintenance of self renewal	Yes	No
Population	Reaches maximum amount of cells before differentiating	Does not reach maximum population

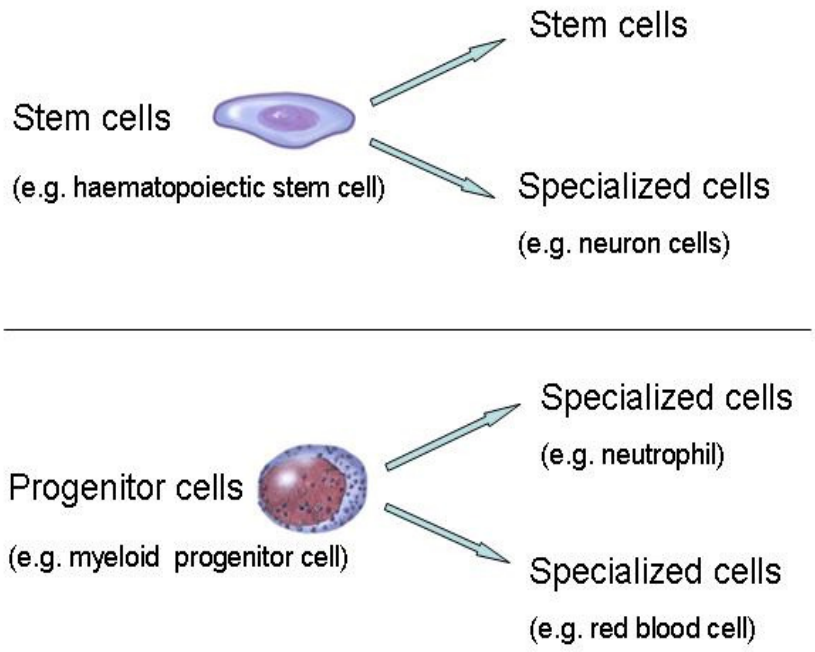

Figure 1.10. Multiplication characteristics of a stem cell and a progenitor cell

The majority of progenitor cell populations remain dormant and possess little activity in the tissue in which they reside[167]. They exhibit slow growth and their main role is to replace damaged and dysfunctional cells[176]. Not all progenitors are mobile and are situated near the tissue of their target differentiation. When the cytokines, growth factors and other cell division enhancing stimulators influence the progenitors, a higher rate of cell division is introduced which leads to the recovery of the damaged tissues[90,169,171].

1.6.1.2. Progenitor stem cells: classification and types

On the basis of their renewal capacity and characteristics, these immature cells are broadly classified into pluripotent, multipotent and unipotent cell types[202,207]. The cells are further categorized on their differentiating properties into three types namely MSC[195,208], hematopoietic stem cells (HSC)[202,209] and embryonic cells[210].

1.6.1.2. a. Mesenchymal Stem Cells (MSC)

MSC are multipotent stem cells that can differentiate into a variety of cell types. MSC have been shown to differentiate into different cell types *in vitro* or *in vivo*. These cell types include osteoblasts, chondrocytes, myocytes, adipocytes, and, as described lately, beta-pancreatic islets cells[195,199,211] (Figure 1.11)

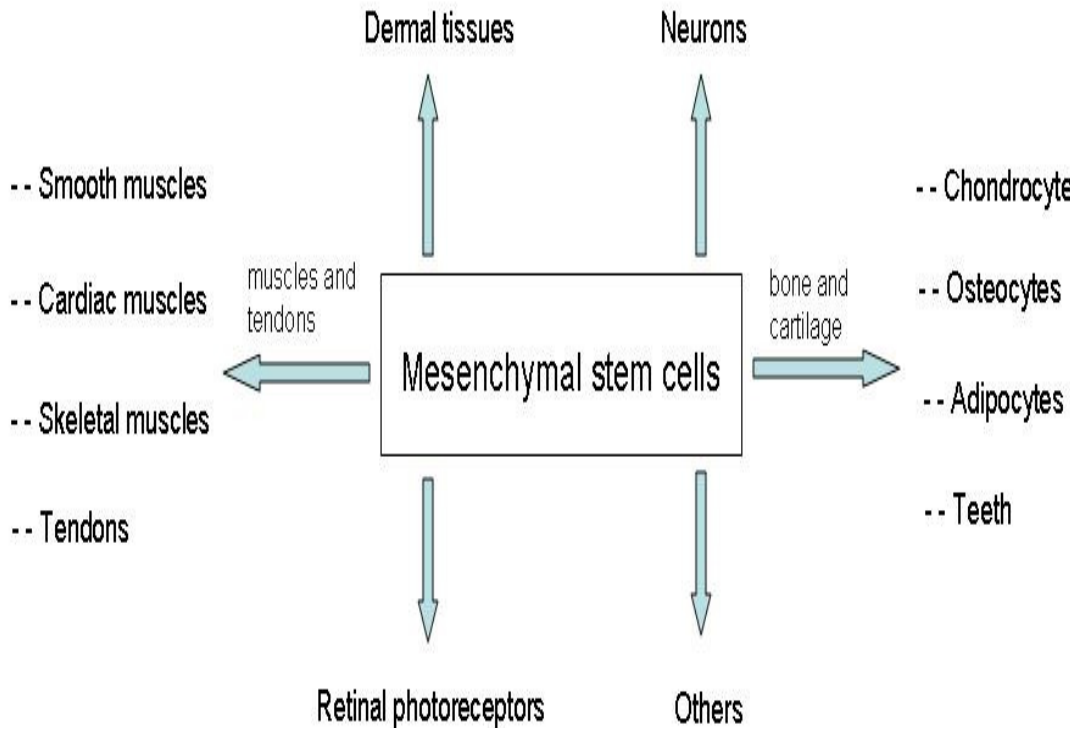

Figure 1.11. Multipotency characteristics of MSC. (Figure adapted from Song *et al* 2004)

Their ability to differentiate into an osteogenic lineage makes it an interesting area of research in the field of vascular calcification[30,212-214].

1.6.1.2. b. Hematopoietic stem cells

HSC are stem cells that give rise to all the blood cell types including myeloid (monocytes, macrophages, neutrophils, basophils, eosinophils, erythrocytes, dendritic cells), and lymphoid lineages[174,188,202].

The hematopoietic tissue contains cells with long-term and short-term regeneration capacities and committed multipotent, oligopotent, and unipotent progenitors[209,215]. As stem cells, they are defined by their ability to form multiple cell types and their ability to self-renew[216]. Morphogically, they are non-adherent, rounded and with a rounded nucleus and low cytoplasm content [216].

1.6.1.2. c. Endothelial progenitor cells (EPC)

EPC are derived from the BM which circulate in the blood and possess the ability to differentiate into endothelial cells that make up the lining of blood vessels. EPC found in adults are thus related to angioblasts, which are the stem cells that form blood vessels during embryogenesis[90,177].

1.6.2. Mesenchymal cells and osteoblastic lineage

Human mesenchymal stem cells (hMSC) are multipotent, capable of differentiating into at least three lineages which are osteogenic, chondrogenic, and adipogenic[199,200,213] (Figure 1.12). This lineage development occurs by a process called transdifferentiation whereby a cell type committed to and progressing along a specific developmental lineage switches into another cell type of a different lineage through genetic reprogramming[199,211].

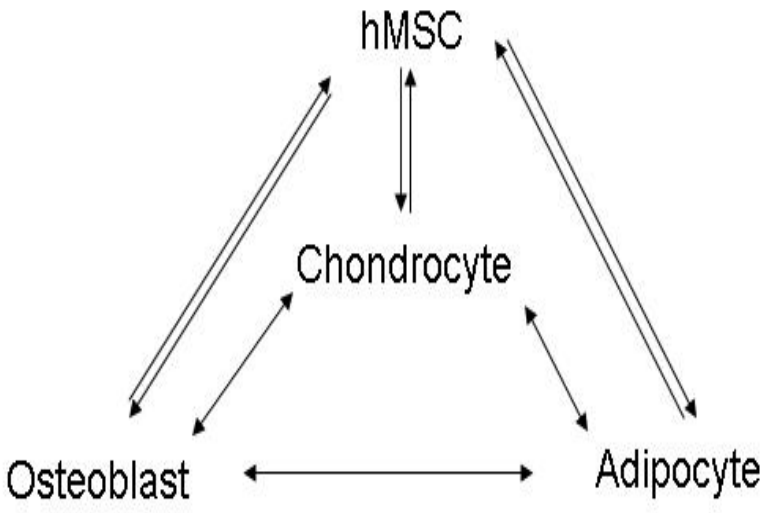

Figure1.12. A transdifferentiation model of hMSC demonstrating osteoblasts, adipocytes, and chondrocytes differentiated from hMSC. (Figure adapted from Song *et al*, 2004)

Osteogenic differentiation of MSC is characterized by three distinct phases; cell proliferation, secretion of extracellular matrix and mineralization of extracellular matrix resulting in mature osteoblasts[30,214]. It has been demonstrated that as osteogenic differentiation progresses the multiple differentiation potentials of mesenchymal cells become more limited, such that terminally committed osteoblasts are unable to differentiate into other cell types[200,217]. The fully differentiated osteoblasts derived from the BM cells have been identified by expression of ALP, bone sialoprotein, OCN, and the elaboration of calcified extracellular matrix[200,203,212].

In vitro studies have characterized the osteogenic potential of hMSC[200]. When cultured in the presence of osteogenic factors hMSC differentiate into an osteogenic lineage, producing bone-like nodules with a mineralized extracellular matrix containing hydroxyapatite. Similar results have also been reported using BM-derived cells[199].

These findings suggest the importance of cell transdifferentiation in the development and maintenance of mammalian tissues and regulation of lineage commitment[195,207]. The *in vitro* differentiation system allows an identification of molecular regulators, such as cell cycle proteins, transcription factors, or other signalling molecules, that control cross-lineage commitment among different cell type[208]. An identification and understanding of the contribution of these cells towards vasculature is an interesting field of study[41]. Considering

the previous and ongoing vascular biology work it may be worth investigating the role of these BM-derived MSC with osteogenic lineage, or osteo-progenitors, towards vascular calcification[41,207].

1.6.3. Osteoblastic progenitor population: contribution towards calcification

On-going vascular research investigations suggest that the immature progenitor BM cells may significantly contribute towards vascular diseases including atherosclerosis and vascular calcification[39,167,207,214].

1.6.3.1. Immature progenitors: from bone marrow to blood circulation

Recruitment of the immature cells to the blood under the influence of cytokines is a process termed as mobilization[183]. This process involves enhancement of the physiological release of stem cells and progenitors from the BM reservoir in response to stress signals during injury and inflammation[39]. The emerging picture of stem cell mobilization involves an interaction between MSC and HSC which regulates both bone and BM remodelling processes, which also mediate progenitor cell proliferation and migration[183,188].

The stem cell mobilization process is initiated by stimulation of marrow cells with cytokines such as granulocyte colony-stimulating factor (G-CSF), resulting in the release of membrane-bound SCF, proliferation of progenitor cells, as well as activation or degradation of adhesion molecules[174,183,218]. Cytokines involved with the increased release of these cells are G-CSF, granulocyte-macrophage colony-stimulating factor (GM-CSF) and SCF[41,147,186]. Chemokines such as SDF-1α and IL-8 are also associated with the mobilisation process[219,220]. These molecules differ in their mode of administration, the time frame required to achieve mobilization, the lineage of cells mobilized, and their efficiency[41,183].

1.6.3.2. Homing and proliferation

Homing is the process in which circulating cells actively cross the BM endothelium barrier and lodge transiently in the BM compartment by activation of adhesion interactions prior to their proliferation[84]. Progenitor cells also home to other organs especially in response to stress signals, transmitted in response to alarm situations such as total body irradiation and can migrate to the spleen prior to bone marrow homing[187,190].

The endothelium is the first anchoring site for homing cells. This endothelium layers are know to express adhesion molecules and stimulating chemokines[201]. Among these chemokines, SDF-1α signalling has been reported as an important factor involved with migration and mobilization of hematopoietic stem cells during vessel wall injury[187,190,221].

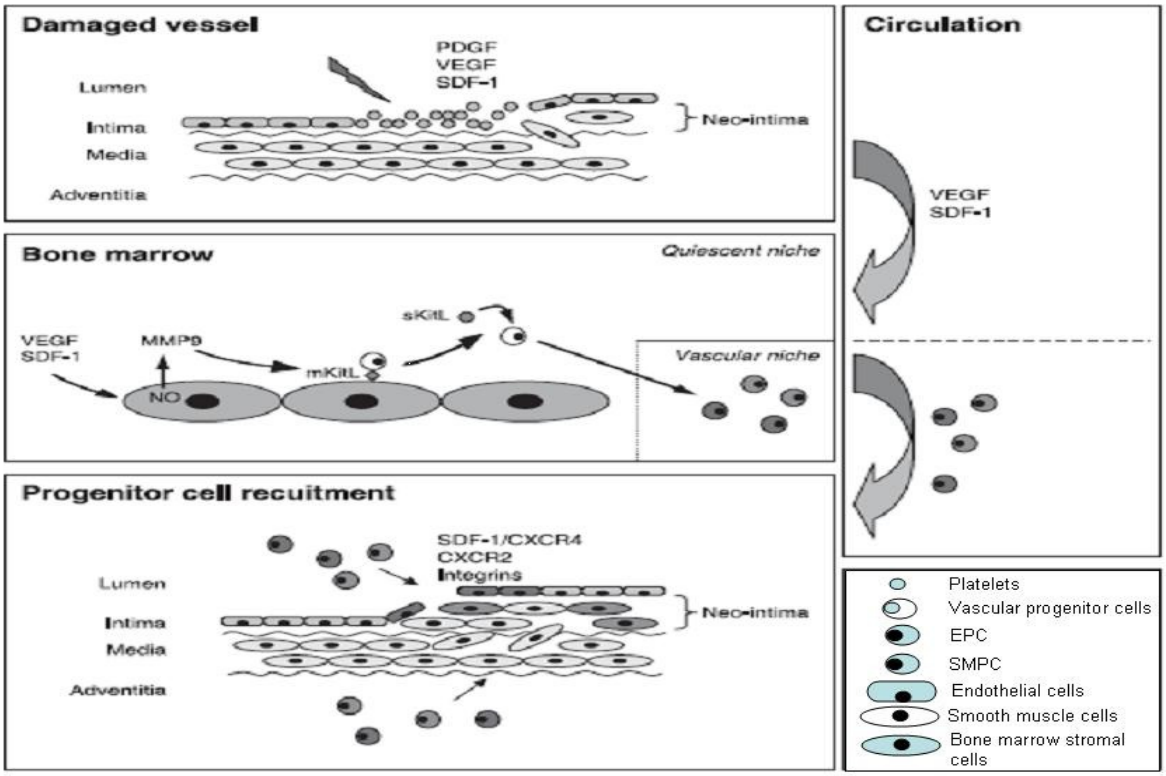

Figure 1.13. Mobilization, homing and recruitment of vascular progenitor cells. (Figure downloaded from Jevon *et al*, 2007)

Vascular damage involves an initial endothelial denudation and platelet accumulation. Platelets, along with neighbouring endothelial and VSMC, secrete growth factors and cytokines including PDGF, VEGF and SDF-1α[165,222]. Among these, PDGF is important for VSMC migration and proliferation[223] while VEGF and SDF-1α are crucial for the mobilization of vascular progenitor cells from the BM reservior[165,223]. Once mobilized,

these vascular progenitor cells are believed to migrate to the site of damage where adhesion chemokines mediate the integration of these cells within vasculature[185,220]. Soon after contact with these molecules the cells are activated causing adhesion to the endothelium through interactions with ICAM-1 or VCAM-1[84,224].

As soon as these immature cells integrate into the endothelial layer the process of proliferation and differentiation commences which contributes to vascular repair and lesion formation[169,225]. As mentioned previously VEGF is considered to be one of the key players in differentiation of the progenitor cells in the vasculature post homing[226]. More recently, factors other than VEGF have been reported to contribute towards the proliferative process[88,227]. G-CSF[228], TGF β[223], PDGF[223] and vascular endothelial cadherin[229] have also been reported to influence the immature cell differentiation into matured endothelial and SMC.

1.6.3.3. Impact and behaviour in a diseased artery

Endothelial cells help to maintain vessel homeostasis and it is believed that EPC have a role in maintaining the integrity of the endothelium[39,230]. EPC are associated with a reduced risk of mortality rate from cardiovascular causes, and it has been suggested that the number of circulating EPC may be a prognostic tool for determining the risk of cardiovascular events[72,177]. Vascular diseases including atherosclerosis, myocardial infarction and intimal hyperplasia have been positively related to the circulating progenitor numbers[72,167,177]. Under ideal vascular conditions, these cells proliferate into SMC which contribute towards vascular repair[39,90,169]. However more recently it was suggested that these cells contribute to vascular lesions resulting from cardiovascular events[169].

These recent vascular studies link these immature cells to osteo-progenitors, the cell type which is known to differentiate in an osteogenic lineage[28,158]. Under the influence of chemo attractants, growth factors and previously mentioned cytokines the progenitors slowly start proliferating towards a SMC and osteoblastic lineage which complicates the disease formation process[28,61,214].

In this investigation, this circulating osteo-progenitors hypothesis will be tested in two mouse models and a human patient cohort diagnosed with peripheral artery diseases. The next Chapter discusses the materials and methods involved in experimental investigations.

CHAPTER 2: GENERAL MATERIALS AND METHODS

2.1. Animal model study of aortic calcification

Vascular calcification was investigated in a mouse model to understand the underlying mechanism and its association with circulating BM-derived osteo-progenitors. Based on the previous studies two mouse models were used in these studies.

2.1.1. Experimental $OPG^{-/-}$ mice

An $OPG^{-/-}$ was considered suitable for the study. The criteria for selecting $OPG^{-/-}$ mice as an experimental model is discussed in Chapter 1 (section 1.3.2). Breeding pairs were originally obtained from Clea Laboratories, Japan. 12 month old male and female mice were selected for the studies. This age was chosen based on previous studies demonstrating vascular calcification is more marked in animals of this age group[1]. The OPG deficiency was originally generated on a C57/BL6 background[1].

2.1.2. Control $OPG^{+/+}$ mice

Male and female $OPG^{+/+}$ mice were selected as the control for all $OPG^{-/-}$ mouse model experiments. The control groups for both male and females were age matched with the experimental group to allow better comparison and interpretation of results. These mice were also obtained from Clea laboratories, Japan.

2.1.3. Calcitriol induced $OPG^{-/-}$ mice

Age matched 8 weeks old $OPG^{-/-}$ and $OPG^{+/+}$ mice were selected for the experiments involving calcitriol administration. 5µg/kg body weight calcitriol injections were administered subcutaneously for 3 consecutive days in both experimental and control mice at 14 weeks (98 days) of age. Mice were culled and aortas harvested at the end of the experiments to assess vascular calcification. A detailed experimental design including the timing of calcitriol administration and tail bleed analysis will be discussed in detail in Chapter 6 (section 6.3 and 6.4).

2.1.4. Ethics approval, animal house facility and breeding

Ethics approvals were obtained from James Cook University (JCU) animal ethics committee prior to commencement of experiments (refer Appendix 1, 2 and 3). During the course of the study all mice were housed in a purpose-built mouse facility at JCU, Townsville, Australia. Water and normal laboratory diet were available *ad libitum*.

2.2. Aortic calcification assessment within the mouse model

2.2.1 Alizarin red-staining

Alizarin red has been demonstrated to identify traces of free calcium in tissue sections[231-233]. 1% alizarin red solution was prepared by dissolving alizarin red sulphonate powder (Tech, QLD, Australia, colour index# 58005) in distilled water (Appendix 4). After mixing the pH was adjusted to 4.1-4.3 using 0.5% ammonium hydroxide. The solution was made freshly for each experiment. Standardisation of staining analysis is discussed in Chapter 3 (section 3.1.1).

2.2.1.1 Protocol

Whole harvested aortas were fixed in 10% formalin for 15 min followed by phosphate buffer saline (PBS) wash for 2 min (Appendix 4). Excess fatty residues were teased off from the outer regions of the aortas to reduce interference in the staining procedure. The tissue was split longitudinally and pinned out on cork prior to staining with 1% alizarin red for 2 hours on a shaker at room temperature (R.T). The tissues were passed through grades of paraformaldehyde (Australian chemical reagents, QLD, Australia) and glycerol (Ajax Fine Chem., Australia) (3:1, 1:1 & 1:3 respectively, Appendix 4). Paraformaldehyde removes excess stain from the tissue, to avoid calcium destaining incubation times did not exceed 2 min.

2.2.1.2 Standardisation of protocol

Since alizarin red whole tissue staining has not been previously described, the protocol was standardised before application in experiments. A detailed discussion of the standardisation can be found in Chapter 3 (section 3.1.1.2 & 3.1.1.3 respectively).

2.2.1.3 Assessing alizarin red-staining

Tissue calcium staining was observed on a dissecting microscope (Nikon, SMZ 800, Japan). Images of all the aortic segments (arch, thoracic arch, supra-renal and infra renal) were digitally photographed (Nikon Cool Pix 4500, Nikon Corporation, Japan) for later computer aided analysis of calcium staining percentage using scion software (Scion Corporation, 4.0.3, USA). The demarcations of the aortic segments are illustrated below in Figure 2.1. The photographic images from each aortic segment in both $OPG^{-/-}$ and $OPG^{+/+}$ mice were analysed. The peripheral area of the aortic segments was outlined using specific software tools and a total surface area was estimated (mm^2). In the next step stained areas within the tissue were selected and estimated (mm^2). The total percentage of calcium staining was estimated using the following calculation:

$$\frac{\text{Alizarin red staining area } (mm^2)}{\text{Total surface area of the aortic segment } (mm^2)} \times 100$$

The calcium staining percentages were compared between $OPG^{-/-}$ and $OPG^{+/+}$ mice and graphically represented.

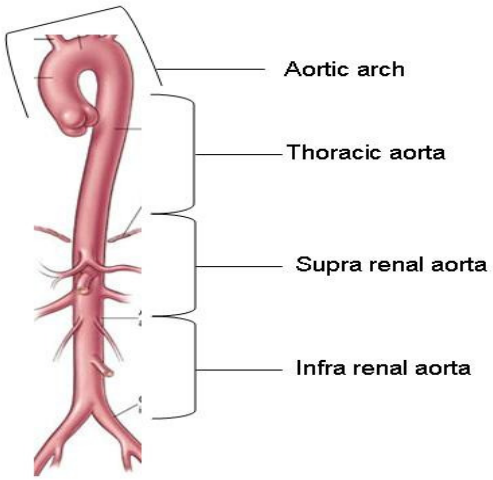

Figure 2.1. Segments of a murine aorta (Figure downloaded from cleavelandclinic.org)

2.3. Extraction of aortic calcium

Total extractable aortic calcium was estimated using a bioassay method involving extraction of calcium from the whole aorta followed by colorimetric estimation of free aortic calcium[234]. Harvested aortas were weighed, segmented and transferred into a 1.5 ml eppendorf tube containing 50 µl of 1N Hydrochloric acid (HCl). Using a drill and sterile plastic drill heads the aortic segments were fragmented and homogenised until the tissue reached near dissolution. An additional 50 µl HCl was mixed to facilitate optimum digestion. Tubes were cooled on ice during the process. The digested samples were incubated overnight on a shaker for maximum extraction of calcium. Samples were then centrifuged at 30,000 x g (18,000 rpm) for 30 min. The supernatant was collected in separate eppendorf tubes and stored and -20^{o}C. The pellets were discarded.

2.4. Quantification of aortic calcium

A Quantichrom^{TM} bioassay was used to estimate the extractable aortic calcium.

This assay is based on phenolsulphonepthalein dye which reacts with free calcium present in the tissue forming a stable blue coloured complex. The intensity of the colour is directly proportional to the calcium concentration and is measured at 595 nm.

A calcium bioassay standard was aliquoted and diluted according to the manufacturer's instructions as outlined below.

No	STD + substrate	Vol (µL)	Calcium (mg/dL)
1	100µL + 0µL	100	20
2	80µL + 20µL	100	16
3	60µL + 40µL	100	12
4	40µL + 60µL	100	8
5	30µL + 70µL	100	6
6	20µL + 80µL	100	4
7	10µL + 90µL	100	2
8	0µL + 100µL	100	0

The standards were stored at 4^{o}C for later use. Prior to commencing the assay all reagents and samples were equilibrated to R.T. A working solution consisting of equal parts of reagent A and reagent B (accompanied with the kit) was prepared. 5 µl of standard and sample solutions were transferred to a clear 96- well plate. Both the standards and samples were run in duplicates. Working solution (1000 µl) was added to each of the wells. The

plate was incubated for 4-5 min at R.T with intermittent mixing. Optical density was measured at 595 nm using a Tecan Plate reader (Qlab, Brisbane, Australia.). The colour formed was stable for 60 min.

Optical density (O.D) for the blank was subtracted from the standard O.D values and plotted against the calcium standard concentrations. The slope was determined using linear regression fitting. The total aortic calcium was calculated by subtracting the blank O.D from the sample O.D and then dividing by the slope as shown is equation 2.1 below. The intra and inter assay reproducibility is discussed in Chapter 3 (section 3.2.3.1 and 3.2.3.2 respectively).

$$\frac{OD_{SAMPLE} - OD_{BLANK}}{Slope} \quad (mg/dL)$$

Equation 2.1. Calculation for estimating aortic calcium (O.D-optical density; mg: milligram; dL: decilitre)

2.5. Protein cytokine studies using ELISA for mouse model studies

Protein cytokine studies were performed on serum samples collected from experimental and control mouse groups. The serum protein levels were statistically correlated to extractable aortic calcium levels to determine any association. Cytokines of interest, stromal cell derived factor (SDF-1 α) and granulocyte colony stimulating factor (G-GSF) were measured by an enzyme linked immunosorbent assay (ELISA). These cytokines were selected as they have been consistently reported to be associated with the release of immature cells from bone marrow into the circulation and to facilitate homing of these cells to vascular lesions[41,174,183,185].

2.5.1. Sample collection, preparation and storage

Tail bleeds were collected from mouse groups into lithium heparin tubes (Microvette, USA). 200 µl of blood was collected per bleed. Bloods were allowed to clot for 2 hours before centrifuging for 20 min at approximately 2000 x g. Serum samples were separated after centrifugation and assayed immediately or aliquoted into 1.5 ml eppendorf tubes and stored at -20^{o}C until required. Repeated thawing and freezing of samples was avoided.

2.5.2. ELISA protocol

Assays were carried out according to the manufacturer's instructions (R & D, Quantikine, USA). Prior to commencing the assay, all reagents and samples were equilibrated to R.T. Standards and serum samples were assayed in duplicates. 50 µl of assay diluent and 50 ul of standard, control or samples were added per well and mixed for 1 min. The plate was incubated for 2 hours at R.T (on a shaker for SDF-1α). Wells were aspirated and washed with ELISA wash buffer. Washings were repeated 4 times. After the final wash any traces of buffer were removed by aspirating or decanting. The plate was inverted and blotted against clean paper towels. 100 µl of conjugate was added to each well and incubated for 2 hours at R.T. Washings were repeated as done in previous step. 200 µl (per well) of substrate solution was added and incubated for 30 min. Colour development was halted by the addition of a stop solution (200 µl, accompanied with the kit) and gentle mixing. The O.D of each plate was determined immediately (signal stable for 30 min) at 570 nm on Tecan plate reader (Qlab, Brisbane, Australia.).

2.5.3. Calculation of standards and estimation of cytokines

Calculation for standards and samples were similar for both SDF-1α and G-CSF. The duplicate readings for standard, samples and control were averaged and subtracted from the averaged zero standards O.D. A standard curve was constructed by plotting the mean absorbance for each standard on the y-axis against concentration; a best fit curve through the points on the graph was drawn. The concentration determined from the standard curve was multiplied by the dilution factor where sample were dilutioned. The intra and inter-assay reproducibility is demonstrated in Chapter 3 (section 3.3.3 and 3.4.3 respectively).

2.6. Flow cytometry analysis

Flow cytometry (FC) (BD FACSCalibur, USA) was used to quantify the BM- derived osteo-progenitors in circulating blood in both mouse groups and patient cohort. Detailed investigation plan for mouse model and patient experiments will be discussed in experimental Chapters 4, 5, 6 and 7.

2.6.1. Collection of tail bleeds

Tail bleeds were collected from both $OPG^{-/-}$ and $OPG^{+/+}$ mice (lithium heparin, Microvette, USA). Where multiple bleeds were required, samples were taken at the same time of the day to minimise variation due to diurnal fluctuations. 150 to 200 µl of blood was collected per tail from all the experimental and control mice.

2.6.2. RBC cell lysis

Red blood cells (RBC) were lysed using ammonium chloride and potassium (ACK) lysis buffer (Appendix 4). Samples were incubated with 1 ml of lysis buffer for 15 min at R.T and centrifuged at 400 x g for 5 min at R.T. The supernatant was discarded and the cell pellet was washed with PBS containing 2 mM ethylene diamine tetra-acetic acid (EDTA). The sample was centrifuged and the supernatant was incubated again in lysis buffer for 10 min at R.T. After incubation the cells were washed and centrifuged as performed in the previous washing step. The supernatant was discarded and the final cell pellet was reconstituted in FC buffer (Appendix 4).

2.6.3. FcR Blocking

Mouse FcR blocking agent (BD biosciences, USA) was used to eliminate any non specific antigen- antibody binding. Samples were incubated with 50µl of FcR (1:50 in FC buffer) at R.T for 15 min. Incubation was followed by centrifugation at 400 x g for 5 min. The supernatant was discarded and the cell pellet reconstituted in 90 µl of FC buffer and transferred to ice.

2.6.4. Primary antibody labelling

The cell suspension was equally divided into two tubes. The cells in the one tube were used for primary OCN antibody labelling and those in the other were for isotype control. 5 µl of unconjugated goat anti-mouse OCN primary antibody (BT biomedical technologies, USA) or isotype control (BD biosciences, 1:100 in FC buffer) was added to the appropriate tubes. Cells were incubated for 30 min at $4^{o}C$.

2.6.5. Secondary antibody labelling

Cells were then washed in PBS buffer and centrifuged at 400 x g for 5 min. The cell pellets were labelled with a fluorescent anti-goat phycoerythrin (PE) secondary antibody (1:75 in FC buffer Jackson's Immunoresearch, USA). 50 µl of the titre antibody was added to both the OCN and isotype labelled cell pellets. Tubes were incubated for 30 min at 4^{o}C. The incubation was carried out in dark conditions to avoid degradation of fluorescent intensity of PE.

2.6.6. Flow cytometry analysis

The cells were washed and centrifuged at 400xg for 5 min. The pellet was reconstituted in FC buffer containing 3% fetal calf serum (FCS) and 0.05 % sodium azide (Appendix 4). The cells were immediately analysed on FC (BD FACSCalibur, USA) to quantify the OCN^{+} MNC population. A detailed FC protocol and technique optimisation is discussed in Chapter 3 (section 3.5 & 3.6).

2.7. Quantification of extractable aortic OCN^{+} population

Immune cells were extracted from aorta of 12 month old male experimental $OPG^{-/-}$ and control $OPG^{+/+}$ mouse group. OCN^{+} population from these extracted cells were further quantified using FC analysis.

2.7.1. Extraction of aortic immune cells by enzymatic digestion

The aortas were harvested from the $OPG^{-/-}$ and $OPG^{+/+}$ mouse groups for this investigation. To quantify the desired cell population the immune cells in the aorta were extracted as a preliminary step. Aortas from mouse were pooled in groups of four to obtain an adequate number of cells for analysis. The aortas were cut into smaller segments and transferred into 1.5 ml eppendorf tube containing 200 µl of 20 mM 4-(2-hydroxyethyl)-1-piperazineethanesulfonic acid (HEPES, Amersco Inc.USA) buffer (Appendix 4). The tissue was homogenised with a drill and clean plastic pestle until a single cell suspension was obtained. The homogenised aorta was removed on a nylon mesh in a petri dish and any remaining lumps of the tissue were homogenised with the end of the syringe. The petri dish

along with the nylon mesh was washed with 10 mM EDTA to recover as many cells as possible. The tissue was then subjected to enzyme digestion by incubating it with 3 ml of a dissociation buffer at 37^{o}C for 1 hour with intermittent mixing. This dissociation buffer consisted of collagenase type XI (125 U/ml, Sigma, USA), hyaluronidase type I-S (600 U/ml, Sigma, USA), DNase type I (60 U/ml, Roche, USA) and collagenase type I (450 U/ml, Sigma, USA) in 20 ml of HEPES buffer (Appendix 4). Post incubation, the cell suspension was passed through a 2 mm nylon mesh to eliminate any smaller tissue lumps. The cell suspension was centrifuged at 450 x g for 30 min. The supernatant was discarded and the cell pellet was used for further analysis.

2.7.2. FcR blocking

Mouse FcR blocking agent (BD biosciences, USA) was used to eliminate any non specific antigen- antibody binding. Cell pellet was incubated with 50µl of FcR (1:50) in FC buffer (Appendix 4) at R.T for 15 min. Incubation was followed by centrifugation at 400 x g for 5 min. The supernatant was discarded and the cell pellet was reconstituted in 90 µl of FC buffer and transferred to ice.

2.7.3. Primary antibody labelling

As described in section 2.6.4, the cell suspension was equally divided into two tubes for primary antibody and isotype control respectively. 5 µl of goat anti-mouse unconjugated OCN primary antibody (BT biomedical technologies, USA) or isotype control (1:100 in FC buffer) was added to the appropriate tubes. Cells were incubated for 30 min at 4^{o}C.

2.7.4. Secondary antibody labelling

Post primary antibody labelling the cells pellets were washed, as in previous steps, and labelled with a fluorescent phycoerythrin (PE) secondary antibody (1:75 in FC buffer, Jackson's Immunoresearch, USA). 50 µl of the titre antibody was added to both the OCN labelled and isotype cell pellets. Tubes were incubated for 30 min at 4^{o}C in dark conditions to avoid degradation of fluorescent intensity of PE.

2.7.5. Flow cytometry analysis

The FC analysis was carried out as performed in section 2.6.6. The cells were immediately analysed on FC to measure the OCN^+ cell population.

2.8. Human patient cohort calcification studies

A patient cohort, suffering from peripheral artery disease and who previously had computed tomography (CT) scans, was also studied. Blood was collected and quantified for OCN^+ MNC population by FC analysis. The calcification volumes from the CT scans were correlated with the OCN^+ MNC population to assess association.

2.8.1. Selection criteria for the patient study

All the selected patients were diagnosed with abdominal aortic aneurysm (AAA) based on CTA. AAA was defined by maximum aorta diameter of ≥ 30 mm. Peripheral artery disease was diagnosed based on appropriate symptoms assessed by a consultant vascular surgeon. Patients were excluded if they had received open surgical or endovascular treatment on their infrarenal aorta or if a Computed Tomographic Angiogram (CTA) was felt to be contra-indicated, as previously described[235]. Patients with serum creatinine of ≥ 120 μM, with inability to lie flat or with contrast allergy were also excluded.

2.8.2. Ethics approval and access to the patient details

Ethics approval for the studies was granted by Ethics committee from JCU (Appendix 3). Written informed consent was obtained from all the recruited patients for the investigation.

2.9. Aortic calcification measurements in patients using CT imaging

The patients' calcification volumes were measured as previously described[235]. Briefly CTA was performed on 16 -slice multi scanner (MX, Philips). Images of abdominal aorta (supra-renal aorta to tibial arteries) were obtained in 20 seconds in 1 breath-hold cycle. The images from the origin of the lowest renal to the bifurcation of the aorta were transferred to a workstation and transformed into a 3 dimensional composite image[235]. Using the volume of interest tool on a workstation, an encircling line was drawn around the aortic images to form a region on interest. The image slices were then previewed to ensure that only calcified aortic section was highlighted and excluded all other vascular structures and adjacent calcified vertebral body areas[235]. The readings were repeated after 24 hours to assess the level of inter and intra observer reproducibility[235]. The results were statistically analysed using SPSS program (15.0, SPSS Inc, USA). The calcification volumes were categorised into high calcified volume and low calcified volume based on the median for the group.

2.10. Quantification of OCN^+ MNC population using flow cytometry analysis

2.10.1. Collection of patient blood samples

Blood samples were obtained following an overnight fast. 20 ml of blood was collected into heparinised tubes (BD vacutainer, Becton Dickinson, USA). The samples were immediately couriered to the JCU, School of Medicine and Dentistry research laboratory for analysis.

2.10.2. Ficoll histopaque technique

The mononuclear cell layer was separated from other blood constituents using a ficoll histopaque (Sigma, USA) gradient technique. Blood samples were diluted 1:2 with PBS and divided into two equal volumes. Each volume of diluted blood sample was carefully layered onto 15 ml ficoll histopaque. Both tubes were centrifuged at 400 x g for 30 min, without brakes to avoid mixing. After centrifugation four layers were obtained; an upper plasma layer, MNC layer followed by a ficoll layer and a final RBC layer at the bottom of the tube. Using a clean glass pipette the MNC layer was removed to a separate tube. The plasma layer was collected post-MNC separation and transferred into 15 ml falcon tubes and stored at -20^{o}C for protein cytokine analysis.

2.10.3. Buffer solutions

Wash buffer containing 2 mM EDTA with 0.5 % chicken albumin (Sigma, USA) was used for intermittent cell washings (Appendix 4). Another 2mM EDTA buffer with 0.5 % bovine serum albumin (BSA) was used as a magnetic separation (MS) buffer (Appendix 4). Cells were treated with BSA buffer during the magnetic enrichment step. A FC buffer containing 3 % FCS and 0.05 % sodium azide (Appendix 4) was used for antibody dilutions.

2.10.4. Centrifugation and cell washing

All protocol steps were separated by washing using the wash buffer containing 2 mM EDTA with 0.5 % chicken albumin. Post washing, the cells were centrifuged for 10 min at 400 x g at R.T. A single cell suspension was prepared using 30 micron nylon mesh.

2.10.5. Trypan blue cell dye exclusion test for cell viability

The dye exclusion test determines the number of viable cells present in a cell suspension. It is based on the principle that live cells possess intact cell membranes that exclude certain dyes, such as trypan blue, eosin, or propidium, whereas dead cells do not. In this test, a cell suspension is mixed with the dye and then visually examined to determine whether cells take up or exclude the dye. The cells in the pellet obtained from the MNC washing step were counted on a haemocytometer. 20 µl of the cell pellet suspension was aliquoted after MNC cell separation and washing. The sample was incubated with an equal volume of 0.4 % trypan blue staining for 3 min. The cell-dye mixture was then transferred on to a haemocytometer slide. The counting procedure and cell calculations are discussed in Chapter 3 (section 3.7.1).

2.10.6. Human FcR blocking

After the MNC counts were estimated 20 µl of FcR block (Miltenyi biotech, USA) was added to every 1 x 10^7 cells in the suspension. 10% donkey serum was also mixed with the solution to enhance the quality of blocking. The final cell suspension was incubated at 20 min at R.T before centrifugation at 400 x g for 10 min. The optimisation for FcR blocking titre is discussed in Chapter 3 (section 3.7.2).

2.10.7. Primary OCN antibody labelling

The cell pellet was resuspended in 90 µl of FC buffer and transferred to ice to maintain cell viability. The suspension was mixed thoroughly and divided equally into two tubes. The cell suspension in one tube was labelled with primary antibody and the other with an isotype control. Both primary OCN antibody (Santa Cruz, USA) and IgG Isotype (BD biosciences, USA) was used at 1:100. Cell suspensions in both tubes were incubated for 30 min at 4^{o}C followed by washing in wash buffer and centrifugation at 400 x g for 10 min. optimisation for primary antibody titre labelling is discussed in Chapter 3 (section 3.7.3).

2.10.8. Secondary PE fluorescent antibody labelling

After cell washing, the primary antibody attached to the cells was tagged with PE secondary antibody (Jackson's Immunoresearch, USA) (1:75). The cells were incubated at 4^{o}C for 30 min in the dark. Cells were washed and centrifuged at 400 x g for 10 min. The cells were maintained in cold conditions throughout to retain cell viability and to prevent capping of antibodies on the cell surfaces. The optimisation for secondary antibody titre labelling is discussed in Chapter 3 (section 3.7.4).

2.10.9. Anti-PE magnetic beads

Post washing, the cell pellets were suspended to 80 µl of MS buffer containing 0.5 % chicken albumin. 20 µl per 10^7 cells of anti-PE beads (Miltenyi, USA) were further added to the suspension. This cell-bead suspension was incubated for 20 min at 4^{o}C in the dark. Cells were washed with MS buffer and centrifuged at 400 x g for 10 min. The magnetically labelled cell pellet was resuspended in 500 µl of MS buffer and maintained on ice. The optimisation for anti-PE bead labelling is discussed in Chapter 3 (section 3.7.5).

2.10.10. Magnetic column separation set up

A mini MACS (magnetic assorting cell separator) and a MS column (Miltenyi Biotech, USA) were used as the maximum number of labelled cells was less than 10^7 cells. The MS column was placed in the magnetic field of the Mini MACS separator. The column was

prepared by rinsing with 500 µl of MS buffer. Once the buffer was eluted from the column, the cell suspension was added. A diagrammatic representation of the magnetic separation protocol is shown below in Figure 2.1.

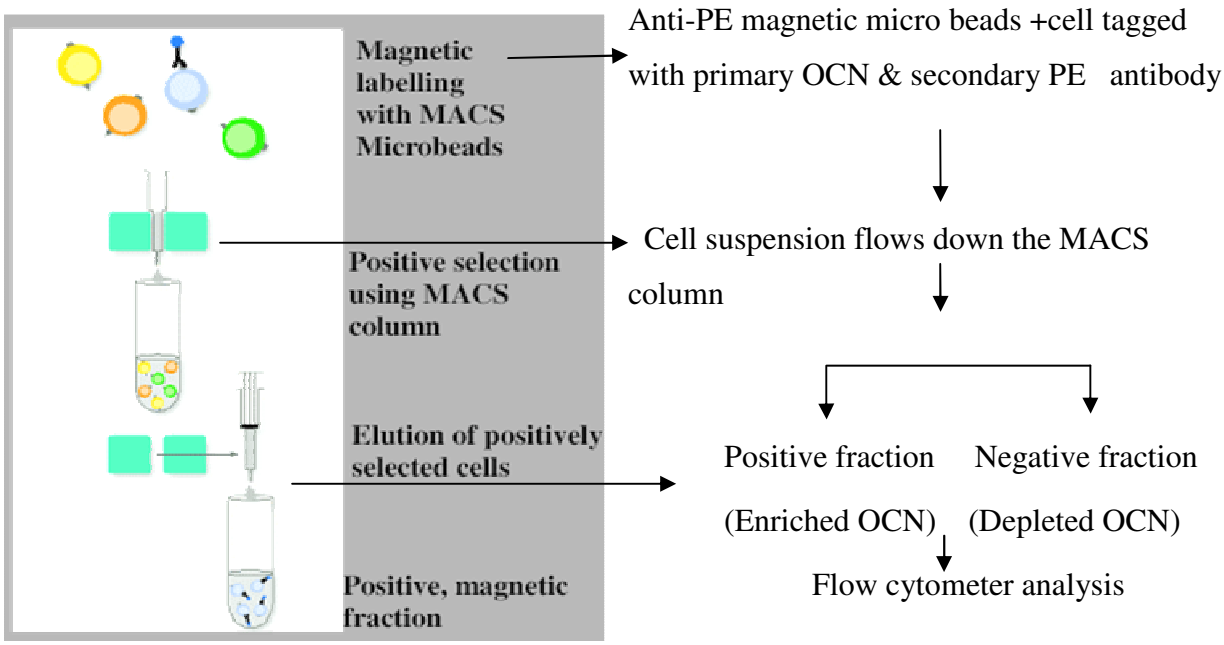

Figure 2.2. Schematic diagram illustrating the magnetic enrichment technique for quantification of OCN^+ MNC.

While the MNC flow down through the column reservoir, the OCN^+ labelled MNC adhere to the micro beads in the column and get separated from the MNC which are not bound by OCN antibody. 500 µl of buffer was twice added after the cell suspension to ensure better separation. New buffer was added only when the column reservoir was empty and the column was never allowed to run dry. The eluted fraction, also termed as negative fraction, was collected separately and stored on ice for later centrifugation. Once all three washes were completed, the column was detached from the Mini MACS separator and placed on a collection tube. 500 µl of MS buffer was added in the column reservoir. The buffer was then immediately flushed out by firmly pushing the plunger (accompanying the column) thus collecting the magnetically labelled cells. This labelled fraction was termed the positive fraction. Both positive and negative fractions were centrifuged at 400 x g for 10 min to elute the anti- PE beads from the MNC.

2.10.11. Flow cytometry analysis of murine and human cells

Although the number of OCN^+ MNC within the circulation of mouse and human blood samples was estimated by FC analysis the protocol steps involved for species was different. A flow chart describing the similarities and differences in the two models is outlined below.

A) For mouse model

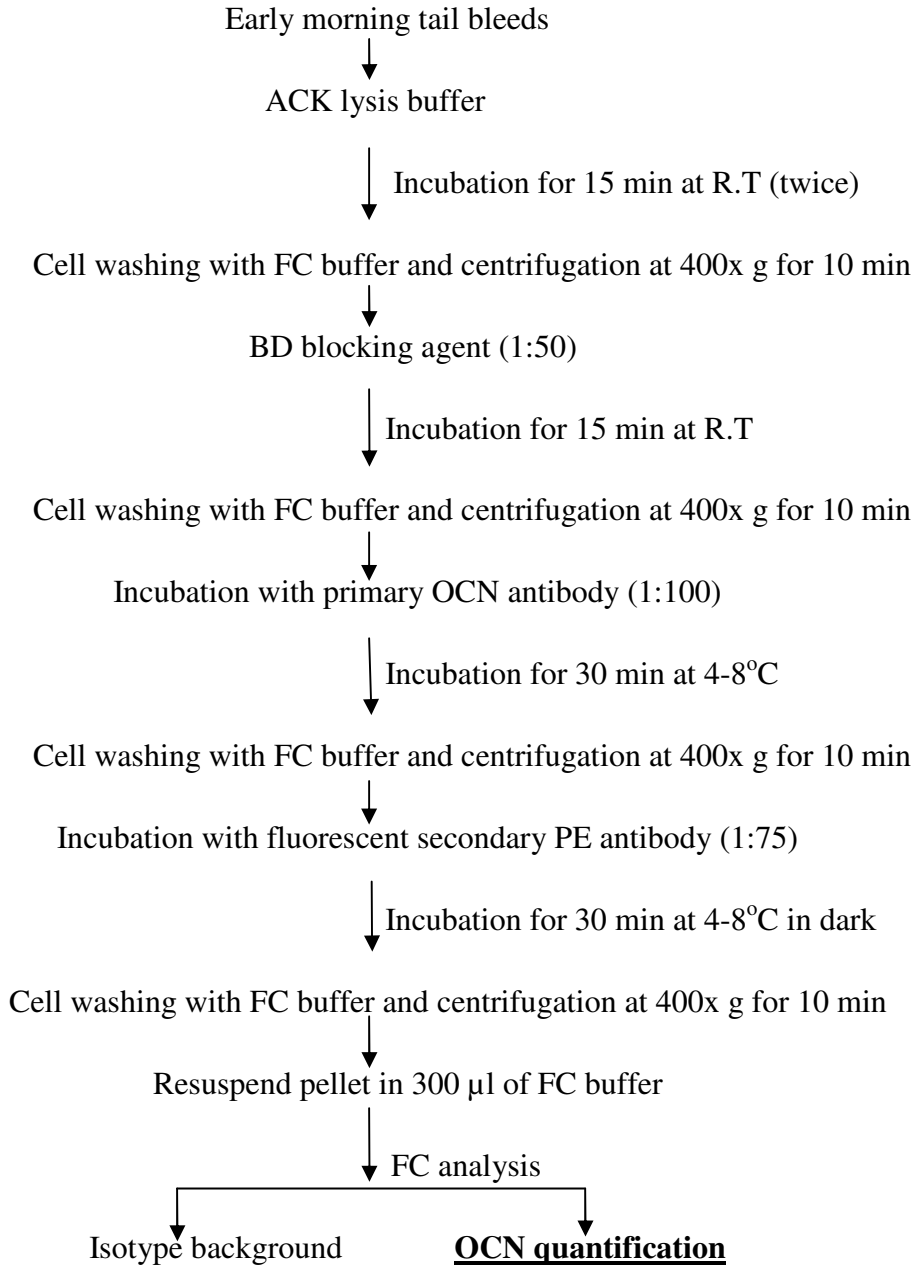

B) For human patient cohort

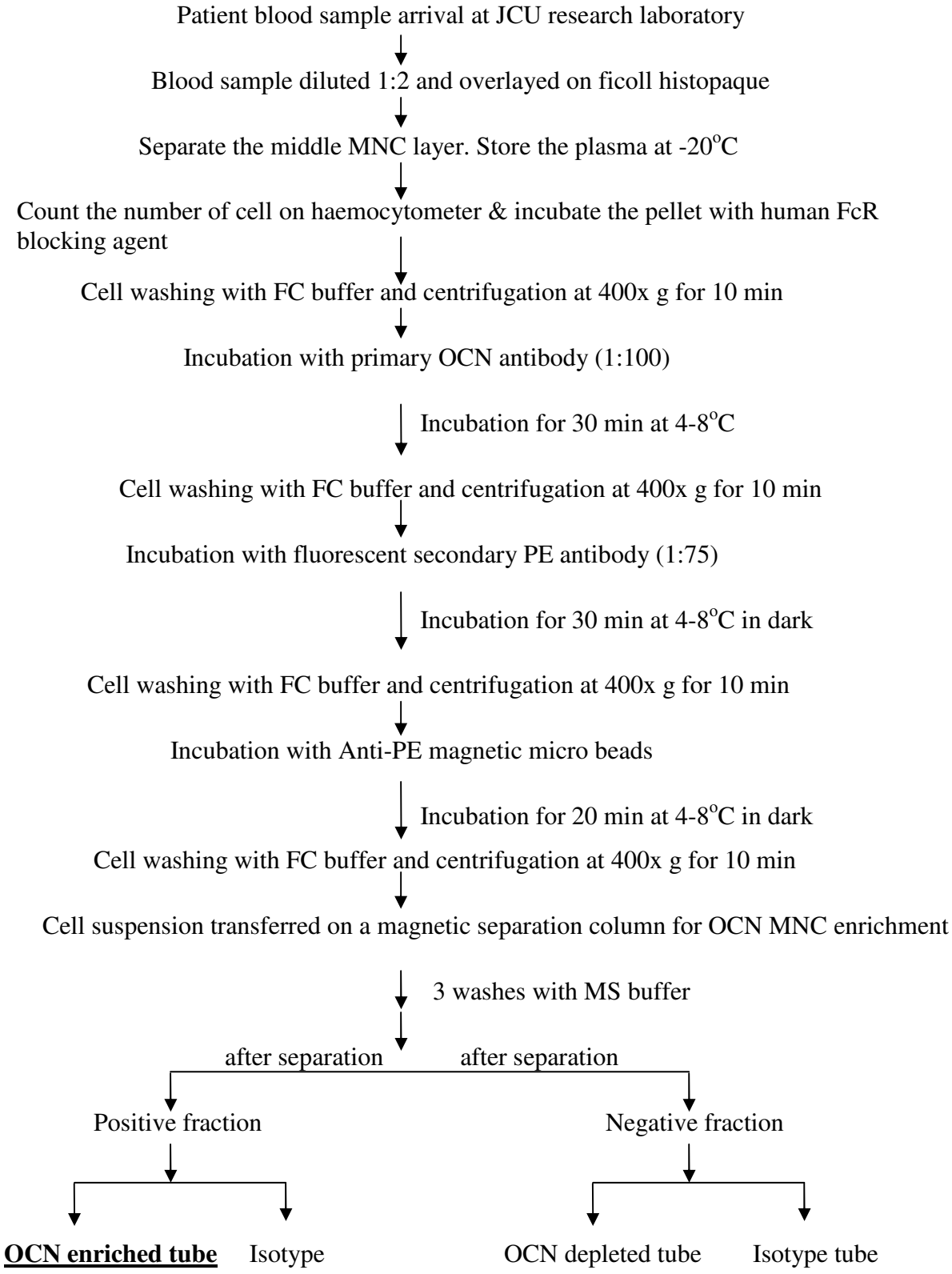

Figure 2.3. Flow cytometry protocol for mouse model (A) and human patient cohort (B) (ACK- ammonium chloride and potassium; FC-flow cytometry; OCN MNC-osteocalcin mononuclear cells; PE-phycoerythrin)

Quantification of OCN^+ MNC in patient blood samples involved an initial separation of MNC from whole blood by ficoll histopaque. The MNC population was labelled with primary OCN antibody and further enriched by magnetic column separation. On the other hand the murine quantification of circulating OCN^+ MNC involved the lysis of RBC by ACK lysis buffer. Although the incubation with primary OCN and fluorescent secondary antibody were similar in both studies, OCN^+ MNC was not enriched in the animal model. There are a couple of reasons for this.

Firstly, only a limited amount of blood sample could be withdrawn during tail bleeds from mice. The maximum amount of peripheral blood that could be obtained from was approximately 200 µl. On the other hand 20 ml of blood was obtained from all the human patients. Hence the limited amount of blood samples obtained from mice tail bleeds was a drawback in separating the MNC layer by ficoll histopaque method.

Secondly, the difference between the MNC counts in both animal and human blood samples is large. MNC obtained from tail bleeds are extremely limited to be set up and enriched on MS column. Also the amount of circulating OCN^+ MNC was found out to be in lower numbers in murine blood samples when compared to patient blood samples. This difference in the MNC counts could be significant in the enrichment step during which some OCN^+ MNC could be lost in the several washing steps prior to magnetic column enrichment. To avoid any loss of desired cell population ficoll hypaque MNC separation and magnetic bead enrichment steps were eliminated from the blood sample preparation for mouse model experiments.

2.10.12. Flow cytometry analysis

Post centrifugation, the cell pellets were resuspended into FC buffer and immediately analysed on FC (BD FACSCalibur, USA). The standardisation of the FC analysis for mouse model and human patient cohort is discussed in Chapter 3 (section 3.7 and section 3.8).

2.11. Protein cytokine studies using ELISA for patient sample investigation

Protein cytokine studies were performed on plasma samples collected from patient blood samples. These plasma samples were obtained from the ficoll histopaque separation of the whole blood. Cytokines of interest such as SDF-1 α, G-GSF and SCF were measured by ELISA technique as performed with mouse serum samples. The plasma cytokine levels were then statistically correlated to circulating OCN^+ MNC and the infra renal aortic calcification volumes estimated by CTA to determine any possible association. These cytokines were selected as they have been consistently reported to be associated with the release of immature cells from BM into the circulation.

2.11.1. Sample collection, preparation and storage

The samples were obtained from the ficoll histopaque separation of the patient blood. The samples received from SNP was immediately layered on ficoll histopaque solution and centrifuged at 400 x g for 30 min. The resultant plasma layer was separated in a 15 ml tube and stored at -20^{o}C for cytokine analysis after obtaining blood samples from the whole cohort. The cytokine analysis for all the plasma samples was performed at the same time to minimise errors between samples. Repeated thawing and freezing of samples was avoided. The ELISA protocol was followed according to section 2.5.2

Calculation for standards and samples was followed according to section 2.5.3. The intra and inter-assay reproducibility for SDF-1α, G-CSF and SCF is demonstrated in Chapter 3 (section 3.9.3, 3.10.3 and 3.11.3 respectively).

2.12. Statistical analysis

All the mouse and human patient data was analysed using SPSS statistics software (15.0, SPSS Inc USA). Data was assessed for normality using Q-Q plots. For all the data which was not normally distributed statistical non-parametric statistical tests were used to assess our hypotheses, including Mann-Whitney U test, paired Wilcoxon test and Spearman correlations. Assay reproducibility was assessed using coefficient of variation. All the data is represented in medians and inter-quartile ranges (IQR).

CHAPTER 3. FEASIBILITY STUDIES AND PROTOCOL OPTIMISATION

3.1. Calcium quantification

Standardisation of aortic calcium staining in whole aorta was the preliminary step since this has not been previously reported[232,233]. From previous reports, it was evident that alizarin red is an ideal reagent to detect calcification in 5µm sections of tissues including aorta, spleen and bone sections[232,236,237]. Based on these reports, an experimental design was set up to standardise optimum aortic staining.

3.1.1. Aortic calcium staining

3.1.1.1 Aim

The aim of this study was to establish a reproducible means of staining calcium in mice aortas. Whole aortas harvested from experimental $OPG^{-/-}$ and control $OPG^{+/+}$ mice were used for the studies.

3.1.1.2 Alizarin red concentration

Different alizarin concentration (0.5 %, 1 %, and 2 %) were tested to determine the optimum staining concentration. It was demonstrated that a 1% solution of alizarin red in distilled water (D/W) suited best for the experiment as staining area could be measured without background staining interference (Figure 3.1).

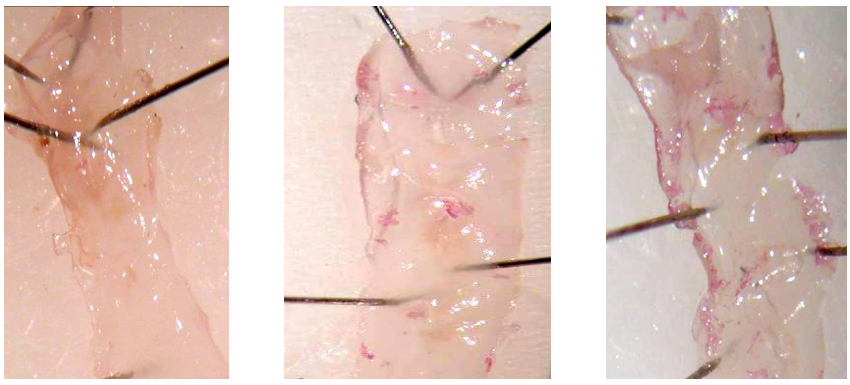

0.5% **1%** 2 %

Figure 3.1. Pictures of aortas stained with different concentrations of alizarin red.

3.1.1.3. Incubation condition

Further experiments were carried out to access optimal incubation time and conditions. Initial incubation periods of 15 min, 30 min, 1 hour and 2 hour on static and shaker conditions were tested to estimate optimum staining conditions (Figure 3.2). A continuous 2 hour staining period while placed on shaker conditions resulted in optimum staining since the alizarin red stained the free calcium more prominently in the mouse aorta at 2 hour shaker conditions than other tested incubation conditions.

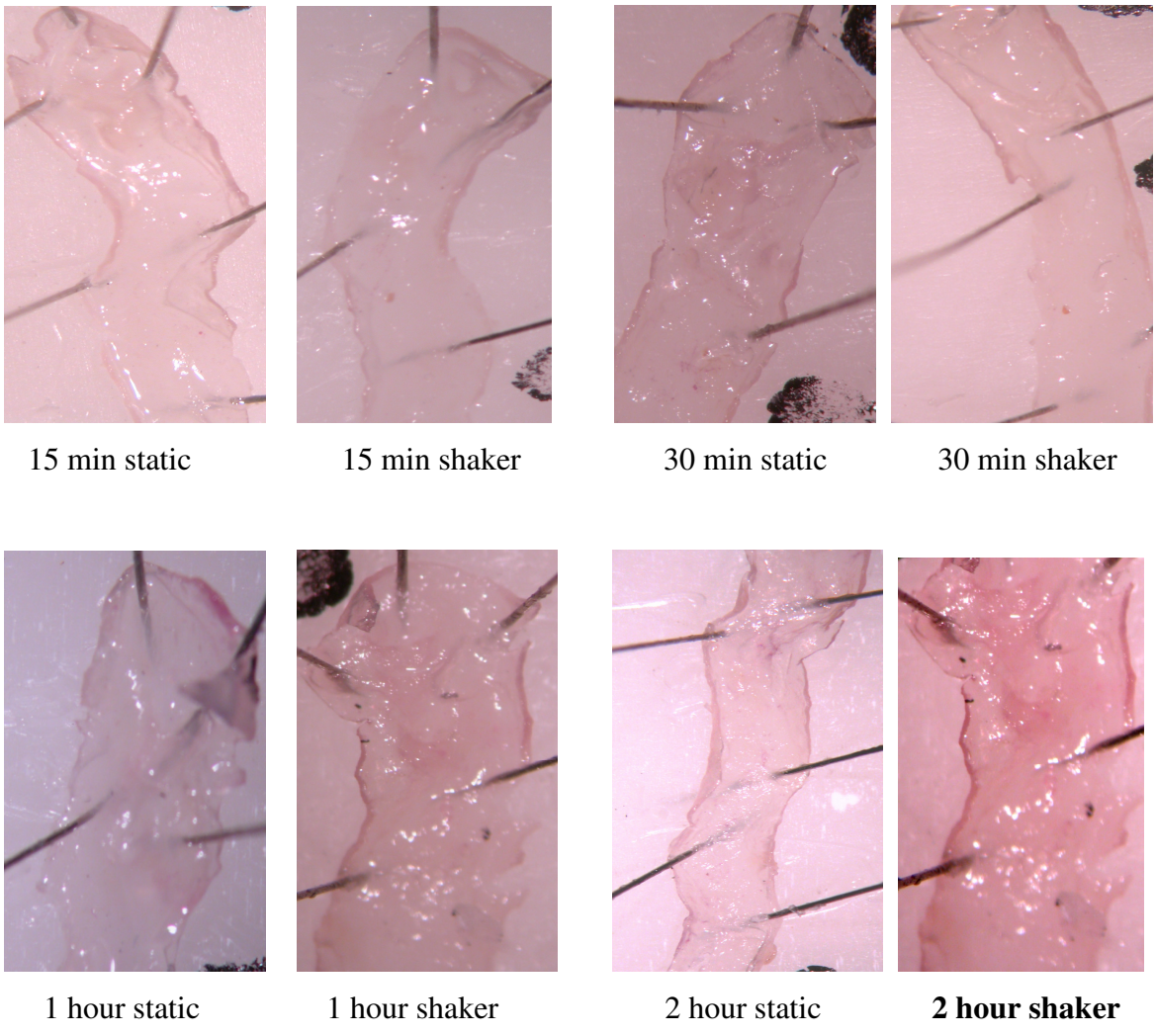

Figure 3.2. Comparison of different staining conditions of mice aortas with alizarin red

3.1.2 Scion software measurements

As discussed in the Chapter 2, computer aided software (Scion^{TM}, USA) was selected for the calcium staining percentage quantification. With assistance from the specific region selecting tool in the software, the total area of the aorta was measured in mm^2. The red areas of calcium staining were then measured in the same manner and reported as percentage of staining area. The measurements were repeated twice on different occasions for intra measurement coefficient of variation. The same measurement style was followed for each aortic section in both $OPG^{-/-}$ and control $OPG^{+/+}$ mice.

3.1.2.1. Intra measurement reproducibility

7 aortas each from $OPG^{-/-}$ and $OPG^{+/+}$ were assessed two separate occasions by the same observer to estimate the intra-observer error. Standard deviations were calculated using Microsoft Excel 2000 (Microsoft Inc. USA). The coefficient of variation in percentage was calculated as follows:

$$\frac{\text{Standard deviation (assessment 1 + assessment 2)}}{\text{Mean assessment value}} \times 100$$

The median intra-observer coefficient of variation for measurements carried out of different aortic regions is shown section in Table 3.1.

Table 3.1. Intra-observer coefficient of variation for alizarin staining area measurements in different aortic regions in experimental $OPG^{-/-}$ and control $OPG^{+/+}$ mouse models.

Aortic regions	Mouse strain	
	$OPG^{-/-}$ (C0V in %)	$OPG^{+/+}$ (COV in %)
Aortic arch	6.94	9.3
Thoracic arch	7.63	8.89
Supra renal	8.66	9.6
Infra renal	8.49	9.09

($OPG^{-/-}$: osteoprotegerin deficient; $OPG^{+/+}$; osteoprotegerin present, COV: coefficient of variation)

3.2. Assay of extractable aortic calcium

As mentioned in the Chapter 2, aortic calcification was also estimated using a commercially available Quantichrom bioassay. The method was initially standardised.

3.2.1. Aim

To assess the reproducibility of aortic calcium measurement by bioassay.

3.2.2. Protocol

Calcium measurements were performed in duplicates. Each plate comprised of standard and sample duplicates. The results were used to calculate intra-assay coefficient of variation.

Calcium amounts (or concentration) were calculated using standard curves as per manufacture's instructions (Quantichrom, USA). Details are provided in Chapter 2 (section 2.4). The Mean (*M*) and Standard Deviation (*SD*) of duplicate readings were calculated by following the equation:

$$\frac{(SD1+ \ldots\ldots +SD7)/7}{(M1+ \ldots\ldots +M7)/7} \times 100$$

Three separate assessments were carried out using different plates on separate days. The *M* and *SD* were averaged from the three separate assessments to generate an average inter-assay coefficient of variation:

$$\frac{(SD\ (Plate\ 1\ M1 + Plate\ 2\ M1) + \ldots\ldots + SD\ (Plate\ 1\ M7 + Plate\ 2\ M7))/7}{(M\ (Plate\ 1\ M1 + Plate\ 2\ M1) + \ldots\ldots + M\ (Plate\ 1\ M7 + Plate\ 2\ M7))/7} \times 100$$

3.2.3. Results and conclusion

3.2.3.1. Intra assay reproducibility

Reproducibility of aortic calcium assay in 12 month old mouse model (study 1)

Intra-assay coefficient of variation for calcium assay standard measurements in a 12 month old mouse model is illustrated in Figure 3.3.

Plate 1 O.D readings (595 nm)

Standard			Mean	Std dev
20	0.7670	0.7670	0.7670	0.0000
16	0.6560	0.6340	0.6450	0.0156
12	0.5440	0.5220	0.5330	0.0156
8	0.3810	0.3640	0.3725	0.0120
6	0.2920	0.2820	0.2870	0.0071
4	0.1910	0.2050	0.1980	0.0099
2	0.1340	0.1360	0.1350	0.0014
0	0.0500	0.0520	0.0510	0.0014
		Mean	0.3736	0.0079
	Intra assay coefficient of variation		**2.10 %**	

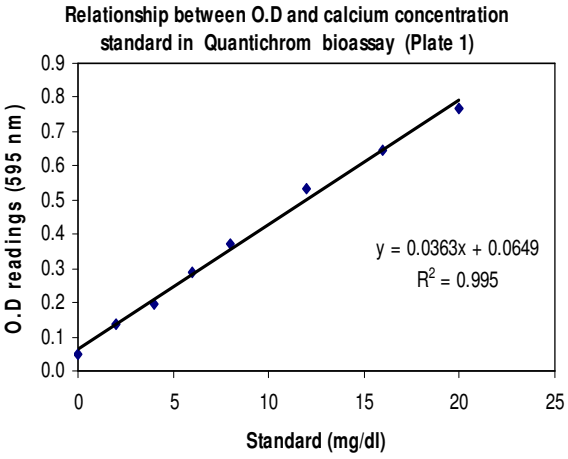

Plate 2 O.D readings (595 nm)

Standard			Mean	Std dev
20	0.7770	0.7690	0.7730	0.0057
16	0.6510	0.6240	0.6375	0.0191
12	0.5240	0.5320	0.5280	0.0057
8	0.3840	0.3610	0.3725	0.0163
6	0.2910	0.2720	0.2815	0.0134
4	0.1810	0.2160	0.1985	0.0247
2	0.1310	0.1380	0.1345	0.0049
0	0.0430	0.0460	0.0445	0.0021
		Mean	0.3713	0.0115
	Intra assay coefficient of variation		**3.09 %**	

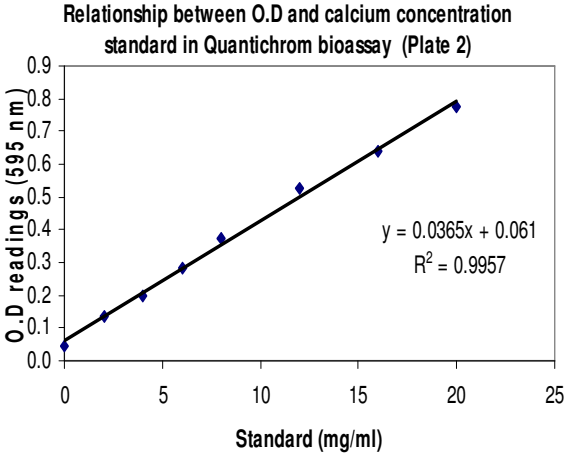

Plate 3

Standard			Mean	Std dev
20	0.7850	0.7630	0.7740	0.0156
16	0.6240	0.6230	0.6235	0.0007
12	0.5120	0.5310	0.5215	0.0134
8	0.3810	0.3780	0.3795	0.0021
6	0.2610	0.2680	0.2645	0.0049
4	0.1800	0.1860	0.1830	0.0042
2	0.1260	0.1280	0.1270	0.0014
0	0.0470	0.0440	0.0455	0.0021
		Mean	0.3648	0.0057
	Intra assay coefficient of variation		**1.56 %**	

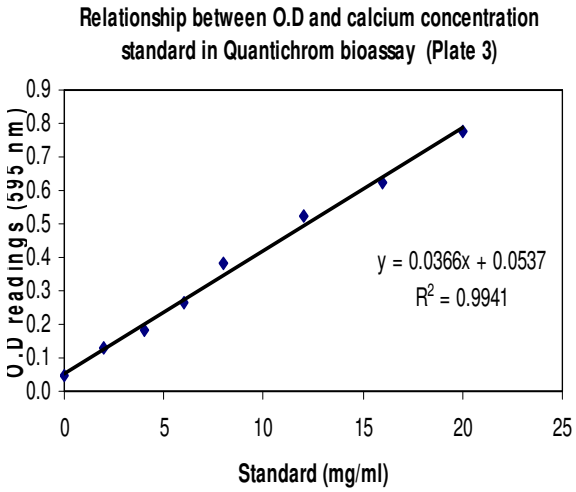

Figure 3.3. Intra-assay assessment of reproducibility for calcium standard assays for 12 month old mouse groups (Std dev: standard deviation; O.D: optical density)

Reproducibility of aortic calcium assay in 14 week old mouse model (study 2)

Intra assay coefficient of variation for calcium assay standard measurements in a 14 week old mouse model is illustrated in Figure 3.4.

Plate 1 O.D readings (595 nm)

Std			Mean	Std dev
20	0.7210	0.7350	0.7280	0.0099
16	0.6860	0.6240	0.6550	0.0438
12	0.5400	0.5240	0.5320	0.0113
8	0.3440	0.3170	0.3305	0.0191
6	0.2520	0.2320	0.2420	0.0141
4	0.1810	0.1950	0.1880	0.0099
2	0.1380	0.1460	0.1420	0.0057
0	0.0700	0.0620	0.0660	0.0057
		Mean	**0.3604**	**0.0149**
	Intra assay coefficient of variation		**4.14 %**	

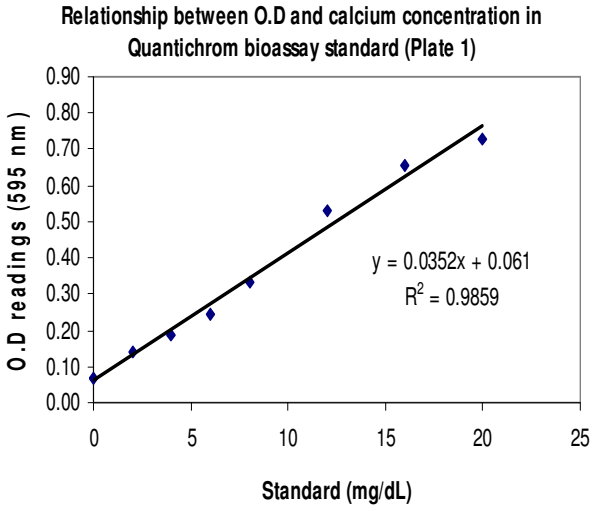

Plate 2

Std	O.D readings (595 nm)		Mean	Std dev
20	0.8130	0.7950	0.8040	0.0127
16	0.7760	0.7140	0.7450	0.0438
12	0.5950	0.5340	0.5645	0.0431
8	0.3740	0.3470	0.3605	0.0191
6	0.2510	0.2300	0.2405	0.0148
4	0.1740	0.1750	0.1745	0.0007
2	0.1390	0.1410	0.1400	0.0014
0	0.0500	0.0520	0.0510	0.0014
		Mean	**0.3850**	**0.0171**

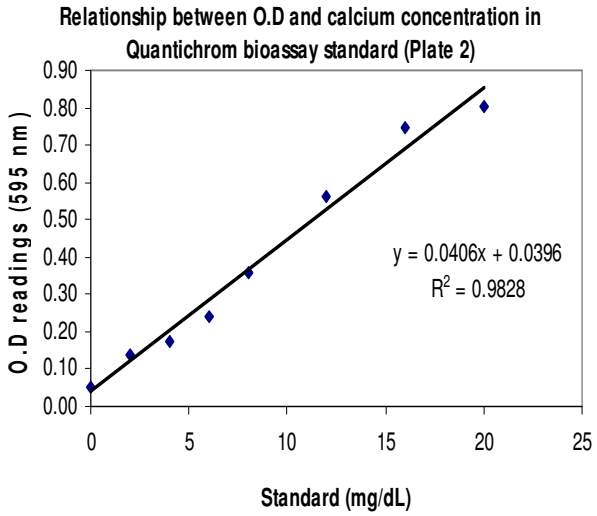

Intra assay coefficient of variation	**4.45 %**

Plate 3

Std			Mean	Std dev
20	0.7130	0.7250	0.7190	0.0085
16	0.6890	0.7140	0.7015	0.0177
12	0.5420	0.5340	0.5380	0.0057
8	0.3850	0.3270	0.3560	0.0410
6	0.2510	0.2300	0.2405	0.0148
4	0.1740	0.1790	0.1765	0.0035
2	0.1390	0.1410	0.1400	0.0014
0	0.0740	0.0690	0.0715	0.0035
	Mean		**0.3679**	**0.0120**

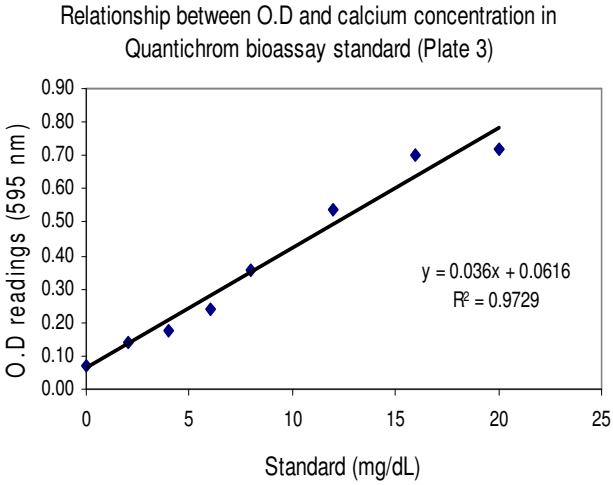

Intra assay coefficient of variation	**3.26%**

Figure 3.4. Intra-assay assessment of reproducibility for calcium standard assays for calcitriol mouse group.

3.2.3.2. Inter-assay reproducibility

Reproducibility of aortic calcium assay in 12 month old mice (study 1)

Table. 3.2. Inter-assay assessment of reproducibility for calcium assay in 12 month old mouse groups

	Mean O.D readings (595 nm)				
Std	Plate 1	Plate 2	Plate 3	Mean	std dev
20	0.7670	0.7730	0.7740	0.7713	0.004
16	0.6450	0.6375	0.6235	0.6353	0.011
12	0.5330	0.5280	0.5215	0.5275	0.006
8	0.3725	0.3725	0.3795	0.3748	0.004
6	0.2870	0.2815	0.2645	0.2777	0.012
4	0.1980	0.1985	0.1830	0.1932	0.009
2	0.1350	0.1345	0.1270	0.1322	0.004
0	0.0510	0.0445	0.0455	0.0470	0.004
			Mean	**0.3699**	**0.007**
		Inter-assay coefficient of variation		**1.79 %**	

Reproducibility of aortic calcium assay in 14 week old mice (study 2)

Table. 3.3. Inter-assay reproducibility of calcium assay in 12 month old mouse groups

	Mean O.D readings (595 nm)				
Std	Plate 1	Plate 2	Plate 3	Mean	std dev
20	0.728	0.8040	0.7190	0.7503	0.0467
16	0.655	0.7450	0.7015	0.7005	0.0450
12	0.532	0.5645	0.5380	0.5448	0.0173
8	0.3305	0.3605	0.3560	0.3490	0.0162
6	0.242	0.2405	0.2405	0.2410	0.0009
4	0.188	0.1745	0.1765	0.1797	0.0073
2	0.142	0.1400	0.1400	0.1407	0.0012
0	0.066	0.0510	0.0715	0.0628	0.0106
			Mean	**0.3711**	**0.0181**
		Inter-assay coefficient of variation		**4.88 %**	

The combined results are illustrated in Figure 3.5. Intra-assay and inter-assay coefficient of variation for the Quantichrom calcium bioassay was between 1 and 5%.

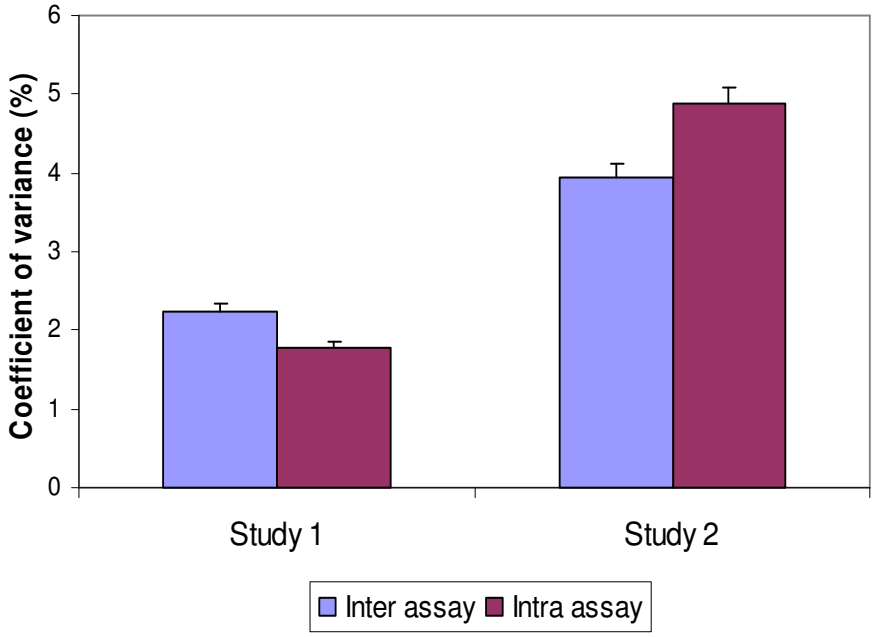

Figure 3.5**.** Intra and inter-assay assessment of reproducibility of the Quantichrom calcium bioassay for study 1 and 2.

3.3. Serum SDF-1α measurments in mouse models

3.3.1. Aim

The aim of this study was to assess the reproducibility of the SDF-1α ELISA kit at both intra and inter-assay levels. Serum samples obtained from tail bleeds of experimental $OPG^{-/-}$ mice (n=11) and control $OPG^{+/+}$ mice (n=11) was analysed. The immunoassay required preparation of standards, antibodies for target protein capture and detection, and involved a multiple-step protocol in its execution, all of which may introduce error.

3.3.2. Protocol

Serum SDF-1α measurements were performed in duplicates. The results were used to calculate intra-assay coefficient of variation.

SDF-1α amounts (or concentrations) were calculated using standard curves as per manufacture's instructions. Details are provided in Chapter 2 (section2.5.3). The mean (*M*)

and standard deviation (*SD*) of duplicate readings were calculated and the intra-assay coefficient of variation using the equation applied in section 3.2.2.

3.3.3. Results and conclusion

3.3.3.1. Intra-assay reproducibility

Intra-assay reproducibility for SDF-1α standard measurements in a 12 month old mouse model are illustrated in Figure 3.6.

Plate 1

Std (ng\ mL)	O.D readings (450 nm)		Mean	Std dev
0	0.0470	0.0490	0.0480	0.0014
0.156	0.0680	0.0710	0.0695	0.0021
0.312	0.1050	0.0940	0.0995	0.0078
0.625	0.1490	0.1460	0.1475	0.0021
1.25	0.2480	0.2440	0.2460	0.0028
2.5	0.6710	0.6860	0.6785	0.0106
5	1.1480	1.1420	1.1450	0.0042
10	1.9990	2.0280	2.0135	0.0205
		Mean	0.5559	0.0065
		Intra assay coefficient of variation	**1.16 %**	

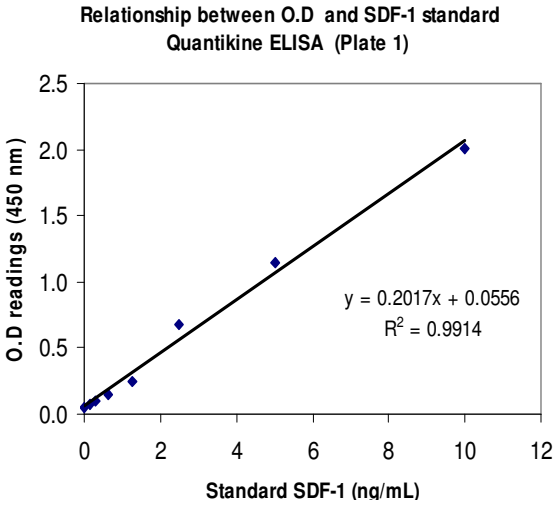

Plate 2

Std (ng\ mL)	O.D readings (450 nm)		Mean	Std dev
0	0.0490	0.0420	0.0455	0.0049
0.156	0.0660	0.0730	0.0695	0.0049
0.312	0.1120	0.1040	0.1080	0.0057
0.625	0.1420	0.1450	0.1435	0.0021
1.25	0.2390	0.2410	0.2400	0.0014
2.5	0.6680	0.6820	0.6750	0.0099
5	1.1410	1.1480	1.1445	0.0049
10	1.9890	2.0110	2.0000	0.0156
		Mean	0.5533	0.0062
		Intra assay coefficient of variation	**1.11 %**	

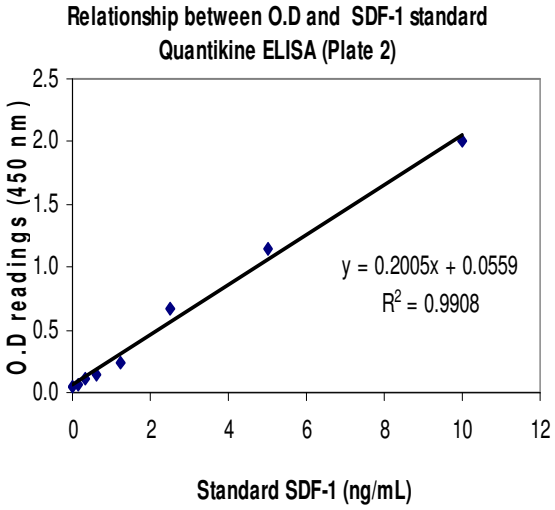

Plate 3

Std (ng\ mL)	O.D readings (450 nm)		Mean	Std dev
0	0.0590	0.0510	0.0550	0.0057
0.156	0.0680	0.0720	0.0700	0.0028
0.312	0.1150	0.1190	0.1170	0.0028
0.625	0.1830	0.1650	0.1740	0.0127
1.25	0.2390	0.2410	0.2400	0.0014
2.5	0.6420	0.6690	0.6555	0.0191
5	1.1460	1.1490	1.1475	0.0021
10	1.9810	2.1210	2.0510	0.0990
		Mean	0.5638	0.0182
		Intra assay coefficient of variation	**3.22 %**	

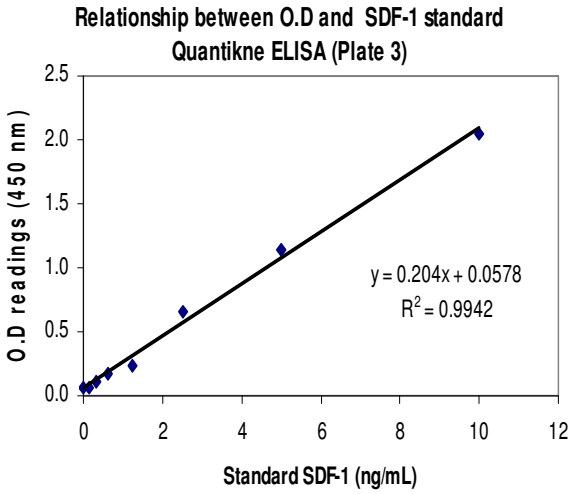

Figure 3.6. Intra-assay assessment of reproducibility for SDF-1 α standard measurements in 12 month old mouse groups.

3.3.3.2. Inter-assay reproducibility

Inter-assay reproducibility was also assessed for SDF-1 α ELISA technique and is illustrated in Table 3.4.

Table 3.4. Inter-assay assessment of reproducibility for SDF-1α standards in a 12 month old mouse groups.

Std (ng\ mL)	Plate 1	Plate 2	Plate 3	Mean	Std dev
0	0.048	0.0455	0.055	0.0495	0.005
0.156	0.0695	0.0695	0.07	0.0697	0.000
0.312	0.0995	0.1080	0.117	0.1082	0.009
0.625	0.1475	0.1435	0.174	0.1550	0.017
1.25	0.246	0.2400	0.24	0.2420	0.003
2.5	0.6785	0.6750	0.6555	0.6697	0.012
5	1.145	1.1445	1.1475	1.1457	0.002
10	2.0135	2.0000	2.051	2.0215	0.026
			Mean	**0.5576**	**0.009**
			Inter assay coefficient of variation	**1.66 %**	

Intra-assay and inter-assay reproducibility for Quantikine SDF-1α ELISA standards was robust with the coefficient of variation between repeats within the same trial falling between 1 and 4 %.

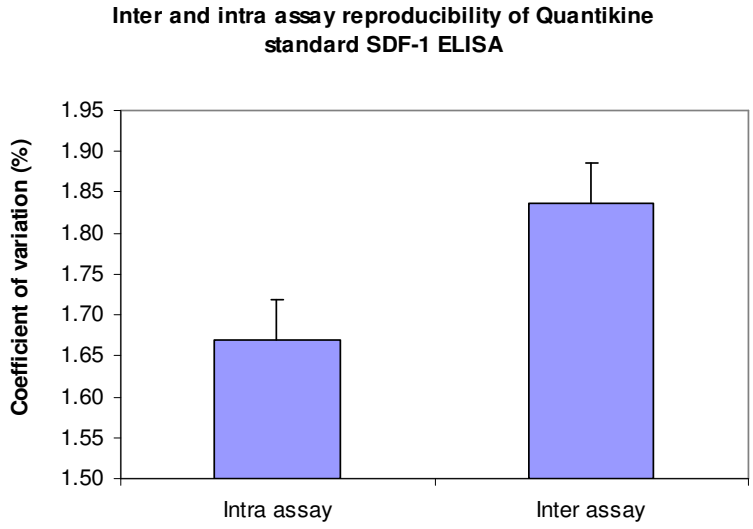

Figure 3.7. Intra and inter-assay assessment of reproducibility in Quantikine mouse SDF-1α ELISA standards.

3.4. Serum G-CSF measurments in mouse models

3.4.1. Aim

The aim of this study was to assess the reproducibility of G-CSF ELISA kit at both intra and inter-assay levels. Serum samples obtained from tail bleeds of $OPG^{-/-}$ mice and control $OPG^{+/+}$ mice were analysed. The immunoassay required preparation of standards, antibodies for target protein capture and detection, and involved a multiple-step protocol in its execution, all of which may introduce error.

3.4.2. Protocol

Serum G-CSF measurements were performed in duplicates. The results were used to calculate intra-assay coefficient of variation.

G-CSF amounts (or concentrations) were calculated using standard curves as per manufacture's instructions. Details are provided in Chapter 2 (section2.5.3). The mean (*M*)

and standard deviation (*SD*) of duplicate readings were calculated and the intra-assay coefficient of variation using the equation applied in section 3.2.3.

3.4.3. Results and conclusion

3.4.3.1. Intra-assay reproducibility

Intra-assay reproducibility for G-CSF standard measurements in a 12 month old mouse model is illustrated in Figure 3.8.

Plate 1

Std (pg\ mL)	O.D readings (450 nm)		Mean	Std dev
900	1.7110	1.7100	1.7105	0.0007
450	0.8940	0.9390	0.9165	0.0318
225	0.4630	0.4460	0.4545	0.0120
112.5	0.3760	0.3880	0.3820	0.0085
56.25	0.2340	0.2380	0.2360	0.0028
28.125	0.1100	0.1200	0.1150	0.0071
14.06	0.0970	0.0920	0.0945	0.0035
0	0.0650	0.0650	0.0650	0.0000
		Mean	**0.4968**	**0.0083**
		Intra assay coefficient of variation	**1.67 %**	

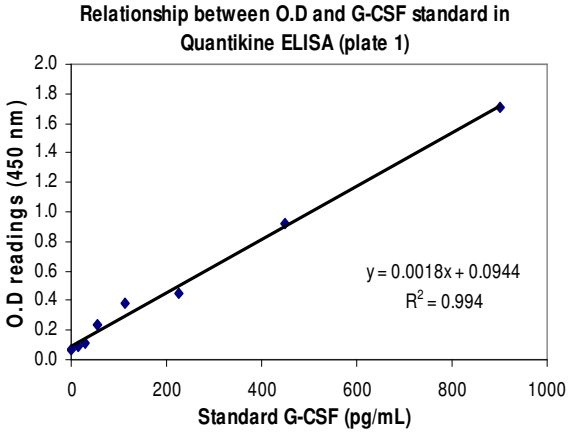

Plate 2

Std (pg\ mL)	O.D readings (450 nm)		Mean	Std dev
900	1.7410	1.7700	1.7555	0.0205
450	0.9130	0.9590	0.9360	0.0325
225	0.5120	0.4960	0.5040	0.0113
112.5	0.3670	0.3880	0.3775	0.0148
56.25	0.2240	0.2650	0.2445	0.0290
28.125	0.1800	0.1950	0.1875	0.0106
14.06	0.1210	0.0920	0.1065	0.0205
0	0.0950	0.0750	0.0850	0.0141
		Mean	**0.5246**	**0.0192**
		Intra assay coefficient of variation	**3.65 %**	

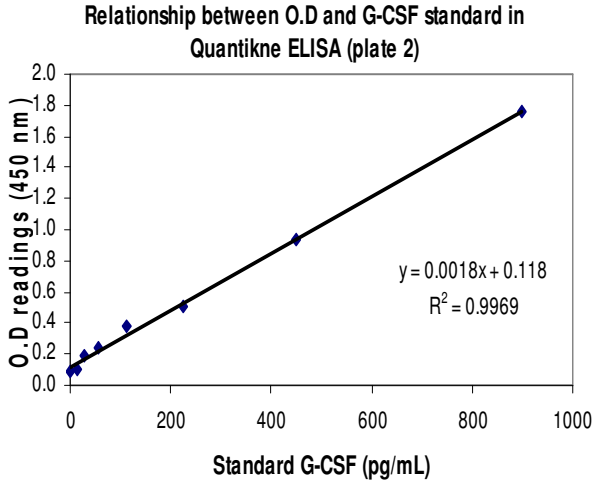

Plate 3

Std (pg\ mL)	O.D readings (450 nm)		Mean	Std dev
900	1.8840	1.6800	1.7820	0.1442
450	1.1000	1.0590	1.0795	0.0290
225	0.6180	0.5760	0.5970	0.0297
112.5	0.3670	0.3380	0.3525	0.0205
56.25	0.3750	0.3930	0.2840	0.0127
28.125	0.1900	0.1950	0.1925	0.0035
4.06	0.1110	0.0920	0.1015	0.0134
0	0.0790	0.0850	0.0820	0.0042
		Mean	**0.5589**	**0.0322**
		Inter assay coefficient of variation	**5.75 %**	

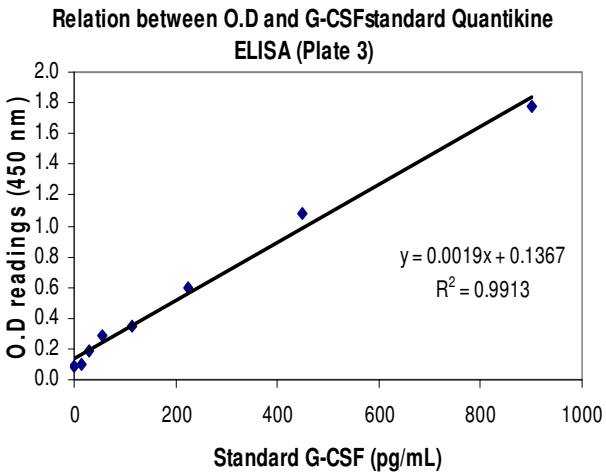

Figure 3.8. Intra-assay assessment of reproducibility for G-CSF standard measurements in 12 month old mouse model.

3.4.3.2. Inter-assay reproducibility

The results are presented graphically in Figure 3.9. Intra-assay and inter-assay reproducibility for Quantikine R&D G-CSF ELISA standards was robust with the coefficient of variation between repeats within the same trial falling between 2 and 7%.

Standard (pg\ mL)	Plate 1	Plate 2	Plate 3	Mean	Std dev
900	1.7105	1.7555	1.7820	1.7493	0.0361
450	0.9165	0.9360	1.0795	0.9773	0.0890
225	0.4545	0.5040	0.5970	0.5185	0.0723
112.5	0.3820	0.3775	0.3525	0.3707	0.0159
56.25	0.2360	0.2445	0.2840	0.2548	0.0256
28.125	0.1150	0.1875	0.1925	0.1650	0.0434
14.06	0.0945	0.1065	0.1015	0.1008	0.0060
0	0.0650	0.0850	0.0820	0.0773	0.0108
			Mean	**0.5267**	**0.0374**
			Inter assay coefficient of variation	**7.10 %**	

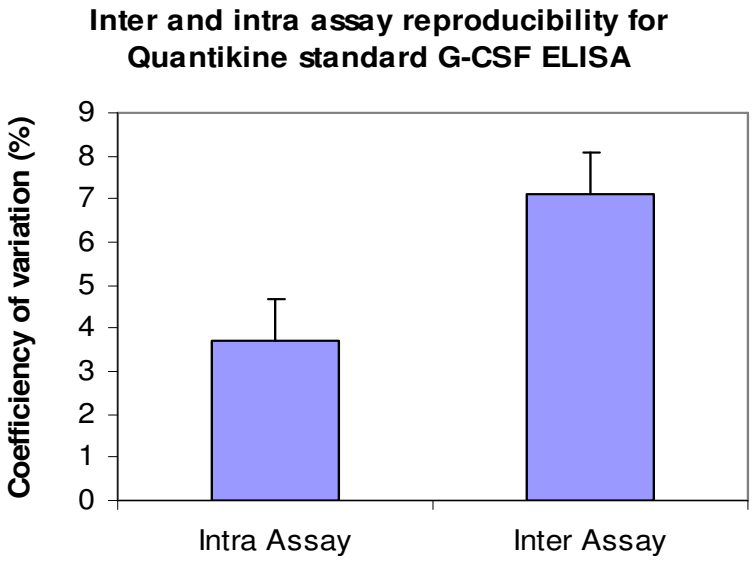

Figure 3.9. Intra and inter-assay assessment of reproducibility in Quantikine mouse G-CSF ELISA standards.

3.5. Flow cytometry standardisation for animal experiments

The flow cytometry (FC) protocol for animal experiments is outlined in Chapter 2 (section 2.6). The analysis of surface marker expressed by FC requires a multi-step protocol which requires optimisation and standardisation. The optimisation of all the stages required for analysis of mice samples is described below.

3.5.1. Tail bleeds time points

For the mouse model experiments in Chapter 5 and 6 , tail bleeds were obtained at four (4) different time points from both male and female (experimental and control groups) to assess day-to-day fluctuation. Multiple tail bleeds on different occasions were obtained taken because the circulating population of interest may vary over time. Repeat assessments also assists in determining inter analysis variability. All bleeds were taken in the mornings (8.30 am-10 am). An internal comparison between experiments was possible because of this multiple bleeds repeated at the same time of the day.

3.5.2. Lysis buffer

A lysis buffer consisting of ammonium chloride and potassium chloride (ACK) was used to achieve the red blood cells (RBC) lysis (Appendix 4). Eliminating the RBC content from the whole blood is crucial as they interfere in the antigen-antibody interaction. A pilot study was carried out before determine the incubation time required for RBC lysis. This step was important in differentiating the dead cells from the viable cell types which was analysed during FC analysis. The following incubation times were examined:

<u>Incubation for 10 min or 20 min</u>

This step did not provide the optimum level of lysis (Figure 3.10 A) as the incubation resulted in incompletely lysis of RBC. The partially lysed RBC interfered with the viable cells which resulted in unclear separation of dead cells from viable cell types. After this, blood was incubated for 20 min at a stretch to check for ideal lysis. However, this also resulted in unconvincing lysis of the RBC (Figure 3.10 B). Overall, the incubation steps for 10 min and 20 min did not result in lysis of RBC.

A further lysis technique was therefore developed. The blood samples were incubated with lysis buffer for an initial phase of 10 min followed by a 5 min washing step and centrifugation at 400x g. The cell pellet obtained was further incubated with lysis buffer for 5 min. A further washing was performed and the cells were analysed by FC using the same instrument settings as previous attempts (Figure 3.10 C). The FC plots showed a desirable level of lysis of RBC evident by a clear separation of lysed RBC from the viable cell types (lymphocytes, monocytes and granulocytes). After repeating the similar lysis protocol for consistent results the method was adopted for future experiments.

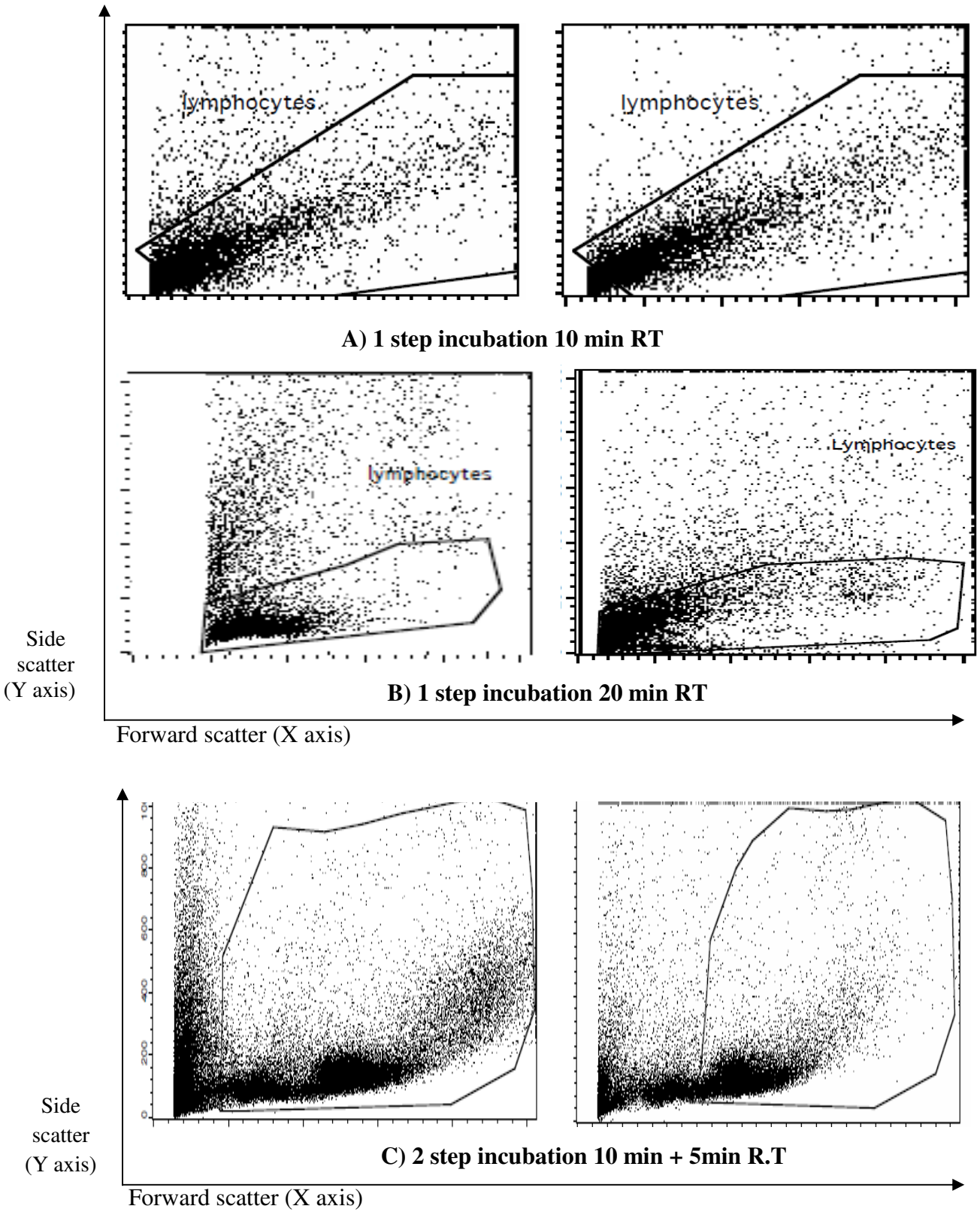

Figure 3.10. Optimisation of ACK lysis buffer using different incubation time periods and conditions

3.5.3. FcR blocking

This step is a pre-requisite for eliminating any non-specific binding of the primary antibody or isotype to the cell antigen surface thus ensuring optimum antigen-antibody binding. Various concentrations of the blocking agent were assessed out to determine the optimum titre of the blocking agent. Dilutions of 1:10 (Figure 3.11 B), 1:50 (Figure 3.11 C), 1:100 (Figure 3.11 A), and 1:500 dilutions were assessed. A titre of 1:50 was found to provide most sufficient blocking of non specific binding.

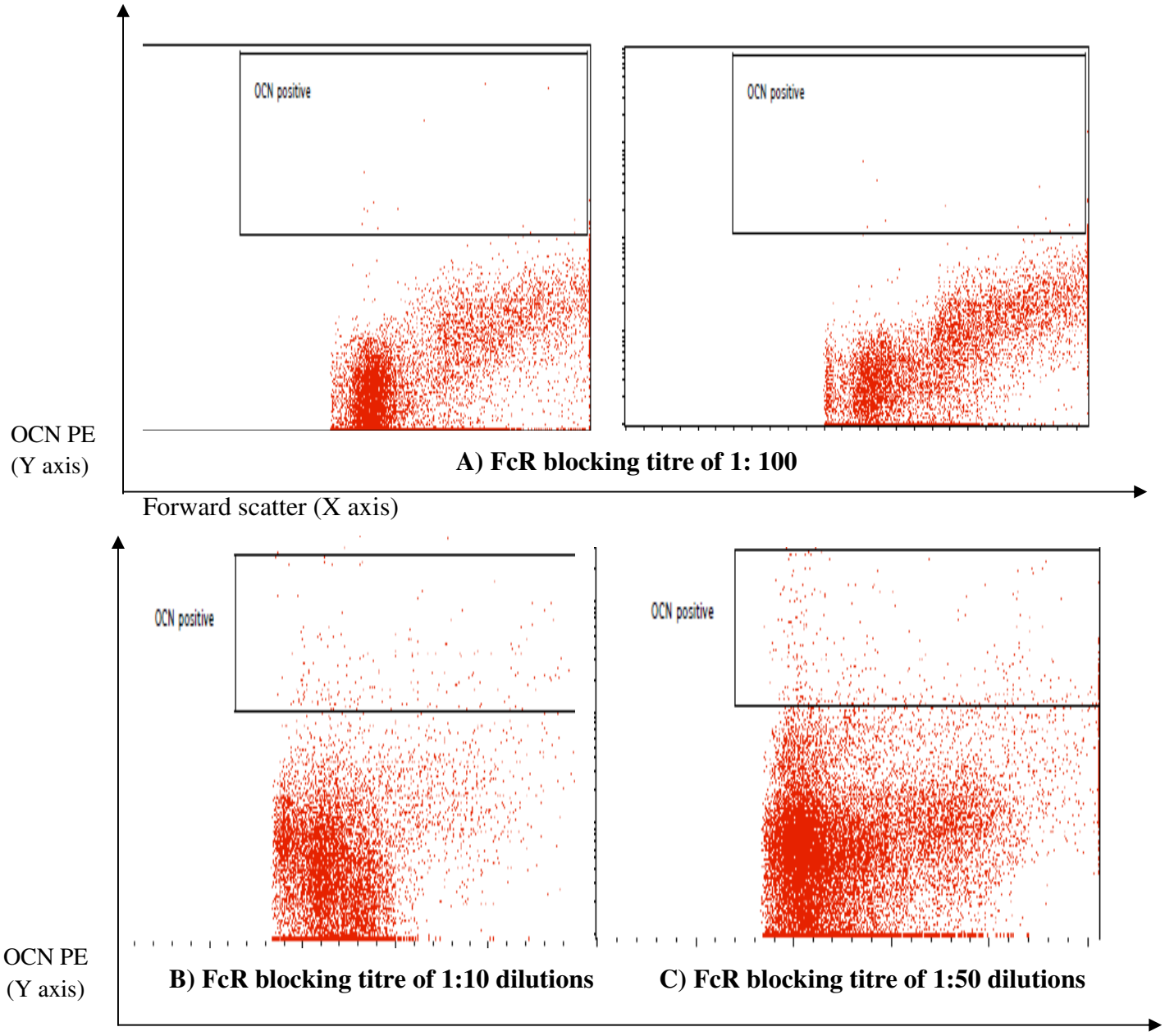

Figure 3.11. Optimisation of appropriate FcR blocking concentration using variable titres

3.5.4. Primary OCN antibody labelling

This step involved the binding of a primary OCN antibody to the cell antigen surface. The appropriate antibody titre would encourage bindings to all OCN antigen expressing cells avoiding non specific binding. This binding step needs to be specific as this is followed by the secondary antibody binding. If the titre of the OCN antibody is less there won't be sufficient binding to cover the entire OCN expressing antigen cell population. To optimise this step different titre of OCN antibody was examined in a pilot study. A series of dilutions including 1:25 (Figure 3.12 B), 1:100 (Figure 3.12 C), 1:500 (Figure 3.12 A), and 1:1000 were tested. 1:100 was worked out to be the most optimum dilution which effectively bound to the primary OCN. This titre was considered to the optimum as both 1:100 and 1:25 dilutions stained equal percentage of OCN population in same blood samples.

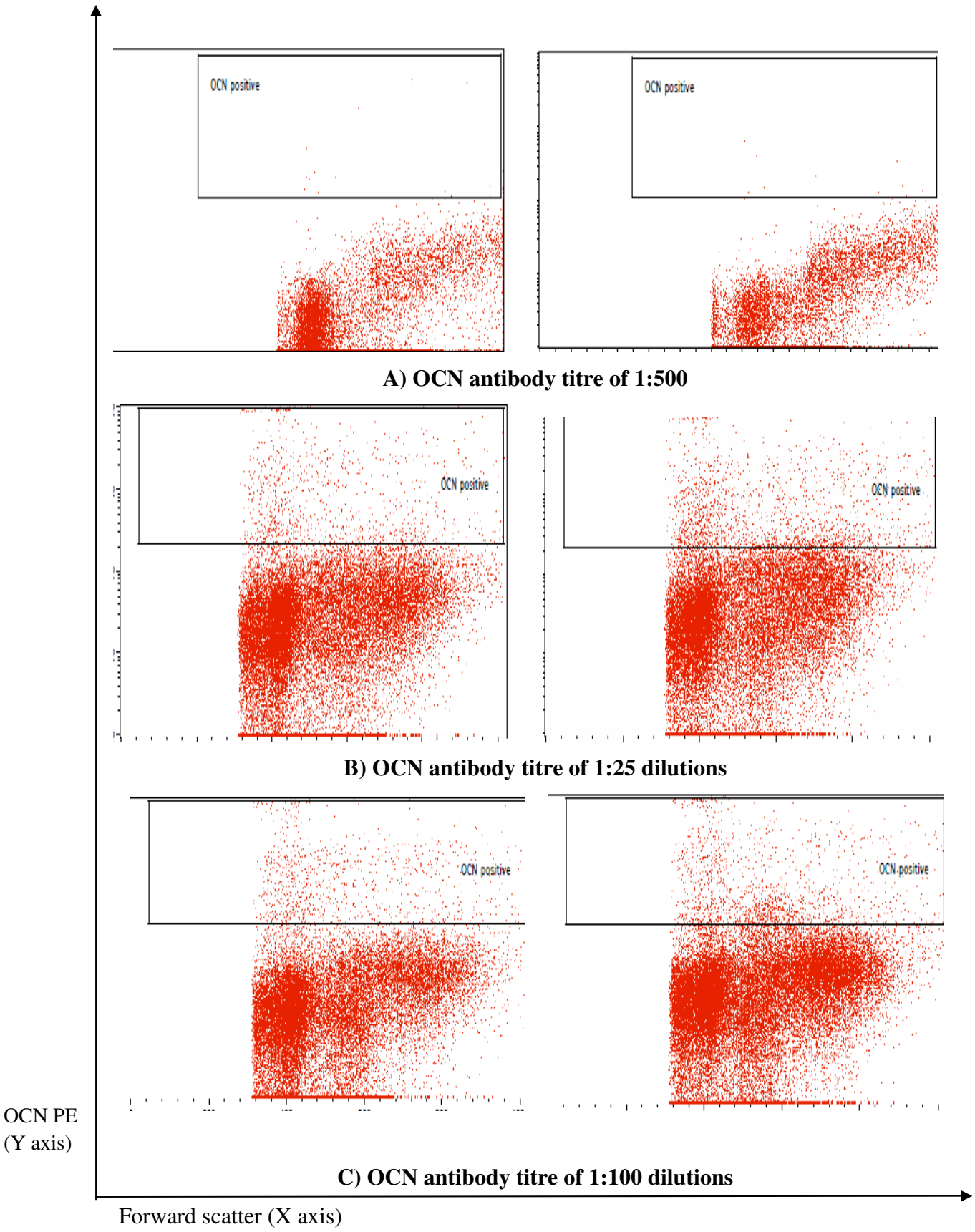

Figure 3.12. Optimisation of appropriate OCN primary antibody dilution using variable titres

3.5.5. Secondary Phycoerythrin (PE) antibody labelling

Secondary antibody titres are equally as important as that of primary antibody to enable assessment sensitivity and specificity.

A PE conjugated secondary antibody was used (Anti-goat, Jacksons Immunoresearch, USA). 1:25 (Figure 3.13 B), 1:100 (Figure 3.13 C), 1:500 (Figure 3.13 A), 1:1000 dilutions were used to work out the required dilution. 1:75 was worked out to be the ideal dilution for effective binding.

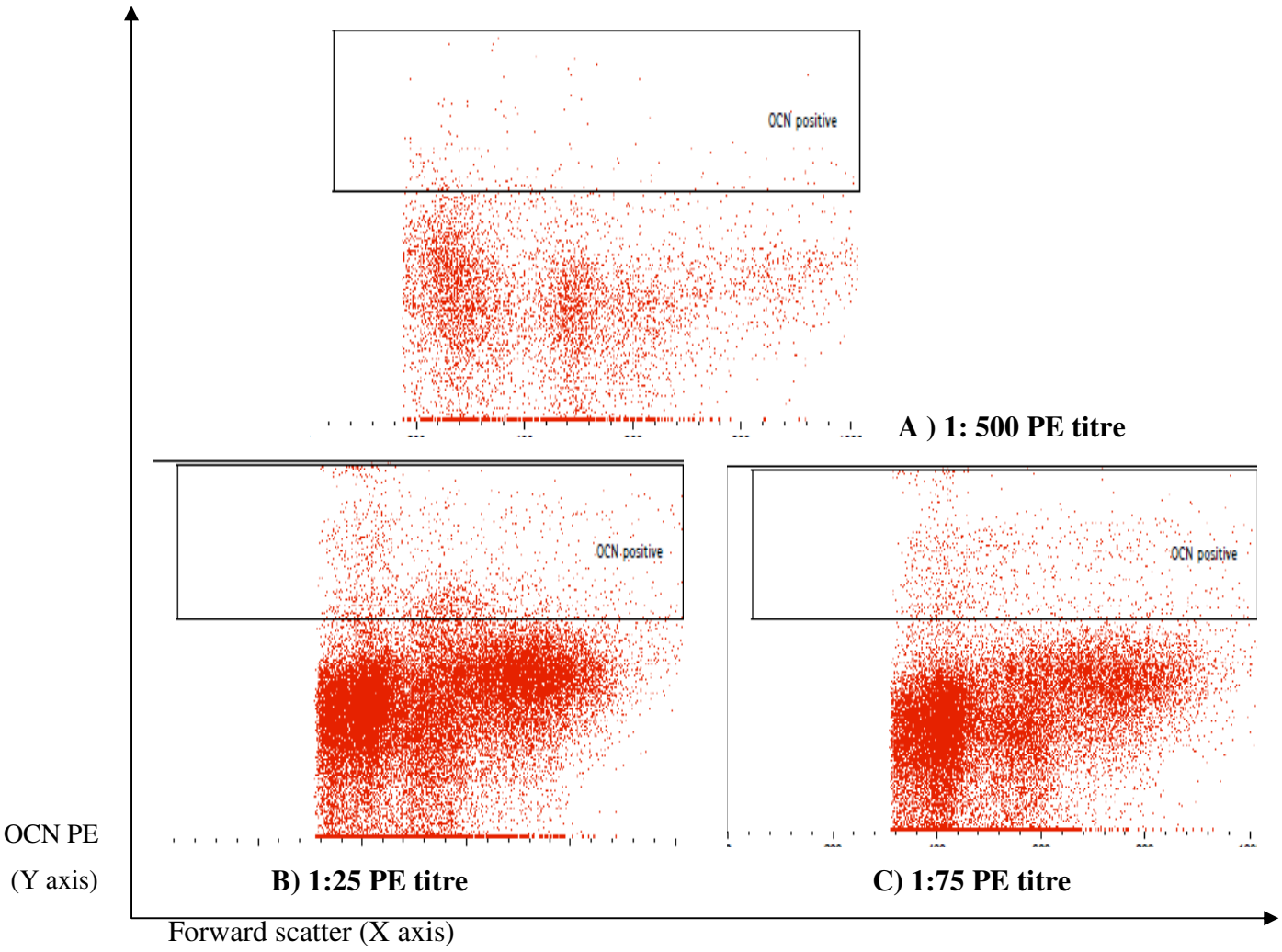

Figure 3.13. Optimisation of appropriate PE secondary antibody dilution using variable titres

3.6. Flow cytometry instrumental and data interpretation of mice OCN expression

3.6.1. Forward scatter (FSC) vs. Side scatter (SSC) settings

On the forward versus side scatter plot the region comprising of viable cells were selected for further analysis. Dead cells (extreme left of the dot plot) were excluded from the gated region (Figure 3.14). Once the first region of interest was selected it was followed on the next dot plot which comprised of OCN (Y axis) versus FSC (X axis). A region statistics was calculated to determine the percentage of OCN^+ MNC. A total number of around 50,000 events were acquired. For consistency between experiments, similar numbers of events were acquired during analysis of all mouse blood samples.

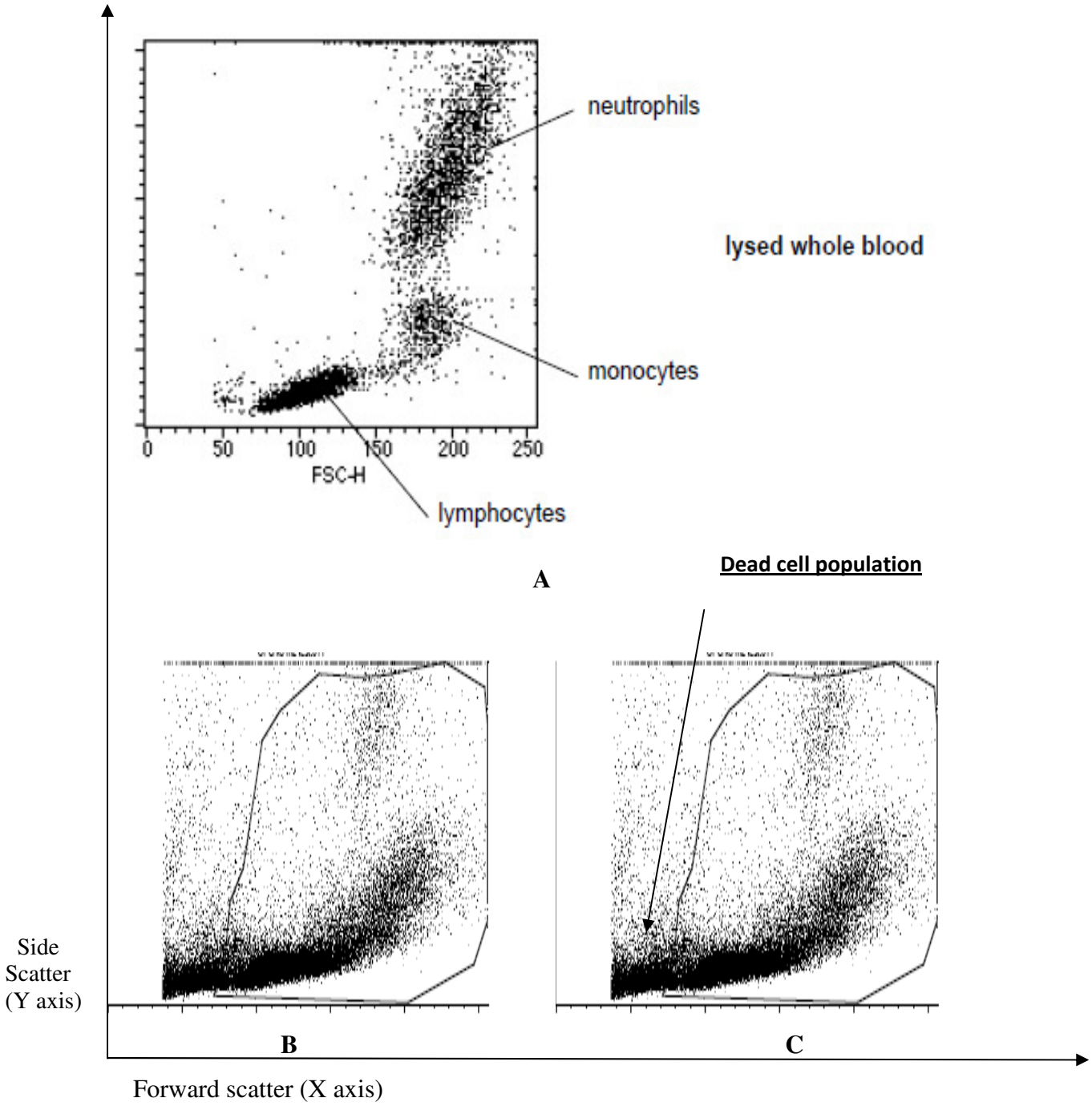

Figure 3.14. Schematic diagram of the basic FSC vs. SSC dot plots acquired during the experiments. A, B, C are examples which represents the first plots from different FC runs. Dead cells were excluded from the analysis. All other viable cells were selected for quantifying the positive cell population.

3.6.2. Unstained population

An unstained sample (without any fluorescent dye) is analysed prior to testing the other samples (Figure 3.15). These readings are applied for standardising the instrument settings for the fluorescent PE channel in the experiments. This step ensures optimum laser power required during the FC analysis for the test samples.

The FSC versus SSC plot used to differentiate and select the viable MNC onto the next dot plot for OCN vs. FSC. Applying this gate filters down the analysis of viable cells which enables in choosing the region of interest.

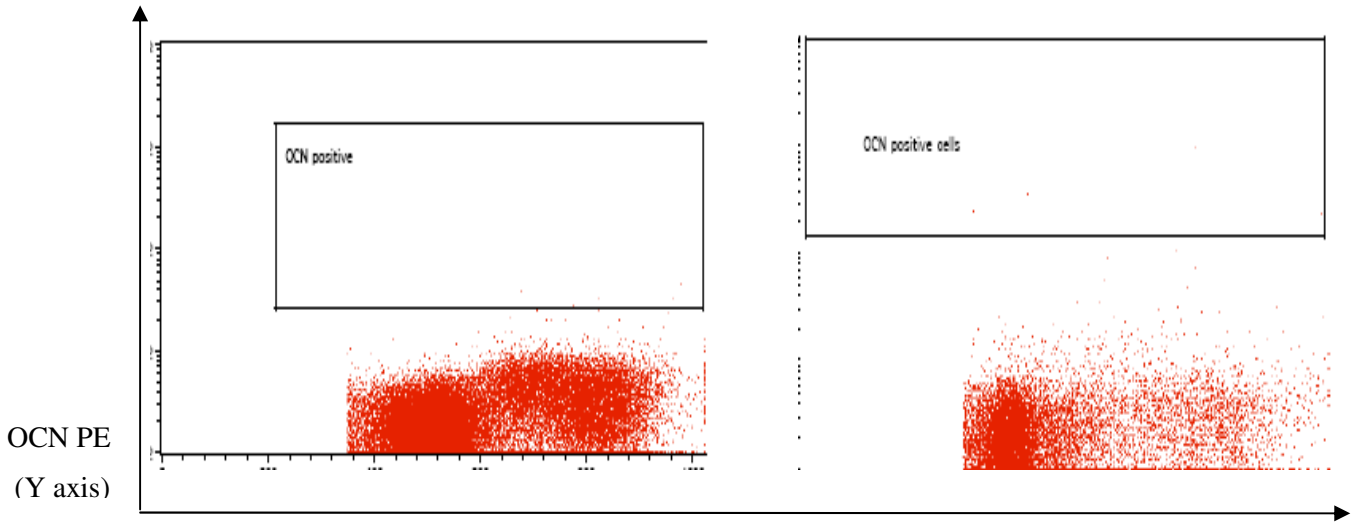

Figure 3.15. Dot plots for an unstained sample gated on SSC (OCN^+) vs. FSC plot.

3.6.3. Establishing appropriate gates for positive staining

An isotype control sample was analysed prior to assessing OCN^+ MNC staining which determined the gates for the positive population. Figure 3.16 below illustrates the gates defined based on the isotype control. Any acquired MNC in this selected region from the subsequent primary antibody stained samples was calculated as OCN^+ expressing population. Ideally, the gate statistics for an isotype tube is close to 'zero'. However this may not be practically possible at all times as during most of analysis there is a small percentage of non-specific background which has to be considered while calculating the final percentage for OCN^+ MNC population. The readings from

OCN^+ staining were subtracted from isotype control reading. Any background positive percentage was eliminated in this way, making the calculations more accurate. This was carried out for each sample during the experiments.

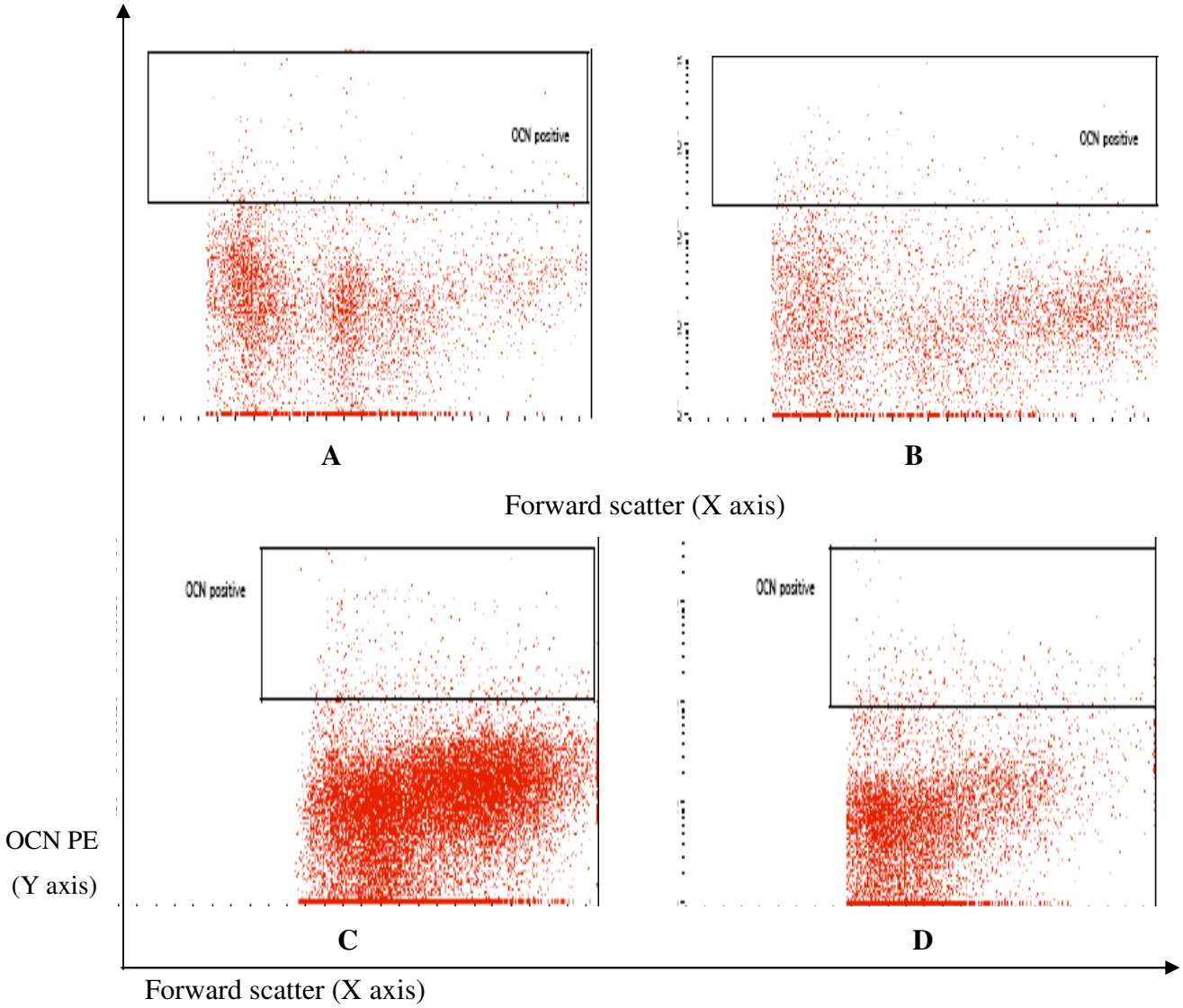

Figure 3.16. Dot plots for isotype controls. A and B represents plots for $OPG^{+/+}$ mice blood while C and D represents plots for $OPG^{-/-}$ mice blood samples.

These plots are illustrated in Figure 3.17 for different blood samples obtained from $OPG^{+/+}$ and $OPG^{-/-}$ mice samples. The region statistics from the isotype plots were subtracted from the OCN^+ staining results to achieve a corrected percentage of OCN^+ staining MNC.

3.6.4. Positive population gating

After the isotype stained samples, the OCN^+ stained samples were immediately assessed. For standardisation, in all the experiments the $OPG^{+/+}$ samples were run followed by $OPG^{-/-}$ samples. This pattern ensured minimal intra experimental error if any. Figure 3.17 represents the gated region from positive samples of both $OPG^{+/+}$ and $OPG^{-/-}$ samples.

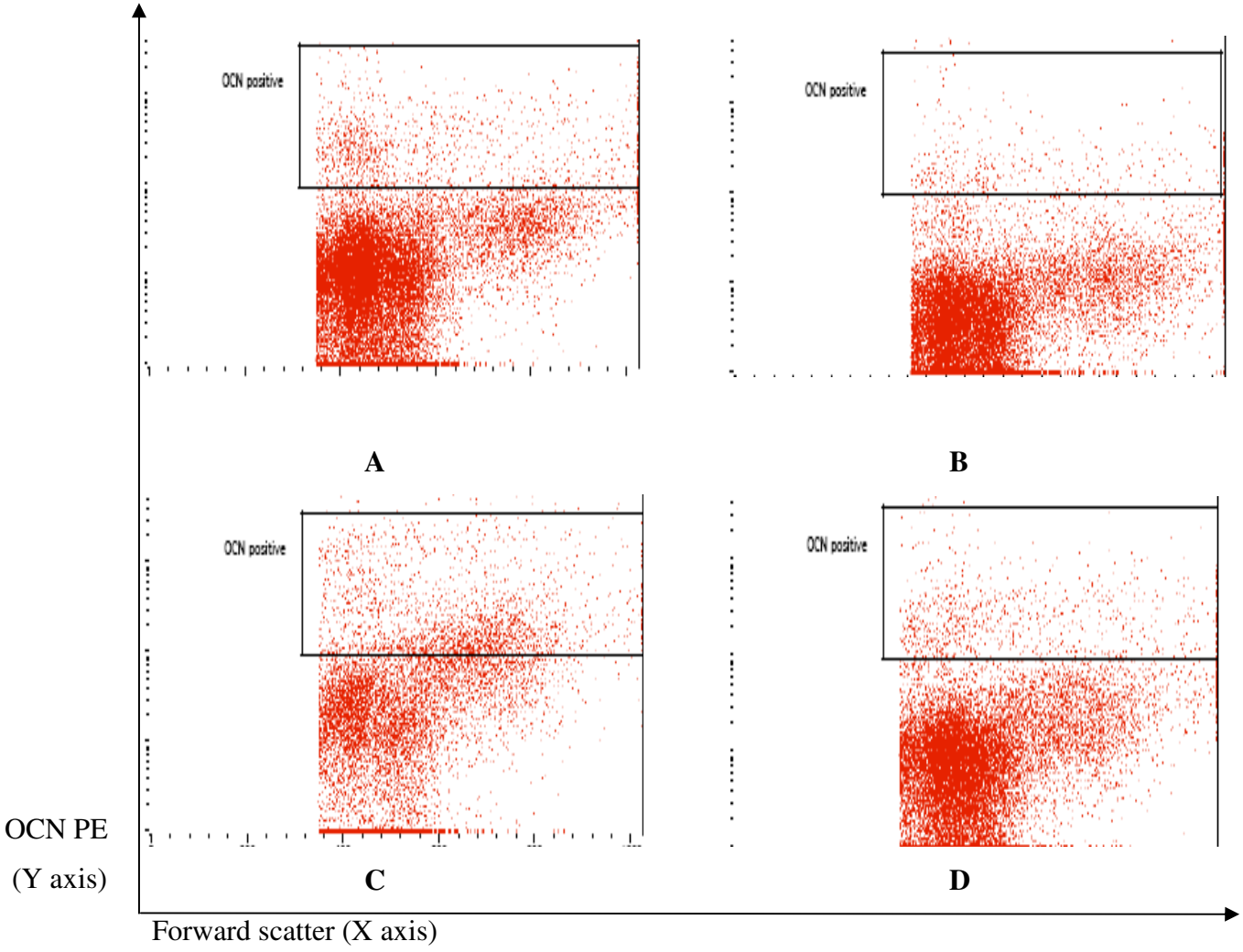

Figure 3.17. Dot plots analysing OCN^+ stained samples. The positively labelled samples were analysed on FC post isotype tubes for each sample. A and B represent plots for $OPG^{-/-}$ samples while C and D corresponds to $OPG^{+/+}$ sample dot plots for OCN^+ MNC population.

3.6.5. Calculation of positive population cell percentage

Statistical analysis was performed to estimate the percentage of circulating OCN^+ MNC in mouse tail bleeds. 'Cell Quest' software (BD biosciences, USA) was used for final FC calculation. Selecting the region statistics option in the Cell Quest FC software displays the total number of cells selected in a particular region of the gates applied in the experiment. For all the samples in the present investigation, two statistical readings were displayed. The first region was the gate which was applied for the basic FSC versus SSC plot. This region is "region 1" or "R1" and it was defined as "All cells" in the gate. The same terminology was used in the region statistics performed for all the samples. The second selected region (gate) was a subset of the first gate. The numbers in this region represent cells potentially expressing OCN^+ MNC. Figure 3.18 below illustrates examples of region statistics for $OPG^{-/-}$ and $OPG^{+/+}$ tail bleed samples. The statistics window details include the region gate names, cell numbers and positive cell percentages for each sample. Other specifics such as sample name, number of events acquired, X-Y parameters and date of the experiment conducted is also displayed.

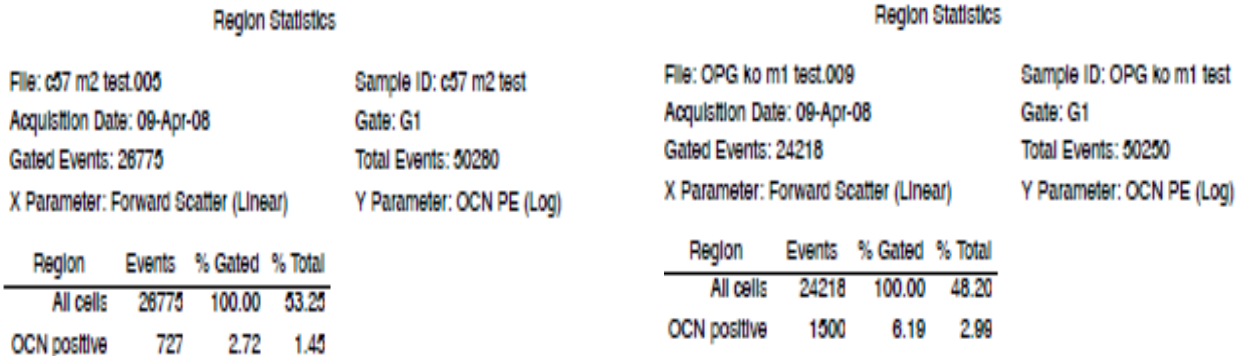

A **B**

Figure 3.18. Examples of FC readouts for blood samples from $OPG^{+/+}$ (A) and $OPG^{-/-}$ (B) mouse blood samples.

3.7. Flow cytometry standardisation for human experiments

Similar to mouse model experiments, optimising FC protocol steps for blood samples obtained from human patient cohort was also important to obtain consistent and reproducible results.

3.7.1. Ficoll histopaque technique for mononuclear separation

A detailed protocol for MNC separation using ficoll hypaque from human blood sample is provided in Chapter 2. Certain parameters were considered for collecting maximum MNC. Blood samples were initially diluted 1:2 before ficoll histopaque overlay. The ficoll hypaque need to be at R.T before use. The ratio between the ficoll histopaque solution and the blood was at 1:2.5 for every separation to ensure optimal MNC recovery as previously described[238]. After layering the blood samples, the tubes were centrifuged at 400xg for 30 min without brakes to avoid any mixing of separated cell layers[170,239]. After MNC recovery, the cells were washed twice with an isotonic buffer consisting of 0.5 % chicken albumin and 2mM EDTA[239]. Washing ensures the elimination of any carry over platelets from blood. Cells were counted on haemocytometer followed by FcR blocking[239].

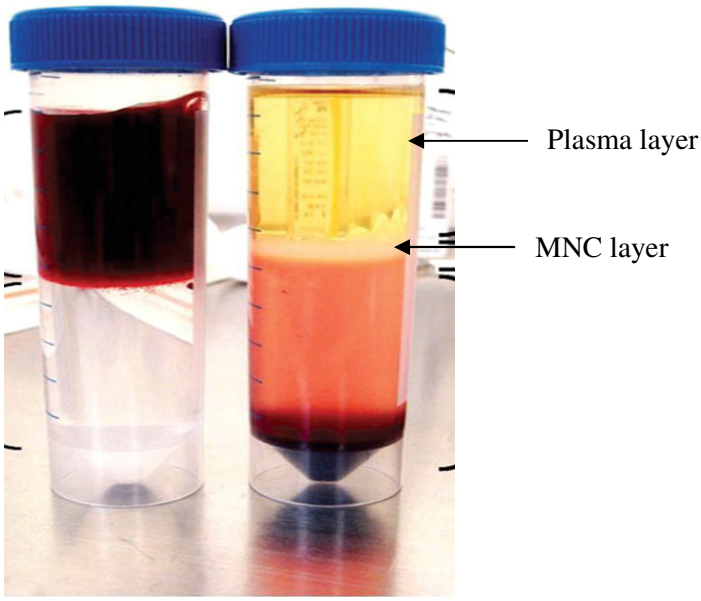

Before centrifugation After centrifugation

Figure 3.19. Mononuclear cell separation by the ficoll histopaque method.

3.7.2. Human FcR blocking

A human FcR block (Miltenyi Biotech, USA) was used. FcR block combined with 10 % donkey serum was used to block the cells. 20 µl of FcR block solution was used for every 10^7 cells. The cells were incubated at R.T for 20 min after which they were washed twice with isotonic buffer for optimal recovery of cells[170,239].

3.7.3. Primary OCN antibody labelling

Once the FcR block was removed by washing the cells with FC buffer, the cell suspension was split up into two equal parts; one for primary OCN and other for isotype control labelling. The appropriate OCN antibody titre was determined before analysing any patient samples. 1:50 (Figure 3.20 B), 1:100 (Figure 3.20 C), 1:500 (Figure 3.20 A) and 1:1000 titres of antibody were assessed by FC analysis. It was noted that an antibody dilution of 1:100 was ideal for optimum antigen-antibody reaction as the percentage of stained OCN^+ MNC was found to be similar for 1:50 and 1:100 dilutions for the same blood samples. An IgG isotype was also used at a similar dilution as the OCN antibody. Using a constant dilution enabled an appropriate comparison for FC results. The cells were incubated at 4^oC for 30 min for optimum antigen-antibody cell binding.

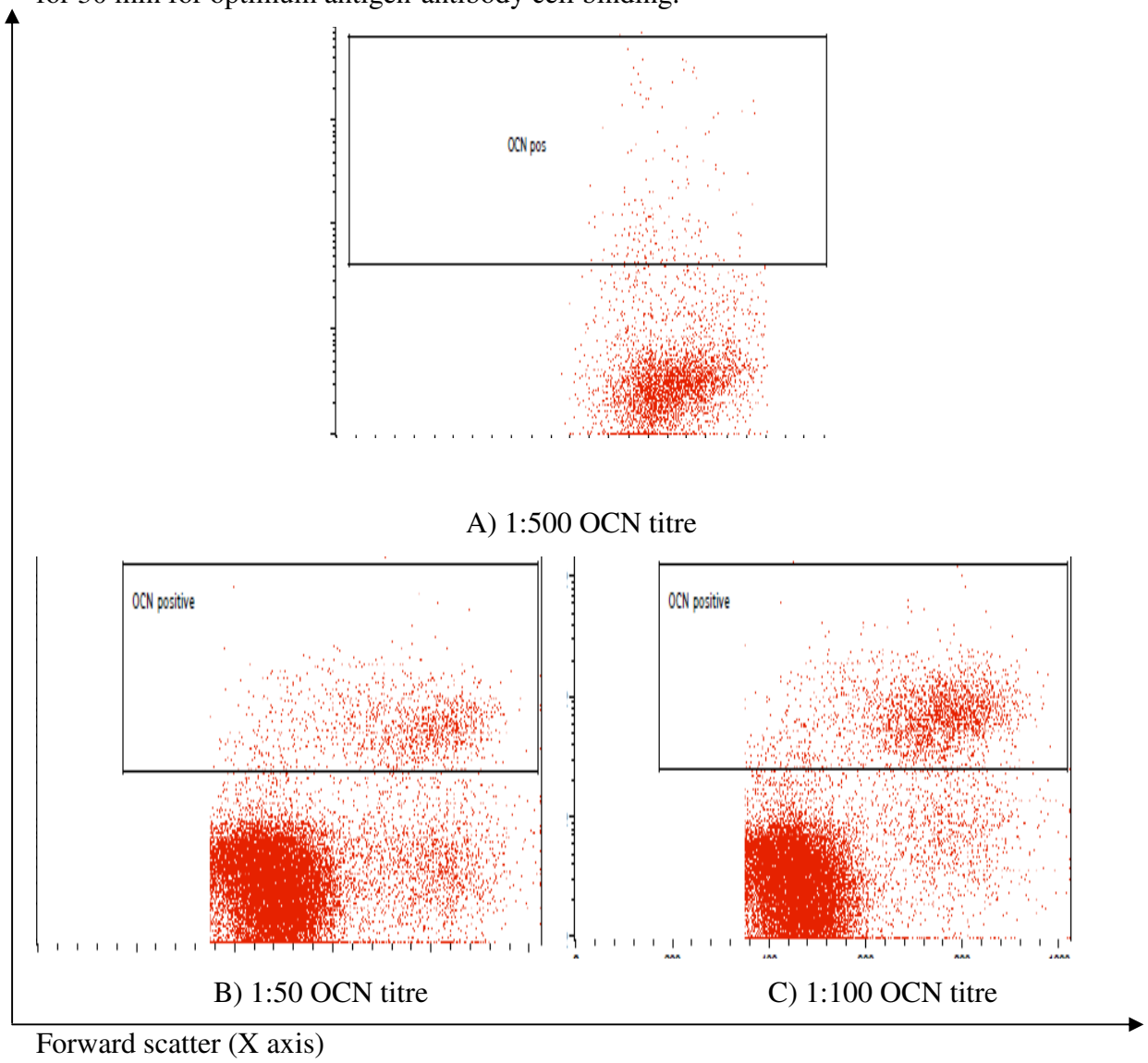

Figure 3.20. Optimisation of primary OCN antibody dilution at variable titres.

3.7.4. Secondary Phycoerythrin (PE) antibody labelling

A PE conjugated secondary antibody (Jacksons Immunoresearch, USA) was used to tag with the antigen- antibody complex. Similar to the primary antibody, a combination of dilutions were tested to identify optimal concentration. 1:50 (Figure 3.21.B), 1:100 (Figure 3.21 C), 1:500 (Figure 3.21 A) and 1:1000 were tested to tag with the primary antibody. 1:100 titre was demonstrated to be the optimum secondary binding as similar fluorescence intensity was also observed for 1:50 dilutions for same blood samples as observed in Figure 3.21 B and C respectively.

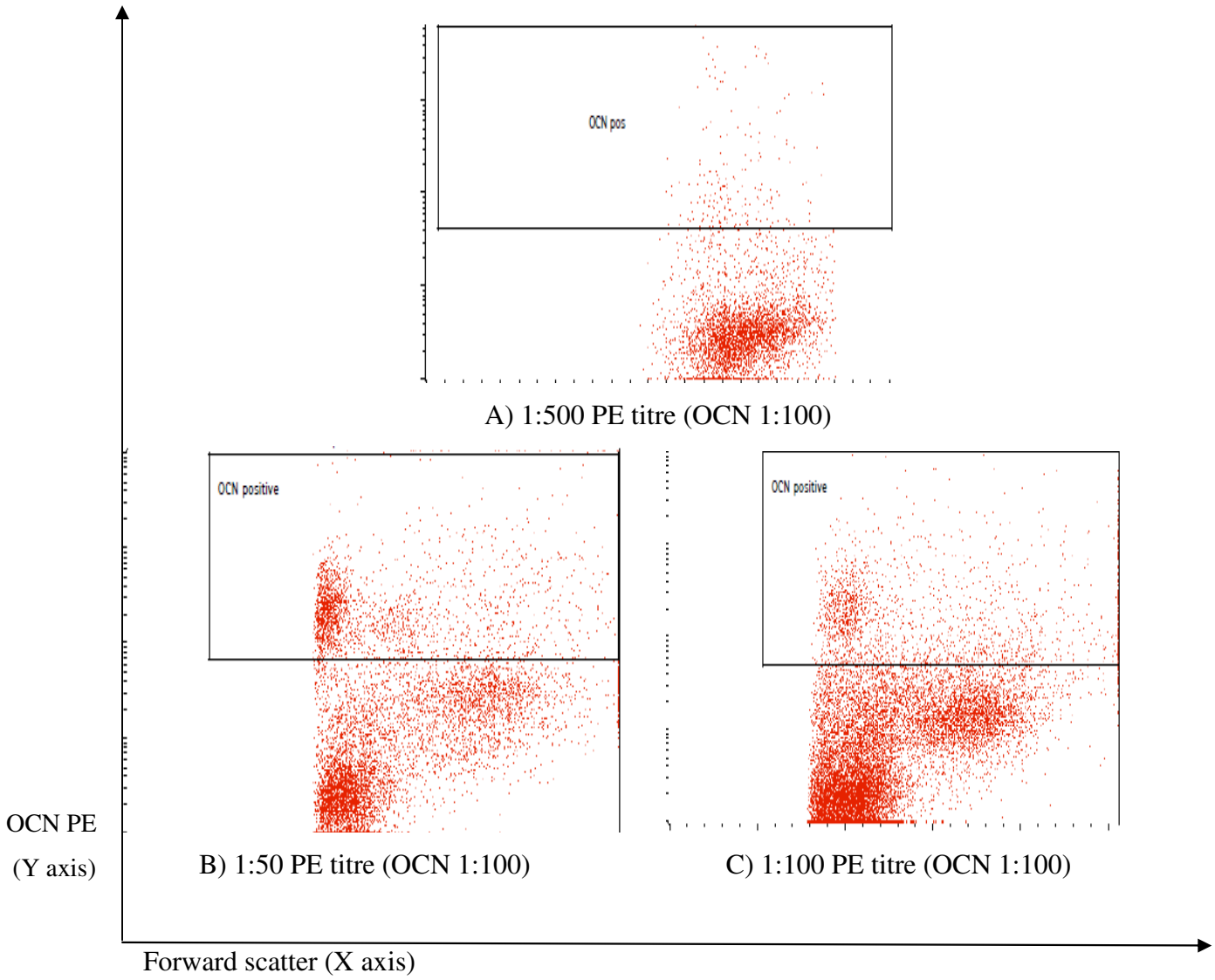

Figure 3.21. Optimisation of fluorescent secondary PE antibody dilution at variable titres.

3.7.5. Anti-PE magnetic beads

Anti-PE magnetic micro beads (Miltenyi, USA) were used for magnetic enrichment of OCN^+ labelled MNC tagged with fluorescent PE secondary antibody. These beads have special magnetic properties which are specific to the PE tagged secondary antibody. During incubation, these beads adhere to the fluorescently labelled PE which is primarily attached to the OCN antigen. Under the magnetic force of the column, these beads, along with the antigen-antibody complex, adhere to the column which is collected as the positively labelled fraction. The eluted fraction is considered negatively labelled. 20 µl of micro beads were used/10^7 cells as per as manufacturers' instructions. Cells were washed with appropriate buffer to remove excess beads attached to the cells and incubated at 4^oC for 20 min.

3.7.6. Magnetic separation (MS) columns

A MS column was used for separation of the positively labelled OCN^+ MNC population. The anti PE beads adhering to the OCN^+ MNC population are enriched under magnetic influence thus pulling out the population of interest. The enrichment step was necessary because the OCN^+ MNC population was limited in circulating blood and analysing blood samples without enrichment may have resulted in some OCN^+ MNC escaping the analysis amidst the large pool of other cellular population.

3.8. FC instrumental settings and data interpretation for human samples

3.8.1. FSC versus SSC settings and unstained population

The FSC and SSC plots were similar to that previously described for mouse model experiments. Briefly, an unstained sample was initially analysed to determine the FSC and SSC on a dot plot. The voltage and laser power was standardised for the fluorescent PE channel. Figure 3.22 represents the dot plots for unstained samples. The primary FSC vs. SSC gate was applied on the fluorescent gate. A near reading of 'zero' in the unstained region of the OCN-PE gate reflects the appropriate instruments for the actual OCN^+ and isotype labelled samples.

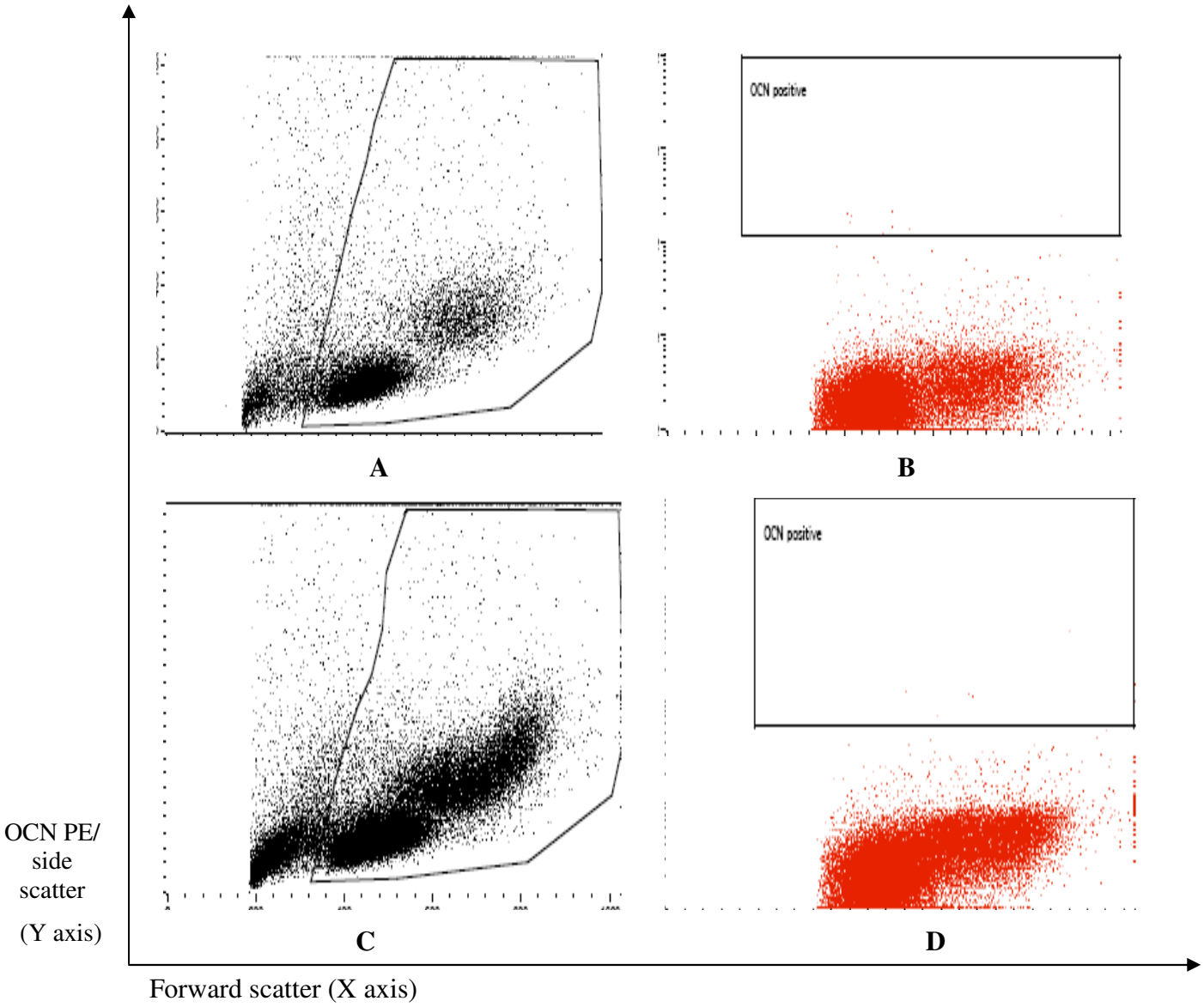

Figure 3.22. Dot plots for unstained samples. A and C represents FSC vs. SSC plots for two of the patient samples. The selected region is then gated on the fluorescent PE channel to obtain a positive population number. For an unstained sample this number is near 'zero' as evident in B and D.

3.8.2. Negatively labelled fraction

The negatively labelled fraction (obtained after MS separation) was labelled with isotype or OCN^+ MNC makers were analysed by FC as described for mice blood samples. Although the findings for the negative fraction was independent of the positive fraction, these results showed if any positively labelled cells escaped the magnetic force of the MS column. This population was demonstrated to be considerably near zero, illustrating minimal cells loss

from the magnetic column during separation. Figure 3.23 represents an example of the plots of negatively labelled samples stained for isotype and OCN^+ MNC.

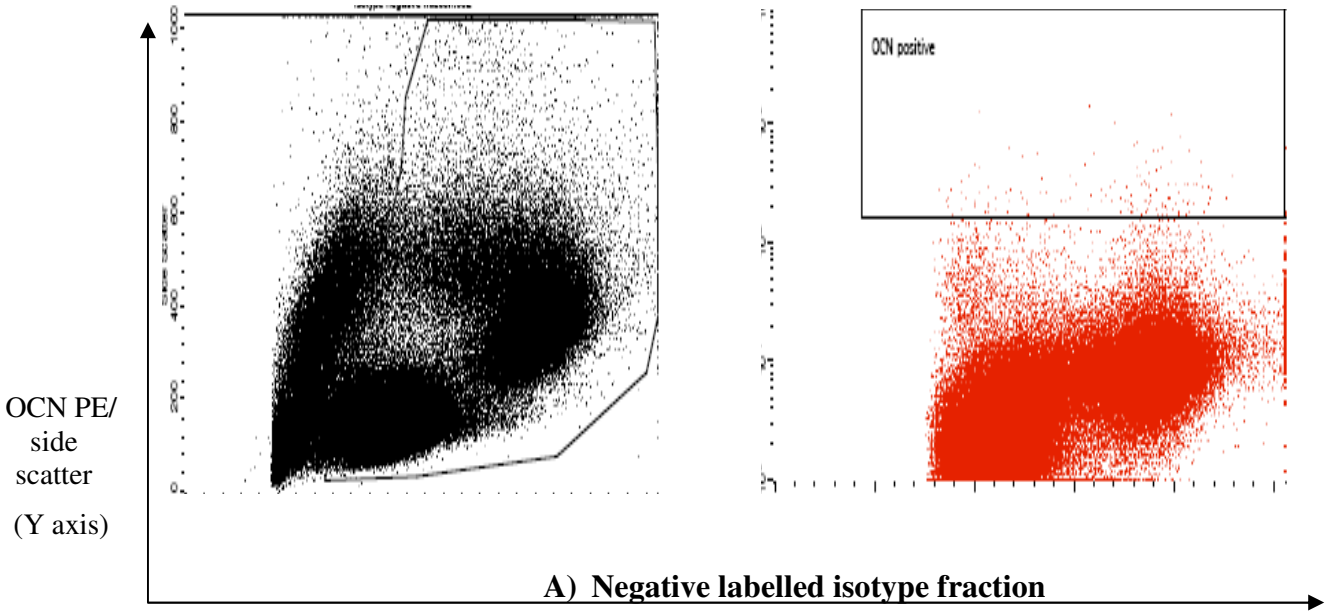

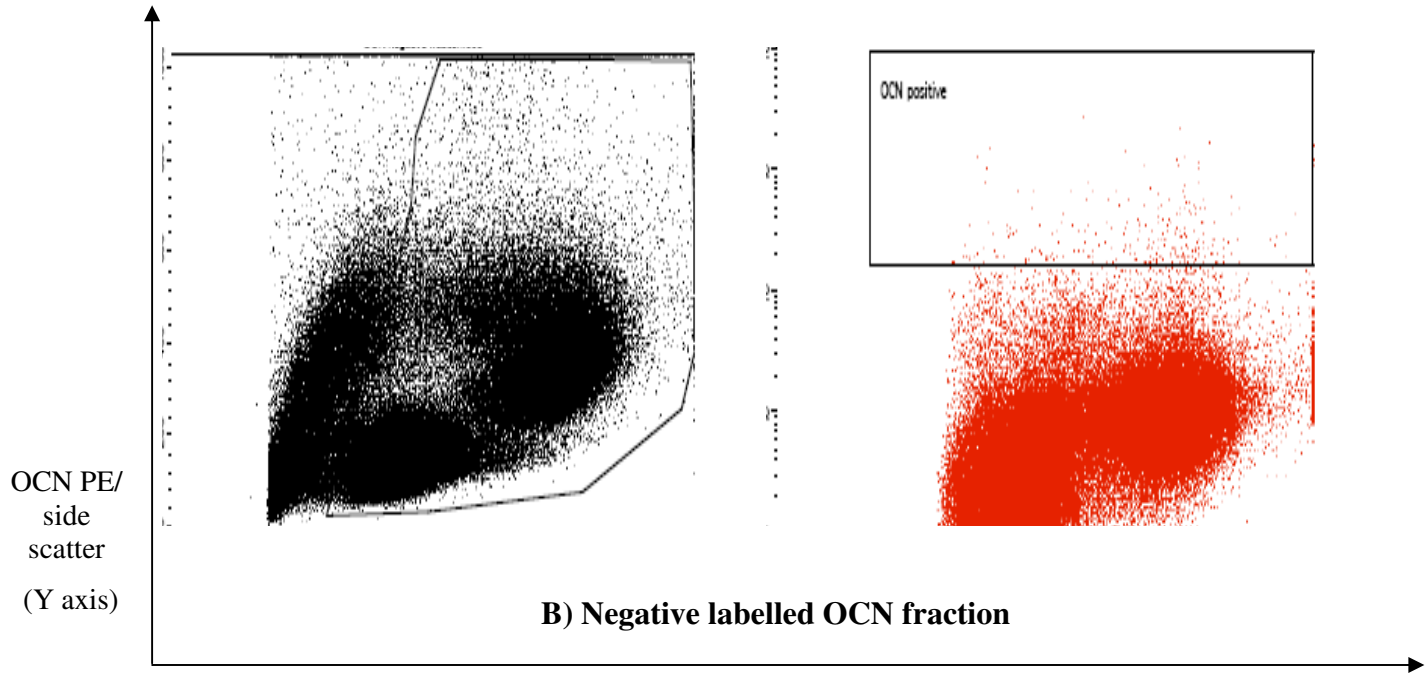

Figure 3.23. Dots plots for negatively labelled sample. A) Samples labelled for isotype B) Samples labelled for OCN^+ MNC. The difference in the OCN-PE gate for both the plots is minimal reflecting the effectiveness of the MS column separation. All the positively labelled cells were enriched on the MS column without cells into the negative fraction.

3.8.3. Positively labelled fraction

A cell count was carried out for this positively labelled fraction using a haemocytometer. After the cell count this fraction was similarly analysed on FC. Examples of these are illustrated in Figure 3.24.

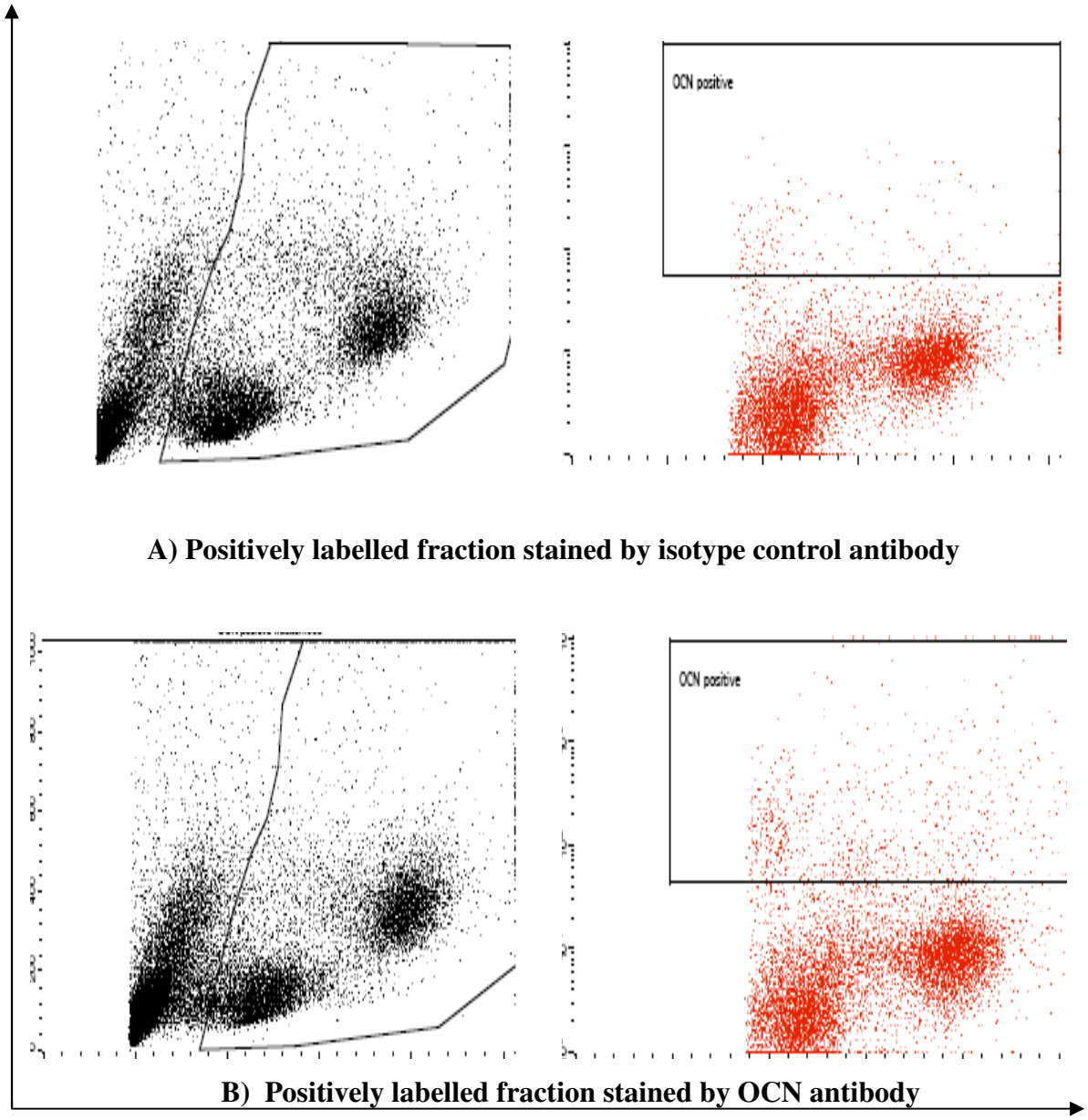

A) Positively labelled fraction stained by isotype control antibody

B) Positively labelled fraction stained by OCN antibody

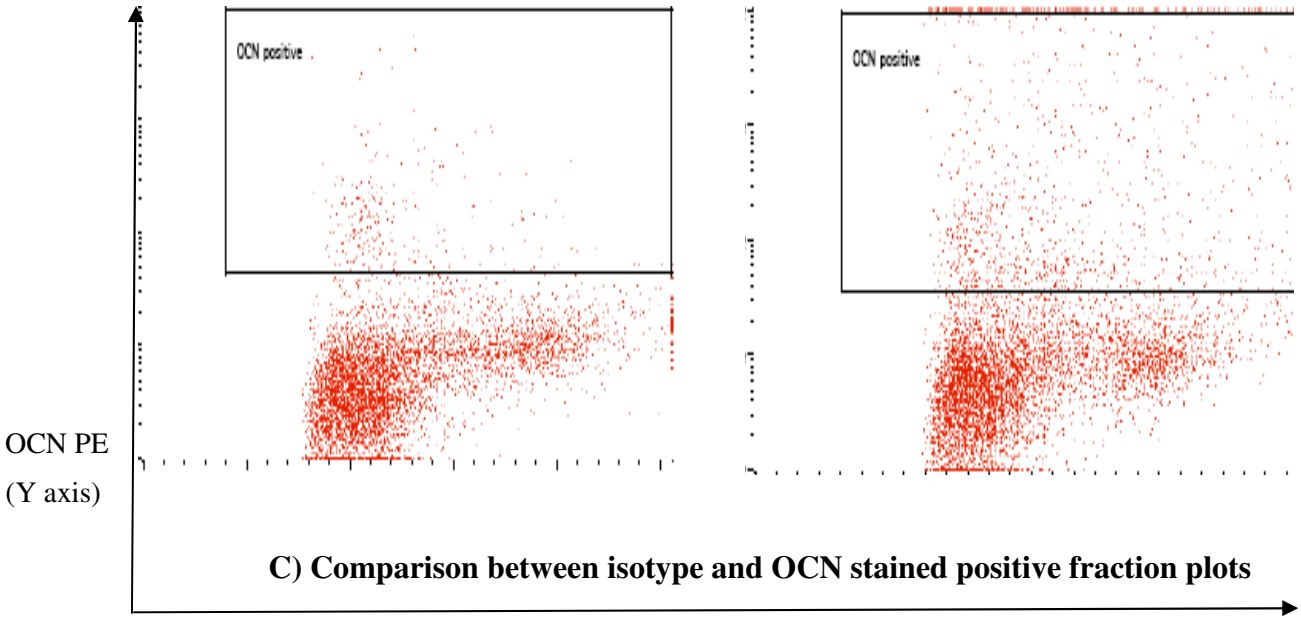

Figure 3.24. Dot plots of OCN positively stained population. A) Positively labelled fraction stained by isotype control antibody B) positively labelled fraction for OCN stained antibody and C) comparison between isotype and OCN stained plots

3.8.4. Calculation of OCN^+ MNC

Once all samples were analysed, statistical analysis was performed using the selected gates. The procedure for setting the gates and selecting the gate statistics were similar to the mouse model experiments (section 3.6.5). Briefly, the region statistics provided an estimate of the percentage OCN^+ MNC. Although the numbers represent the percentage of cells, the actual population percentage is calculated on the basis of the total MNC counts estimated before and after the magnetic separation step.

The cell counts were made at the following stages of the experiment

1) An initial MNC count was performed after the cells were separated and washed from whole blood.
2) A second cell count was performed after the blocking step and before labelling the cells with OCN primary and isotype antibodies.

3) A third cell count was performed after the magnetic separation was performed. This result in the positively gated cells counts identified in FC analysis was used to estimate the percentage of OCN^+ MNC.

$$\frac{\text{Cells positive for OCN}}{\text{Total number of MNC in positively labelled fraction}} \times 100 = \%\ OCN^+\ MNC$$

3.9. Plasma SDF-1α measurments in human patient cohort

3.9.1. Aim

The aim of this study was to assess reproducibility of the human Quantikine SDF-1 α ELISA kit (R & D, USA) at both intra and inter-assay levels. Plasma obtained from human patient blood samples was analysed. The immunoassay required preparation of standards, antibodies for target protein capture and detection, and involved a multiple-step protocol in its execution, all of which may introduce error.

3.9.2. Protocol

SDF-1α measurements were performed in duplicates. The results were used to calculate an intra assay coefficient of variation.

SDF-1α amounts (or concentration) were calculated using standard as per manufacture's instructions. Details are provided in Chapter 2 (section 2.11.3). The mean and standard deviation of duplicate standard curve concentration points were obtained from colorimetric analysis. These readings were averaged and the intra-assay coefficient of variation for each plate (expressed as %) was calculated.

3.9.3. Results and conclusion

3.9.3.1. Intra assay reproducibility

Intra-assay reproducibility for SDF-1α standard measurements for human patient samples is illustrated in Figure 3.25.

Plate 1

Std (pg\ mL)	O.D readings(492 nm)		Mean	Std dev.
10,000	0.3770	0.3750	0.3760	0.0014
5,000	0.2460	0.2490	0.2475	0.0021
2500	0.0990	0.0930	0.0960	0.0042
1250	0.0480	0.0490	0.0485	0.0007
625	0.0220	0.0240	0.0230	0.0014
312	0.0140	0.0150	0.0145	0.0007
156	0.0160	0.0160	0.0160	0.0000
		Mean	**0.1174**	**0.0015**
		Intra assay coefficient of variation	**1.29 %**	

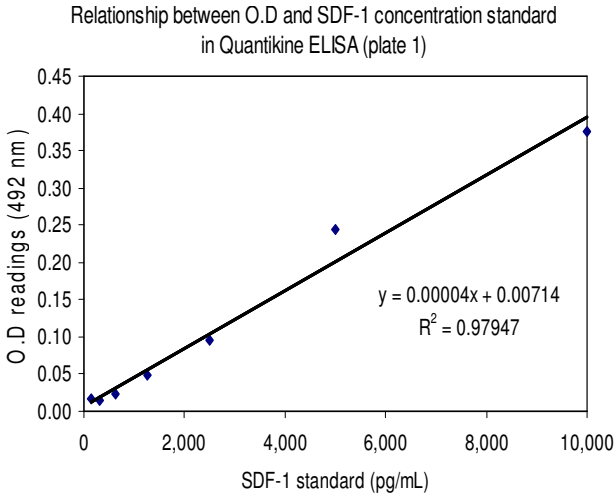

Plate 2

Std (pg\ mL)	O.D readings(492 nm)		Mean	Std dev.
10,000	0.3950	0.4240	0.4095	0.0205
5,000	0.2510	0.2470	0.2490	0.0028
2500	0.1010	0.1030	0.1020	0.0014
1250	0.0470	0.0490	0.0480	0.0014
625	0.0260	0.0290	0.0275	0.0021
312	0.0180	0.0140	0.0160	0.0028
156	0.0140	0.0170	0.0155	0.0021
		Mean	**0.1239**	**0.0047**
		Intra assay coefficient of variation	**3.83 %**	

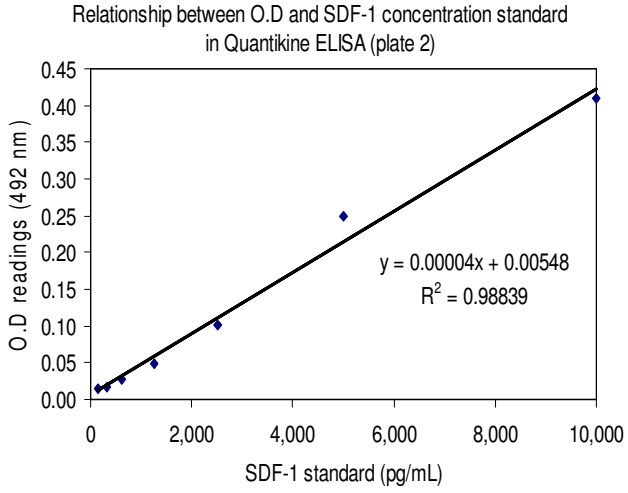

Figure 3.25. Intra-assay assessment of reproducibility for Quantikine standard SDF-1α measurements in human plasma samples.

3.9.3.2. Inter-assay reproducibility

Inter-assay reproducibility was also assessed for reproducibility of the SDF-1 α ELISA technique and is illustrated in Table 3.5.

Table 3.5. Inter-assay assessment of reproducibility for SDF-1α standards in a human patient cohort

Std (pg\ mL)	Plate 1	Plate 2	Mean	Std dev.
10,000	0.3760	0.4095	0.3928	0.0237
5,000	0.2475	0.2490	0.2483	0.0011
2500	0.0960	0.1020	0.0990	0.0042
1250	0.0485	0.0480	0.0483	0.0004
625	0.0230	0.0275	0.0253	0.0032
312	0.0145	0.0160	0.0153	0.0011
156	0.0160	0.0155	0.0158	0.0004
		Mean	**0.1206**	**0.0048**
		Inter assay coefficient of variation	**4.01 %**	

Intra-assay and inter-assay reproducibility for Quantikine SDF-1α ELISA standards was robust with the coefficient of variation between repeats within the same trial falling between 3 and 5 %.

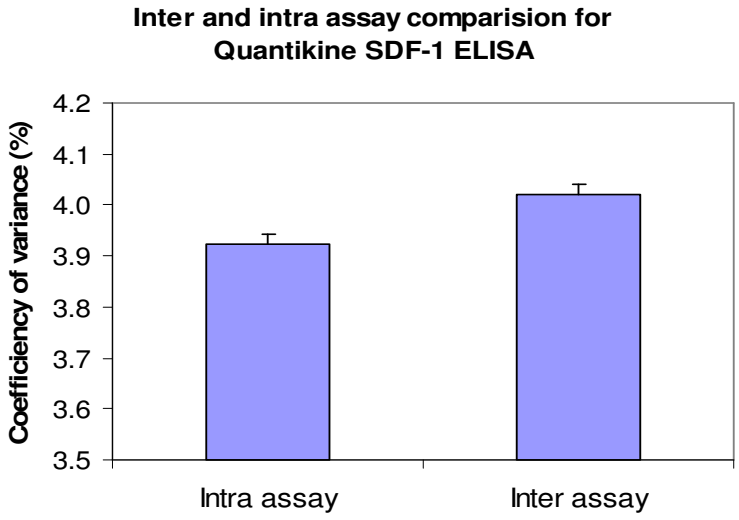

Figure 3.26. Intra and inter- assay assessment of reproducibility for Quantikine SDF-1 α ELISA standards in human plasma samples.

3.10. Plasma G-CSF measurments in human patient cohort

3.10.1. Aim

The aim of this study was to assess reproducibility of the human Quantikine G-CSF ELISA kit (R & D, USA) at both intra and inter-assay levels. Plasma obtained from human patient blood samples was analysed. The immunoassay required preparation of standards, antibodies for target protein capture and detection, and involved a multiple-step protocol in its execution, all of which may introduce error.

3.10.2. Protocol

Plasma G-CSF measurements were performed in duplicates. The results were used to calculate an intra-assay coefficient of variation.

Plasma G-CSF amounts (or concentration) was calculated using standard curves as per manufacture's instructions. Details are provided in Chapter 2 (section 2.11.3). The mean and standard deviation of standard curve concentration points were obtained from colorimetric analysis. The mean and standard deviation were averaged and the intra-assay coefficient of variation for each plate (expressed as %) was calculated.

3.10.3. Results and conclusion

3.10.3.1. Intra-assay reproducibility

Plate 1

Std(pg/mL)	O.D readings(492 nm)		Mean	Std dev.
2500	0.6010	0.6060	0.6035	0.0035
1250	0.3150	0.3180	0.3165	0.0021
625	0.1590	0.1650	0.1620	0.0042
312	0.0820	0.0930	0.0875	0.0078
158	0.0650	0.0530	0.0590	0.0085
78	0.0270	0.0280	0.0275	0.0007
39	0.0185	0.0185	0.0185	0.0000
		Mean	**0.1821**	**0.0038**
		Intra assay coefficient of variation	**2.10 %**	

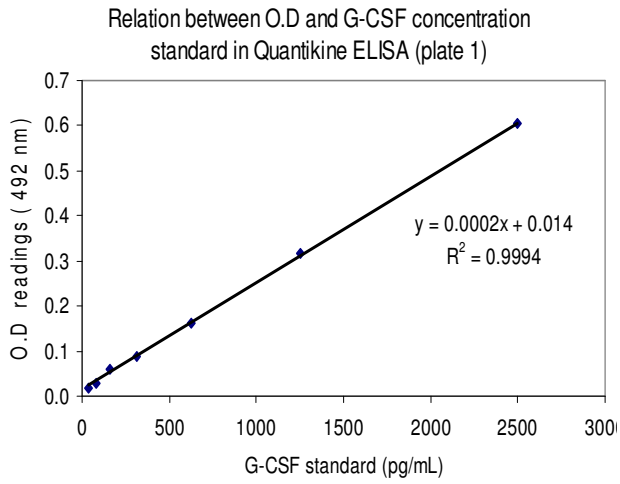

Plate 2

Std(pg/mL)	O.D readings(492 nm)		Mean	Std dev.
2500	0.6100	0.6060	0.6080	0.0028
1250	0.3150	0.3210	0.3180	0.0042
625	0.1690	0.1650	0.1670	0.0028
312	0.0830	0.0910	0.0870	0.0057
158	0.0610	0.0570	0.0590	0.0028
78	0.0320	0.0380	0.0350	0.0042
39	0.0290	0.0220	0.0255	0.0049
		Mean	**0.1856**	**0.0039**
		Intra assay coefficient of variation	**2.12 %**	

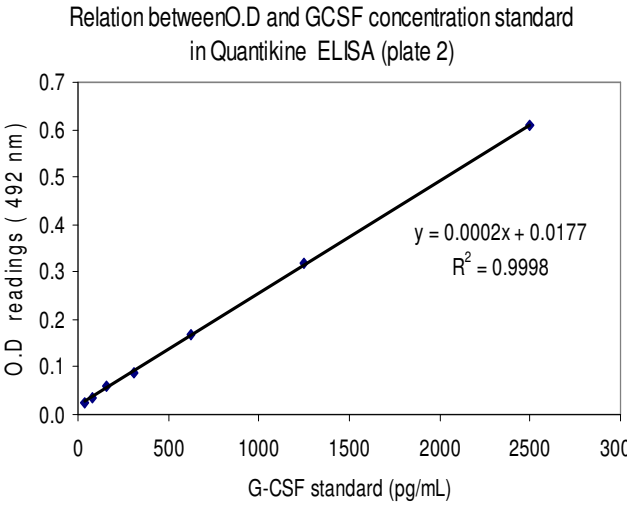

Figure 3.27. Intra-assay assessment of reproducibility for Quantikine standard G-CSF measurements in human plasma samples.

3.10.3.2. Inter-assay reproducibility

Inter-assay reproducibility was also assessed for reproducibility of the G-CSF ELISA technique and is illustrated in Table 3.6.

Table 3.6 Inter-assay assessment of reproducibility for G-CSF standards in a human patient cohort

Std (pg\ mL)	Plate 1	Plate 2	Mean	Std dev.
2500	0.6035	0.6080	0.6058	0.0032
1250	0.3165	0.3180	0.3173	0.0011
625	0.162	0.1670	0.1645	0.0035
312	0.0875	0.0870	0.0873	0.0004
158	0.059	0.0590	0.0590	0.0000
78	0.0275	0.0350	0.0313	0.0053
39	0.0185	0.0255	0.0220	0.0049
		Mean	**0.1839**	**0.0026**
		Intra assay coefficient of variation	**1.42 %**	

Intra-assay and inter-assay reproducibility for Quantikine G-CSF ELISA standards was robust with the coefficient of variation between repeats within the same trial falling between 1 and 3 %.

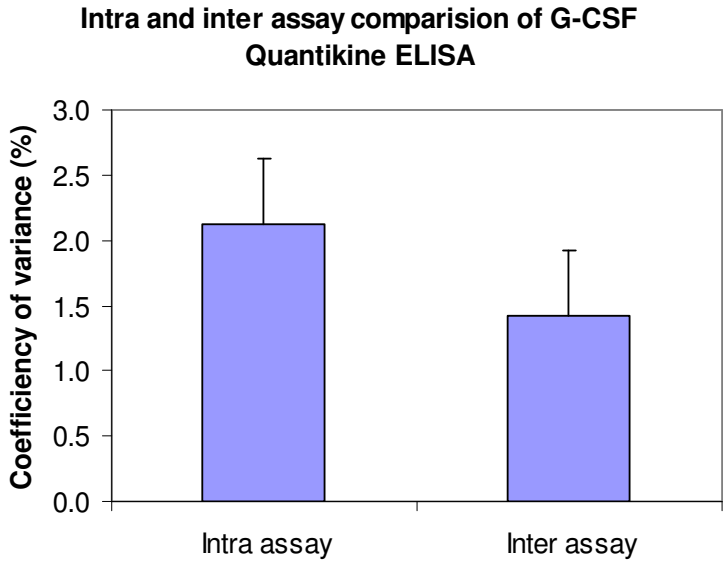

Figure 3.28. Intra and inter-assay assessment of reproducibility for Quantikine G-CSF ELISA standards in human plasma samples.

3.11. Plasma SCF measurments in human patient cohort

3.11.1. Aim

The aim of this study was to assess reproducibility of the human Quantikine SCF ELISA kit (R & D, USA) at both intra and inter-assay levels. Plasma obtained from human patient blood samples was analysed. The immunoassay required preparation of standards, antibodies for target protein capture and detection, and involved a multiple-step protocol in its execution, all of which may introduce error.

3.11.2. Protocol

SCF measurements were performed in duplicates. These results were used to calculate the intra-assay coefficient of variability.
Plasma SCF amounts (or concentrations) were calculated as per manufacture's instructions. Details are provided in Chapter 2 (section 2.11.3). The mean and standard deviation of standard curve concentration points were obtained from colorimetric analysis. The mean and standard deviation were averaged and the intra-assay coefficient of variation for each plate (expressed as %) was calculated.

3.11.3. Results and conclusion

3.11.3.1. Intra-assay reproducibility

Plate1

Standard (pg/mL)	O.D readings (592 nm)		Mean	Std dev
2000	0.5120	0.5010	0.5065	0.0078
1000	0.3230	0.3270	0.3250	0.0028
500	0.2380	0.2430	0.2405	0.0035
250	0.1490	0.1520	0.1505	0.0021
125	0.1030	0.1000	0.1015	0.0021
62.5	0.0750	0.0700	0.0725	0.0035
31.2	0.0460	0.0570	0.0515	0.0078
		Mean	0.1640	0.0042
	Intra assay coefficient of variation		**2.58 %**	

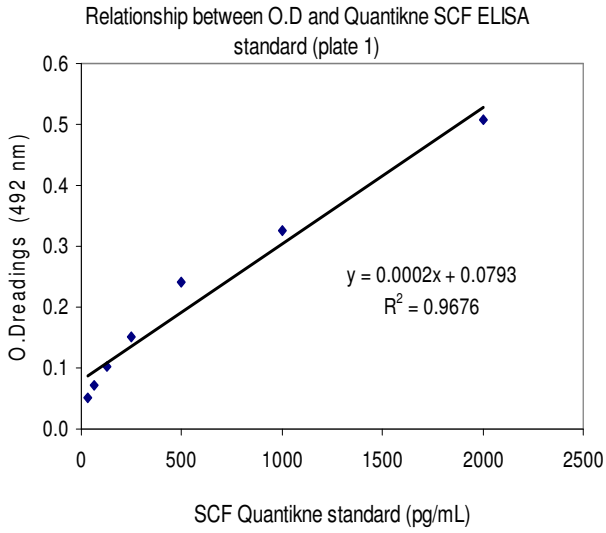

Plate 2

Standard pg/mL)	O.D readings (592 nm)		Mean	Std dev
2000	0.5150	0.5100	0.5125	0.0035
1000	0.3470	0.3390	0.3430	0.0057
500	0.2260	0.2310	0.2285	0.0035
250	0.1560	0.1530	0.1545	0.0021
125	0.1020	0.1000	0.1010	0.0014
62.5	0.0810	0.0780	0.0795	0.0021
31.2	0.0520	0.0480	0.0500	0.0028
		Mean	0.2099	0.0030
	Intra assay coefficient of variation		**1.44 %**	

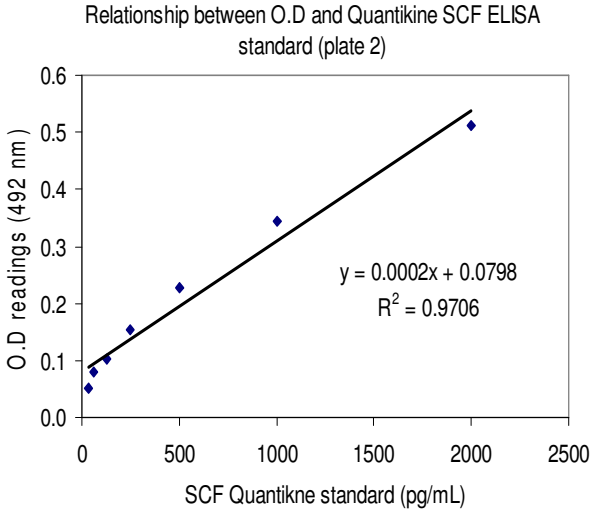

Figure 3.29. Intra-assay assessment of reproducibility for Quantikine standard SCF measurements in human plasma samples.

3.11.3.2. Inter assay reproducibility

Inter-assay coefficient of variation was also assessed for reproducibility of the SCF ELISA technique and is illustrated in Table 3.7.

Table 3.7. Inter-assay assessment of reproducibility for SCF standards in a human patient cohort

Std (pg\ mL)	Plate 1	Plate 2	Mean	Std dev.
2000	0.5065	0.5125	0.5095	0.0042
1000	0.3250	0.3430	0.3340	0.0127
500	0.2405	0.2285	0.2345	0.0085
250	0.1505	0.1545	0.1525	0.0028
125	0.1015	0.1010	0.1013	0.0004
62.5	0.0725	0.0795	0.0760	0.0049
31.2	0.0515	0.0500	0.0508	0.0011
		Mean	0.2084	0.0049
		Inter assay coefficient of variation	**2.37 %**	

Intra-assay and inter-assay reproducibility for Quantikine R&D SCF ELISA standards was robust with the coefficient of variation between repeats within the same trial falling between 1 and 3%. The results are presented graphically in Figure 3.30.

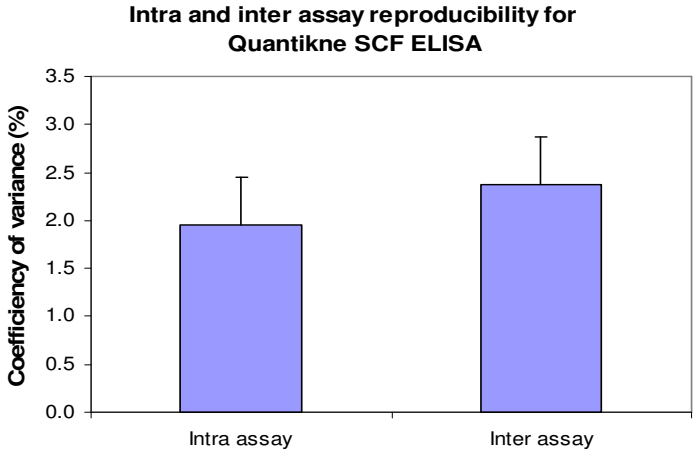

Figure 3.30. Intra and inter-assay assessment of reproducibility assessment for Quantikine SCF ELISA standards in human plasma samples.

CHAPTER 4. AORTIC CALCIFICATION IN 12 MONTH OLD OPG$^{-/-}$ MOUSE MODEL AND ITS ASSOCIATION WITH STEM CELL MOBILISING CYTOKINES

4.1. Introduction

Over the past two decades vascular calcification has been studied in mouse models, emphasizing the role of various proteins that regulate this process[2,61,97]. In addition to vascular calcification, these models have focused attention on bone mineralization suggesting that both processes could be mechanically interlinked[1,3,28,123,125]. A variety of mouse models have been employed to study the mechanisms underlying vascular calcification including mouse models deficient in matrix gla[59,61], OPG[57,58,62],OPN[61] and ApoE[38,57,61]. A detailed review of some of these mouse models is provided in Chapter 1 (section 1.3)

In this Chapter the severity of aortic calcification was estimated by two methods, namely aortic calcium staining and total aortic calcium quantification by bioassay method. The SDF-1α and G-CSF cytokine concentrations were also estimated in order to relate them to the severity of aortic calcification. These cytokines were investigated as they are reported to mobilize progenitors from the BM and facilitate their homing to the vasculature[183,186,188,218].

4.2. OPG$^{-/-}$ as an experimental mouse model

As discussed in Chapter 1, OPG is a recently identified member of the TNF receptor gene super family[118], which inhibits osteoclast development[112,136]. In this vascular calcification investigation an OPG$^{-/-}$ mouse model system was considered appropriate since targeted gene deletion of OPG has be reported to increase osteoclast activity with bone loss[113,136], hypercalcemia[118] and vascular calcification[57,58]. One of the main rationales for selecting this particular model was that calcification within the aorta of these mice develops independently of atherosclerosis or other related vascular diseases[58,61,62]. Along with vascular calcification, the OPG$^{-/-}$ mice also developed severe osteoporosis resulting in bone loss[34,112,136], bone fractures[34,129] and decrease in bone mineral density[118,129]. Hence, this model was deemed suitable to investigate the role of osteoblasts, their possible origin and role in vascular calcification. Studies also report that the absence of OPG increases the area

of calcification in vasculature which resultantly increases the plaque burden by converting SMC to osteogenic lineage[9,13,27,162]. Calcified arteries in $OPG^{-/-}$ mice have been demonstrated to express several bone matrix proteins, including collagen type I[18,122], MGP[15,59,108], OCN[4,61], osteonectin[4,31], and BMP- 2[31,61] indicating a possible role for these bone related proteins in the pathogenesis of vascular calcification. The sample size used for both mouse model studies described in this Chapter is tabulated below.

Investigation	Mice type and gender	
	$OPG^{-/-}$ Males	$OPG^{+/+}$ Males
Alizarin red calcium staining	7	7
Total aortic calcium quantification	11	11
SDF-1α	11	11
G-CSF	11	11

4.3. Aortic calcium staining

Aortic calcium was determined by two techniques as described in Chapter 2. The first was a visual staining method demonstrating the percentage of calcium staining within the whole aorta and secondly, a bioassay system which quantified the total amount of extractable aortic calcium. Use of both methods gave two independent means of assessing vascular calcification in experimental $OPG^{-/-}$ and control $OPG^{+/+}$ mice.

4.3.1. Protocol

In an initial study the percentage of alizarin red-staining in aortas harvested from $OPG^{-/-}$ (n=7) and $OPG^{+/+}$ (n=7) male mice was assessed. A detailed protocol and method optimization is discussed in Chapter 2 (section 2.2) and 3 (section 3.1) respectively. The staining areas were defined in the digital photos of the whole aortas using computer aided Scion software™. Four aortic regions were examined: aortic arch (A.A), thoracic aorta (T.A), suprarenal (S.R) and infra renal (I.R). Whole aortic staining was determined by averaging the results of all four regions. Results between experimental $OPG^{-/-}$ and control $OPG^{+/+}$ (wild type) mice were compared.

4.3.2. Results

Alizarin red-staining was greater in the aortas of $OPG^{-/-}$ mice compared to $OPG^{+/+}$ mice (Figure 4.1). Infrarenal calcium staining was found to be similar in the $OPG^{-/-}$ and $OPG^{+/+}$ mice. Total aortic staining was significantly greater in $OPG^{-/-}$ (median 0.92 %, IQR 0.81-1.0, n=7) when compared to $OPG^{+/+}$ (median 0.53 %, IQR 0.47-0.58, p=0.01, n=7).

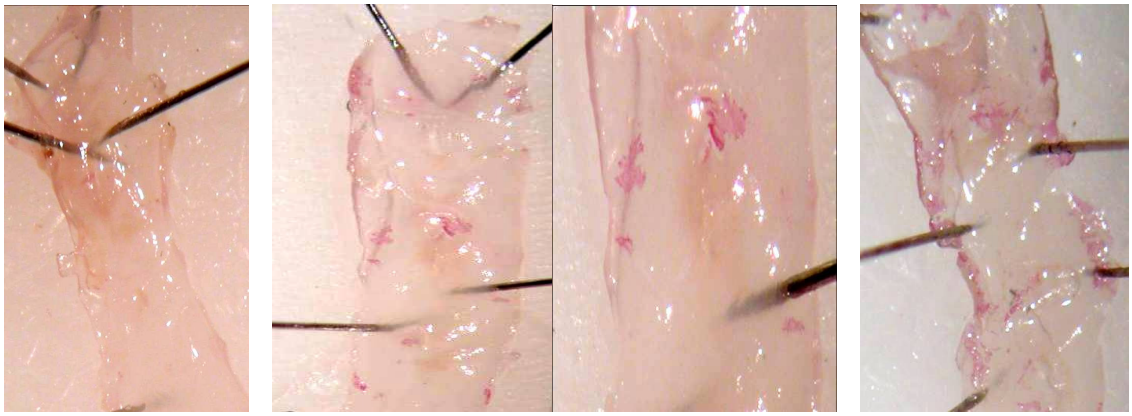

$OPG^{+/+}$ (10 x) (A) | $OPG^{-/-}$ (10 x) (B) | $OPG^{-/-}$ (40 x) (C) | $OPG^{-/-}$ (10 x) (D)

Figure 4.1. Examples of aortic arch calcium staining (red areas) in $OPG^{-/-}$ and $OPG^{+/+}$ mouse groups. Red areas of staining were observed in a greater proportion in $OPG^{-/-}$ than in $OPG^{+/+}$ mouse group.

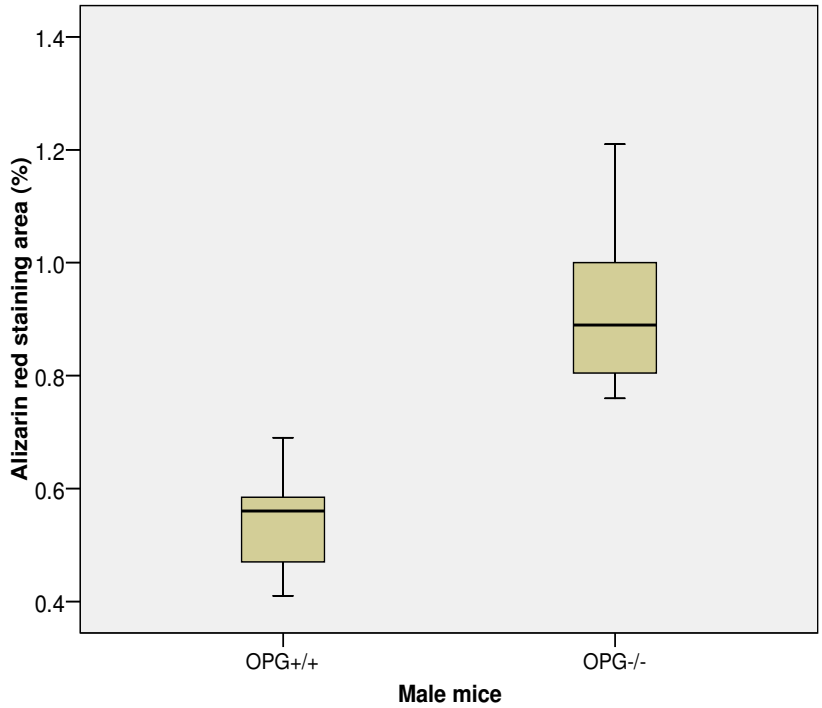

Figure 4.2. Box plots representing alizarin red-staining percentage in the whole aorta of $OPG^{-/-}$ and $OPG^{+/+}$ mouse groups. Results are displayed as median and IQR statistical box plots.

SPSS statistical box plot demonstrated unequal aortic staining distribution in both $OPG^{-/-}$ and $OPG^{+/+}$ mice (Figure 4.2). Median staining percentages was found out to be greater in $OPG^{-/-}$ (0.92 %, 0.81-1.0, n=7) compared to $OPG^{+/+}$ percentage (0.53 %, 0.47-0.58, p=0.01, n=7).

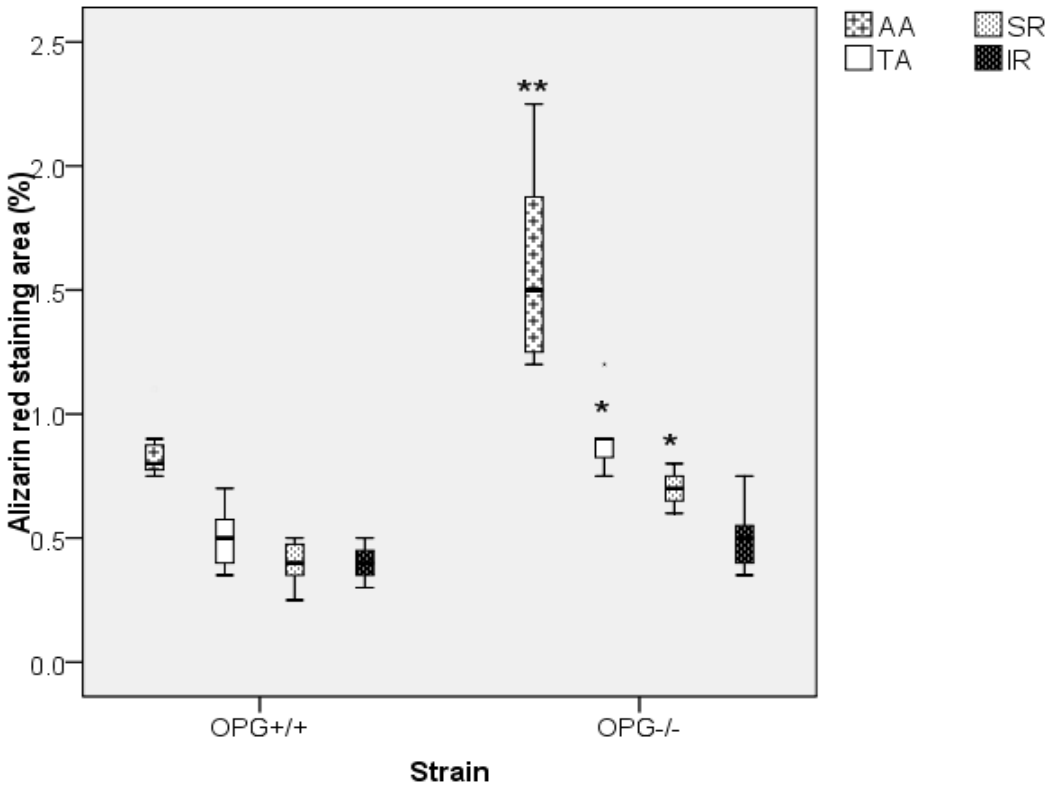

Figure. 4.3. Box plot representing alizarin red-staining percentage in the aortic regions of $OPG^{-/-}$ and $OPG^{+/+}$ mouse groups. Results are displayed as median and IQR statistical box plots. (A.A: aortic arch; T.A: thoracic arch; S.R: Supra renal; I.R: infra renal). * denotes statistical significance.

Alizarin red-staining was significantly greater in A.A, T.A and S.R of $OPG^{-/-}$ mice compared to $OPG^{+/+}$ mice. I.R staining was similar in $OPG^{-/-}$ as illustrated in Figure 4.3 and tabulated in Table 4.1. Results were compared using with non-parametric Mann Whitney U test as the staining percentage results were not normally distributed.

4.4. Total extractable aortic calcium quantification

Extractable aortic calcium was estimated as a second measurement of aortic calcification.

4.4.1. Protocol

Details of the method are provided in Chapter 2 (section 2.4). Intra and Inter-assay reproducibility were assessed (Chapter 3, section 3.2.3). Briefly, total calcium was extracted from harvested aortas of 12 month old $OPG^{-/-}$ (n=11) and $OPG^{+/+}$ male (n=11) mice by hydrochloric acid (HCl) digestion. The samples were analyzed by colorimetric estimation of free calcium using a 96-well method. Total aortic calcium was compared in experimental and control groups.

4.4.2. Results

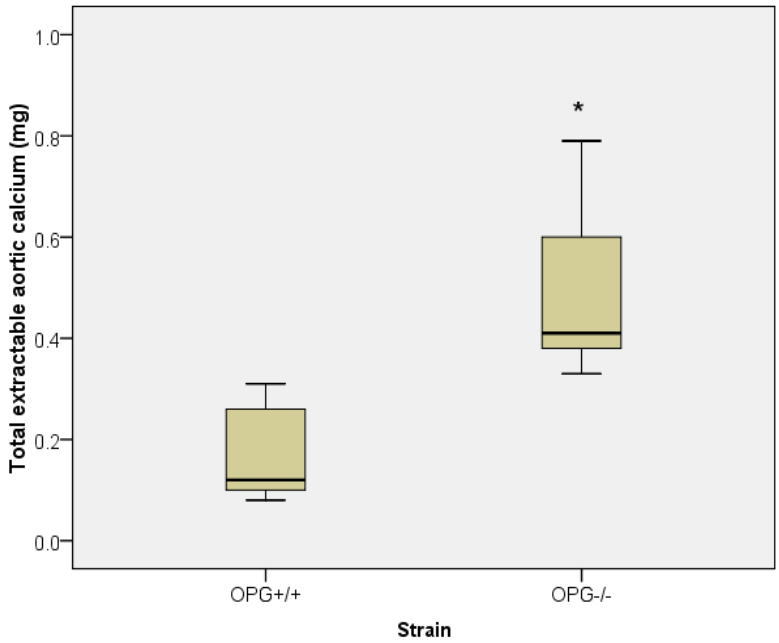

Figure 4.4. Box plot representing total extractable aortic calcium in experimental $OPG^{-/-}$ and control $OPG^{+/+}$ male mouse group. Results are displayed as median and IQR statistical box plots. * denotes statistical significance.

Total extractable calcium was demonstrated to be significantly greater in the aortas of $OPG^{-/-}$ compared to control mice (Figure 4.4). A summary of our estimation of aortic calcification in $OPG^{-/-}$ and $OPG^{+/+}$ mice aortic sections are given in Table 4.1.

Table 4.1. Comparison of alizarin red-staining and calcium quantification in $OPG^{-/-}$ and $OPG^{+/+}$ mouse groups.

Assessment	$OPG^{-/-}$		$OPG^{+/+}$		p value
	Median	IQR	Median	IQR	
Alizarin red staining (%)					
Whole aorta	0.89	0.81-1.0	0.56	0.47-0.58	0.001
Aortic arch	1.40	1.23-1.81	0.80	0.78-0.88	0.01
Thoracic	0.88	0.81-0.9	0.50	0.4-0.58	0.01
Suprarenal	0.73	0.65-0.8	0.40	0.35-.0.48	0.01
Infrarenal	0.5	0.34-0.56	0.40	0.23-0.41	0.165
Extractable calcium (mg)	0.49	0.38-0.6	0.18	0.1-0.26	0.01

4.5. SDF-1α and aortic calcium

Serum SDF-1α concentration was estimated by a standard quantitative sandwich ELISA technique. Mouse serum concentration of SDF-1α was determined and compared in $OPG^{-/-}$ (n=11) and experimental $OPG^{-/-}$ and $OPG^{+/+}$ group. Intra and Inter-assay reproducibility was assessed. Tail bleeds were drawn from the same mouse groups which were used for studying quantification of total aortic calcium.

4.5.1. Protocol

The protocol for the serum SDF-1α estimation is detailed in Chapter 2 (section 2.5) and optimization methods are given in Chapter 3 (section 3.3). Briefly, serum samples (10 ul) collected via tail bleeds from both $OPG^{+/+}$ (n=11) mice were added to an ELISA plate pre-coated with monoclonal antibody specific for SDF-1α (R & D Quantikine, USA). After a series of washings and addition of secondary antibody and other reagents the concentration of SDF-1α was colorimetrically estimated and compared between experimental and control mouse groups.

4.5.2. Results

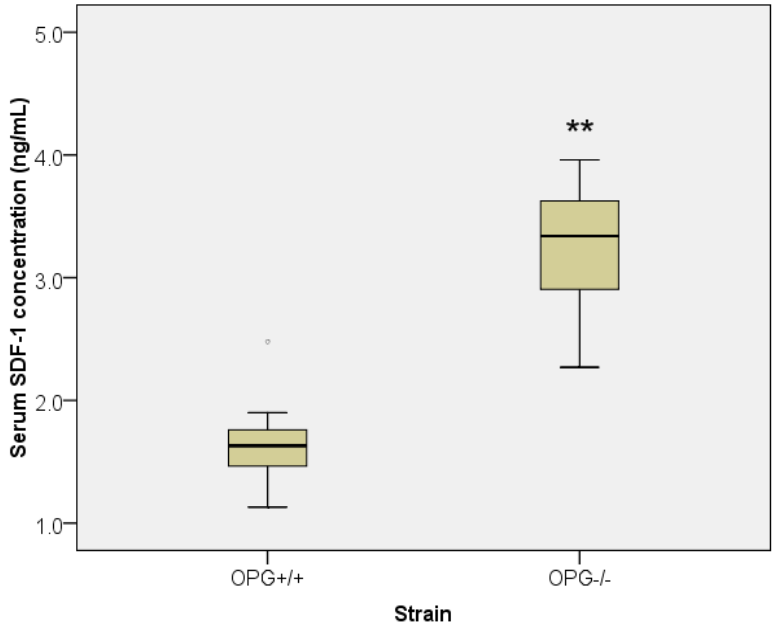

Figure 4.5. Box plot representing serum SDF-1α concentration comparison between experimental $OPG^{-/-}$ and control $OPG^{+/+}$ mouse group. Results are displayed as median and IQR plots. * denotes statistical significance.

Total serum SDF-1α concentration was significantly greater in $OPG^{-/-}$ compared to $OPG^{+/+}$ mice. Results were compared by Mann Whitney U test since data was not normally distributed. Serum concentration results of SDF-1α are shown below in Table 4.2.

4.6. G-CSF and aortic calcium

4.6.1. Protocol

Serum concentration of G-CSF was estimated by a sandwich ELISA technique (R & D Quantikine, USA). The protocol for the serum G-CSF estimation is detailed in Chapter 2 (section 2.5) and optimization in Chapter 3 (section 3.4). Serum G-CSF concentration was determined and compared in experimental $OPG^{-/-}$ and $OPG^{+/+}$ mouse groups.

4.6.2. Results

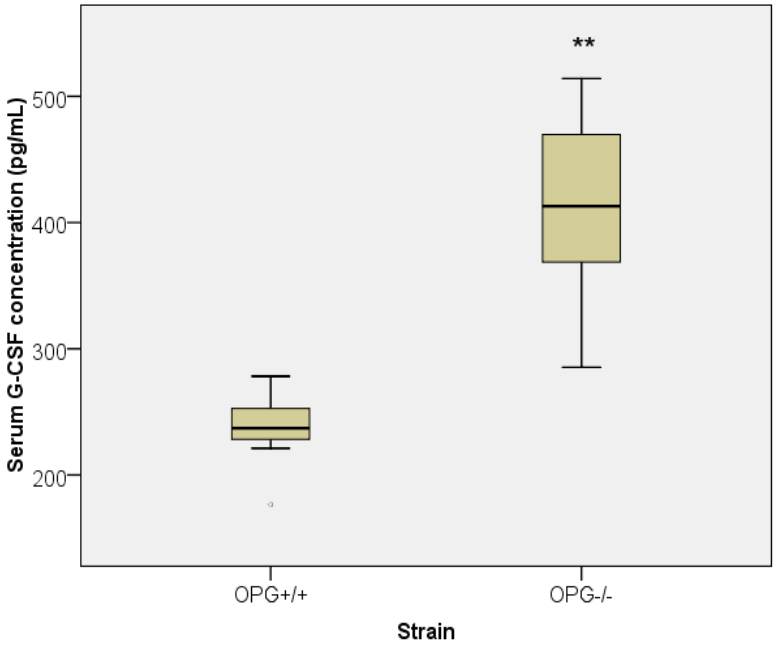

Figure 4.6. Box plot representing G-CSF concentration comparison between experimental $OPG^{-/-}$ and control $OPG^{+/+}$ mouse groups. . Results are displayed as median and IQR plots. * denotes statistical significance.

Total serum G-CSF concentration was significantly greater in $OPG^{-/-}$ compared to control mice. Results were compared by Mann Whitney U test since data was not normally distributed. Serum concentration results of G-CSF are shown below in Table 4.2.

Table 4.2. Comparison of SDF-1α and G-CSF serum concentrations in $OPG^{-/-}$ and $OPG^{+/+}$ mouse groups.

Assessment / Cytokine of Interest	$OPG^{-/-}$		$OPG^{+/+}$		p value
	Median	IQR	Median	IQR	
SDF-1α (ng/mL)	3.26	3.03- 3.59	1.65	1.44-1.72	0.01
G-CSF (pg/mL)	412.7	398.6-430.94	236.2	228.2-260	0.01

The serum concentrations of the SDF-1 α and G-CSF concentrations were greater in $OPG^{-/-}$ mouse group.

4.7. Correlation with extractable aortic calcium

The correlation of circulating SDF-1α and G-CSF concentration in mouse serum samples and total extractable aortic calcium was statistically stronger in experimental $OPG^{-/-}$ group (Figure 4.7).

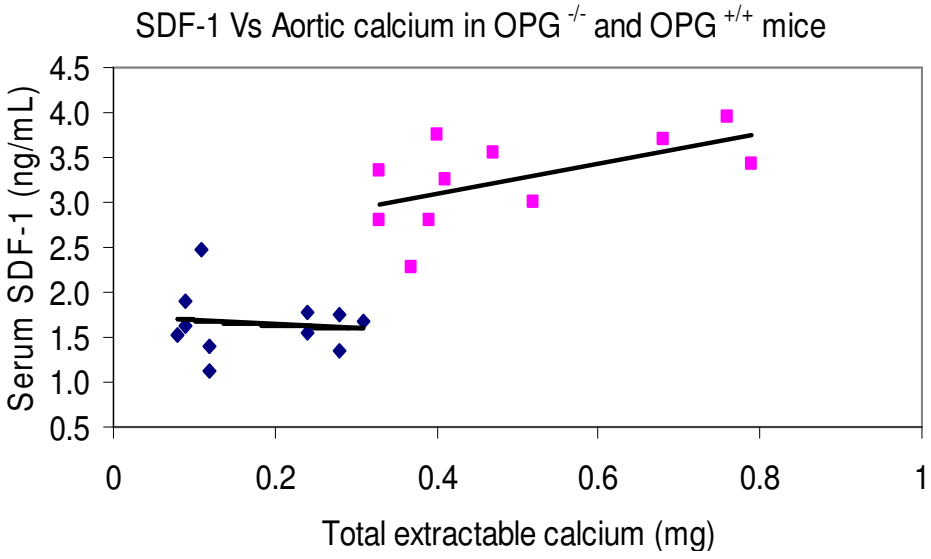

A

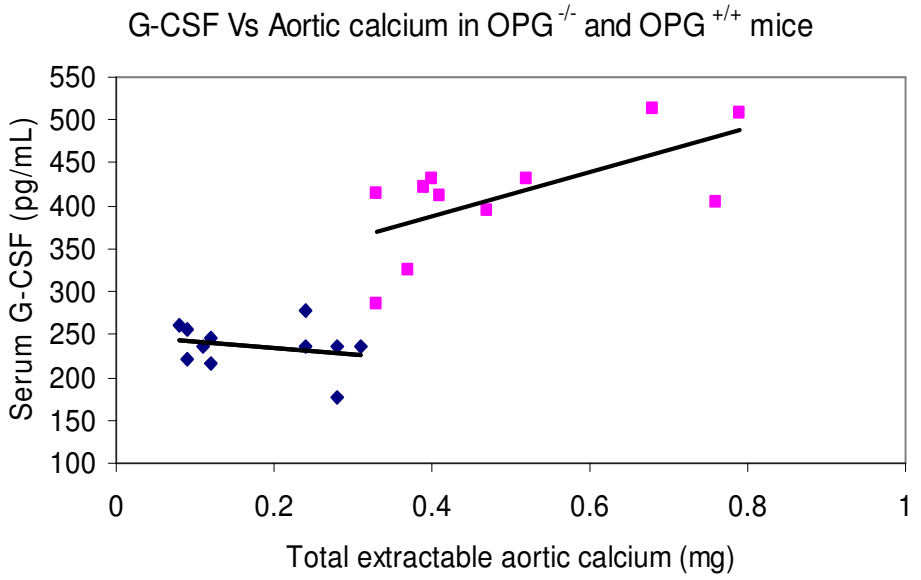

B

Figure 4.7. Scatter plot illustrating the association of serum SDF-1 α (A) and G-CSF (B) concentration with total extractable aortic calcium in $OPG^{-/-}$ and $OPG^{+/+}$ mouse groups. (◊- $OPG^{+/+}$, □- $OPG^{-/-}$)

Spearman's correlation coefficient statistics indicated that the concentration of SDF-1α was strongly correlated to extractable aortic calcium at 0.683 (n=11, p=0.01) in $OPG^{-/-}$ group (Figure 4.7A) while in $OPG^{+/+}$ group the correlation was weaker at 0.453 (n=11, p=0.21).

Similarly the G-CSF concentration was also strongly correlated to the extractable aortic calcium at 0.704 in $OPG^{-/-}$ group (Figure 4.7B) while in $OPG^{+/+}$ group the correlation was comparatively weaker at 0.432.

4.8. Discussion

The findings from this investigation support an association between OPG and vascular calcification as previously reported[1,2,58,135]. Research groups have demonstrated aortic calcium staining in tissue sections[52,58], however whole aortic staining has not been previously reported. This study demonstrates that aortic calcium can be assessed in whole aorta using calcification estimation by alizarin red-staining and the calcium bioassay method. Calcium staining percentage was significantly greater in the aortas of 12 month old male $OPG^{-/-}$ mouse group compared to age matched control $OPG^{+/+}$ mouse group. The distribution of calcium staining varied from different aortic regions. Alizarin red-staining was greatest in the A.A followed by T.A, S.R and I.R aortic sections. This variation in staining pattern could be possible because varied gene expressions within different regions of the aorta that may determine either a protective role or make the aortic region susceptible to mineralization. One of the probable reasons for this could be that VSMC contributing to the different regions of the aorta arise from different embryological sites. These VSMC arise from various precursor sites which would be expected to have different gene expression and propensity to be stimulated to carry out calcification in the separate segments of aorta[240]. Overall calcium staining was 2-fold greater in aortas of $OPG^{-/-}$ mice compared to $OPG^{+/+}$ controls (Figure 4.2 and Table 4.1).

In the second part of the study, serum samples were analyzed for the circulating SDF-1 α and G-CSF cytokine levels. These cytokines promote the release of immature cells from BM environment into the peripheral circulation[41,185,186]. Further, SDF-1 α and G-CSF also facilitate the recruitment and homing of undifferentiated circulating cells to diseased arteries[54,185]. The current studies demonstrated that the circulating concentration of both of these cytokines were significantly higher in $OPG^{-/-}$ when compared to control $OPG^{+/+}$ mice

suggesting that there could be an increased BM cellular release in mice susceptible to vascular calcification. These findings will be related to the hypotheses later in Chapter 5.

Following serum cytokine studies, total extractable aortic calcium was measured from both mouse groups. It was observed that the aortic calcium levels were significantly elevated in experimental $OPG^{-/-}$ group than the control ones. These findings relate to the results from the first part of the investigation in which calcium staining percentage was found to be higher in $OPG^{-/-}$ group. The circulating cytokine concentrations were also reported to be significantly associated with the calcium levels indicating that the release of BM cell population and aortic calcium may be linked. This observation will be further tested with a circulating cell theory in Chapters 5, 6 and 7.

Overall, the investigation undertaken in this Chapter suggests that vascular calcification occurs in the aortas of old $OPG^{-/-}$ mice and that this mouse model can be investigated to further test the research hypothesis. The role of circulating BM- derived osteo-progenitors in the pathogenesis of vascular calcification will be discussed in detail in the next Chapter using these 12 month old $OPG^{-/-}$ mouse model.

CHAPTER 5. ASSESSMENT OF ASSOCIATION BETWEEN CIRCULATING OCN^+ MNC, AORTIC CALCIUM & AORTIC OCN^+ POPULATION IN $OPG^{-/-}$ MOUSE MODEL

5.1. Introduction

In the previous Chapter aortic calcification was estimated in a 12 month $OPG^{-/-}$ mouse model by alizarin red-staining and calcium bioassay. The extent of aortic calcification in this older $OPG^{-/-}$ model was also correlated to the serum levels of SDF-1α and G-CSF.
In this Chapter circulating OCN^+ MNC in peripheral blood was quantified in a similar 12 month old $OPG^{-/-}$ mouse groups. Further their association with aortic calcium content and the extractable aortic OCN^+ population in $OPG^{-/-}$ mice was investigated. This study was undertaken as circulating OCN^+ cells are believed to be derived from the BM [28,192]. Due to their osteogenic potential outside the BM, they are also referred as osteo-progenitors[33,88,215,241].

5.2. Osteo-progenitors in bone marrow

The BM is known to be a vast reservoir for immature cells which have the potential to develop into different lineages after release into the peripheral circulation[41,167,177,183]. These immature cells are termed as progenitor stem cells. Based on their potential to differentiate further these cells are broadly classified into mesenchymal[30,195,211], hematopoietic[209,211,215] and endothelial progenitor cells[40,177,181]. Amongst all these cell types, there exists a small pool of cells which have been reported to form an osteogenic lineage[30,33,52,214]. This micro-population of cells residing in the BM is also known as osteo-progenitors or BM side population[242]. The term derives from the ability of these cells to develop into an osteogenic, or bone-like forming cells, lineage[167]. The osteo-progenitor population comprises a small population of the BM (about 1-2 %) and cells of this lineage are specifically known for their non-adherent nature[214,243]. Further information on circulating bone marker positive cells such as OCN in vasculature is discussed in Chapter 1.

5.3. OCN^+ MNC in 12 month old $OPG^{-/-}$ male and female mouse groups

OCN^+ MNC were quantified in these studies by FC, 12 month old $OPG^{-/-}$ males and female mice were selected for the investigation (n=10 from both groups).

5.3.1. Protocol

The protocol for the quantification of circulating OCN^+ MNC population is detailed in Chapter 2 (section 2.6). The optimization of the technique is discussed in Chapter 3 (section 3.5 and 3.6). Briefly, ten (10) experimental $OPG^{-/-}$ and ten age matched control $OPG^{+/+}$ males and females were selected for the study. Early morning tail bleed samples were processed and analyzed for OCN^+ MNC by FC. At the end of the study, animals were sacrificed and aortas harvested and stored at -20^{o}C until calcium was extracted and quantified. The experimental time lines are detailed in Figure 5.1.

5.3.2. Analysis

Circulating OCN^+ MNC data was not normally distributed. Therefore the data were compared between $OPG^{-/-}$ and $OPG^{+/+}$ mice using Mann Whitney U test. Data was presented as statistical box plots.

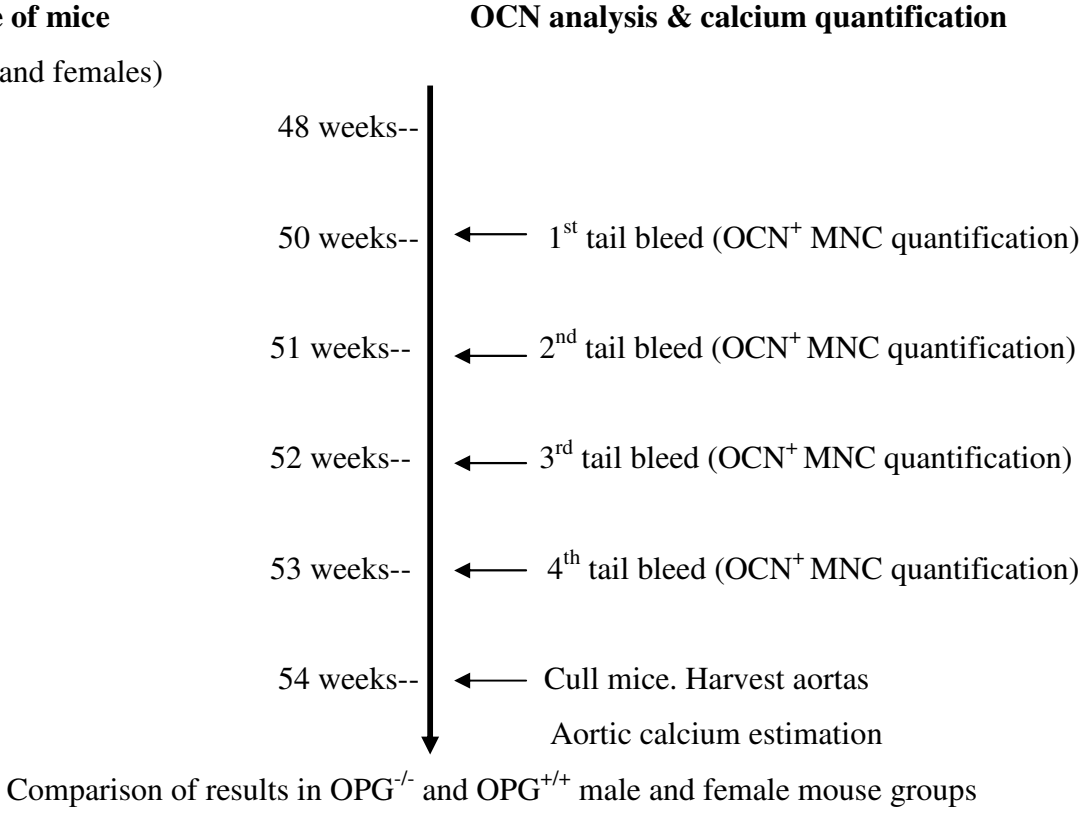

Figure 5.1. Experimental design for quantification of circulating OCN^+ MNC in $OPG^{-/-}$ and $OPG^{+/+}$ mouse groups.

5.4. Results for male mouse group

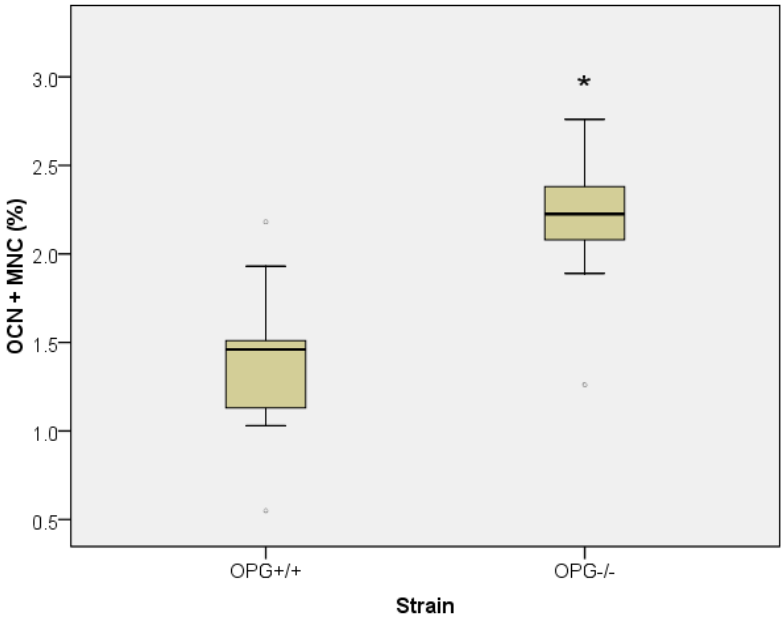

A

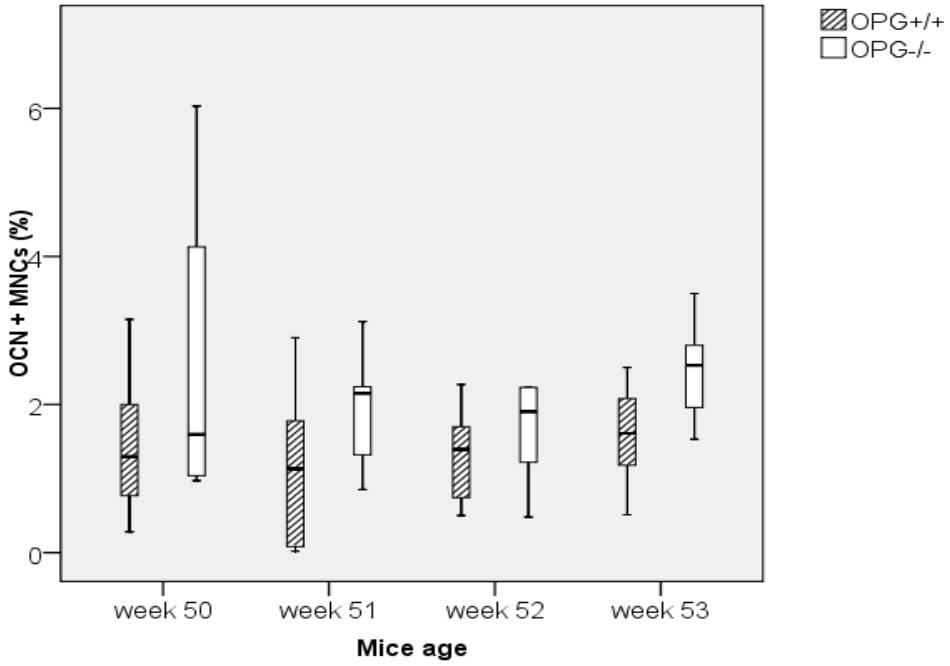

B

Figure 5.2. Box plots representing the circulating OCN^+ MNC comparison in experimental $OPG^{-/-}$ and control $OPG^{+/+}$ male mouse group (A) and median OCN^+ MNC distribution from individual mouse (4 tail bleeds) from both mouse groups (B). * denotes statistical significance.

The median percentage of circulating OCN^+ MNC was significantly greater in male $OPG^{-/-}$ (median 2.23 %, IQR 2.11-2.37, n=10) when compared $OPG^{+/+}$ group (median 1.46 %, IQR 1.2-1.51, n=10, p=0.02). The readings were not normally distributed throughout the four week study period. However the median percentage was higher in $OPG^{-/-}$ males during all the four week of OCN^+ MNC quantification (Figure 5.2 B).

5.5. Results for female mouse group

Figure 5.3 represents the median and IQR values of circulating OCN^+ MNC percentage in tail bleeds obtained from the female mouse group.

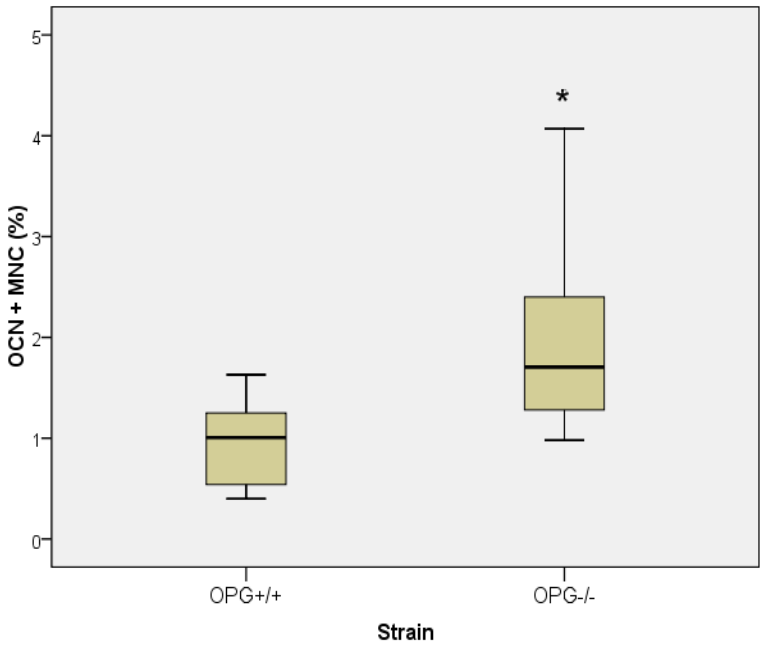

A

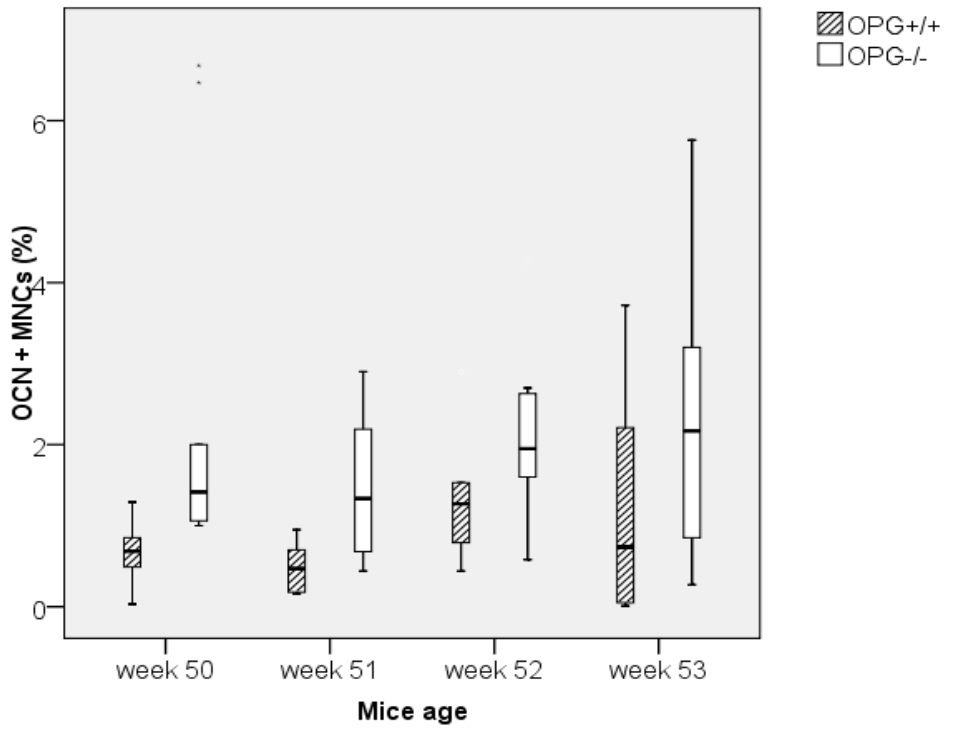

B

Figure 5.3. Box plots representing the percentage of circulating OCN^+ MNC comparison between experimental $OPG^{-/-}$ and control $OPG^{+/+}$ female mouse group (A) and median OCN^+ MNC distribution from individual mouse (4 tail bleeds) for both groups (B).

The median percentage of circulating OCN^+ MNC was significantly greater in female $OPG^{-/-}$ (median 2.14 %, IQR 1.35- 2.34, n=10) as compared to $OPG^{+/+}$ (median 0.98, IQR 0.57-1.23, n=10, p=0.02). The readings were not normally distributed through the period of study however the median percentage was higher in $OPG^{-/-}$ females during all the four week of OCN^+ MNC quantification. A summary of the results is tabulated in the Table 5.1.

Table 5.1. OCN^+ MNC were estimated by calculating the median results from tail bleeds analyzed from each group and gender (n=10 each) of mice obtained at 50, 51, 52 and 53 weeks of age.

Mice	Age of mice (in weeks)	$OPG^{-/-}$		$OPG^{+/+}$	
		Median	IQR	Median	IQR
Males	50	1.60	1.08-3.62	1.30	0.78-1.97
	51	2.15	1.32-2.24	1.13	0.08-1.72
	52	1.91	1.35-2.20	1.40	0.85-1.66
	53	2.53	1.98-2.79	1.61	1.23-2.04
Females	50	1.42	1.06-1.95	0.69	0.50-0.83
	51	1.34	0.83-1.99	0.47	0.23-0.67
	52	1.95	1.66-2.63	1.27	0.87-1.52
	53	2.17	1.15-2.96	0.74	0.08-1.95

5.6. Aortic calcium quantification in male and female $OPG^{-/-}$ and $OPG^{+/+}$ mouse groups

At 54 weeks of age the aortas from both male and female mouse groups were harvested. Total aortic calcium was extracted and quantified using a bioassay as performed in Chapter 4 (section 4.4). Results were compared between the experimental $OPG^{-/-}$ and control $OPG^{+/+}$ groups.

5.6.1. Protocol

Total extractable aortic calcium quantification was performed as described in Chapter 2 (section 2.4). Briefly, aortas were harvested from $OPG^{-/-}$ (males and females, n=10) and $OPG^{+/+}$ control mice (males and females, n=10). Total aortic calcium was extracted and concentrations were estimated.

5.6.2. Analysis

Results indicated that calcium concentration was not normally distributed. Therefore they were compared between $OPG^{-/-}$ and $OPG^{+/+}$ mice using non parametric Mann Whitney U test. Data was presented as statistical box plots.

5.6.3. Results for male and female mouse groups

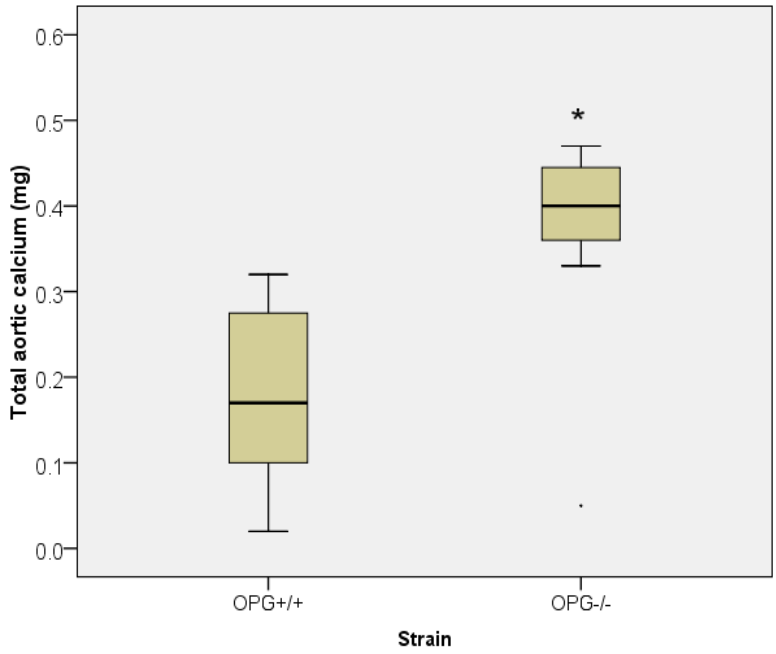

Figure 5.4. Box plot representing the comparison of total extractable aortic calcium in 12 month old male experimental $OPG^{-/-}$ and control $OPG^{+/+}$ mouse groups. The readings were found not to be normally distributed and hence non-parametric statistical test, Mann Whitney U statistical significance test was applied. * denotes statistical significance.

The amount of total calcium extracted from the aorta of $OPG^{-/-}$ mice was significantly greater than for $OPG^{+/+}$ mice.

Similarly in females, the extractable calcium was demonstrated to be significantly greater in the aortas of $OPG^{-/-}$ female mice compared to control mice. A comparison between $OPG^{-/-}$ and $OPG^{+/+}$ (males and females) total extractable aortic calcium content is tabulated below in Table 5.2.

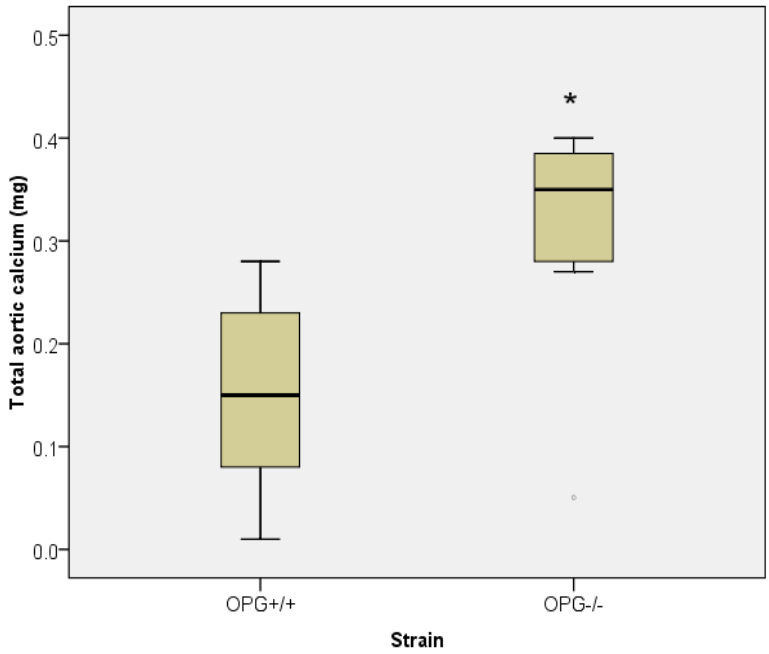

Figure 5.5. Box plot representing the comparison of total extractable aortic calcium in 12 month old female experimental $OPG^{-/-}$ and control $OPG^{+/+}$ mouse groups. The readings were found not to be normally distributed and hence non-parametric statistical test, Mann Whitney U statistical significance test was applied. * denotes statistical significance.

Table 5.2. Total extractable aortic calcium comparison between $OPG^{-/-}$ and $OPG^{+/+}$ (males and females) mouse groups.

Mice	Assessment	$OPG^{-/-}$		$OPG^{+/+}$		p value
		Median	IQR	Median	IQR	
Males (n=10)	Extractable calcium (mg)	0.41	0.39-0.51	0.18	0.1-0.28	0.02
Females (n=10)	Extractable calcium (mg)	0.30	0.19-0.4	0.15	0.08-0.23	0.02

5.7. Aortic OCN^+ population in 12 month old $OPG^{-/-}$ male mouse group

Aortic OCN^+ population was also assessed in $OPG^{-/-}$ mouse model. This study was undertaken to investigate the association between the BM-derived osteo-progenitors (section 5.3) and the OCN^+ cells deposited in the mouse aorta. The deposited OCN^+ cell population was also compared in a three-way association with the total aortic calcium content.

5.7.1. Protocol

A detailed protocol is described in Chapter 2 (section 2.7). Briefly, 12 month old male experimental $OPG^{-/-}$ (n=16) and age matched control $OPG^{+/+}$ (n=16) were selected for the study. Aortas were harvested and subjected to enzymatic digestion to obtain aortic immune cells. Aortas from each group were pooled in groups of four (4 batches for both groups) to obtain sufficient cells for analysis. The mashed aortas were digested in an appropriate dissociation buffer (Appendix 4). The extracted cells were labeled with primary OCN antibody followed by fluorescent secondary PE antibody. The cell suspension was analyzed on FC to determine the aortic OCN^+ cell population in the experimental $OPG^{-/-}$ and control $OPG^{+/+}$ mouse group.

5.7.2. Results

The result for the quantification of aortic OCN^+ population is illustrated in Figure 5.6 below.

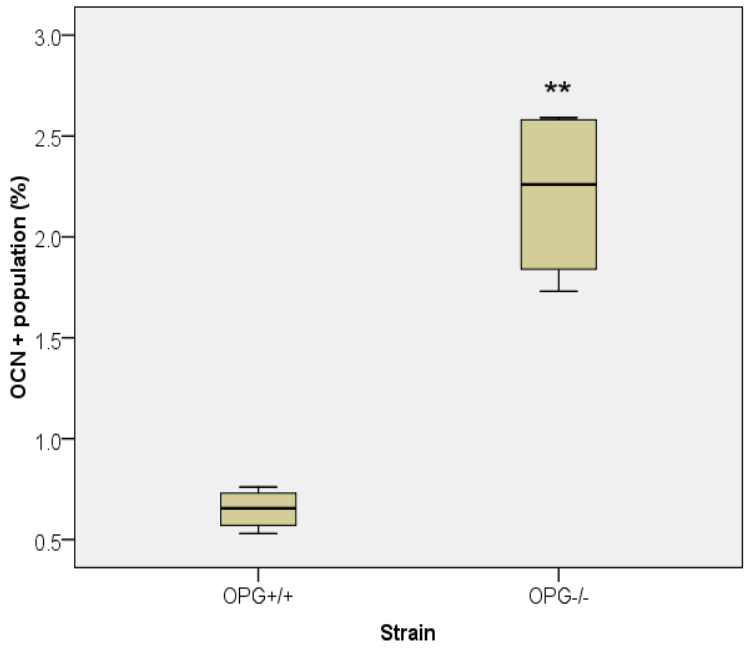

Figure 5.6. Box plot representing the aortic OCN^+ population comparison between experimental $OPG^{-/-}$ and control $OPG^{+/+}$ mouse group. The readings were found not to be normally distributed and hence non-parametric statistical test, Mann Whitney U statistical significance test was applied. * denotes statistical significance.

The median percentage of aortic OCN^+ population in this investigation was found to be significantly greater in experimental $OPG^{-/-}$, 2.23 % (1.8- 2.52, n=4), compared to $OPG^{+/+}$ mouse group, 0.66 % (0.59-0.72, p=0.0001, n=4).

5.8. Association between circulating OCN^+ MNC, aortic calcification and extractable aortic OCN^+ population

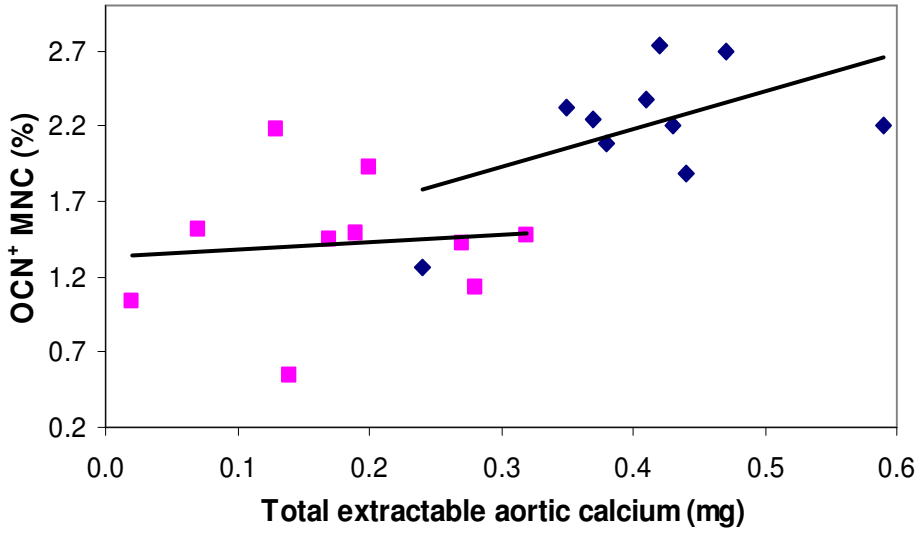

Figure 5.7. Scatter plot illustrating the association between circulating OCN^+ MNC and total extractable aortic calcium in male $OPG^{-/-}$ and $OPG^{+/+}$ mouse groups. (□- $OPG^{+/+}$, ◊- $OPG^{-/-}$)

In the male $OPG^{-/-}$ mouse group the total extractable aortic calcium was significantly correlated with the percentage of OCN^+ MNC. This correlation, however, was not significant in the $OPG^{+/+}$ control group. The statistical difference and spearman's correlation coefficient is summarized in Table 5.3.

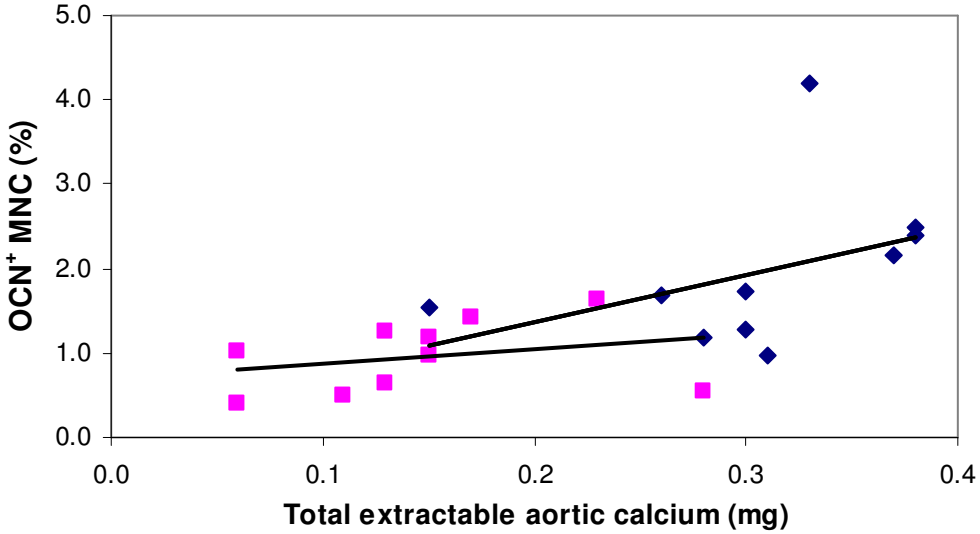

Figure 5.8. Scatter plot illustrating the association between circulating OCN^+ MNC and extractable aortic calcium in female $OPG^{-/-}$ and $OPG^{+/+}$ mouse groups. (□- $OPG^{+/+}$, ◊- $OPG^{-/-}$)

Similarly in the female $OPG^{-/-}$ mouse group the total extractable aortic calcium was significantly correlated with the percentage of OCN^{+} MNC. This correlation, however, was not significant in the $OPG^{+/+}$ control group. The statistical difference and spearman's correlation coefficient is summarized in Table 5.3.

Table 5.3. Association between OCN^{+} MNC percentage and aortic calcification in $OPG^{-/-}$ and $OPG^{+/+}$ (males and females) mouse groups. * denotes statistical significance.

.

Gender	Spearman's correlation coefficient(r value)	
	$OPG^{-/-}$	$OPG^{+/+}$
Males	0.525*	0.391
Females	0.564*	0.410

5.9. Discussion

Vascular calcification in $OPG^{-/-}$ mice and its association with circulating SDF-1α and G-CSF concentrations was demonstrated in the Chapter 4. The investigations undertaken in this Chapter examines a possible association between the percentage of circulating OCN^{+} MNC, aortic calcification and aortic OCN^{+} MNC population in an experimental $OPG^{-/-}$ mice. Osteo-progenitors with bone forming abilities (OCN^{+} cells), make up a small percentage of the BM stroma and are also found in extremely low numbers in peripheral blood[28,41,167,207]. Previous reports have demonstrated a positive association of these osteogenic cells with osteoporosis and other bone related diseases[1,123-125,128,244]. However speculation still exists over the role for these cells in the pathogenesis of vascular calcification[1,2,38,41]. The reports from these studies are unconvincing and do not present a clear conclusion.

As discussed in the Chapter 1, vascular calcification and bone-related diseases are inter-related to a considerable extent[1,2,124,125]. For a human skeletal system to function normally, an osteoclast-osteoblast balance is crucial[1,112,130,136,245]. The OPG- RANK- RANKL interaction plays a central role in controlling the normal bone turnover [136,137,246,247]. RANK is a protein necessary to elevate the calcium levels of osteoclasts in the bone[161,246].

RANKL, on the other hand, has been described to be a protein necessary for the promotion of osteo-resorption[137,246,248]. OPG inhibits this RANK-RANKL interaction thus playing an important role in inhibiting the differentiation of osteoblastic precursors into mature osteoblasts and thus regulate bone formation[61,112,118,126,246]. However in the absence of OPG this osteoclast-osteoblast balance is hampered resulting in excess bone resorption and loss of bone mineral density[1,61,123,249]. This excess bone loss has been reported to be associated with vascular calcification, suggesting that it may be a direct consequence of this bone loss[34,35,124,125]. Even in the experimental mouse model, knocking out the OPG protein resulted in elevated calcification in both male and female groups compared to the control mice groups. Mineralization and bone loss was related and reported in various tissue sections within the vasculature[61,97,118]. The hypothesis put forward here is that in the process of counter-balancing this excess bone loss BM may stimulate the release of osteo-progenitors from marrow environment. The over produced progenitor cells, with bone forming abilities may enter peripheral circulation and home to diseased vasculature, thus mineralizing the vascular lesions[1,58,118,123,249].

The complied results from the investigations in this Chapter along with Chapter 4 suggest that circulating OCN^+ MNC population is elevated in a mouse model system in which osteoclast inhibitors such as OPG are knocked out. This circulating population was also demonstrated to be associated with aortic calcium and aortic OCN^+ population deposited within the vasculature. These results suggest three-way linkage between the release of BM osteo-progenitor population, its presence in peripheral circulation and its further deposition within aortic tissues in $OPG^{-/-}$ mice.

In Chapter 4, we demonstrated a positive association between the total aortic calcium content and the stem cell mobilizing cytokines such as SDF-1α and G-CSF in circulating serum samples of $OPG^{-/-}$ mice. These findings from Chapter 4 could be related to the OCN^+ population increase in $OPG^{-/-}$ aorta as SDF-1α and G-CSF stimulate the release of osteo-progenitors from the BM as a direct result of excess bone loss, as observed in $OPG^{-/-}$ mice. Further, these cytokines may also facilitate homing of the OCN^+ population to diseased lesions, suggesting a possible role for osteo-progenitors towards vascular calcification.

Recent reports, however, have questioned the demonstration of vascular calcification in an older $OPG^{-/-}$ model as it is known to have a number of limitations. Firstly, the severity of vascular calcification is minimal within vasculature of these mice developing only a low to moderate degree of calcification[61,138]. The percentage of aorta undergoing mineralization is

also inconsistent and low, between 1 to 2%, as reported in Chapter 4. Secondly, the localization of calcification reported in the $OPG^{-/-}$ model is extremely region specific within the vasculature[138], a finding reflected in the results from Chapter 4. Also, the time span required to develop calcification in existing knockout mouse models is long[61,97]. However, more recently it was reported that the process of calcification can also be stimulated in younger $OPG^{-/-}$ mice using a calcitriol infusion[138].

Overall, the results obtained from this Chapter supports the initial hypotheses that BM-derived osteo-progenitors may contribute towards aortic calcification. Further investigation, however, is required in a calcitriol induced $OPG^{-/-}$ mouse model in which aortic calcification is reported to develop more rapidly than in the 12 month old $OPG^{-/-}$ model[138]. The next Chapter discusses the association of OCN^{+} MNC and total aortic calcification in a calcitriol induced younger $OPG^{-/-}$ mouse model.

CHAPTER 6. INVESTIGATION OF OCN^+ MNC AND AORTIC CALCIFICATION IN A CALCITRIOL TREATED $OPG^{-/-}$ MOUSE MODEL

6.1. Introduction

In this Chapter, the effect of calcitriol on the circulating OCN^+ MNC was investigated. The correlation of this population was also studied with the extractable aortic calcium content. A comparison between 12 month old $OPG^{-/-}$ model without calcitriol and 14 week old $OPG^{-/-}$ model with calcitriol doses was studied to determine the influence of calcitriol on the extent of vascular calcification.

A recent report suggested that administration of calcitriol in 14 week old $OPG^{-/-}$ mice increased the degree of aortic calcification within the vasculature of the young mice[138]. These reports formed a basis for the present investigation in this Chapter.

6.2. The mode of action of calcitriol

Calcitriol or 1α, 25-dihydroxyvitamin D3 has been implicated in the induction of vascular calcification[1-3]. It is metabolized in a two step process within the body to the hormonally-active form known as 1,25-dihydroxycholecalciferol[139]. The first step occurs within the liver where cholecalciferol is hydroxylated to 25-hydroxycholecalciferol by the enzyme 25-hydroxylase[138,142]. The second step occurs in the kidneys where 25-hydroxycholecalciferol serves as a substrate for 1-alpha-hydroxylase, yielding 1, 25-dihydroxycholecalciferol, the biologically active form[1,3].

6.3. Experimental design

Eight week old (56 days, n=12) male experimental $OPG^{-/-}$ and age matched control $OPG^{+/+}$ mice were selected for the study. All mice were fed a normal chow diet throughout the study. At 14 weeks of age (98 days) the $OPG^{-/-}$ and $OPG^{+/+}$ mice were injected subcutaneously with 5 µg/kg body weight of calcitriol (Tocris Biosciences, USA) for 3 consecutive days (days 98, 99 and 100) as described in Chapter 2. Tail bleeds were analyzed by FC analysis to estimate the percentage of OCN^+ MNC in circulating blood during the course of the experiment. Serum samples were collected before (75 days) and after (106 days) calcitriol injections (not shown in the figure). At the end of the study (106

days), aortas were harvested and stored at -20°C until later estimation of extractable calcium. A brief experimental design is illustrated in Figure 6.1.

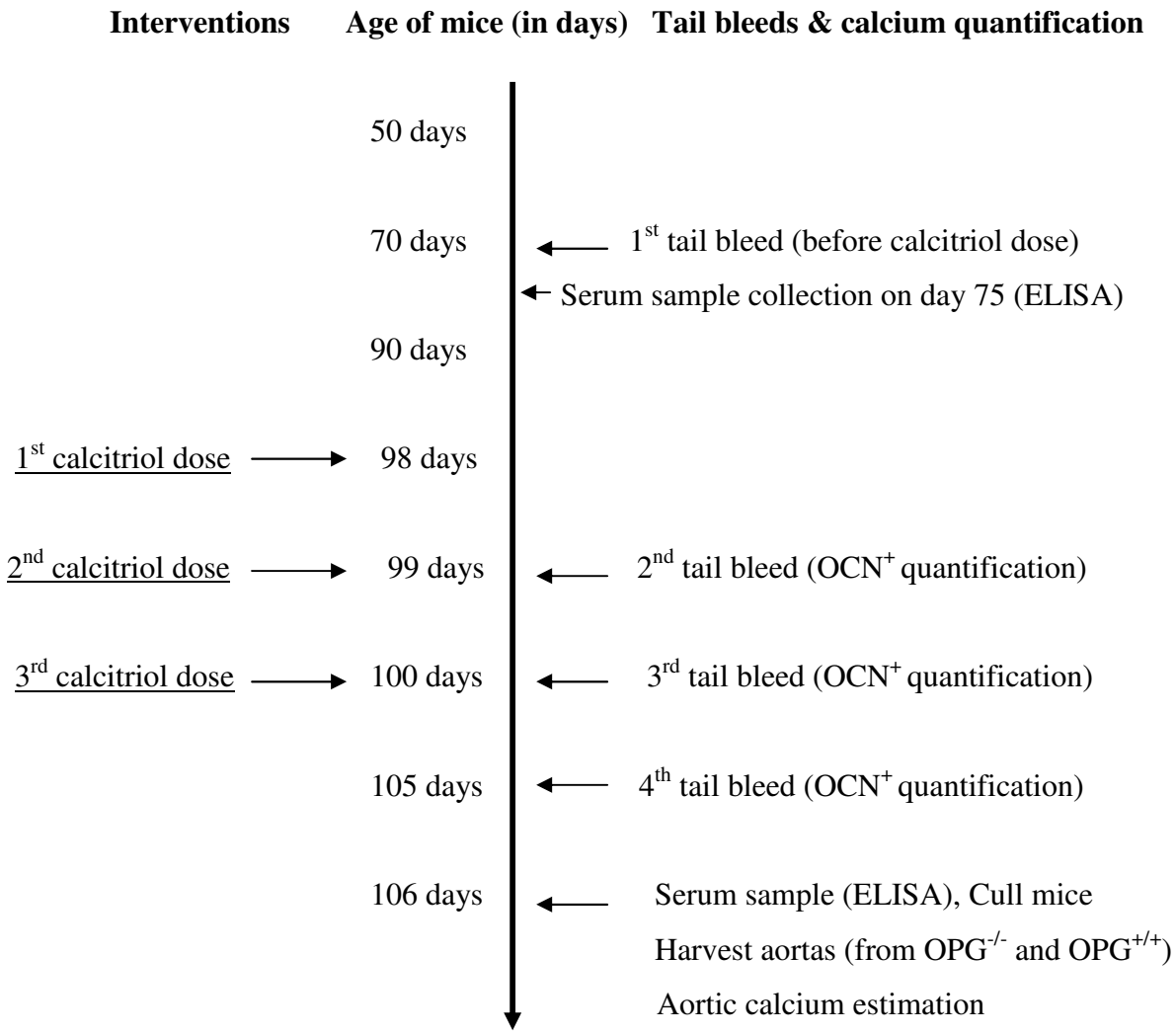

Figure 6.1. Experimental design for calcitriol administered vascular calcification studies

6.4. OCN^+ MNC estimation

6.4.1. Protocol

The circulating OCN^+ MNC were quantified at different time points before and after calcitriol injections. 12 mice from each group (8 weeks old) were selected for the study. A detailed protocol and the FC standardization is outlined in Chapter 2 (section 2.6) and Chapter 3 (section 3.5 and 3.6) respectively.

6.4.2. Results

The median percentage comparison of the percentage of OCN^+ MNC for the two groups is illustrated in Figure 6.2.

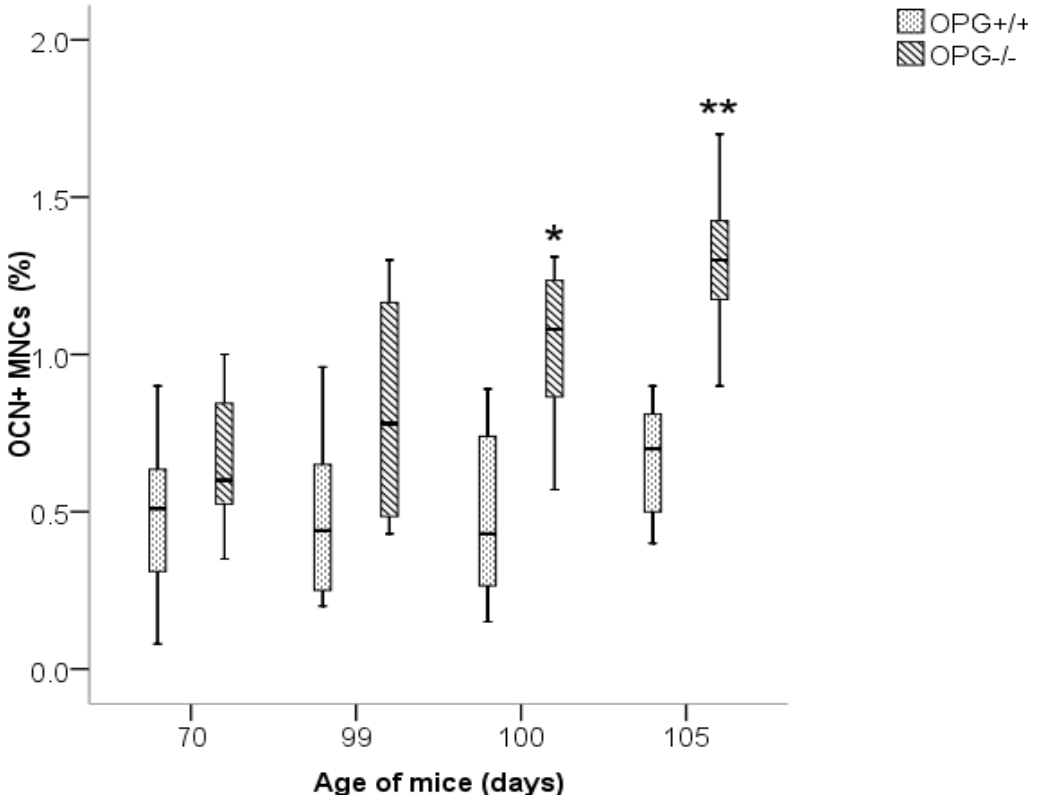

Figure 6.2. Box plot representing the percentage of circulating OCN^+ MNC between experimental $OPG^{-/-}$ and control $OPG^{-/-}$ mouse groups receiving calcitriol. * denotes statistical significance.

The percentage of circulating OCN^+ MNC in 15 week old mice was significantly greater in $OPG^{-/-}$ mice compared to the $OPG^{+/+}$ group seven days after the first calcitriol injection (at 105 days).

The median and the IQR results for all the tail bleeds (before and after calcitriol injections) in experimental $OPG^{-/-}$ and control $OPG^{+/+}$ male mice is tabulated in Table 6.1.

Table 6.1. Effect of calcitriol on circulating OCN^+ MNC in experimental $OPG^{-/-}$ and control $OPG^{+/+}$ male mouse groups.

	$OPG^{-/-}$ (Experimental)		$OPG^{+/+}$ (Control)		
Age and relation to calcitriol doses	Median	IQR	Median	IQR	Significance (p value)
70 days (No calcitriol)	0.75	0.51-0.85	0.48	0.31-0.63	0.08
99 days(post 1st calcitriol dose)	0.79	0.48-1.13	0.49	0.26-0.62	0.04
100 days (post 2nd calcitriol dose)	1.05	0.89-1.23	0.54	0.26-0.67	0.02*
105 days(1 week post 1st calcitriol dose)	1.30	0.86-1.4	0.70	0.51-0.81	0.01**

As observed in the OCN^+ MNC percentage, calcitriol administration also resulted in the increase of OCN^+ MNC cell numbers/ml of blood in $OPG^{-/-}$ group (8 x 10^3 cells/ml, IQR 6 x10^3- 8.3 x 10^3, 105 age point) when compared to that before calcitriol doses (3.1 x10^3 cells/ml, IQR 1.6 x10^3-3.3 x10^3, p=0.01, 70 day age point). The increase at this time point was not significant in $OPG^{+/+}$ group. Figure 6.3 illustrates the significant increase in the OCN^+ population/ml blood of $OPG^{-/-}$ experimental mice.

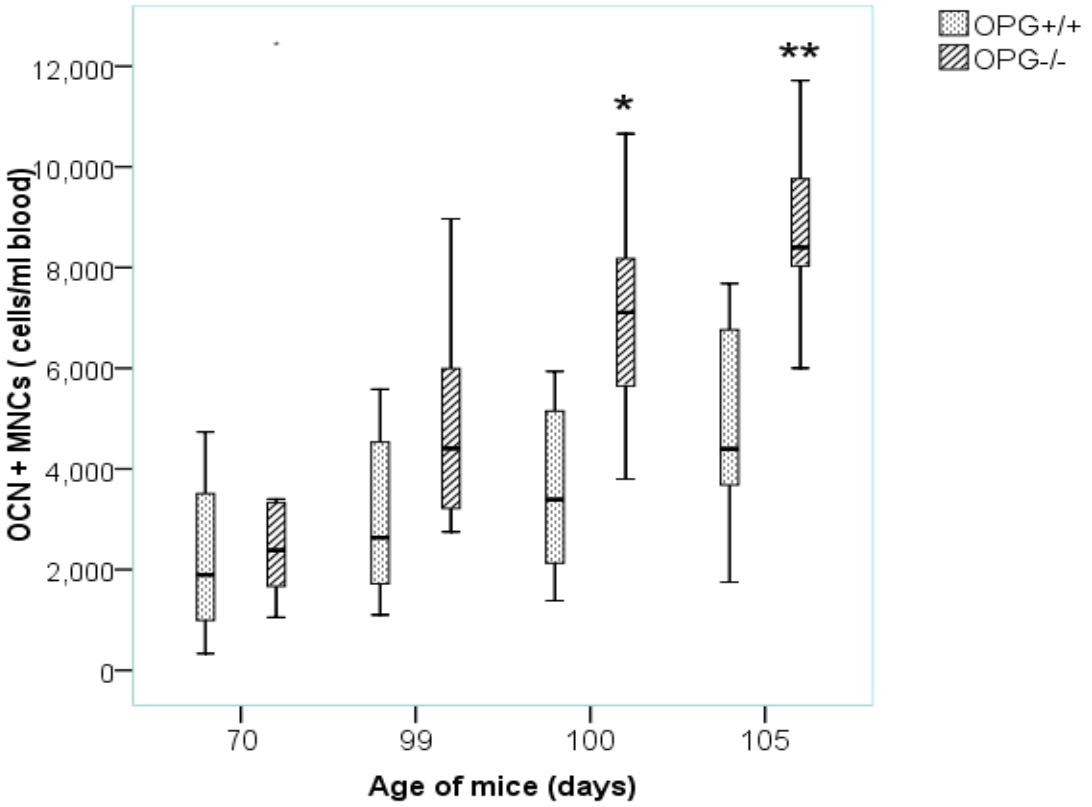

Figure 6.3. Box plot representing the comparison of circulating OCN^+ MNC population between experimental $OPG^{-/-}$ and control $OPG^{+/+}$ mouse group receiving calcitriol. * denotes statistical significance.

6.5. Aortic calcium quantification

6.5.1. Protocol

After OCN^+ MNC estimation experimental $OPG^{-/-}$ (n=12) and control $OPG^{+/+}$ (n=12) mice were culled and aortas were harvested. Total aortic calcium was extracted and quantified using a bioassay described in Chapter 4 (section 4.4). A detailed protocol and the optimization are given in Chapter 2 (section 2.4) and 3 (section 3.2) respectively. Results were compared between the experimental $OPG^{-/-}$ and control $OPG^{+/+}$ groups.

6.5.2. Results

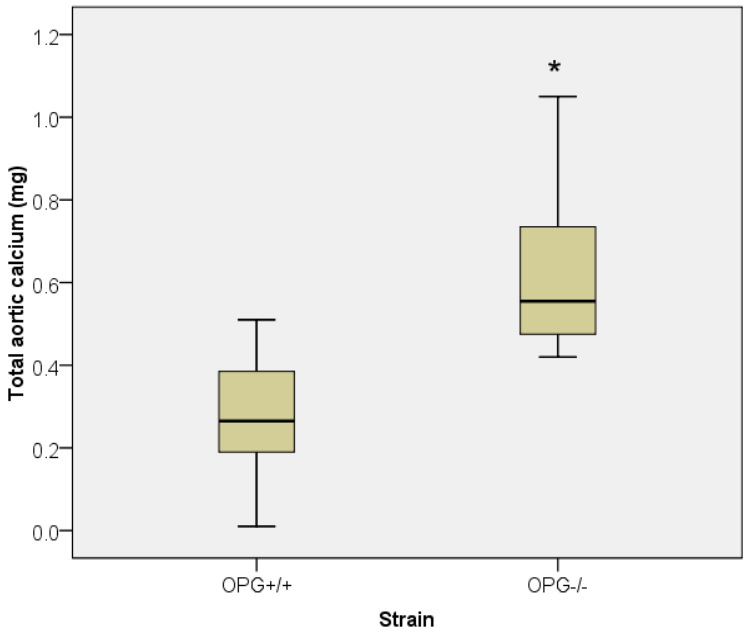

Figure 6.4. Box plots representing the total extractable aortic calcium comparison between experimental $OPG^{-/-}$ and control $OPG^{+/+}$ male mouse groups. The data was found not to be normally distributed and hence a non parametric Mann Whitney U test was used to assess statistical significance. * denotes statistical significance.

6.6. Correlative association for circulating OCN^{+} MNC and total calcium in calcitriol model

The association between circulating OCN^{+} MNC and total aortic calcium content was investigated for experimental $OPG^{-/-}$ and control $OPG^{+/+}$ mouse groups in relation to calcitriol doses. The correlation coefficient for both mouse groups is illustrated in Figure 6.5.

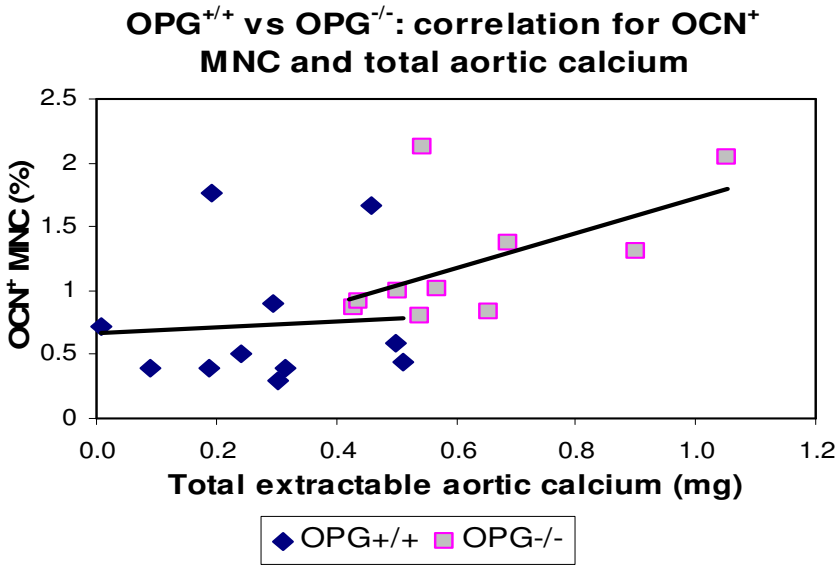

Figure 6.5. Scatter plot illustrating the association of total aortic calcification with circulating OCN^+ MNC percentage in $OPG^{-/-}$ and $OPG^{+/+}$ mice obtained 1 week after the 1st calcitriol dose.

The OCN^+ MNC was weakly correlated with total aortic calcification before calcitriol doses (r=0.31, not shown in the Figure). However 1 week after the first calcitriol dose the correlation was statistically significant (r=0.64, p<0.01) in $OPG^{-/-}$ mice while it was weakly correlated in $OPG^{+/+}$ mice (r=0.34, p<0.09).

6.7. $OPG^{-/-}$ mouse model: with calcitriol vs. without calcitriol

The total extractable aortic calcium in the 15 week old $OPG^{-/-}$ male mouse group that received calcitriol was significantly greater (0.64 mg, IQR 0.49-0.71, n=12) than that measured in the earlier cumulative assessment on 12 month old $OPG^{-/-}$ male mouse group without calcitriol (Chapter 4 and 5, 0.41 mg, IQR 0.38-0.47, n=18, p=0.02). The median and the IQR comparison between the older $OPG^{-/-}$ male mice without calcitriol model and the young $OPG^{-/-}$ male mice with calcitriol model is illustrated in Figure 6.6.

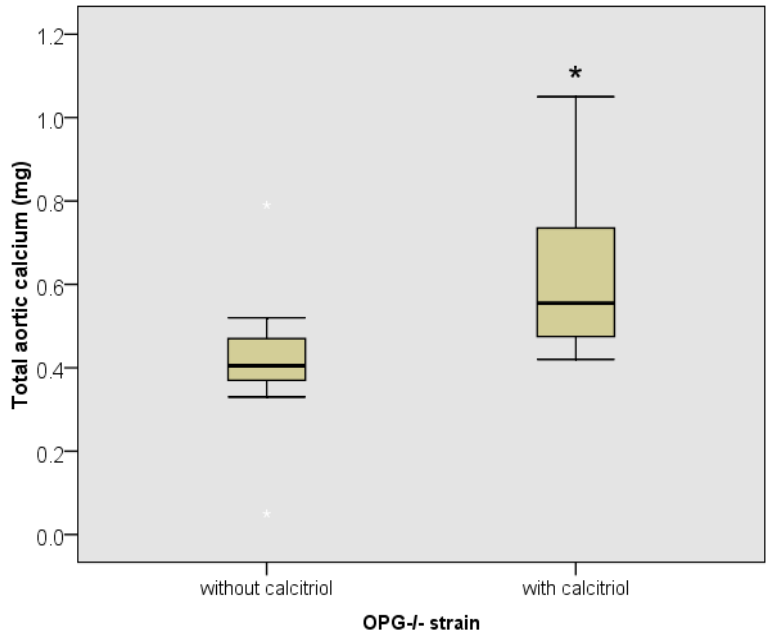

Figure 6.6. Box plot representing the comparison for 12 month old $OPG^{-/-}$ (n=18) male mouse group without calcitriol model and the 14 week old $OPG^{-/-}$ male group (n=12) with calcitriol. * denotes statistical significance.

6.8. Discussion

The investigation described in this Chapter demonstrates a positive association between the circulating OCN^{+} MNC population and the total extractable aortic calcium in a calcitriol induced $OPG^{-/-}$ mouse model. The present investigation supports the hypothesis which tests the association of BM-derived osteo-progenitors with aortic calcification.

The 14 week old $OPG^{-/-}$ mice used in the calcitriol model demonstrated greater severity of aortic calcification than the 12 month old $OPG^{-/-}$ without calcitriol investigated in Chapter 4 and 5. The results obtained in this Chapter confirm the role of calcitriol in accelerating vascular calcification within a mouse model as suggested previously[138].

In the present analysis, it was noted that calcitriol doses instigated a significant increase in circulating OCN^{+} MNC in younger experimental $OPG^{-/-}$ mouse group. However, this OCN^{+} MNC percentage was found to be lower than the circulating OCN^{+} MNC demonstrated in the 12 month old $OPG^{-/-}$ model without calcitriol. This was thought to be possible due the young age of the $OPG^{-/-}$ mice (15 weeks vs. 54 weeks). The younger age of the $OPG^{-/-}$ mice

may limit the amount of time for the osteo-progenitors such as OCN^+ cells to be released from the BM environment. However, in spite of OCN^+ MNC population being lower in younger calcitriol $OPG^{-/-}$ model, it was found that the amount of extractable aortic calcium was significantly greater than that reported in 12 month old $OPG^{-/-}$ model without calcitriol (Chapter 4 and 5). The correlation of the circulating OCN^+ MNC population with the amount of total extractable aortic calcium was stronger in calcitriol induced $OPG^{-/-}$ male mouse group in comparison to the 12 month old $OPG^{-/-}$ mouse groups suggesting a positive influence of calcitriol towards vascular calcification.

This study also addresses some of the controversies questioning the application of an older $OPG^{-/-}$ model for vascular calcification model[58,61,97,138]. Previous reports suggested that the time frame required by the older $OPG^{-/-}$ models to develop calcification was a major concern[5,6]. This was also evident in the $OPG^{-/-}$ model investigated in Chapter 4 and 5. These 50-54 weeks old mice reflect slow calcium accumulation in the $OPG^{-/-}$ vasculature. It has also been reported that the vasculature of these mice develop low to moderate degree of calcification[7,8]. Immunohistochemistry studies, in older $OPG^{-/-}$ mice, also reported a limited percentage of calcium deposition throughout the vasculature[138]. Further, the extent of calcification development within vasculature of these $OPG^{-/-}$ mice was extremely region specific[1,7,8].

Calcitriol, on the other hand, is known to be important for the development, growth, and maintenance of a healthy skeleton[138,139]. A physiological dose of vitamin D3 has the effect of promoting both bone resorption and formation[139]. However, high-dose calcitriol increases bone resorption by activating osteoclastogenesis and inhibiting the expression of OPG[7]. It was suggested that osteoclastogenesis in $OPG^{-/-}$ mice was accelerated by treatment with calcitriol which resulted in increased serum calcium level[139]. Microscopy analysis of the aortic tissues in these experiments also demonstrated an increased level of calcium deposition in the medial layer of the in $OPG^{-/-}$ aorta after 3 subsequent doses of calcitriol injections[138].

During the present calcitriol studies in this Chapter, it was observed that in both mouse groups the circulating OCN^+ MNC population were similar before the 1st calcitriol injection in $OPG^{-/-}$ and $OPG^{+/+}$ model at 70 day age time point. This was expected because of the young age of the $OPG^{-/-}$ mice. Investigations from Chapter 4 and 5 also indicated that the time frame for aortic calcification in these $OPG^{-/-}$ mice is approximately 50-54 weeks. The percentage of OCN^+ MNC population started increasing significantly only after the 3rd dose

of calcitriol (100 day time point). This increase in the circulating OCN^+ MNC in $OPG^{-/-}$ group was most significant one week after the first calcitriol injection (105 days age time point). At this point of time, the mortality rates and the deteriorating health in the $OPG^{-/-}$ group did not allow further quantification of circulating OCN^+ MNC.

One week after the first calcitriol injections the mortality rate was 16 % and 8% in $OPG^{-/-}$ and $OPG^{+/+}$ group respectively. Some of the surviving $OPG^{-/-}$ mice demonstrated spinal deformities symptoms such as restricted movement, arched back bone and inability to stand on the hind legs for food and water. At this time, all the mice were culled total aortic calcium was quantified.

After the calcitriol investigations in $OPG^{-/-}$ mouse model, which related to the results obtained in the older $OPG^{-/-}$ model, the current hypotheses was further tested in a human patient cohort to confirm our mouse model findings. The next Chapter investigates the association of circulating OCN^+ MNC population and aortic calcification volumes measured in a human patient cohort diagnosed from peripheral artery diseases.

CHAPTER 7. ASSOCIATION BETWEEN CIRCULATING OCN^+ MNC POPULATION, STEM CELL MOBILISING CYTOKINES AND CALCIFICATION VOLUMES IN A PATIENT COHORT

7.1. Introduction

Studies described in Chapter 5 and 6 investigated the association of circulating OCN^+ MNC with the aortic calcification levels in two $OPG^{-/-}$ mouse models. In this Chapter, a human patient cohort investigation was undertaken to assess the correlation between circulating OCN^+ MNC and the calcification volumes in patients diagnosed with peripheral artery diseases.

7.2. Measurement of aortic calcification volumes in patients

Patients diagnosed with peripheral artery diseases and requiring CTA were considered for the study. Patients were reviewed by a vascular consultant and a detailed examination was carried out.

7.2.1. Ethics approval and patient selection criteria

Approval for the human studies was obtained from The JCU Ethics Committee (Appendix 3). Written informed consent was obtained from all participants. Patients included in the study had symptoms of intermittent claudication and clinical evidence of lower limb ischemia. These patients, according to the treating physician, required a CTA to further assess their peripheral arteries[235]. In our clinical study, 10 patients (≈ 44% of the total cohort) had an AAA (aortic diameter≥ 30 mm) in addition to symptoms of intermittent claudication while 13 patients (56 %) did not have an AAA (aortic diameter ≤ 30 mm). The difference between the aortic diameters for both these group was statistically significant (p=0.0001, n=23). Also, as indicated in table 7.1, patients diagnosed with AAA along with occlusive PAD symptoms had higher prevalence of risk factors such as smoking, hypertension, CHD and dyslipidemia compared to subjects who simply had intermittent claudication (smoking: p=0.01, hypertension: p= 0.03, CHD: p=0.03, dyslipidemia: p=0.01). Patients were excluded if they had received previous open surgical or endovascular treatment of their infrarenal aorta or if a CTA was felt to be contra-indicated. Also, patients with either abnormal serum creatinine, an inability to lie down flat on their back or with any contrast allergy were excluded from the study[235].

7.2.2. CTA analysis

For selected patients, CTA images were analyzed, as previously described[131,235], to quantify infrarenal aortic calcification volume. A detailed methodology is described in Chapter 2 (section 2.8).

7.3. Patient recruitment and blood sample collection

At recruitment, patients were requested to visit their nearest Sullivan Nicolaides Pathology for early morning blood samples which were obtained following an overnight fast. Blood samples (20 ml) were collected into heparinised tubes (4 ml X 5 tubes, BD vacutainer, Becton Dickinson, USA) to avoid coagulation. The samples were immediately couriered to JCU, School of Medicine & Dentistry research laboratory for further analysis.

7.4. Experimental design

7.4.1. OCN^+ MNC analysis

The detailed protocol and optimization of the quantification of circulating OCN^+ population in human patient cohort is described in Chapter 2 (section 2.10) and 3 (section 3.6 and 3.7) respectively. Briefly, MNC were separated from the blood sample using a ficoll separation technique. Plasma was stored at -20^oC for later analysis of SDF-1α, G-CSF and SCF concentrations. After performing an initial MNC cell count an FcR blocking step was carried out (Miltenyi biotech, USA) preventing the nonspecific binding prior to exposure to primary anti- OCN antibody (Goat anti-mouse, Biomedical technologies, USA). The primary OCN antibody labeling step was followed by fluorescent secondary PE antibody (Donkey anti-goat, Jacksons Immunoresearch, USA) binding step. Further, these cells were incubated with appropriate volumes of anti-PE magnetic micro beads (Miltenyi Biotech, USA). These anti-PE beads adhere to the fluorescent PE tag which is already attached to the OCN antibody. The magnetically labeled cells were then passed through MS columns where MNC labeled with OCN antibody were enriched. Post MS enrichment, both OCN^+ and OCN^- MNC fractions were quantified on FC as discussed in Chapter 2 (section 2.10).

7.4.2. SDF-1α, G-CSF and SCF ELISA

The plasma, separated as a part of MNC extraction, was stored at -20^oC prior to determination of circulating SDF-1α, G-CSF and SCF concentrations, as described in Chapter 2 (section 2.11.1, 2.11.2 and 2.11.3 respectively). All the ELISA's were carried out

according to the manufacturer's instructions (R& D Quantikine, USA). In short, for all ELISA kits, plasma was plated on a pre-antibody coated plate. Plates containing the plasma- antibody complex were then incubated with a fluorescent secondary antibody. After washings, the plasma concentrations of the cytokines were colorimetrically estimated at 492 nm at a corrected reference wavelength of 592 nm. The results were correlated with the circulating OCN^+ MNC percentages and the infra-renal aortic calcification volumes.

7.5. Results

7.5.1. Association of patient age, gender and calcification volumes

Prior to laboratory analysis of blood samples, general patient background information and patient history, including age, sex, smoking habits, hypertension, coronary heart disease history and dyslipidaemia conditions were recorded. An infra renal aortic CTA analysis was performed to measure the calcification volumes in these patients[131,235]. A summary of patients' clinical characteristics is presented in Table 7.1.

Table 7.1. Comparison of risk factors for patients who did and did not have AAA

Risk Factors	IC patients who also had AAA (n=10)	IC patients who did not have AAA (n=13)	P value
Smoking	9 (90 %)	9 (70%)	0.01
Diabetes	4 (40%)	7 (54%)	1.0
Hypertension	9 (90%)	8 (62%)	0.03
Coronary heart disease	9 (90%)	8 (62%)	0.03
Dyslipidemia	9 (90%)	9 (70%)	0.01

Shown are numbers (%) or median (interquartile ranges)

IC= Intermittent claudication

Intermittent claudication was defined by an appropriate history obtained by a vascular specialist, a positive Edinburgh claudication questionnaire and confirmation of significant stenosis (>50%) or occlusion of lower limb arteries on CTA. AAA was defined by a maximum aortic diameter of ≥30mm. Hypertension was defined by a history of high blood pressure or receiving treatment to reduce blood pressure. Diabetes was defined by a fasting

blood glucose ≥ 7.0 mM, or history of, or treatment for hyperglycaemia. Smoking status was classified into current smokers (smoked within the last month), ex-smokers (given up for more than one month) and never smokers. Dyslipidemia was defined by history of diagnosis or treatment for high cholesterol or fats[250].

As would be expected, the percentage of males included in this study was greater than females (17 males and 6 females) as peripheral artery diseases are more prevalent in men[63,66,74,75,153]. The median age for the cohort was 75 years and 83 % of the cohort had a smoking habit. 48 % of the patient cohort had a history of diabetes. A CTA was performed and calcification volumes were measured as previously described[235]. These calcification volumes were found to be moderately correlated to the patient age (Figure 7.1).

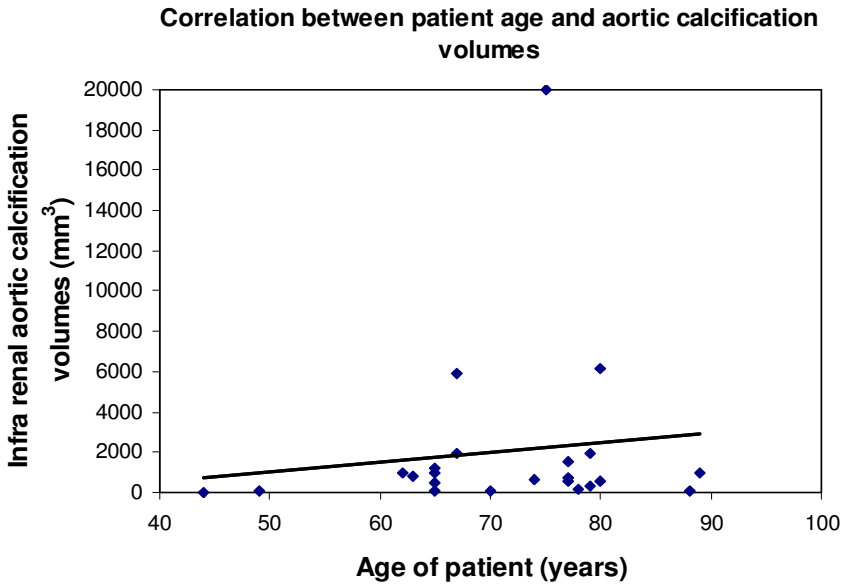

Figure 7.1. Scatter plot illustrating a positive correlation between infra renal aortic calcification volumes and patient age. Spearman's correlation coefficient indicated a correlation value of 0.45.

Patients were categorized into two groups: 1) patients with calcification volumes ≥ median 2) patients with calcification volumes ≤ median. The median of the calcification volumes for the data set was calculated to be 805 mm^3 (IQR 242.5.5-1384.5).

7.5.2. Circulating OCN^+ MNC population

The circulating OCN^+ MNC were analyzed by FC analysis. A total of 23 patient samples were assessed. A statistical box plot illustrating median and IQR of OCN^+ MNC for the two patient groups is illustrated in Figure 7.2.

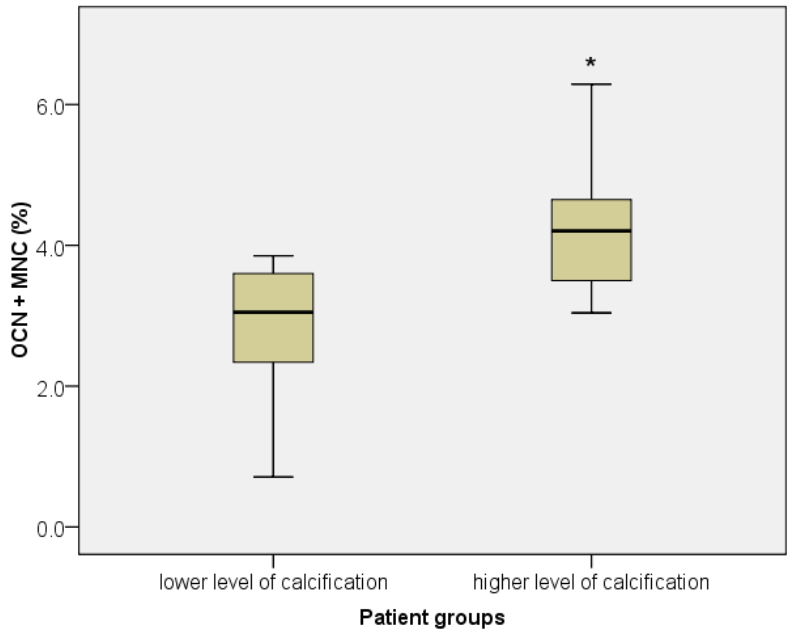

Figure 7.2. Box plot representing the percentage of circulating OCN^+ MNC for the two calcification groups. The data was found not to be normally distributed and hence a non parametric Mann Whitney U test was used to assess statistical significance within the groups. * denotes statistical significance.

Patients with more severe aortic calcification (calcification volume ≥ median i.e. $805cm^3$, had a greater percentage of circulating OCN^+ MNC (median 4.07 %, IQR 3.76-4.39, n=12) than those with less severe aortic calcification (median 3.10 %, IQR 2.32-3.60, n=11, p=0.01).

Similar to OCN^+ MNC percentage, OCN^+ MNC/ml blood was also calculated from the cell counts and was tested for statistical significance (Figure 7.3).

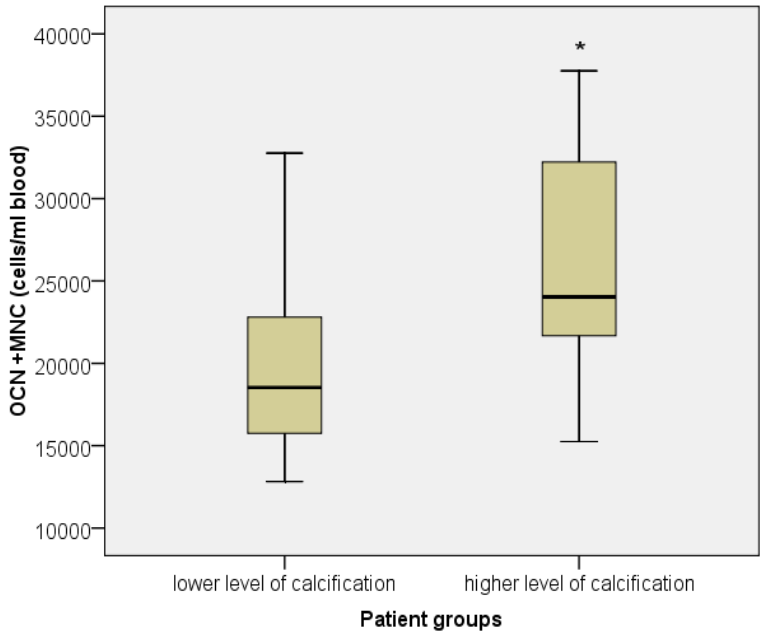

Figure 7.3. Box plot representing the number of circulating OCN^+ MNC/ ml patient blood in the two calcification groups. The data was found not to be normally distributed and hence a non parametric Mann Whitney U test was used to assess statistical significance within the groups. * denotes statistical significance.

Patients with more severe aortic calcification (calcification volume ≥ median i.e. 805 cm^3 had a greater number of circulating OCN^+ MNC/ml blood than those with less severe aortic calcification. The results are summarized in Table 7.2.

Table 7.2. Comparison of the OCN^+ MNC population in patients with high and low amounts of aortic calcification.

Patient groups → Assessment ↓	High calcification group (≥805mm^3) n=12		Low calcification group (≤805mm^3) n=11		p value
	Median	IQR	Median	IQR	
OCN^+ MNC %	4.07	3.76-4.39	3.10	2.32-3.60	0.01
OCN^+ MNC cells/ml	2.28 x 10^4	2.16-3.20	1.95 x 10^4	1.64-2.40	0.03

7.5.3. Plasma SDF-1α, G-CSF and SCF concentration

Plasma samples obtained from the 23 patients were analyzed for stem cell mobilizing cytokines as described in section 7.4.7.

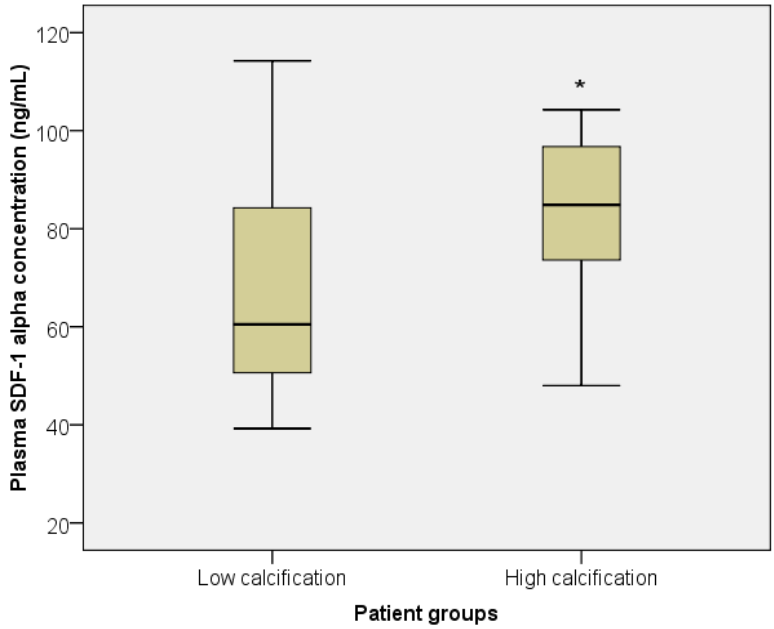

Figure 7.4. Box plot representing the circulating plasma SDF-1α concentrations in patient with peripheral artery disease in relation to aortic calcification. The data was found not to be normally distributed and hence a non parametric Mann Whitney U test was used to assess statistical significance within the groups. * denotes statistical significance.

Patients with more severe aortic calcification (calcification volume ≥ median i.e. 805 cm^3) had higher circulating plasma concentration of SDF-1α, than those with less severe aortic calcification.

Circulating plasma G-CSF concentration was also analyzed in patients included in the study (Figure 7.5).

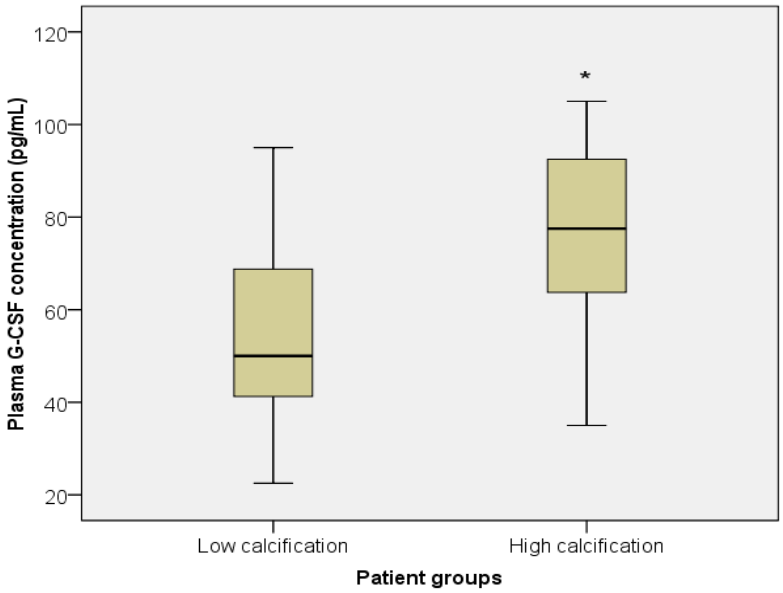

Figure 7.5. Box plot representing the circulating plasma G-CSF concentrations in patients with peripheral artery disease in relation to aortic calcification. The data was found not to be normally distributed and hence a non parametric Mann Whitney U test was used to assess statistical significance within the groups. * denotes statistical significance.

Patients with more severe aortic calcification (calcification volume ≥ median i.e. 805 cm^3) had higher circulating plasma concentration of G-CSF than those with less severe aortic calcification.

Finally, circulating plasma SCF concentration was also analyzed in patient samples (Figure 7.6).

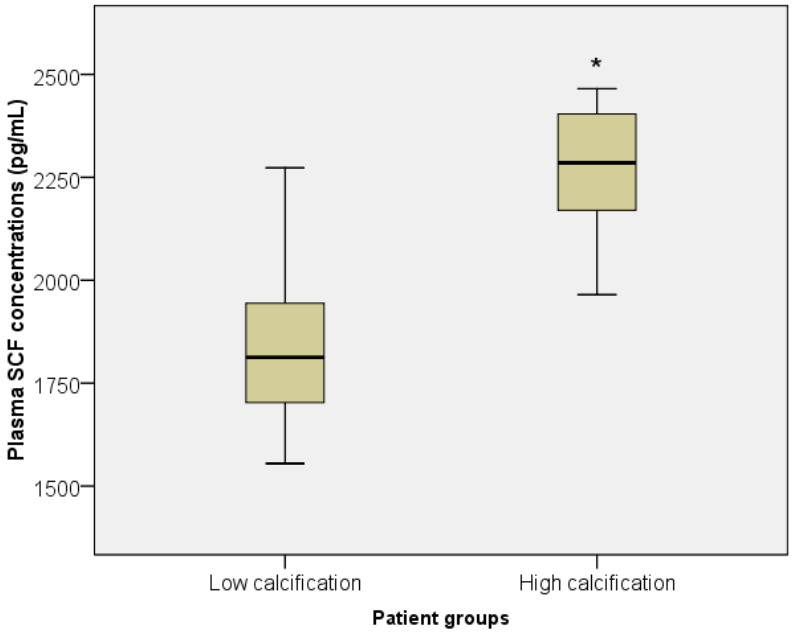

Figure 7.6. Box plot representing the circulating plasma SCF concentrations in patient with peripheral in relation to aortic calcification. The data was found not to be normally distributed and hence a non parametric Mann Whitney U test was used to assess statistical significance within the groups. * denotes statistical significance.

Patients with more severe aortic calcification (calcification volume ≥ median i.e. 805 cm^3) had higher circulating plasma concentrations of G-CSF than those with less severe aortic calcification; however the difference was not significant.
The results for all the three stem cell mobilizing cytokines are summarized in Table 7.3

Table 7.3. Comparison of plasma stem cell mobilizing cytokine concentrations in patients in relation to aortic calcification

Patient groups → Assessment ↓	High calcification group (>805mm^3) n=12		Low calcification group (<805mm^3) n=11		p value
	Median	IQR	Median	IQR	
SDF-1α (ng/mL)	85	74-94.5	60.5	50.63-84	0.04
G-CSF (pg/mL)	77.5	65.63-92.5	50	41.2-68.75	0.03
SCF (pg/mL)	2285	2180-2401	1813	1703-1944	0..001

7.6. Correlation studies

A correlative association between circulating OCN^+ MNC in patient blood samples, the plasma cytokine concentrations, and the calcification volumes were assessed.

7.6.1. OCN^+ MNC population, calcification volumes and patient age

The correlation between the percentage of OCN^+ circulating MNC and aortic calcification volumes were assessed (Figure 7.7).

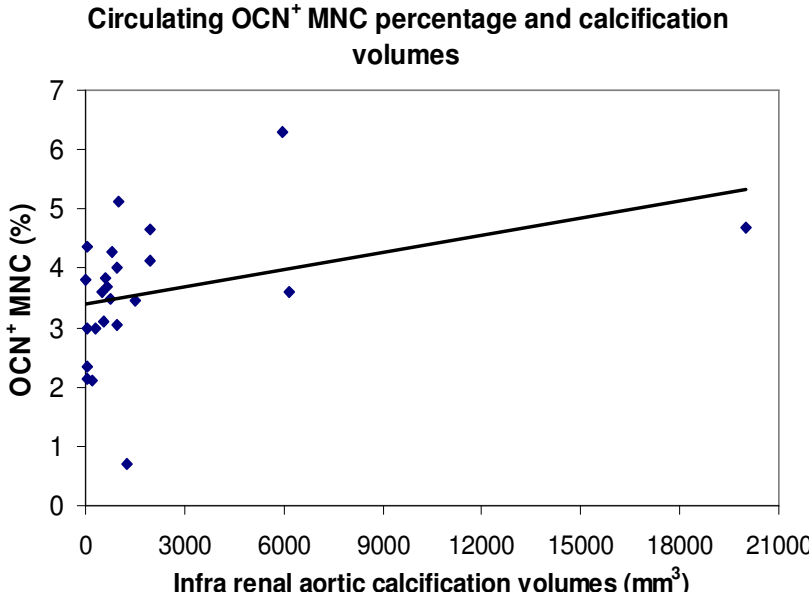

Figure 7.7. Scatter plot illustrating the correlation between circulating OCN^+ MNC percentage and infra renal aortic calcification volumes. Spearman's correlation coefficient was used to test statistical correlation since the study group was comparatively small.

The spearman correlation coefficient between the circulating OCN^+ MNC percentage and infra renal aortic calcification volumes was found to be 0.475 (n=23, p=0.02). A correlation was also observed between number of OCN^+ MNC per ml of blood and the infra renal aortic calcification volumes (r=0.501, n=23, p=0.02, not shown in Figure).

The amount of correlation OCN^+ MNC with patient age was also assessed (Figure 7.8)

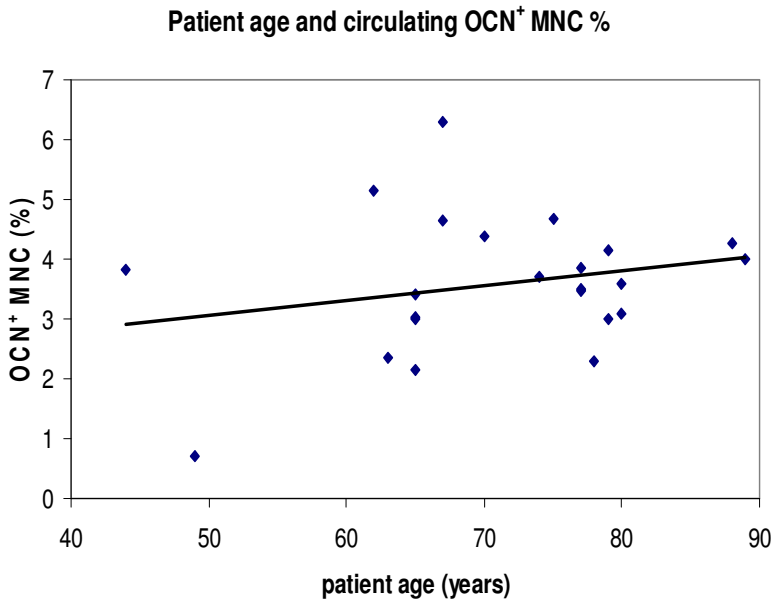

Figure 7.8. Scatter plot illustrating the correlation between patient age and percentage of circulating OCN^+ MNC.

The spearman correlation coefficient between the circulating OCN^+ MNC percentage and patient age was found to be 0.510 (n=23, p=0.01). A correlation was also observed between number of OCN^+ MNC per ml of blood and the infra renal aortic calcification volumes (r=0.495, n=23, p=0.01, not shown in Figure). Table 7.4 shows a compiled result for the correlation values.

Table 7.4. A summary of correlation coefficients between aortic calcification volumes and circulating OCN^+ MNC or age.

Assessment parameters	Spearman's corrleation coefficient
OCN^+ MNC (percent)	0.475
OCN^+ MNC/ ml blood	0.501
Patient age	0.510

7.6.2. Calcification volumes with plasma SDF-1α, G-CSF and SCF concentrations

The spearman correlation coefficient between the plasma SDF-1 α concentration and infra renal aortic calcification volumes was found to be 0.480 (n=23, p=0.01, Figure 7.9)

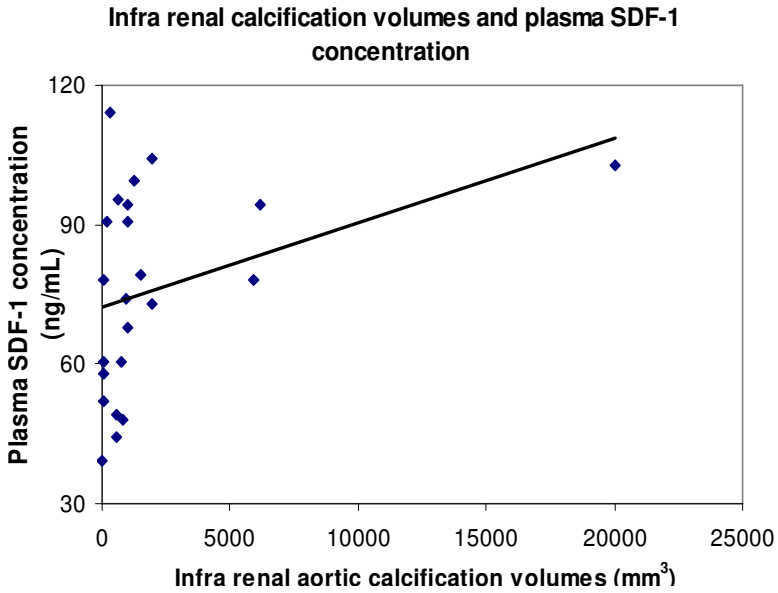

Figure 7.9. Scatter plot illustrating the correlation between plasma SDF-1 α concentration and infra renal aortic calcification volumes.

The plasma concentrations for G-CSF was also statistical correlated with the infra renal aortic calcification volumes (Figure 7.10).

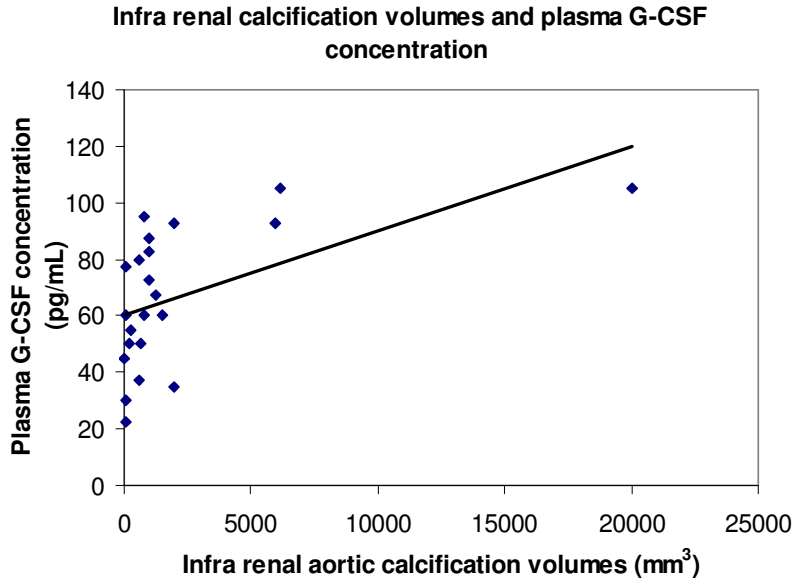

Figure 7.10. Scatter plot illustrating the correlation between plasma G-CSF concentration and infra renal aortic calcification volumes.

The correlation between the plasma G-CSF concentration and infra renal aortic calcification volumes was found to be 0.522 (n=23, p=0.01).

The spearman's correlation coefficient between plasma concentrations for SCF was also statistical correlated with the infra renal aortic calcification volumes (Figure 7.11).

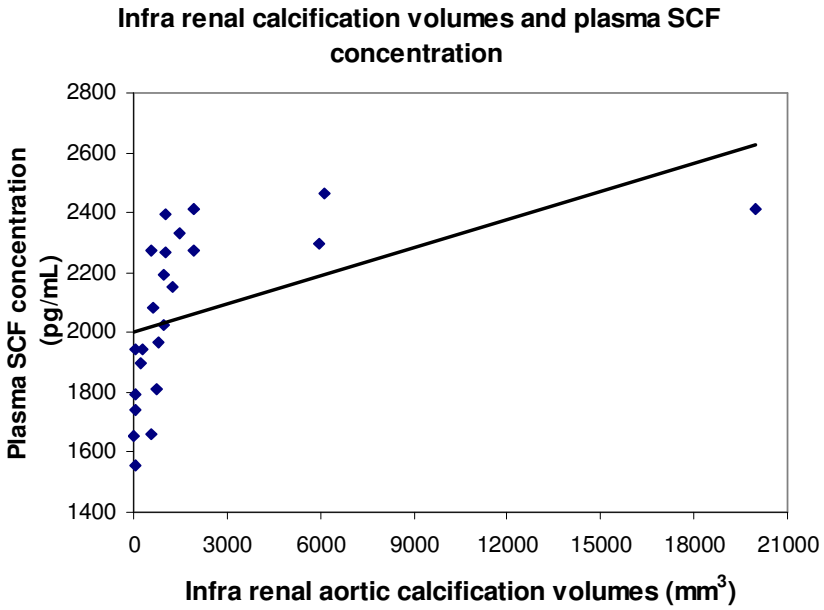

Figure 7.11. Scatter plot illustrating the correlation between plasma SCF concentration and infra renal aortic calcification volumes.

The correlation between the plasma SCF concentration and infra renal aortic calcification volumes was found to be 0.480 (n=23, p=0.03).

7.6.3. Circulating OCN^+ MNC with SDF-1α, G-CSF and SCF concentration

Circulating OCN^+ MNC percentage was analyzed for statistical correlation with plasma SDF-1α concentrations in patient cohort (Figure 7.12).

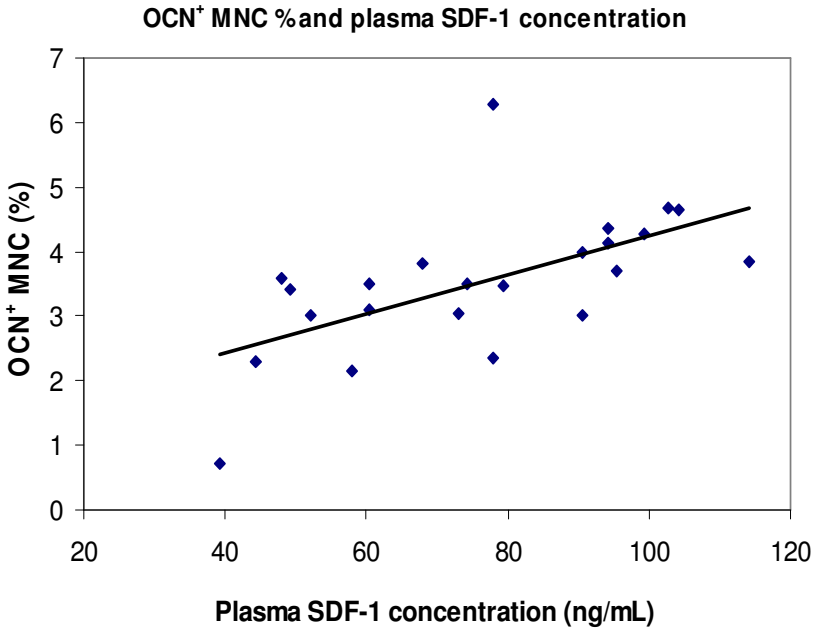

Figure 7.12. Scatter plot illustrating the correlation between plasma SDF-1 α concentration and percentage of circulating OCN^+ MNC.

The spearman correlation coefficient between the plasma SDF-1α concentration and OCN^+ MNC percentage was found to be statistically strong at 0.597 (n=23, p=0.003). The OCN^+ MNC/ml blood population (not shown in the Figure) was also observed to be statistically correlated (r-0.462, p=0.03, n=23).

The association of circulating OCN^+ MNC percentage with plasma G-CSF concentrations was also assessed (Figure 7.13).

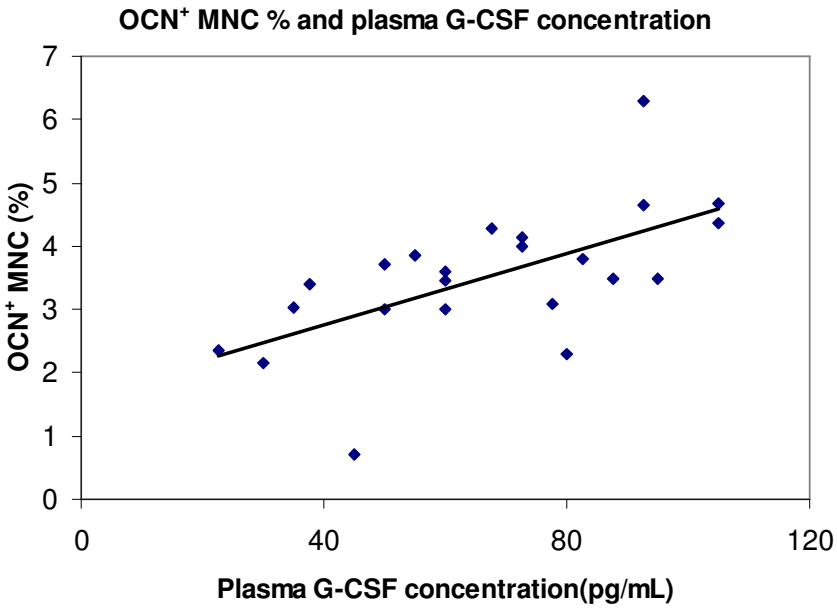

Figure 7.13. Scatter plot illustrating the correlation between plasma G-CSF concentration and percentage of circulating OCN^+ MNC.

The spearman correlation coefficient between the plasma G-CSF concentration and circulating OCN^+ MNC percentage was found to be strong at 0.641 (n=23, p=0.001). The OCN^+ MNC/ml blood population (not shown in the Figure) was also observed to be statistically correlated (r-0.671, p=0.001, n=23).

The association of circulating OCN^+ MNC percentage with plasma SCF concentrations was also assessed (Figure 7.14).

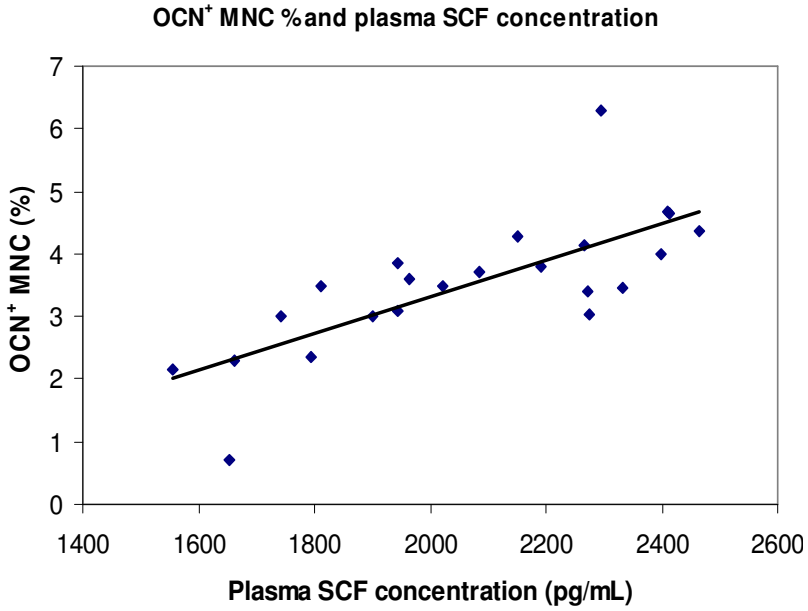

Figure 7.14. Scatter plot illustrating the correlation between plasma SCF concentration and the percentage of circulating OCN^+ MNC. Spearman's correlation coefficient was used to test statistical correlation since the study group was comparatively small.

The spearman correlation between the plasma SCF concentration and OCN^+ MNC percentage was found to be strong at 0.654 (n=23, p=0.001). The OCN^+ MNC /ml blood population (not shown in the Figure) was also observed to be statistically correlated (r-0.610, p=0.003, n=23).

The compiled results for correlation statistics between all the stem cell mobilizing cytokines and OCN^+ MNC population are given in Table 7.5.

Table 7.5. A summary of the correlation coefficient for the association between the number of circulating OCN^+ MNC population and stem cell mobilizing cytokines.

Stem cell mobilizing cytokines in human patient cohort (n=23)	Spearman's correlation coefficient	
	OCN^+ MNC (percent)	OCN^+ MNC (per ml blood)
SDF-1α (ng/mL)	0.597	0.462
G-CSF (pg/mL)	0.641	0.671
SCF (pg/mL)	0.654	0.610

7.7. Discussion

The investigations undertaken in this Chapter reported, for the first time, a possible association between the BM-derived osteo-progenitors and aortic calcification in a patient cohort suffering from peripheral artery diseases. Along with the circulating osteo-progenitors, the plasma concentration of stem cell mobilizing cytokines such as SDF-1α, G-CSF, and SCF was also investigated in this Chapter. Further, their correlation with the aortic calcification volumes and circulating osteo-progenitors was studied. The results reflected the findings obtained from the mouse model investigations from Chapter 5 and 6. The present findings supported the hypotheses that immature BM-derived osteo-progenitors are released from the BM environment into peripheral circulation followed by homing to the diseased arteries. Further, these immature cells integrate, proliferate and develop into bone-like cells in the diseased vessel wall which results in the mineralization of the vasculature as previously supported[182,183,243]. This channeling and proliferating of the immature cells was found to be induced by cytokines such as SDF-1α and G-CSF concentrations in circulating blood[90,185,186,218,224].

The circulating OCN^+ MNC in blood samples obtained from patients diagnosed with peripheral artery diseases was quantified. Patients were categorized into two groups based on their total infra renal aortic calcification volume content. The measured calcification volumes were correlated moderately with circulating OCN^+ MNC population. Patients with greater amounts of aortic calcification had higher circulating percentage of OCN^+ MNC.

Interestingly, patients in the high calcification group showed a 4-fold increase in the OCN^+ MNC percentage was in comparison to that reported in normal healthy individuals (4.1 % vs. 0.93 %)[239].

Another aspect of this study was to investigate the association of circulating stem cell mobilizing cytokines with the severity of aortic calcification. As discussed in Chapter 1, cytokines such as G-CSF, SDF-1α and SCF are known for mobilizing immature cells from the BM into peripheral circulation and facilitate their homing towards vascular lesions[186,188,218]. The protein ELISA analysis observed that the plasma concentrations of SDF-1α and G-CSF were approximately 2-3 fold higher in patients with aortic calcification than those observed in healthy subjects (normal G-CSF: 27 pg/mL[251]; normal SDF-1α: 34 ng/mL[251]). Plasma SCF levels, however, were close to the normal values (normal SCF: 2.5 ng/mL[251]). A positive association between these cytokine concentrations, aortic calcification volumes and OCN^+ MNC suggests a role of circulating osteo-progenitors in arterial mineralization. This 3-way association was also observed by our $OPG^{-/-}$ mouse model investigation in Chapter 4.

Circulating OCN^+ MNC were moderately associated with higher and lower levels of infra renal calcification volumes measured by CTA. Also, the calcification volumes showed a stronger overall association with the patient age hence confirming that the severity of calcification progressively increased with the age for the patients selected in the experimental cohort, a finding also been reported previously in literature[34,63,67].

The circulating OCN^+ MNC population also demonstrated a positive correlation to the patient age for both the calcification groups. Patients with higher calcification volumes reported a higher percentage of circulating OCN^+ MNC, thus demonstrating a possible 3-way association between patient age, higher calcification volume and elevated circulating progenitor population. It was also observed that the OCN^+ MNC percentage was higher in male patients than females suggesting that males may be at a higher risk of developing calcification within their vasculature and hence make them more prone to cardiovascular events as previously reported[66,150,252].

Although a positive correlation pattern was observed throughout the patient study for the calcification volumes and BM-derived OCN^+ MNC population, there may be a need for a larger cohort size in order to establish the confidence in the statistical correlation. A larger cohort investigation could also assist in confirming the hypothesis and the results obtained

from the mouse model studies. Overall this human patient investigation suggests an association between BM-derived osteo-progenitors and their contribution towards vascular calcification with the assistance from circulating cytokines.

A general discussion with conclusion and future directions arising from this research investigation is detailed in the next Chapter.

CHAPTER 8: GENERAL DISCUSSION AND FUTURE DIRECTIONS

8.1. Discussion

This investigation suggests, for the first time, an association between circulating OCN^+ MNC and aortic calcification in two mouse models and a human patient cohort with peripheral artery disease. It also suggests that stem cell mobilizing cytokines could be involved with the release of osteo-progenitors and may facilitate their homing to the vasculature. These findings are supportive evidence for the hypothesis that BM-derived cells play a role in the pathogenesis of vascular calcification.

For centuries, vascular calcification was considered a passive process which occurred as a nonspecific response to tissue injury or necrosis[1,3,82,97]. Calcification was believed to be directly associated with atherosclerotic plaque burden, sharing similar risk factors and leading to cardiovascular morbidity and mortality[3,14,21,22,34,42,43,67,95]. Research in the past has reported it to be a degenerative process leading to uncontrolled precipitation of calcium phosphate[1-3,23,25]. Several passive theories were put forward defining the mechanism by which calcification occurred in arteries[1,37] including loss of inhibition. Other theories suggest mechanisms depending on induction of bone formation, circulation of nucleational complexes and cell apoptosis[1,3,52,61,97].

Research in the past two decades suggests vascular calcification to be an active cellular mechanism[45,253]. Genetic vascular research also suggests that vascular calcification can be studied as an independent factor from atherosclerosis[2,14,15,34,42,52]. This research suggests that following endothelial damage, VSMC from the medial layer of the artery migrate to the intimal layer via the *vasa vasorum* and contribute to atherosclerosis progression[253]. Nevertheless, more recent studies have claimed that the media may not be the only source for VSMC in vascular lesions. It was further speculated these VSMC may originate from sources external to the vasculature[178,253]. This hypothesis was supported by investigations in which VSMC progenitors were identified in circulating blood[169,178]. Further BM transplant experiment conducted in animal models also suggested that external sources such as the BM may contribute to atherosclerosis progression[193,194]. This novel hypothesis was termed as the circulating cell theory. Recently, circulating BM-derived cells have also been suggested to contribute towards vascular calcification[158,177,182,243,254]. The BM population with osteogenic potential is referred to as osteo-progenitors[214]. The concept of osteo-

progenitors, however, is vaguely understood and the behaviour of these immature cells in the vasculature has been controversial and demands further research.

Following the development of this concept, research groups have reported various *in vivo* and *in vitro* studies which suggest a positive association between the BM-derived cells and their contribution towards the pathogenesis of vascular diseases including atherosclerosis[39,169,193,241] and vascular calcification[30,41,194,207]. The osteogenic potential of adult vascular cells has been demonstrated *in vitro* and *in vivo*. The lineages of these cells, which are similar to that of marrow stromal cells and their capacity for self-renewal, demonstrated that they are of a MSC origin which forms a significant proportion of BM stroma[30,195,200,211,214,217]. Researchers have claimed that the majority of VSMC in neointimal lesions in animal models of atherosclerosis were of BM origin[39,169,193,227]. BM transplant experiments investigated in mouse models by several groups also indicated that BM-derived progenitor cells could potentially achieve a VSMC lineage and hence contribute to lesion formation[169,171,178,192]. *In vitro* differentiation studies also indicate that these immature cells derived from various mouse models differentiate into osteoclast-like cells in the presence of several chemo attractants and growth factors ideal for osteogenic lineage[30,159,243,255]. Evidence from hMSC line studies also supports the hypotheses that BM cells play a crucial role towards the pathogenesis of vascular diseases[30,199,200,214]. Human OCN^+ cells have also been reported to stimulate mineralization both *in vitro*[30,157,158,217] and when injected into mice[192,217,241]. Osteoclast and osteoblast-like cells have also been demonstrated within areas of vascular calcification in both human[169,222] and mouse aortas[194,217,241].

Along with *in vitro* investigations, immunohistochemistry studies have also identified the osteoblast-like bone markers after BM transplants in mouse models. These findings support the contribution of the circulating progenitors towards pathogenesis of vascular calcification[58,59,96,97,166]. Along with the histological findings, the role of certain cytokines such as SDF-1α and G-CSF in BM cell mobilization has also been studied. The studies indicate a possible association between the release of immature cells and the advent of osteoblast-like cells in vascular lesions[41,147,183,185,188,219].

In spite of all the evidence, the contribution of immature BM- derived progenitors is not clear[256]. Recent studies in $ApoE^{-/-}$ mice show that local vessel wall progenitors are more important in giving rise to VSMC in intimal atherosclerotic lesions than those derived from the BM[244,257]. Evidence remains inconclusive about the exact mechanism by which these

BM cells are released into peripheral circulation and further initialize the process of mineralization in diseased arteries[167,183,205,218]. In this investigation, a positive role for BM-derived osteo-progenitor cells towards pathogenesis of vascular calcification was hypothesized (Figure 8.1).

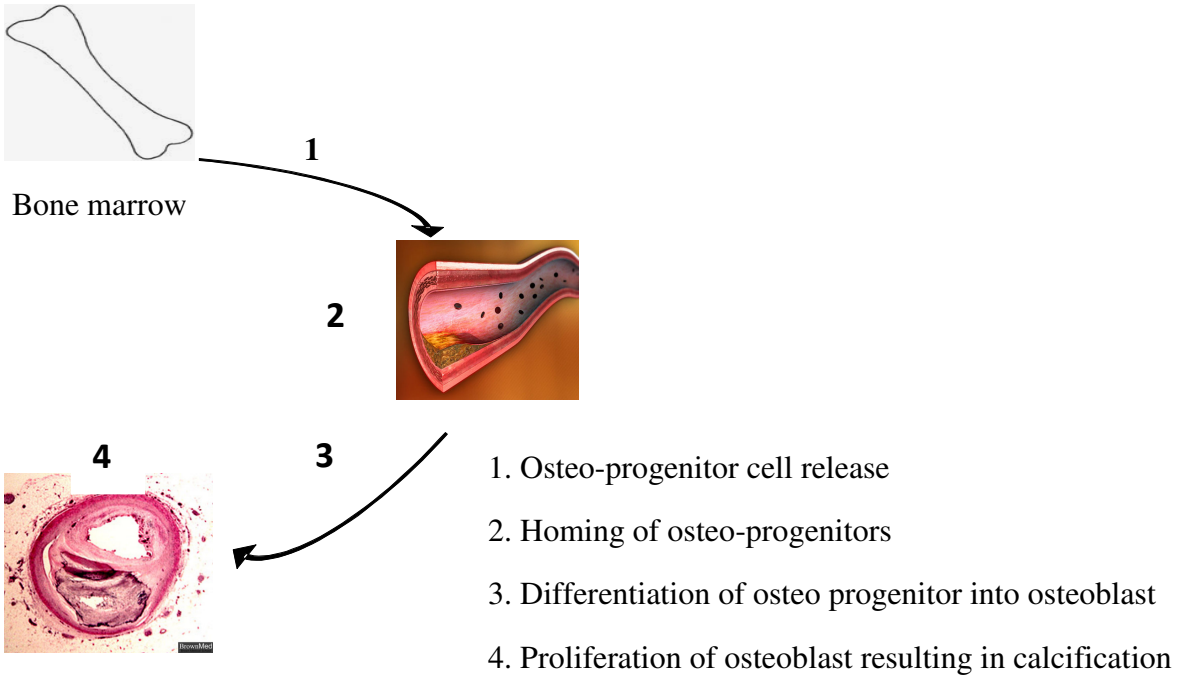

Figure 8.1. Circulating cell theory: This theory suggest that BM-derived osteo-progenitors home to diseased arteries where they contribute towards vascular calcification.

Aortic calcification was assessed in an $OPG^{-/-}$ mouse model along with quantification of circulating OCN^{+} MNC from peripheral blood. This circulating OCN^{+} MNC population was observed to be significantly increased in $OPG^{-/-}$ mice and positively associated with the aortic calcium levels. To further assess the homing of these cells to vasculature, the OCN^{+} population deposited in the vessel wall in $OPG^{-/-}$ mice was analysed. The results showed a three-way association between the circulating BM-derived OCN^{+} MNC, bone forming cells within the vasculature and the severity of vascular calcification. Protein cytokine studies performed in $OPG^{-/-}$ mice also suggested a role for stem cell mobilising cytokines in stimulating the release of immature osteo-progenitors from the BM environment. Under the influence of chemo-attractants these bone marker-positive cells may home to the diseased arteries. This cell population may further undergo osteogenic differentiation in the lesions thus promoting vessel mineralisation as previously described[185,186].

Although the existing $OPG^{-/-}$ mouse model was assessed for calcification it was found to have some limitations[61,138]. The degree of calcification in these $OPG^{-/-}$ mice was observed

to be only moderate[58,59,61,138]. To investigate the hypotheses of this thesis more thoroughly, a modified animal model was required in which the mineralization process occurred rapidly and involved a greater degree of calcification[138]. During the course of the investigation an independent group demonstrated a modified mouse model system which involved the subcutaneous administration of calcitriol which acted as a catalyst in inducing rapid mineralization of vascular tissues[138]. *In vitro* studies, in the past, have also indicated that excess calcitriol can increase calcium uptake into smooth muscle cells[139-141]. This modified calcitriol model was adapted in young $OPG^{-/-}$ mice for the further investigation of the hypotheses.

Further studies demonstrated an increase in the circulating OCN^{+} MNC population in $OPG^{-/-}$ mouse groups which received calcitriol. This circulating OCN^{+} MNC increase was less in the younger $OPG^{-/-}$ model with calcitriol in comparison to the older $OPG^{-/-}$ model without calcitriol. However, the total extractable aortic calcium content was significantly higher in calcitriol induced $OPG^{-/-}$ mice indicating that calcium deposits in the aorta at a quicker rate with the infusion of calcitriol. One reason for the lower circulating OCN^{+} MNC population could be the short period of study. The limited amount of time after calcitriol administration may not be sufficient for the release of immature BM cells into the peripheral circulation. The younger age of the $OPG^{-/-}$ mice in calcitriol model was also considered to be crucial in the difference of circulating cells. The association between the total extractable aortic calcium and the circulating OCN^{+} MNC was stronger in calcitriol induced $OPG^{-/-}$ model than in 12 month old $OPG^{-/-}$ model without calcitriol emphasizing the influence of calcitriol in accelerating aortic calcification.

To further confirm the results from mouse model experiments, an investigation of a human patient cohort was undertaken. These patients were diagnosed with peripheral artery disease and recruited from The Townsville General Hospital during a period from 2007 to 2009. The OCN^{+} MNC population was quantified from circulating blood samples from the patients and correlated with the infra renal aortic calcification volumes measured by CTA as previously described[235] . Calcification volumes were found to be greater associated in older patients and males, an observation which has been reported in other studies[258,259]. The calcification volumes were found to be associated with the circulating OCN^{+} MNC percentage thought to originate from the BM environment. As observed in the mouse model studies, plasma cytokine levels of G-CSF and SCF were positively correlated with the calcification volumes and OCN^{+} population. These results suggest a role for stem cell mobilizing cytokines in stimulating the immature progenitor cells from BM environment. It

is suggested that after the release of OCN^+ MNC into the peripheral circulation chemo attractants such as SDF-1α facilitate cell homing and survival in diseased lesions. Further, it was also thought that under ideal proliferative conditions these osteo-progenitor cells differentiate into osteoblasts within the vasculature. This process results in the vessel wall mineralization thus contributing to the complexity of the disease formation. The results obtained from the current studies are suggestive and further investigation is required to confirm the behavior of these circulating osteo-progenitors in the vessel wall.

8.2. Limitations

Despite providing consistent data which indicates that OCN^+ MNC are associated with aortic calcification in two mouse models and a patient cohort these studies do have a number of limitations meaning that the definitive role of these cells in vascular calcification still requires further investigation.

Firstly, both mouse models employed were based on OPG deficiency. These $OPG^{-/-}$ mice are reported to undergo osteoporosis along with vascular calcification. Thus it is possible that the increased OCN^+ MNC was related to the bone loss occurring in osteoporosis rather than the aortic calcification in these animals. The finding that the OCN^+ MNC increase in response to the vascular calcification promoting agent calcitriol and their association with aortic calcification in humans do however suggest that the osteo-progenitor cells are important in the calcification process.

The role of OPG within the vasculature is also not entirely clear. While depletion of OPG in mouse models is reported to induce vascular calcification, in patients serum OPG levels are positively associated with peripheral artery disease. This variation of results in mouse model and human patient has lead to the questioning of the protective role of OPG in the vasculature. The human cohort investigated in this study was small. A larger cohort would be ideal to confirm the association between circulating osteo-progenitors and aortic calcification. Also, unavailability of a control healthy group for comparative studies was considered to be drawback in these studies. This could not be achieved because of the limited patient cohort and the complicated recruitment criteria for the patients in whom patients were excluded from the study if they had received previous open surgical or endovascular treatment of their infrarenal aorta. Moreover, the patients investigated in our study included some patients who had AAA in addition to occlusive PAD. While independent studies for these two groups would have been ideal, we were not powered to analyse these groups separately.

8.3. Conclusion

In conclusion, the current study suggests an association between cells previously identified as osteogenic progenitors and aortic calcification. The novel hypothesis that the BM-derived osteo-progenitor population contributes to the pathogenesis of vascular calcification was supported, in part, by the studies reported. A human patient cohort analysis reflected the animal model results suggesting a role for immature BM cells with osteogenic potential in calcification. Overall, the study supports a new pathway involved in arterial calcification and this may impact on current treatment strategies for this condition.

8.4. Future directions

Further work is necessary to confirm the role of these BM-derived immature cells in the vasculature. This may be achieved by tracing the circulatory path of these immature cells and determining their final lineage. BM cell populations could be extracted from the marrow environment and labelled with green fluorescent protein GFP dye which has been reported to tag immature cells without influencing their lineage. This fluorescently labeled population could then be injected back *in vivo*. Further these tagged cells could be traced in the peripheral circulation via *in vivo* imaging techniques.

Another way of investigating the influence of these osteo-progenitors would be to block the effect of stem cell mobilizing cytokines using anti-cytokine blocking agents. Controlling this mobilizing activity would reduce the release of osteo-progenitors from the marrow environment and thus assist in determining their contribution towards the severity of vascular calcification.

For animal investigations, designing a mouse model which does not develop osteoporosis would be ideal for further vascular calcification studies. Designing such a system could resolve controversies in the existing knockout mouse models which considers that arterial calcification is invariably observed as a result of osteoporosis hence questions the role of circulating cells in vascular calcification progression.

Further investigations could also extend the type of pathologies being investigated and could form a basis for collaboration with other external groups. Since calcification is also linked to other clinical conditions such as atherosclerosis, diabetes, obesity and bone related disorders, this investigation could build on the work achieved by other research groups with broader clinical perspectives.

BIBLIOGRAPHY

1. Abedin M, Tintut Y, Demer LL. Vascular calcification: mechanisms and clinical ramifications. Arterioscler Thromb Vasc Biol. 2004 Jul;24(7):1161-70.
2. Cannata-Andia JB, Rodriguez-Garcia M, Carrillo-Lopez N, Naves-Diaz M, Diaz-Lopez B. Vascular calcifications: pathogenesis, management, and impact on clinical outcomes. J Am Soc Nephrol. 2006 Dec;17(12 Suppl 3):S267-73.
3. Giachelli CM. Vascular calcification mechanisms. J Am Soc Nephrol. 2004 Dec;15(12):2959-64.
4. Shanahan CM. Vascular calcification--a matter of damage limitation? Nephrol Dial Transplant. 2006 May;21(5):1166-9.
5. Cardiovascular diseases in Australia: A snapshot, 2004-05. Australian Bureau of Statistics. 2005;4821.0.55.001.
6. Shao JS, Cai J, Towler DA. Molecular mechanisms of vascular calcification: lessons learned from the aorta. Arterioscler Thromb Vasc Biol. 2006 Jul;26(7):1423-30.
7. Speer MY, Giachelli CM. Regulation of cardiovascular calcification. Cardiovasc Pathol. 2004 Mar-Apr;13(2):63-70.
8. Jono S, Shioi A, Ikari Y, Nishizawa Y. Vascular calcification in chronic kidney disease. J Bone Miner Metab. 2006;24(2):176-81.
9. Moe SM, Chen NX. Pathophysiology of vascular calcification in chronic kidney disease. Circ Res. 2004 Sep 17;95(6):560-7.
10. London GM, Guerin AP, Marchais SJ, Metivier F, Pannier B, Adda H. Arterial media calcification in end-stage renal disease: impact on all-cause and cardiovascular mortality. Nephrol Dial Transplant. 2003 Sep;18(9):1731-40.
11. Doherty TM, Asotra K, Fitzpatrick LA, et al. Calcification in atherosclerosis: bone biology and chronic inflammation at the arterial crossroads. Proc Natl Acad Sci U S A. 2003 Sep 30;100(20):11201-6.
12. Bellasi A, Raggi P. Diagnostic and prognostic value of coronary artery calcium screening. Curr Opin Cardiol. 2005 Sep;20(5):375-80.
13. Wexler L, Brundage B, Crouse J, et al. Coronary artery calcification: pathophysiology, epidemiology, imaging methods, and clinical implications. A statement for health professionals from the American Heart Association. Writing Group. Circulation. 1996 Sep 1;94(5):1175-92.

14. Watson KE, Demer LL. The atherosclerosis-calcification link? Curr Opin Lipidol. 1996 Apr;7(2):101-4.
15. Mazzini MJ, Schulze PC. Proatherogenic pathways leading to vascular calcification. Eur J Radiol. 2006 Mar;57(3):384-9.
16. Ketteler M, Westenfeld R, Schlieper G, Brandenburg V. Pathogenesis of vascular calcification in dialysis patients. Clin Exp Nephrol. 2005 Dec;9(4):265-70.
17. O'Neill WC. Vascular calcification: not so crystal clear. Kidney Int. 2007 Feb;71(4):282-3.
18. Parhami F, Bostrom K, Watson K, Demer LL. Role of molecular regulation in vascular calcification. J Atheroscler Thromb. 1996;3(2):90-4.
19. Young MJ, Adams JE, Anderson GF, Boulton AJ, Cavanagh PR. Medial arterial calcification in the feet of diabetic patients and matched non-diabetic control subjects. Diabetologia. 1993 Jul;36(7):615-21.
20. Lehto S, Niskanen L, Suhonen M, Ronnemaa T, Laakso M. Medial artery calcification. A neglected harbinger of cardiovascular complications in non-insulin-dependent diabetes mellitus. Arterioscler Thromb Vasc Biol. 1996 Aug;16(8):978-83.
21. Casscells W, Hassan K, Vaseghi MF, et al. Plaque blush, branch location, and calcification are angiographic predictors of progression of mild to moderate coronary stenoses. Am Heart J. 2003 May;145(5):813-20.
22. Hisar I, Ileri M, Yetkin E, et al. Aortic valve calcification: its significance and limitation as a marker for coronary artery disease. Angiology. 2002 Mar-Apr;53(2):165-9.
23. Block GA, Hulbert-Shearon TE, Levin NW, Port FK. Association of serum phosphorus and calcium x phosphate product with mortality risk in chronic hemodialysis patients: a national study. Am J Kidney Dis. 1998 Apr;31(4):607-17.
24. Yang H, Curinga G, Giachelli CM. Elevated extracellular calcium levels induce smooth muscle cell matrix mineralization in vitro. Kidney Int. 2004 Dec;66(6):2293-9.
25. Cozzolino M, Dusso AS, Slatopolsky E. Role of calcium-phosphate product and bone-associated proteins on vascular calcification in renal failure. J Am Soc Nephrol. 2001 Nov;12(11):2511-6.

26. Giachelli CM, Speer MY, Li X, Rajachar RM, Yang H. Regulation of vascular calcification: roles of phosphate and osteopontin. Circ Res. 2005 Apr 15;96(7):717-22.
27. O'Brien KD, Kuusisto J, Reichenbach DD, et al. Osteopontin is expressed in human aortic valvular lesions. Circulation. 1995 Oct 15;92(8):2163-8.
28. Vattikuti R, Towler DA. Osteogenic regulation of vascular calcification: an early perspective. Am J Physiol Endocrinol Metab. 2004 May;286(5):E686-96.
29. Boskey AL, Maresca M, Ullrich W, Doty SB, Butler WT, Prince CW. Osteopontin-hydroxyapatite interactions in vitro: inhibition of hydroxyapatite formation and growth in a gelatin-gel. Bone Miner. 1993 Aug;22(2):147-59.
30. Jaiswal N, Haynesworth SE, Caplan AI, Bruder SP. Osteogenic differentiation of purified, culture-expanded human mesenchymal stem cells in vitro. J Cell Biochem. 1997 Feb;64(2):295-312.
31. Zebboudj AF, Shin V, Bostrom K. Matrix GLA protein and BMP-2 regulate osteoinduction in calcifying vascular cells. J Cell Biochem. 2003 Nov 1;90(4):756-65.
32. Monsoro-Burq AH, Duprez D, Watanabe Y, et al. The role of bone morphogenetic proteins in vertebral development. Development. 1996 Nov;122(11):3607-16.
33. Towler DA, Shao JS, Cheng SL, Pingsterhaus JM, Loewy AP. Osteogenic regulation of vascular calcification. Ann N Y Acad Sci. 2006 Apr;1068:327-33.
34. Hofbauer LC, Brueck CC, Shanahan CM, Schoppet M, Dobnig H. Vascular calcification and osteoporosis--from clinical observation towards molecular understanding. Osteoporos Int. 2007 Mar;18(3):251-9.
35. Kiel DP, Kauppila LI, Cupples LA, Hannan MT, O'Donnell CJ, Wilson PW. Bone loss and the progression of abdominal aortic calcification over a 25 year period: the Framingham Heart Study. Calcif Tissue Int. 2001 May;68(5):271-6.
36. Parhami F, Garfinkel A, Demer LL. Role of lipids in osteoporosis. Arterioscler Thromb Vasc Biol. 2000 Nov;20(11):2346-8.
37. Rodriguez Garcia M, Naves Diaz M, Cannata Andia JB. Bone metabolism, vascular calcifications and mortality: associations beyond mere coincidence. J Nephrol. 2005 Jul-Aug;18(4):458-63.
38. Shroff RC, Shanahan CM. The vascular biology of calcification. Semin Dial. 2007 Mar-Apr;20(2):103-9.

39. Roberts N, Jahangiri M, Xu Q. Progenitor cells in vascular disease. J Cell Mol Med. 2005 Jul-Sep;9(3):583-91.
40. Blann AD, Woywodt A, Bertolini F, et al. Circulating endothelial cells. Biomarker of vascular disease. Thromb Haemost. 2005 Feb;93(2):228-35.
41. Manolagas SC, Jilka RL. Bone marrow, cytokines, and bone remodeling. Emerging insights into the pathophysiology of osteoporosis. N Engl J Med. 1995 Feb 2;332(5):305-11.
42. Falk E. Pathogenesis of atherosclerosis. J Am Coll Cardiol. 2006 Apr 18;47(8 Suppl):C7-12.
43. Berliner JA, Navab M, Fogelman AM, et al. Atherosclerosis: basic mechanisms. Oxidation, inflammation, and genetics. Circulation. 1995 May 1;91(9):2488-96.
44. Vink A, Schoneveld AH, Richard W, et al. Plaque burden, arterial remodeling and plaque vulnerability: determined by systemic factors? J Am Coll Cardiol. 2001 Sep;38(3):718-23.
45. Shioi A, Mori K, Jono S, et al. Mechanism of atherosclerotic calcification. Z Kardiol. 2000;89 Suppl 2:75-9.
46. Tanimura A, McGregor DH, Anderson HC. Calcification in atherosclerosis. I. Human studies. J Exp Pathol. 1986 Summer;2(4):261-73.
47. Liaw L, Almeida M, Hart CE, Schwartz SM, Giachelli CM. Osteopontin promotes vascular cell adhesion and spreading and is chemotactic for smooth muscle cells in vitro. Circ Res. 1994 Feb;74(2):214-24.
48. O'Brien ER, Garvin MR, Stewart DK, et al. Osteopontin is synthesized by macrophage, smooth muscle, and endothelial cells in primary and restenotic human coronary atherosclerotic plaques. Arterioscler Thromb. 1994 Oct;14(10):1648-56.
49. Olesen P, Nguyen K, Wogensen L, Ledet T, Rasmussen LM. Calcification of human vascular smooth muscle cells: associations with osteoprotegerin expression and acceleration by high-dose insulin. Am J Physiol Heart Circ Physiol. 2007 Feb;292(2):H1058-64.
50. Proudfoot D, Shanahan CM. Molecular mechanisms mediating vascular calcification: role of matrix Gla protein. Nephrology (Carlton). 2006 Oct;11(5):455-61.
51. Wada T, McKee MD, Steitz S, Giachelli CM. Calcification of vascular smooth muscle cell cultures: inhibition by osteopontin. Circ Res. 1999 Feb 5;84(2):166-78.

52. Bostrom K, Watson KE, Stanford WP, Demer LL. Atherosclerotic calcification: relation to developmental osteogenesis. Am J Cardiol. 1995 Feb 23;75(6):88B-91B.
53. Hunter GK, Goldberg HA. Nucleation of hydroxyapatite by bone sialoprotein. Proc Natl Acad Sci U S A. 1993 Sep 15;90(18):8562-5.
54. Lomashvili K, Garg P, O'Neill WC. Chemical and hormonal determinants of vascular calcification in vitro. Kidney Int. 2006 Apr;69(8):1464-70.
55. Hirsch D, Azoury R, Sarig S, Kruth HS. Colocalization of cholesterol and hydroxyapatite in human atherosclerotic lesions. Calcif Tissue Int. 1993 Feb;52(2):94-8.
56. Schinke T, Karsenty G. Vascular calcification--a passive process in need of inhibitors. Nephrol Dial Transplant. 2000 Sep;15(9):1272-4.
57. Bennett BJ, Scatena M, Kirk EA, et al. Osteoprotegerin inactivation accelerates advanced atherosclerotic lesion progression and calcification in older ApoE-/- mice. Arterioscler Thromb Vasc Biol. 2006 Sep;26(9):2117-24.
58. Bucay N, Sarosi I, Dunstan CR, et al. osteoprotegerin-deficient mice develop early onset osteoporosis and arterial calcification. Genes Dev. 1998 May 1;12(9):1260-8.
59. Luo G, Ducy P, McKee MD, et al. Spontaneous calcification of arteries and cartilage in mice lacking matrix GLA protein. Nature. 1997 Mar 6;386(6620):78-81.
60. George J, Afek A, Abashidze A, et al. Transfer of endothelial progenitor and bone marrow cells influences atherosclerotic plaque size and composition in apolipoprotein E knockout mice. Arterioscler Thromb Vasc Biol. 2005 Dec;25(12):2636-41.
61. Wallin R, Wajih N, Greenwood GT, Sane DC. Arterial calcification: a review of mechanisms, animal models, and the prospects for therapy. Med Res Rev. 2001 Jul;21(4):274-301.
62. Morony S, Tintut Y, Zhang Z, et al. Osteoprotegerin inhibits vascular calcification without affecting atherosclerosis in ldlr(-/-) mice. Circulation. 2008 Jan 22;117(3):411-20.
63. Allison MA, Criqui MH, Wright CM. Patterns and risk factors for systemic calcified atherosclerosis. Arterioscler Thromb Vasc Biol. 2004 Feb;24(2):331-6.
64. Ishimura E, Okuno S, Kitatani K, et al. Different risk factors for peripheral vascular calcification between diabetic and non-diabetic haemodialysis patients--importance of glycaemic control. Diabetologia. 2002 Oct;45(10):1446-8.

65. Maser RE, Wolfson SK, Jr., Ellis D, et al. Cardiovascular disease and arterial calcification in insulin-dependent diabetes mellitus: interrelations and risk factor profiles. Pittsburgh Epidemiology of Diabetes Complications Study-V. Arterioscler Thromb. 1991 Jul-Aug;11(4):958-65.

66. Leng GC, Lee AJ, Fowkes FG, et al. Incidence, natural history and cardiovascular events in symptomatic and asymptomatic peripheral arterial disease in the general population. Int J Epidemiol. 1996 Dec;25(6):1172-81.

67. Iribarren C, Sidney S, Sternfeld B, Browner WS. Calcification of the aortic arch: risk factors and association with coronary heart disease, stroke, and peripheral vascular disease. JAMA. 2000 Jun 7;283(21):2810-5.

68. Hughson WG, Mann JI, Garrod A. Intermittent claudication: prevalence and risk factors. Br Med J. 1978 May 27;1(6124):1379-81.

69. Heliovaara M, Karvonen MJ, Vilhunen R, Punsar S. Smoking, carbon monoxide, and atherosclerotic diseases. Br Med J. 1978 Feb 4;1(6108):268-70.

70. Midgette AS, Baron JA, Rohan TE. Do cigarette smokers have diets that increase their risks of coronary heart disease and cancer? Am J Epidemiol. 1993 Mar 1;137(5):521-9.

71. Price JF, Mowbray PI, Lee AJ, Rumley A, Lowe GD, Fowkes FG. Relationship between smoking and cardiovascular risk factors in the development of peripheral arterial disease and coronary artery disease: Edinburgh Artery Study. Eur Heart J. 1999 Mar;20(5):344-53.

72. Vasa M, Fichtlscherer S, Aicher A, et al. Number and migratory activity of circulating endothelial progenitor cells inversely correlate with risk factors for coronary artery disease. Circ Res. 2001 Jul 6;89(1):E1-7.

73. Bernin P, Theorell T, Sandberg CG. Biological correlates of social support and pressure at work in managers. Integr Physiol Behav Sci. 2001 Apr-Jun;36(2):121-36.

74. Bigaard J, Tjonneland A, Thomsen BL, Overvad K, Heitmann BL, Sorensen TI. Waist circumference, BMI, smoking, and mortality in middle-aged men and women. Obes Res. 2003 Jul;11(7):895-903.

75. Krupski WC. The peripheral vascular consequences of smoking. Ann Vasc Surg. 1991 May;5(3):291-304.

76. Smith FB, Lowe GD, Fowkes FG, et al. Smoking, haemostatic factors and lipid peroxides in a population case control study of peripheral arterial disease. Atherosclerosis. 1993 Sep;102(2):155-62.
77. Stevens RJ, Kothari V, Adler AI, Stratton IM. The UKPDS risk engine: a model for the risk of coronary heart disease in Type II diabetes (UKPDS 56). Clin Sci (Lond). 2001 Dec;101(6):671-9.
78. Schulze MB, Rimm EB, Li T, Rifai N, Stampfer MJ, Hu FB. C-reactive protein and incident cardiovascular events among men with diabetes. Diabetes Care. 2004 Apr;27(4):889-94.
79. Ritchie SA, Connell JM. The link between abdominal obesity, metabolic syndrome and cardiovascular disease. Nutr Metab Cardiovasc Dis. 2007 May;17(4):319-26.
80. Rimm EB, Giovannucci EL, Willett WC, et al. Prospective study of alcohol consumption and risk of coronary disease in men. Lancet. 1991 Aug 24;338(8765):464-8.
81. Golledge J, Jones L, Oliver L, Quigley F, Karan M. Folic acid, vitamin B12, MTHFR genotypes, and plasma homocysteine. Clin Chem. 2006 Jun;52(6):1205-6.
82. Jayalath RW, Mangan SH, Golledge J. Aortic calcification. Eur J Vasc Endovasc Surg. 2005 Nov;30(5):476-88.
83. Geng YJ, Libby P. Progression of atheroma: a struggle between death and procreation. Arterioscler Thromb Vasc Biol. 2002 Sep 1;22(9):1370-80.
84. Frenette PS, Subbarao S, Mazo IB, von Andrian UH, Wagner DD. Endothelial selectins and vascular cell adhesion molecule-1 promote hematopoietic progenitor homing to bone marrow. Proc Natl Acad Sci U S A. 1998 Nov 24;95(24):14423-8.
85. Tedgui A, Mallat Z. Apoptosis, a major determinant of atherothrombosis. Arch Mal Coeur Vaiss. 2003 Jun;96(6):671-5.
86. Llodra J, Angeli V, Liu J, Trogan E, Fisher EA, Randolph GJ. Emigration of monocyte-derived cells from atherosclerotic lesions characterizes regressive, but not progressive, plaques. Proc Natl Acad Sci U S A. 2004 Aug 10;101(32):11779-84.
87. Tanimura A, McGregor DH, Anderson HC. Matrix vesicles in atherosclerotic calcification. Proc Soc Exp Biol Med. 1983 Feb;172(2):173-7.
88. Grunewald M, Avraham I, Dor Y, et al. VEGF-induced adult neovascularization: recruitment, retention, and role of accessory cells. Cell. 2006 Jan 13;124(1):175-89.

89. Bucala R, Spiegel LA, Chesney J, Hogan M, Cerami A. Circulating fibrocytes define a new leukocyte subpopulation that mediates tissue repair. Mol Med. 1994 Nov;1(1):71-81.
90. Urbich C, Dimmeler S. Endothelial progenitor cells: characterization and role in vascular biology. Circ Res. 2004 Aug 20;95(4):343-53.
91. Spring H, Schuler T, Arnold B, Hammerling GJ, Ganss R. Chemokines direct endothelial progenitors into tumor neovessels. Proc Natl Acad Sci U S A. 2005 Dec 13;102(50):18111-6.
92. Schwartz SM, Virmani R, Rosenfeld ME. The good smooth muscle cells in atherosclerosis. Curr Atheroscler Rep. 2000 Sep;2(5):422-9.
93. Bostrom K. Proinflammatory vascular calcification. Circ Res. 2005 Jun 24;96(12):1219-20.
94. Frink RJ, Achor RW, Brown AL, Jr., Kincaid OW, Brandenburg RO. Significance of calcification of the coronary arteries. Am J Cardiol. 1970 Sep;26(3):241-7.
95. Guerin AP, London GM, Marchais SJ, Metivier F. Arterial stiffening and vascular calcifications in end-stage renal disease. Nephrol Dial Transplant. 2000 Jul;15(7):1014-21.
96. Niederhoffer N, Lartaud-Idjouadiene I, Giummelly P, Duvivier C, Peslin R, Atkinson J. Calcification of medial elastic fibers and aortic elasticity. Hypertension. 1997 Apr;29(4):999-1006.
97. Atkinson J. Arterial calcification. Mechanisms, consequences and animal models. Pathol Biol (Paris). 1999 Sep;47(7):677-84.
98. LeGeros RZ, Contiguglia SR, Alfrey AC. Pathological calcifications associated with uremia: two types of calcium phosphate deposits. Calcif Tissue Res. 1973 Oct 23;13(3):173-85.
99. Moe SM, Reslerova M, Ketteler M, et al. Role of calcification inhibitors in the pathogenesis of vascular calcification in chronic kidney disease (CKD). Kidney Int. 2005 Jun;67(6):2295-304.
100. Lomashvili KA, Cobbs S, Hennigar RA, Hardcastle KI, O'Neill WC. Phosphate-induced vascular calcification: role of pyrophosphate and osteopontin. J Am Soc Nephrol. 2004 Jun;15(6):1392-401.
101. Towler DA. Inorganic pyrophosphate: a paracrine regulator of vascular calcification and smooth muscle phenotype. Arterioscler Thromb Vasc Biol. 2005 Apr;25(4):651-4.

102. Farzaneh-Far A, Proudfoot D, Shanahan C, Weissberg PL. Vascular and valvar calcification: recent advances. Heart. 2001 Jan;85(1):13-7.
103. Roy ME, Nishimoto SK. Matrix Gla protein binding to hydroxyapatite is dependent on the ionic environment: calcium enhances binding affinity but phosphate and magnesium decrease affinity. Bone. 2002 Aug;31(2):296-302.
104. Shanahan CM, Cary NR, Metcalfe JC, Weissberg PL. High expression of genes for calcification-regulating proteins in human atherosclerotic plaques. J Clin Invest. 1994 Jun;93(6):2393-402.
105. Brancaccio D, Biondi ML, Gallieni M, et al. Matrix GLA protein gene polymorphisms: clinical correlates and cardiovascular mortality in chronic kidney disease patients. Am J Nephrol. 2005 Nov-Dec;25(6):548-52.
106. Bostrom K, Tsao D, Shen S, Wang Y, Demer LL. Matrix GLA protein modulates differentiation induced by bone morphogenetic protein-2 in C3H10T1/2 cells. J Biol Chem. 2001 Apr 27;276(17):14044-52.
107. Price PA, Chan WS, Jolson DM, Williamson MK. The elastic lamellae of devitalized arteries calcify when incubated in serum: evidence for a serum calcification factor. Arterioscler Thromb Vasc Biol. 2006 May;26(5):1079-85.
108. Otawara Y, Price PA. Developmental appearance of matrix GLA protein during calcification in the rat. J Biol Chem. 1986 Aug 15;261(23):10828-32.
109. Loeser R, Carlson CS, Tulli H, Jerome WG, Miller L, Wallin R. Articular-cartilage matrix gamma-carboxyglutamic acid-containing protein. Characterization and immunolocalization. Biochem J. 1992 Feb 15;282 (Pt 1):1-6.
110. Schoppet M, Al-Fakhri N, Franke FE, et al. Localization of osteoprotegerin, tumor necrosis factor-related apoptosis-inducing ligand, and receptor activator of nuclear factor-kappaB ligand in Monckeberg's sclerosis and atherosclerosis. J Clin Endocrinol Metab. 2004 Aug;89(8):4104-12.
111. Emery JG, McDonnell P, Burke MB, et al. Osteoprotegerin is a receptor for the cytotoxic ligand TRAIL. J Biol Chem. 1998 Jun 5;273(23):14363-7.
112. Lacey DL, Timms E, Tan HL, et al. Osteoprotegerin ligand is a cytokine that regulates osteoclast differentiation and activation. Cell. 1998 Apr 17;93(2):165-76.
113. Kiechl S, Werner P, Knoflach M, Furtner M, Willeit J, Schett G. The osteoprotegerin/RANK/RANKL system: a bone key to vascular disease. Expert Rev Cardiovasc Ther. 2006 Nov;4(6):801-11.

114. Browner WS, Lui LY, Cummings SR. Associations of serum osteoprotegerin levels with diabetes, stroke, bone density, fractures, and mortality in elderly women. J Clin Endocrinol Metab. 2001 Feb;86(2):631-7.

115. Kiechl S, Schett G, Wenning G, et al. Osteoprotegerin is a risk factor for progressive atherosclerosis and cardiovascular disease. Circulation. 2004 May 11;109(18):2175-80.

116. Kim SM, Lee J, Ryu OH, et al. Serum osteoprotegerin levels are associated with inflammation and pulse wave velocity. Clin Endocrinol (Oxf). 2005 Nov;63(5):594-8.

117. Shin JY, Shin YG, Chung CH. Elevated serum osteoprotegerin levels are associated with vascular endothelial dysfunction in type 2 diabetes. Diabetes Care. 2006 Jul;29(7):1664-6.

118. Simonet WS, Lacey DL, Dunstan CR, et al. Osteoprotegerin: a novel secreted protein involved in the regulation of bone density. Cell. 1997 Apr 18;89(2):309-19.

119. Giachelli CM, Liaw L, Murry CE, Schwartz SM, Almeida M. Osteopontin expression in cardiovascular diseases. Ann N Y Acad Sci. 1995 Apr 21;760:109-26.

120. Speer MY, McKee MD, Guldberg RE, et al. Inactivation of the osteopontin gene enhances vascular calcification of matrix Gla protein-deficient mice: evidence for osteopontin as an inducible inhibitor of vascular calcification in vivo. J Exp Med. 2002 Oct 21;196(8):1047-55.

121. Demer LL, Tintut Y. Osteopontin. Between a rock and a hard plaque. Circ Res. 1999 Feb 5;84(2):250-2.

122. Moe SM, O'Neill KD, Duan D, et al. Medial artery calcification in ESRD patients is associated with deposition of bone matrix proteins. Kidney Int. 2002 Feb;61(2):638-47.

123. Danilevicius CF, Lopes JB, Pereira RM. Bone metabolism and vascular calcification. Braz J Med Biol Res. 2007 Apr;40(4):435-42.

124. Frye MA, Melton LJ, 3rd, Bryant SC, et al. Osteoporosis and calcification of the aorta. Bone Miner. 1992 Nov;19(2):185-94.

125. Raisz LG. Pathogenesis of osteoporosis: concepts, conflicts, and prospects. J Clin Invest. 2005 Dec;115(12):3318-25.

126. Sattler AM, Schoppet M, Schaefer JR, Hofbauer LC. Novel aspects on RANK ligand and osteoprotegerin in osteoporosis and vascular disease. Calcif Tissue Int. 2004 Jan;74(1):103-6.

127. Ouchi Y, Akishita M, de Souza AC, Nakamura T, Orimo H. Age-related loss of bone mass and aortic/aortic valve calcification--reevaluation of recommended dietary allowance of calcium in the elderly. Ann N Y Acad Sci. 1993 Mar 15;676:297-307.
128. Rubin MR, Silverberg SJ. Vascular calcification and osteoporosis--the nature of the nexus. J Clin Endocrinol Metab. 2004 Sep;89(9):4243-5.
129. Schulz E, Arfai K, Liu X, Sayre J, Gilsanz V. Aortic calcification and the risk of osteoporosis and fractures. J Clin Endocrinol Metab. 2004 Sep;89(9):4246-53.
130. Teitelbaum SL. Bone resorption by osteoclasts. Science. 2000 Sep 1;289(5484):1504-8.
131. Adler Y, Fisman EZ, Shemesh J, et al. Spiral computed tomography evidence of close correlation between coronary and thoracic aorta calcifications. Atherosclerosis. 2004 Sep;176(1):133-8.
132. Knudsen ST, Foss CH, Poulsen PL, Andersen NH, Mogensen CE, Rasmussen LM. Increased plasma concentrations of osteoprotegerin in type 2 diabetic patients with microvascular complications. Eur J Endocrinol. 2003 Jul;149(1):39-42.
133. Murshed M, Schinke T, McKee MD, Karsenty G. Extracellular matrix mineralization is regulated locally; different roles of two gla-containing proteins. J Cell Biol. 2004 Jun 7;165(5):625-30.
134. Tintut Y, Demer LL. Recent advances in multifactorial regulation of vascular calcification. Curr Opin Lipidol. 2001 Oct;12(5):555-60.
135. Min H, Morony S, Sarosi I, et al. Osteoprotegerin reverses osteoporosis by inhibiting endosteal osteoclasts and prevents vascular calcification by blocking a process resembling osteoclastogenesis. J Exp Med. 2000 Aug 21;192(4):463-74.
136. Kong YY, Yoshida H, Sarosi I, et al. OPGL is a key regulator of osteoclastogenesis, lymphocyte development and lymph-node organogenesis. Nature. 1999 Jan 28;397(6717):315-23.
137. Schoppet M, Preissner KT, Hofbauer LC. RANK ligand and osteoprotegerin: paracrine regulators of bone metabolism and vascular function. Arterioscler Thromb Vasc Biol. 2002 Apr 1;22(4):549-53.
138. Orita Y, Yamamoto H, Kohno N, et al. Role of osteoprotegerin in arterial calcification: development of new animal model. Arterioscler Thromb Vasc Biol. 2007 Sep;27(9):2058-64.

139. Rajasree S, Umashankar PR, Lal AV, Sarma PS, Kartha CC. 1,25-dihydroxyvitamin D3 receptor is upregulated in aortic smooth muscle cells during hypervitaminosis D. Life Sci. 2002 Mar 1;70(15):1777-88.

140. Inoue T, Kawashima H. 1,25-Dihydroxyvitamin D3 stimulates 45Ca2+-uptake by cultured vascular smooth muscle cells derived from rat aorta. Biochem Biophys Res Commun. 1988 May 16;152(3):1388-94.

141. Kreutz M, Andreesen R, Krause SW, Szabo A, Ritz E, Reichel H. 1,25-dihydroxyvitamin D3 production and vitamin D3 receptor expression are developmentally regulated during differentiation of human monocytes into macrophages. Blood. 1993 Aug 15;82(4):1300-7.

142. Teng M, Wolf M, Ofsthun MN, et al. Activated injectable vitamin D and hemodialysis survival: a historical cohort study. J Am Soc Nephrol. 2005 Apr;16(4):1115-25.

143. Kodama H, Nose M, Niida S, Yamasaki A. Essential role of macrophage colony-stimulating factor in the osteoclast differentiation supported by stromal cells. J Exp Med. 1991 May 1;173(5):1291-4.

144. Jono S, Ikari Y, Shioi A, et al. Serum osteoprotegerin levels are associated with the presence and severity of coronary artery disease. Circulation. 2002 Sep 3;106(10):1192-4.

145. Watanabe Y, Suzuki M, Oyama Y, et al. Cellular component of vascular calcification. Fibroblasts are essential for calcium deposition in cultured cells. Nephron. 2002 Dec;92(4):840-5.

146. Chen NX, Moe SM. Arterial calcification in diabetes. Curr Diab Rep. 2003 Feb;3(1):28-32.

147. Mundy GR, Boyce B, Hughes D, et al. The effects of cytokines and growth factors on osteoblastic cells. Bone. 1995 Aug;17(2 Suppl):71S-5S.

148. Reynolds JL, Joannides AJ, Skepper JN, et al. Human vascular smooth muscle cells undergo vesicle-mediated calcification in response to changes in extracellular calcium and phosphate concentrations: a potential mechanism for accelerated vascular calcification in ESRD. J Am Soc Nephrol. 2004 Nov;15(11):2857-67.

149. Nitta K, Akiba T, Uchida K, et al. Serum osteoprotegerin levels and the extent of vascular calcification in haemodialysis patients. Nephrol Dial Transplant. 2004 Jul;19(7):1886-9.

150. Ziegler S, Kudlacek S, Luger A, Minar E. Osteoprotegerin plasma concentrations correlate with severity of peripheral artery disease. Atherosclerosis. 2005 Sep;182(1):175-80.

151. Udagawa N, Takahashi N, Jimi E, et al. Osteoblasts/stromal cells stimulate osteoclast activation through expression of osteoclast differentiation factor/RANKL but not macrophage colony-stimulating factor: receptor activator of NF-kappa B ligand. Bone. 1999 Nov;25(5):517-23.

152. Ikeda T, Shirasawa T, Esaki Y, Yoshiki S, Hirokawa K. Osteopontin mRNA is expressed by smooth muscle-derived foam cells in human atherosclerotic lesions of the aorta. J Clin Invest. 1993 Dec;92(6):2814-20.

153. Anand DV, Lahiri A, Lim E, Hopkins D, Corder R. The relationship between plasma osteoprotegerin levels and coronary artery calcification in uncomplicated type 2 diabetic subjects. J Am Coll Cardiol. 2006 May 2;47(9):1850-7.

154. Avignon A, Sultan A, Piot C, Elaerts S, Cristol JP, Dupuy AM. Osteoprotegerin is associated with silent coronary artery disease in high-risk but asymptomatic type 2 diabetic patients. Diabetes Care. 2005 Sep;28(9):2176-80.

155. Nishiura R, Fujimoto S, Sato Y, et al. Elevated Osteoprotegerin Levels Predict Cardiovascular Events in New Hemodialysis Patients. Am J Nephrol. 2008 Sep 19;29(3):257-63.

156. Severson AR, Ingram RT, Fitzpatrick LA. Matrix proteins associated with bone calcification are present in human vascular smooth muscle cells grown in vitro. In Vitro Cell Dev Biol Anim. 1995 Dec;31(11):853-7.

157. Udagawa N, Takahashi N, Akatsu T, et al. Origin of osteoclasts: mature monocytes and macrophages are capable of differentiating into osteoclasts under a suitable microenvironment prepared by bone marrow-derived stromal cells. Proc Natl Acad Sci U S A. 1990 Sep;87(18):7260-4.

158. Cheng SL, Yang JW, Rifas L, Zhang SF, Avioli LV. Differentiation of human bone marrow osteogenic stromal cells in vitro: induction of the osteoblast phenotype by dexamethasone. Endocrinology. 1994 Jan;134(1):277-86.

159. Mori K, Shioi A, Jono S, Nishizawa Y, Morii H. Dexamethasone enhances In vitro vascular calcification by promoting osteoblastic differentiation of vascular smooth muscle cells. Arterioscler Thromb Vasc Biol. 1999 Sep;19(9):2112-8.

160. Canfield AE, Doherty MJ, Wood AC, et al. Role of pericytes in vascular calcification: a review. Z Kardiol. 2000;89 Suppl 2:20-7.

161. Collin-Osdoby P, Rothe L, Anderson F, Nelson M, Maloney W, Osdoby P. Receptor activator of NF-kappa B and osteoprotegerin expression by human microvascular endothelial cells, regulation by inflammatory cytokines, and role in human osteoclastogenesis. J Biol Chem. 2001 Jun 8;276(23):20659-72.
162. Pritzker LB, Scatena M, Giachelli CM. The role of osteoprotegerin and tumor necrosis factor-related apoptosis-inducing ligand in human microvascular endothelial cell survival. Mol Biol Cell. 2004 Jun;15(6):2834-41.
163. Girasole G, Passeri G, Jilka RL, Manolagas SC. Interleukin-11: a new cytokine critical for osteoclast development. J Clin Invest. 1994 Apr;93(4):1516-24.
164. Wozney JM, Rosen V, Celeste AJ, et al. Novel regulators of bone formation: molecular clones and activities. Science. 1988 Dec 16;242(4885):1528-34.
165. Hellstrom M, Kalen M, Lindahl P, Abramsson A, Betsholtz C. Role of PDGF-B and PDGFR-beta in recruitment of vascular smooth muscle cells and pericytes during embryonic blood vessel formation in the mouse. Development. 1999 Jun;126(14):3047-55.
166. Kim KM. Calcification of matrix vesicles in human aortic valve and aortic media. Fed Proc. 1976 Feb;35(2):156-62.
167. Jevon M, Dorling A, Hornick PI. Progenitor cells and vascular disease. Cell Prolif. 2008 Feb;41 Suppl 1:146-64.
168. Saiura A, Sata M, Hirata Y, Nagai R, Makuuchi M. Circulating smooth muscle progenitor cells contribute to atherosclerosis. Nat Med. 2001 Apr;7(4):382-3.
169. Sata M, Fukuda D, Tanaka K, Kaneda Y, Yashiro H, Shirakawa I. The role of circulating precursors in vascular repair and lesion formation. J Cell Mol Med. 2005 Jul-Sep;9(3):557-68.
170. Khosla S, Eghbali-Fatourechi GZ. Circulating cells with osteogenic potential. Ann N Y Acad Sci. 2006 Apr;1068:489-97.
171. Sata M, Saiura A, Kunisato A, et al. Hematopoietic stem cells differentiate into vascular cells that participate in the pathogenesis of atherosclerosis. Nat Med. 2002 Apr;8(4):403-9.
172. Cunningham KS, Gotlieb AI. The role of shear stress in the pathogenesis of atherosclerosis. Lab Invest. 2005 Jan;85(1):9-23.
173. Kumamoto M, Nakashima Y, Sueishi K. Intimal neovascularization in human coronary atherosclerosis: its origin and pathophysiological significance. Hum Pathol. 1995 Apr;26(4):450-6.

174. Abkowitz JL, Robinson AE, Kale S, Long MW, Chen J. Mobilization of hematopoietic stem cells during homeostasis and after cytokine exposure. Blood. 2003 Aug 15;102(4):1249-53.

175. Jansen J, Hanks S, Thompson JM, Dugan MJ, Akard LP. Transplantation of hematopoietic stem cells from the peripheral blood. J Cell Mol Med. 2005 Jan-Mar;9(1):37-50.

176. Rehman J, Li J, Orschell CM, March KL. Peripheral blood "endothelial progenitor cells" are derived from monocyte/macrophages and secrete angiogenic growth factors. Circulation. 2003 Mar 4;107(8):1164-9.

177. Hill JM, Zalos G, Halcox JP, et al. Circulating endothelial progenitor cells, vascular function, and cardiovascular risk. N Engl J Med. 2003 Feb 13;348(7):593-600.

178. Simper D, Stalboerger PG, Panetta CJ, Wang S, Caplice NM. Smooth muscle progenitor cells in human blood. Circulation. 2002 Sep 3;106(10):1199-204.

179. Shi Q, Rafii S, Wu MH, et al. Evidence for circulating bone marrow-derived endothelial cells. Blood. 1998 Jul 15;92(2):362-7.

180. Boos CJ, Goon PK, Lip GY. Endothelial progenitor cells in the vascular pathophysiology of hypertension: arterial stiffness, ageing and more. J Hum Hypertens. 2006 Jul;20(7):475-7.

181. Shintani S, Murohara T, Ikeda H, et al. Mobilization of endothelial progenitor cells in patients with acute myocardial infarction. Circulation. 2001 Jun 12;103(23):2776-9.

182. Caplice NM, Doyle B. Vascular progenitor cells: origin and mechanisms of mobilization, differentiation, integration, and vasculogenesis. Stem Cells Dev. 2005 Apr;14(2):122-39.

183. Cottler-Fox MH, Lapidot T, Petit I, et al. Stem cell mobilization. Hematology Am Soc Hematol Educ Program. 2003:419-37.

184. Heissig B, Hattori K, Dias S, et al. Recruitment of stem and progenitor cells from the bone marrow niche requires MMP-9 mediated release of kit-ligand. Cell. 2002 May 31;109(5):625-37.

185. Lataillade JJ, Clay D, Dupuy C, et al. Chemokine SDF-1 enhances circulating CD34(+) cell proliferation in synergy with cytokines: possible role in progenitor survival. Blood. 2000 Feb 1;95(3):756-68.

186. Petit I, Szyper-Kravitz M, Nagler A, et al. G-CSF induces stem cell mobilization by decreasing bone marrow SDF-1 and up-regulating CXCR4. Nat Immunol. 2002 Jul;3(7):687-94.

187. Kollet O, Spiegel A, Peled A, et al. Rapid and efficient homing of human CD34(+)CD38(-/low)CXCR4(+) stem and progenitor cells to the bone marrow and spleen of NOD/SCID and NOD/SCID/B2m(null) mice. Blood. 2001 May 15;97(10):3283-91.

188. Lapidot T, Petit I. Current understanding of stem cell mobilization: the roles of chemokines, proteolytic enzymes, adhesion molecules, cytokines, and stromal cells. Exp Hematol. 2002 Sep;30(9):973-81.

189. Wright DE, Wagers AJ, Gulati AP, Johnson FL, Weissman IL. Physiological migration of hematopoietic stem and progenitor cells. Science. 2001 Nov 30;294(5548):1933-6.

190. Sreerekha PR, Divya P, Krishnan LK. Adult stem cell homing and differentiation in vitro on composite fibrin matrix. Cell Prolif. 2006 Aug;39(4):301-12.

191. Atkinson C, Horsley J, Rhind-Tutt S, et al. Neointimal smooth muscle cells in human cardiac allograft coronary artery vasculopathy are of donor origin. J Heart Lung Transplant. 2004 Apr;23(4):427-35.

192. Shimizu K, Sugiyama S, Aikawa M, et al. Host bone-marrow cells are a source of donor intimal smooth- muscle-like cells in murine aortic transplant arteriopathy. Nat Med. 2001 Jun;7(6):738-41.

193. Caplice NM, Bunch TJ, Stalboerger PG, et al. Smooth muscle cells in human coronary atherosclerosis can originate from cells administered at marrow transplantation. Proc Natl Acad Sci U S A. 2003 Apr 15;100(8):4754-9.

194. Yoon YS, Park JS, Tkebuchava T, Luedeman C, Losordo DW. Unexpected severe calcification after transplantation of bone marrow cells in acute myocardial infarction. Circulation. 2004 Jun 29;109(25):3154-7.

195. Pittenger MF, Mackay AM, Beck SC, et al. Multilineage potential of adult human mesenchymal stem cells. Science. 1999 Apr 2;284(5411):143-7.

196. Prockop DJ. Marrow stromal cells as stem cells for nonhematopoietic tissues. Science. 1997 Apr 4;276(5309):71-4.

197. Randall TD, Weissman IL. Characterization of a population of cells in the bone marrow that phenotypically mimics hematopoietic stem cells: resting stem cells or mystery population? Stem Cells. 1998;16(1):38-48.

198. Kondo M, Wagers AJ, Manz MG, et al. Biology of hematopoietic stem cells and progenitors: implications for clinical application. Annu Rev Immunol. 2003;21:759-806.

199. Song L, Tuan RS. Transdifferentiation potential of human mesenchymal stem cells derived from bone marrow. FASEB J. 2004 Jun;18(9):980-2.

200. Jaiswal RK, Jaiswal N, Bruder SP, Mbalaviele G, Marshak DR, Pittenger MF. Adult human mesenchymal stem cell differentiation to the osteogenic or adipogenic lineage is regulated by mitogen-activated protein kinase. J Biol Chem. 2000 Mar 31;275(13):9645-52.

201. Hattori K, Heissig B, Tashiro K, et al. Plasma elevation of stromal cell-derived factor-1 induces mobilization of mature and immature hematopoietic progenitor and stem cells. Blood. 2001 Jun 1;97(11):3354-60.

202. Morrison SJ, Wandycz AM, Hemmati HD, Wright DE, Weissman IL. Identification of a lineage of multipotent hematopoietic progenitors. Development. 1997 May;124(10):1929-39.

203. Pereira RF, Halford KW, O'Hara MD, et al. Cultured adherent cells from marrow can serve as long-lasting precursor cells for bone, cartilage, and lung in irradiated mice. Proc Natl Acad Sci U S A. 1995 May 23;92(11):4857-61.

204. To LB, Haylock DN, Simmons PJ, Juttner CA. The biology and clinical uses of blood stem cells. Blood. 1997 Apr 1;89(7):2233-58.

205. Carmeliet P. Developmental biology. One cell, two fates. Nature. 2000 Nov 2;408(6808):43, 5.

206. Clarke DL, Johansson CB, Wilbertz J, et al. Generalized potential of adult neural stem cells. Science. 2000 Jun 2;288(5471):1660-3.

207. Majka SM, Jackson KA, Kienstra KA, Majesky MW, Goodell MA, Hirschi KK. Distinct progenitor populations in skeletal muscle are bone marrow derived and exhibit different cell fates during vascular regeneration. J Clin Invest. 2003 Jan;111(1):71-9.

208. Majumdar MK, Thiede MA, Mosca JD, Moorman M, Gerson SL. Phenotypic and functional comparison of cultures of marrow-derived mesenchymal stem cells (MSCs) and stromal cells. J Cell Physiol. 1998 Jul;176(1):57-66.

209. Zhang J, Niu C, Ye L, et al. Identification of the haematopoietic stem cell niche and control of the niche size. Nature. 2003 Oct 23;425(6960):836-41.

210. Shamblott MJ, Axelman J, Wang S, et al. Derivation of pluripotent stem cells from cultured human primordial germ cells. Proc Natl Acad Sci U S A. 1998 Nov 10;95(23):13726-31.

211. Jiang Y, Jahagirdar BN, Reinhardt RL, et al. Pluripotency of mesenchymal stem cells derived from adult marrow. Nature. 2002 Jul 4;418(6893):41-9.

212. Reyes JM, Fermanian S, Yang F, et al. Metabolic changes in mesenchymal stem cells in osteogenic medium measured by autofluorescence spectroscopy. Stem Cells. 2006 May;24(5):1213-7.

213. Yoo JU, Barthel TS, Nishimura K, et al. The chondrogenic potential of human bone-marrow-derived mesenchymal progenitor cells. J Bone Joint Surg Am. 1998 Dec;80(12):1745-57.

214. Haynesworth SE, Goshima J, Goldberg VM, Caplan AI. Characterization of cells with osteogenic potential from human marrow. Bone. 1992;13(1):81-8.

215. Balsam LB, Wagers AJ, Christensen JL, Kofidis T, Weissman IL, Robbins RC. Haematopoietic stem cells adopt mature haematopoietic fates in ischaemic myocardium. Nature. 2004 Apr 8;428(6983):668-73.

216. Takakura N, Watanabe T, Suenobu S, et al. A role for hematopoietic stem cells in promoting angiogenesis. Cell. 2000 Jul 21;102(2):199-209.

217. Kadiyala S, Young RG, Thiede MA, Bruder SP. Culture expanded canine mesenchymal stem cells possess osteochondrogenic potential in vivo and in vitro. Cell Transplant. 1997 Mar-Apr;6(2):125-34.

218. Lapidot T, Dar A, Kollet O. How do stem cells find their way home? Blood. 2005 Sep 15;106(6):1901-10.

219. Gazitt Y, Liu Q. Plasma levels of SDF-1 and expression of SDF-1 receptor on CD34+ cells in mobilized peripheral blood of non-Hodgkin's lymphoma patients. Stem Cells. 2001;19(1):37-45.

220. Jin DK, Shido K, Kopp HG, et al. Cytokine-mediated deployment of SDF-1 induces revascularization through recruitment of CXCR4+ hemangiocytes. Nat Med. 2006 May;12(5):557-67.

221. Morrison SJ, Wandycz AM, Akashi K, Globerson A, Weissman IL. The aging of hematopoietic stem cells. Nat Med. 1996 Sep;2(9):1011-6.

222. Oh H, Bradfute SB, Gallardo TD, et al. Cardiac progenitor cells from adult myocardium: homing, differentiation, and fusion after infarction. Proc Natl Acad Sci U S A. 2003 Oct 14;100(21):12313-8.

223. Hirschi KK, Rohovsky SA, D'Amore PA. PDGF, TGF-beta, and heterotypic cell-cell interactions mediate endothelial cell-induced recruitment of 10T1/2 cells and their differentiation to a smooth muscle fate. J Cell Biol. 1998 May 4;141(3):805-14.

224. Wysoczynski M, Reca R, Ratajczak J, et al. Incorporation of CXCR4 into membrane lipid rafts primes homing-related responses of hematopoietic stem/progenitor cells to an SDF-1 gradient. Blood. 2005 Jan 1;105(1):40-8.

225. Sahara M, Sata M, Matsuzaki Y, et al. Comparison of various bone marrow fractions in the ability to participate in vascular remodeling after mechanical injury. Stem Cells. 2005 Aug;23(7):874-8.

226. Asahara T, Takahashi T, Masuda H, et al. VEGF contributes to postnatal neovascularization by mobilizing bone marrow-derived endothelial progenitor cells. EMBO J. 1999 Jul 15;18(14):3964-72.

227. Bauer SM, Bauer RJ, Liu ZJ, Chen H, Goldstein L, Velazquez OC. Vascular endothelial growth factor-C promotes vasculogenesis, angiogenesis, and collagen constriction in three-dimensional collagen gels. J Vasc Surg. 2005 Apr;41(4):699-707.

228. Felix R, Cecchini MG, Fleisch H. Macrophage colony stimulating factor restores in vivo bone resorption in the op/op osteopetrotic mouse. Endocrinology. 1990 Nov;127(5):2592-4.

229. Chang SH, Oh CD, Yang MS, et al. Protein kinase C regulates chondrogenesis of mesenchymes via mitogen-activated protein kinase signaling. J Biol Chem. 1998 Jul 24;273(30):19213-9.

230. Willerson JT, Kereiakes DJ. Endothelial dysfunction. Circulation. 2003 Oct 28;108(17):2060-1.

231. Kelly WL, Bryden MM. A modified differential stain for cartilage and bone in whole mount preparations of mammalian fetuses and small vertebrates. Stain Technol. 1983 May;58(3):131-4.

232. McLeod MJ. Differential staining of cartilage and bone in whole mouse fetuses by alcian blue and alizarin red S. Teratology. 1980 Dec;22(3):299-301.

233. Rousseaux CG. Automated differential staining for cartilage and bone in whole mount preparations of vertebrates. Stain Technol. 1985 Sep;60(5):295-7.

234. Hernandez L, Park KH, Cai SQ, Qin L, Partridge N, Sesti F. The antiproliferative role of ERG K+ channels in rat osteoblastic cells. Cell Biochem Biophys. 2007;47(2):199-208.

235. Jayalath RW, Jackson P, Golledge J. Quantification of abdominal aortic calcification on CT. Arterioscler Thromb Vasc Biol. 2006 Feb;26(2):429-30.

236. Doehring LC, Kaczmarek PM, Ehlers E, et al. Arterial calcification in mice after freeze-thaw injury. Ann Anat. 2006 May;188(3):235-42.

237. Doherty TM, Fitzpatrick LA, Inoue D, et al. Molecular, endocrine, and genetic mechanisms of arterial calcification. Endocr Rev. 2004 Aug;25(4):629-72.

238. Eghbali-Fatourechi GZ, Modder UI, Charatcharoenwitthaya N, et al. Characterization of circulating osteoblast lineage cells in humans. Bone. 2007 May;40(5):1370-7.

239. Eghbali-Fatourechi GZ, Lamsam J, Fraser D, Nagel D, Riggs BL, Khosla S. Circulating osteoblast-lineage cells in humans. N Engl J Med. 2005 May 12;352(19):1959-66.

240. Majesky MW. Developmental basis of vascular smooth muscle diversity. Arterioscler Thromb Vasc Biol. 2007 Jun;27(6):1248-58.

241. Tanaka K, Sata M, Natori T, et al. Circulating progenitor cells contribute to neointimal formation in nonirradiated chimeric mice. FASEB J. 2008 Feb;22(2):428-36.

242. Lamagna C, Bergers G. The bone marrow constitutes a reservoir of pericyte progenitors. J Leukoc Biol. 2006 Oct;80(4):677-81.

243. Friedenstein AJ, Chailakhyan RK, Gerasimov UV. Bone marrow osteogenic stem cells: in vitro cultivation and transplantation in diffusion chambers. Cell Tissue Kinet. 1987 May;20(3):263-72.

244. Hak AE, Pols HA, van Hemert AM, Hofman A, Witteman JC. Progression of aortic calcification is associated with metacarpal bone loss during menopause: a population-based longitudinal study. Arterioscler Thromb Vasc Biol. 2000 Aug;20(8):1926-31.

245. Roodman GD. Advances in bone biology: the osteoclast. Endocr Rev. 1996 Aug;17(4):308-32.

246. Stejskal D, Bartek J, Pastorkova R, Ruzicka V, Oral I, Horalik D. Osteoprotegerin, RANK, RANKL. Biomed Pap Med Fac Univ Palacky Olomouc Czech Repub. 2001 Dec;145(2):61-4.

247. Aubin JE, Bonnelye E. Osteoprotegerin and its ligand: a new paradigm for regulation of osteoclastogenesis and bone resorption. Osteoporos Int. 2000;11(11):905-13.

248. Kaneda T, Nojima T, Nakagawa M, et al. Endogenous production of TGF-beta is essential for osteoclastogenesis induced by a combination of receptor activator of NF-kappa B ligand and macrophage-colony-stimulating factor. J Immunol. 2000 Oct 15;165(8):4254-63.

249. Vogt MT, San Valentin R, Forrest KY, Nevitt MC, Cauley JA. Bone mineral density and aortic calcification: the Study of Osteoporotic Fractures. J Am Geriatr Soc. 1997 Feb;45(2):140-5.

250. Golledge J, Jayalath R, Oliver L, Parr A, Schurgers L, Clancy P. Relationship between CT anthropometric measurements, adipokines and abdominal aortic calcification. Atherosclerosis. 2008 Mar;197(1):428-34.

251. Ibelgaufts H. Cytokine Concentrations in Biological Fluids Accessed, 2006.

252. Vliegenthart R, Oudkerk M, Hofman A, et al. Coronary calcification improves cardiovascular risk prediction in the elderly. Circulation. 2005 Jul 26;112(4):572-7.

253. Ross R. The pathogenesis of atherosclerosis: a perspective for the 1990s. Nature. 1993 Apr 29;362(6423):801-9.

254. Han CI, Campbell GR, Campbell JH. Circulating bone marrow cells can contribute to neointimal formation. J Vasc Res. 2001 Mar-Apr;38(2):113-9.

255. Amano H, Yamada S, Felix R. Colony-stimulating factor-1 stimulates the fusion process in osteoclasts. J Bone Miner Res. 1998 May;13(5):846-53.

256. Bentzon JF, Weile C, Sondergaard CS, Hindkjaer J, Kassem M, Falk E. Smooth muscle cells in atherosclerosis originate from the local vessel wall and not circulating progenitor cells in ApoE knockout mice. Arterioscler Thromb Vasc Biol. 2006 Dec;26(12):2696-702.

257. Bentzon JF, Sondergaard CS, Kassem M, Falk E. Smooth muscle cells healing atherosclerotic plaque disruptions are of local, not blood, origin in apolipoprotein E knockout mice. Circulation. 2007 Oct 30;116(18):2053-61.

258. Weintraub HS. Identifying the vulnerable patient with rupture-prone plaque. Am J Cardiol. 2008 Jun 16;101(12A):3F-10F.

259. Pitt B, Rubenfire M. Risk stratification for the detection of preclinical coronary artery disease. Circulation. 1999 May 25;99(20):2610-2.

APPENDIX 1. ETHICS APPROVAL FOR MOUSE MODEL STUDIES

JAMES COOK UNIVERSITY
Townsville Qld 4811 Australia

Tina Langford, Ethics Administrator, Research Office. Ph: 07 4781 4342; Fax: 07 4781 5521

ETHICS REVIEW COMMITTEE **Animal Ethics Committee** *APPROVAL FOR ANIMAL BASED RESEARCH OR TEACHING*						
PRINCIPAL INVESTIGATOR	**Prof Jonathan Golledge**					
CO-INVESTIGATORS	Dr Monsur Kazi; Mr Shripad Pal; Dr Julie Mudd, Dr Mirko Karan; Dr Corey Moran; Mrs Frances Wood; Ms Mariya Goray; Dr Bradford Cullen (Medicine)					
SCHOOL	Medicine					
PROJECT TITLE	**Regulation of calcification and differences of gene expression in vascular diseases**					
APPROVAL DATE	4 Apr 2006	**EXPIRY DATE**	31 Dec 2007		**CATEGORY**	**4**

This project has been allocated Ethics Approval Number with the following conditions:	**A**	**1099**

1. All subsequent records and correspondence relating to this project must refer to this number.
2. That there is NO departure from the approved protocols unless prior approval has been sought from the Animal Ethics Committee.
3. The Principal Investigator is to advise the responsible Ethics Monitor appointed by the Ethics Review Committee:
   - periodically of the progress of the project;
   - when the project is completed, suspended or prematurely terminated for any reason.
4. In compliance with the *Australian Code of Practice for the Care and Use of Animals for Scientific Purposes*, and the *Queensland Animal Care and Protection Act 2001*, it is **MANDATORY** that you provide an annual report on the progress of your project. This report must also detail animal usage, and any unexpected event or serious adverse effect that may have occurred during the study.

NAME OF RESPONSIBLE MONITOR	Summers, Prof Phillip
EMAIL ADDRESS	phillip.summers@jcu.edu.au
ASSESSED AT MEETING **APPROVED** **Professor Phillip Summers** **Chair, Animal Ethics -Committee**	**Date:** 4 Apr 2006 **Date:** 4 Apr 2006
Tina Langford Ethics Officer **Research Office** Tina.Langford@jcu.edu.au	Date: 13 April 2006

APPENDIX 2. AMENDMENT FOR MOUSE MODEL STUDIES

JAMES COOK UNIVERSITY
Townsville Qld 4811 Australia

Tina Langford, Ethics Officer, Research Office. Ph: 07 4781 4342; Fax: 07 4781 5521

ETHICS REVIEW COMMITTEE **Animal Ethics Committee** *APPROVAL FOR ANIMAL BASED RESEARCH OR TEACHING*						
PRINCIPAL INVESTIGATOR	**Prof Jonathan Golledge**					
OTHER INVESTIGATORS	Mr Shripad Pal; Dr Julie Mudd; Dr Mirko Karan; Dr Corey Moran; Mrs Frances Wood; Ms Mariya Goray; Mr Bradford Cullen; Dr Ann Van Campenhout; Dr Catherine Rush (Medicine & Dentistry) & Dr Lynn Woodward (Pharmacy & Molecular Sciences)					
SCHOOL	Medicine & Dentistry					
PROJECT TITLE	**Regulation of calcification and differences of gene expression in vascular diseases**					
APPROVAL DATE	4 Apr 06	**EXPIRY DATE**	1 Feb 09		**CATEGORY**	**4**

This project has been allocated Ethics Approval Number with the following conditions:	**A**	**1099**

1. All subsequent records and correspondence relating to this project must refer to this number.
2. That there is NO departure from the approved protocols unless prior approval has been sought from the Animal Ethics Committee.
3. The Principal Investigator is to advise the responsible Ethics Monitor appointed by the Ethics Review Committee:
   - periodically of the progress of the project;
   - when the project is completed, suspended or prematurely terminated for any reason.
4. In compliance with the *Australian Code of Practice for the Care and Use of Animals for Scientific Purposes*, and the *Queensland Animal Care and Protection Act 2001*, it is **MANDATORY** that you provide an annual report on the progress of your project. This report must also detail animal usage, and any unexpected event or serious adverse effect that may have occurred during the study.

NAME OF RESPONSIBLE MONITOR	Summers, Prof Phillip
EMAIL ADDRESS	phillip.summers@jcu.edu.au
ASSESSED AT MEETING **3 June 08: Amendment approved: Subcutaneous injection of Calcitriol; Additional animals 40 C57BL/6 & 40 OPG Knockout** **APPROVED** **Professor Phillip Summers** **Chair, Animal Ethics Committee**	**Date:** 4 Apr 06 **Date:** 4 Apr 06
Tina Langford Ethics Officer **Research Office** Tina.Langford@jcu.edu.au	Date: 10 Jun 2008

APPENDIX 3. ETHICS APPROVAL FOR HUMAN INVESTIGATION

JAMES COOK UNIVERSITY
Townsville Qld 4811 Australia

Tina Langford, Ethics Officer, Research Office. Ph: 07 4781 4342; Fax: 07 4781 5521

ETHICS REVIEW COMMITTEE
Human Research Ethics Committee
APPROVAL FOR RESEARCH OR TEACHING INVOLVING HUMAN SUBJECTS

PRINCIPAL INVESTIGATOR	**Professor Jonathan Golledge**				
CO-INVESTIGATOR(S)	Dr Mirko Karan; Dr Corey Moran; Mr Adam Parr; Mr Shripad Pal (Medicine & Dentistry) & Frank Quigley (Queensland Health)				
SCHOOL	Medicine & Dentistry				
PROJECT TITLE	**The role of differences in circulating factors in the pathogenesis of vascular disease**				
APPROVAL DATE	18 Sep 2005	**EXPIRY DATE**	18 Sep 2011	**CATEGORY**	**1**
This project has been allocated Ethics Approval Number with the **following conditions**:				**H**	**2196**

1. All subsequent records and correspondence relating to this project must refer to this number.
2. That there is **NO** departure from the approved protocols unless prior approval has been sought from the Human Research Ethics Committee.
3. The Principal Investigator **must advise** the responsible Ethics Monitor appointed by the Ethics Review Committee:
   - periodically of the progress of the project;
   - when the project is completed, suspended or prematurely terminated for any reason;
   - if serious or adverse effects on participants occur; and if any
   - unforeseen events occur that might affect continued ethical acceptability of the project.
4. In compliance with the National Health and Medical Research Council (NHMRC) *"National Statement on Ethical Conduct in Human Research"* (2007), it is **MANDATORY** that you provide an annual report on the progress and conduct of your project. This report must detail compliance with approvals granted and any unexpected events or serious adverse effects that may have occurred during the study.

NAME OF RESPONSIBLE MONITOR	Turner, Richard
EMAIL ADDRESS:	richard.turner@jcu.edu.au
ASSESSED AT MEETING **APPROVED** **Professor Peter Leggat** **Chair, Human Research Ethics Committee**	***Date:*** 18 Sep 2005 ***Date:*** 18 Sep 2005
Tina Langford Ethics Officer **Research Office** Tina.Langford@jcu.edu.au	Date: 26 November 2008

APPENDIX 4. REAGENTS AND SOLUTIONS

1 X PHOSPHATE BUFFERED SALINE (PBS)

For 1000 ml (stock 10X)

8gm of Nacl

0.2gm of KCl

1.44gm of Na_2HPO_4

0.24gm of KH_2PO_4

Adjust pH to 7.4. Adjust volume to 1L with additional distilled H_2O.Sterilize by autoclaving.

For 100 ml (working 1 X)

10 ml of stock solution

90 ml of D/W

1 % ALIZARIN RED STAIN

1 gram of Alizarin red S powder (grade)

100 ml of distilled water (D/W)

Mix the solution. Adjust the pH to 4.1-4.3 using 0.5% ammonium hydroxide. The pH is critical, make fresh.

GRADES OF PARAFORMALDEHYDE AND GLYCEROL

For 1: 3

10 ml of glycerol and 30 ml of paraformaldehyde

For 1:1

15 ml of glycerol and 15 ml of paraformaldehyde

For 3:1

30 ml of glycerol and 10 ml of paraformaldehyde

3% FLOW CYTOMETRY BUFFER

100 ml of 1x PBS

3 % fetal bovine serum (FBS)

0.05 gm Sodium Azide

Mix well. Adjust pH to 7.4. Sterilize by autoclaving. Store at 4°C

ACK LYSIS BUFFER

For 1000 ml (stocking solution 10 X)

8.29g NH_4Cl

1g $KHCO_3$

37.2mg Na2-EDTA

100 ml D/W

Adjust pH- 7.2 to 7.4 with 1N HCL. Sterilize using 0.2µm filter; store at 4°C

For 100 ml (working 1 X)

10 ml of stock solution

90 ml of D/W. Sterilize using 0.2µm filter. Use at room temperature

0.5 % CHICKEN ALBUMIN BUFFER FOR WASHING CELLS

100 ml of 1X PBS

0.5 2mM of EDTA

% Chicken albumin (grade)

Mix well. Adjust pH to 7.2. Sterilize by autoclaving. Store at 2-8^{o}C

MAGNETIC SEPERATION BUFFER

100 ml of 1X PBS

0.5 % bovine serum albumin (BSA)

2mM of EDTA

Adjust pH to 7.2. Degas the buffer. Sterilize by autoclaving. Store at 2-8^{o}C

DISSOCIATION BUFFER FOR EXTRACTION OF IMMUNE CELLS

Per 20 ml

2mg of Collagenase type XI

3mg of Hyaluronidase type I-S

0.6 mg of DNase I

72 mg of Collagenase I

1x PBS (with calcium and magnesium)

Hepes (20mM)

APPENDIX 5. COMMUNICATIONS ARISING FROM THIS WORK

1. CONFERENCES AND PRESENTATIONS

Pal S.N, Rush C, Golledge J. Circulating bone marrow-derived osteo-progenitors in vasculature contributes towards vascular calcification. Australia and New-Zealand Microcirculation Society (ANZMS) Queenstown, New Zealand, August 2009 (oral presentation)

Pal S. N, Rush C, Golledge J. Circulating bone marrow-derived osteo-progenitors are associated with aortic calcification. Australian society for medical research (ASMR) Brisbane, QLD, Australia. May 2009 (poster presentation)

Pal S.N, Rush C, Woodward L, Golledge J. Bone marrow derived osteo-progenitors in Vasculature: A Calcification linkage. Townsville Festival of Life Sciences, Townsville, QLD, Australia. October 2008 (poster presentation)

Pal S.N, Mirko Karan, Jonathan Golledge. Role of Progenitor cells in vascular calcification. Atherosclerosis Thrombosis Vascular Biology (ATVB) scientific research conference, Chicago, U.S.A. April 2007 (poster presentation)

2. PAPERS

Pal S.N, Golledge J, Osteo-progenitors in vascular calcification: A circulating cell theory towards disease progression. *J Atheroscler Thromb*, 2011, Manuscript in Press

Pal S.N, Clancy. P, Golledge. J. Circulating concentrations of stem cell mobilizing cytokines are associated with levels of osteo-progenitor cells and aortic calcification severity. *Circ J*. 2011, March 8 (Epub ahead of print)

Pal S.N, Rush C, Parr A, Van Campenhout A, Golledge J. Osteocalcin positive mononuclear cells are associated with the severity of aortic calcification. *Atherosclerosis*. 2010 May; 210(1):88-93.)

Pal S.N, Rush C, Golledge J. Circulating bone marrow- derived osteo-progenitors in vasculature contributes towards vascular calcification. *J Vasc Res*.2009; 46(S2): 34. (Abstract)

Golledge J, Van Campenhout A, **Pal S. N**, Rush C. Bone marrow-derived cells and arterial disease. *J Vasc Surg*. 2007 Sep; 46(3):590-600.

3. AWARDS

PhD completion grant leading to thesis submission from James Cook University (2009)

Travel grant to attend ANZMS scientific conference held in Queenstown, New Zealand from School of Medicine and Dentistry, James Cook University (2009)

Best Poster award for the Life Science Festival, James Cook University. (2008)

Graduate Research Studies (GRS) grant from James Cook University (2008)

Travel grant to attend ATVB scientific conference held in Chicago, USA from School of Medicine and Dentistry, James Cook University (2007)